The evolution of complete metamorphosis in insects

Inaugural-Dissertation

to obtain the academic degree

Doctor rerum naturalium (Dr. rer. nat.)

submitted to the Department of Biology, Chemistry, Pharmacy

of Freie Universität Berlin

by

Christin Manthey

2022

This thesis was conducted between November 2017 and May 2022, under the supervision of Prof. Dr. Jens Rolff (Freie Universität Berlin) and Dr. Paul Johnston (Freie Universität Berlin and Leibniz-Institute of Freshwater Ecology and Inland Fisheries Berlin). The work was carried out at Freie Universität Berlin.

1st Reviewer: Prof. Dr. Jens Rolff

2nd Reviewer: Sophie Armitage, PhD.

Date of defense: 04.07.2022

To Loke.

TABLE OF CONTENTS

TABLE OF CONTENTS ..... **I**

ZUSAMMENFASSUNG **1**

SUMMARY **5**

CHAPTER I: GENERAL INTRODUCTION **8**

Objectives 21

References 25

CHAPTER II: COMPLETE METAMORPHOSIS AND MICROBIOTA TURNOVER IN INSECTS **34**

Abstract 34

Introduction 35

Materials and Methods 39

Results 47

Discussion 51

Acknowledgements 55

References 55

CHAPTER III: IMMUNE GENE REGULATION IN THE GUT DURING METAMORPHOSIS IN TWO HOLO- VERSUS A HEMIMETABOLOUS INSECT **63**

Abstract 63

Introduction 64

Material and Methods 67

Results 73

Discussion 77

Acknowledgements 80

References 80

CHAPTER IV: COMPLETE METAMORPHOSIS AND FAST LARVAL GROWTH IN INSECTS **87**

TABLE OF CONTENTS

Abstract 87

Introduction 88

Methods 92

Results 96

Discussion 101

Acknowledgements 105

References 105

CHAPTER V: GENERAL DISCUSSION 111

Outlook 118

Conclusion 119

References 120

APPENDICES 127

Appendix chapter II 127

Appendix chapter III 194

Appendix chapter IV 200

References 220

ACKNOWLEDGEMENTS 221

PUBLICATIONS 223

DECLARATION OF INDEPENDENCE 224

ZUSAMMENFASSUNG

Metamorphose, die Verwandlung (*Meta*) der Gestalt (*Morphe*), ist ein häufig vorkommendes Phänomen im Tierreich, in dem Metamorphose mehrmals unabhängig voneinander evolviert ist. Die dramatischsten Veränderungen treten in der erfolgreichsten Tiergruppe auf: den Insekten, die mehr als 60 % aller lebenden Tiere umfassen. Innerhalb der Gruppe der Insekten machen die Holometabolen (z.B. Käfer, Schmetterlinge, Fliegen und Bienen) mehr als 80 % aller Arten aus. Holometabole Insekten durchlaufen eine vollständige Metamorphose. In einem zwischen dem Larven- und Adultstadium liegendem, nicht fressenden Puppenstadium wird die gesamte larvale Anatomie radikal umgebaut, einschließlich des Verdauungstrakts, der Apoptose und Proliferation durchläuft. Die zweite große Gruppe von Insekten, die Hemimetabolen (z.B. Heuschrecken, Wanzen und Libellen), durchlaufen eine unvollständige Metamorphose. Im Vergleich zu den Holometabolen vollzieht sich die Metamorphose bei den hemimetabolen Insekten allmählicher, weniger drastisch und ohne Puppenstadium.

Die Holometabolie ist eine der wichtigsten evolutionären Innovationen, die die enorme und einzigartige Artenvielfalt der Insekten erklären. Wie jedoch die Entwicklung des Puppenstadiums mit dem Erfolg der Insekten zusammenhängt, ist unbekannt. Die Umgestaltung des Larvendarms stellt eine große Herausforderung für die Darmmikrobiota dar, da der Darm während der Verpuppung ausgetauscht wird, was bei Hemimetabola nicht der Fall ist. Dies gibt holometabolen Insekten die einzigartige Möglichkeit, einen Wechsel zwischen der larvalen und der adulten Mikrobiota herbeizuführen und Nischenverschiebungen zu erleichtern, indem das Insekt spezialisierte Symbionten für eine lebensphasenspezifische Ernährung, Ökologie und Physiologie

erwerben kann - eine kaum untersuchte adaptive Hypothese, die die Evolution der Puppe erklären könnte.

In Kapitel II untersuchte ich mithilfe von 16S rRNA-Gen Metabarcodierung, 18 verschiedene pflanzenfressende Insektenarten aus fünf Ordnungen holometaboler und drei Ordnungen hemimetaboler Insekten. Beim Vergleich von larvalen und adulten Exemplaren stellte ich eine wesentlich höhere Beta-Diversität und damit einen Mikrobiota-Austausch bei holometabolan verglichen mit hemimetabolen Insekten fest. Meine Ergebnisse bekräftigen die Idee, dass die Verpuppung die Möglichkeit bietet, die Darmmikrobiota zu verändern und somit Nischenverschiebungen zu erleichtern. Dieser mögliche Effekt der Erleichterung von Nischenverlagerungen könnte den selektiven Vorteil der Evolution der vollständigen Metamorphose erklären.

Die einzigartige Möglichkeit, die mikrobielle Zusammensetzung während der Entwicklung holometaboler Insekten zu verändern, indem der Darm während der vollständigen Metamorphose umgestaltet wird, setzt das Insekt auch einem höheren Infektionsrisiko aus. Holometabole müssen demnach ihre Darmmikrobiota kontrollieren und eine Immunantwort einleiten, um Infektionskrankheiten während der Metamorphose zu vermeiden.

In Kapitel III habe ich mithilfe von RNA Sequenzierung die Expression von Immuneffektor-Genen im Darm während der Metamorphose bei zwei holometabolen und einem hemimetabolen Insekt verglichen. Bei den beiden Holometabola fand ich hohe Abundanzen von unterschiedlich exprimierten Immuneffektoren im Darm während der Larven-Puppen-Häutung; bei den Hemimetabola wurden keine derart hohen Abundanzen während der Nymphen-Erwachsenen-

Häutung beobachtet. Meine Ergebnisse bestätigen, dass die vollständige Metamorphose allein eine prophylaktische Immunantwort, die die Mikrobiota während der Darmrekonstruktion kontrolliert, als adaptive Antwort in Holometabola auslöst.

Eine weitere kaum untersuchte, aber sich nicht auszuschließende Hypothese, die den Erfolg holometaboler Insekten erklärt, könnte darin bestehen, dass die Evolution des Puppenstadiums Wachstum und Differenzierung entkoppelt. Das meiste Wachstum ist bei holometabolen Insekten auf das Larvenstadium beschränkt, während die meiste Entwicklung in der Puppe stattfindet, was ein schnelles Larvenwachstum ermöglicht.

In Kapitel IV führte ich eine Literaturrecherche durch und berechnete Wachstumsraten und Verhältnisse. Ich verglich 33 Arten aus drei holo- und sieben hemimetabolen Insektenordnungen. Ich fand ein schnelleres Larvenwachstum, höhere Wachstumsquotienten und viel höhere Varianzen für diese Messungen bei holometabolen im Vergleich zu hemimetabolen Insekten. Außerdem fand ich bei Holometabolen viel kürzere Wachstumszeiten der Larvenstadien als bei hemimetabolen Insekten. Meine Ergebnisse bestärken die Hypothese der Entkopplung von Wachstum und Differenzierung in holometabolen Insekten, die ein schnelles Larvenwachstum ermöglicht.

In der vorliegenden Arbeit untersuchte ich zwei kaum betrachtete und sich nicht gegenseitig ausschließende Hypothesen zur Erklärung der Evolution der Puppe bei holometabolen Insekten, die den Großteil der Tierdiversität ausmachen. Ich konnte einen Wechsel der Mikrobiota nachweisen, der auch unter der Kontrolle der Darmimmunität des Insektenwirts steht und es Holometabolen ermöglicht, während der Entwicklung verschiedene Nischen zu besetzen. Die zweite Hypothese, die besagt, dass die Entkopplung von Wachstum und Differenzierung ein

schnelles Larvenwachstum ermöglicht, wird durch die von mir gefundenen schnelleren Larvenwachstumsraten bei holometabolen im Vergleich zu hemimetabolen Insekten unterstützt. Die Erleichterung von Nischenverschiebungen durch Veränderungen in der Darmmikrobiota könnte als wesentlicher Treiber der Evolution der Puppe angesehen werden. Der Mikrobiota-Austausch könnte auch durch andere selektive Faktoren wie die Wachstumsrate angetrieben werden. Schnelles Larvenwachstum könnte ein selektiver Faktor für die Entkopplung von Wachstum und Differenzierung sein, was letztlich zur Evolution der Puppe bei holometabolen Insekten geführt haben könnte.

SUMMARY

Metamorphosis, the change (*meta*) in form (*morphe*), is a common phenomenon in the animal kingdom, where it has evolved several times independently. The most dramatic metamorphic changes occur in the most successful group of animals: the insects, which comprise more than 60% of all living animals. Within the group of insects, the Holometabola (e.g. beetles, butterflies, flies and bees) comprise more than 80% of all insect species. Holometabolous insects undergo complete metamorphosis. In a non-feeding pupal life stage, intercalated between the larval and adult stages, their entire anatomy is radically remodelled, including the digestive tract, which undergoes apoptosis and proliferation. The second major group of insects, the Hemimetabola (e.g. grasshoppers, true bugs, and dragonflies), undergo incomplete metamorphosis. Compared to Holometabola, hemimetabolous insects metamorphose more gradually, less drastically and without a pupal stage.

Holometaboly is one of the key evolutionary innovations explaining insects' enormous and unique biodiversity. However, how the evolution of the pupal stage is related to the success of insects is unknown. The remodelling of the larval gut poses a significant challenge to the gut microbiota, as the gut is replaced during pupation, which does not occur in Hemimetabola. It gives holometabolous insects the unique opportunity to drive a change between the larval and adult microbiota, facilitating niche shifts by allowing the insect to acquire specialised symbionts for a life-stage specific diet, ecology and physiology- one barely studied adaptive hypothesis explaining the evolution of the pupa.

SUMMARY

In chapter II, using 16S rRNA gene metabarcoding, I studied 18 different herbivorous insect species from five orders of holometabolous and three orders of hemimetabolous insects. Comparing larval and adult specimens, I found a much higher beta-diversity and hence microbiota turnover in holometabolous insects than in hemimetabolous insects. My results support the idea that the pupa offers the opportunity to change the gut microbiota and hence facilitates niche shifts. This possible effect of niche shift facilitation could explain a selective advantage of the evolution of complete metamorphosis.

The unique opportunity to change the microbial composition throughout insect development by gut remodelling during complete metamorphosis also puts holometabolous insects at a higher risk of infections. Holometabola must control their gut microbiota and initiate an immune response to avoid infectious diseases during metamorphosis.

In chapter III, using RNAseq, I compared the expression of immune effector genes in the gut during metamorphosis in two holometabolous and a hemimetabolous insects. I found high read count abundances of differentially expressed immune effectors in the gut at the larval-pupal moult in the two Holometabola; no such high abundances were observed at the nymphal-adult moult in Hemimetabola. My findings confirm that only complete metamorphosis elicits a prophylactic immune response as an adaptive response in holometabolous insects, which controls the microbiota during gut replacement.

Another barely studied and not mutually exclusive hypothesis explaining the success of holometabolous insects could be that intercalating the pupal stage decouples growth and

differentiation. Most growth is confined to the larval stages in holometabolous insects, while most development occurs in the pupa, allowing for fast larval growth.

In chapter IV, I conducted a literature review and calculated growth rates and ratios. I compared 33 species from three holo- and seven hemimetabolous insect orders. I found faster larval growth, higher growth ratios, and much higher variances for those traits in holometabolous than hemimetabolous insects. I also found much shorter growth periods of the larval stages in holometabolous than hemimetabolous insects. My results support the decoupling of the growth and differentiation hypothesis in holometabolous insects, allowing fast larval growth.

In this thesis, I investigated two barely studied and not mutually exclusive hypotheses explaining the evolution of the pupa in holometabolous insects, which constitute the majority of animal diversity. I could show a microbiota turnover in holometabolous insects, which is also under the control of the host gut immunity and allows the Holometabola to occupy different niches throughout development. The second hypothesis, which proposes that decoupling growth and differentiation allows for fast larval growth, is supported by my findings of faster larval growth rates in holometabolous than hemimetabolous insects. The facilitation of niche shifts by changes in the gut microbiota could be considered an essential driver of the evolution of the pupa. The microbiota turnover could also be driven by other selective factors such as growth rate. Fast larval growth could be a selective factor for decoupling growth and differentiation, ultimately resulting in the evolution of the pupa in holometabolous insects.

CHAPTER I: GENERAL INTRODUCTION

"Von Gestalten zu künden, die in neue Körper verwandelt wurden, treibt mich der Geist. […]"
(Ovid, Metamorphosen)

For centuries, dramatic morphological transitions from a caterpillar to a butterfly or a tadpole to a frog have fascinated naturalists (Merian & Knibbeler, 2017). Metamorphosis, the change (*meta*) in form (*morphe*), is a widespread phenomenon in the animal kingdom (Laudet, 2011; E. E. Werner, 1988). Depending on its definition, metamorphosis is considered for an even wider variety of organisms, including animals, flowering plants, fungi, and some marine algae. In a symposium at the 2006 Society for Integrative and Comparative Biology (SICB) annual meeting in Orlando, FL (USA), fourteen scientists discussed metamorphosis and compared its notions (Bishop et al., 2006). Their various definitions of metamorphosis have some similarities and some differences among them. The three main similarities across most of the definitions are that (i) metamorphosis includes a major morphological change, (ii) a change in the adaptive landscape, and (iii) the pre-metamorphic stage is post-embryonic (Bishop et al., 2006). In the animal kingdom, metamorphosis evolved independently several times, including well-studied examples in fish, amphibians and insects that meet all three criteria but differ in the degree of morphological change.

The most dramatic metamorphosis occurs in the most successful group of animals: the insects. Insects comprise more than 60% of all living animals (Grimaldi & Engel, 2005; Mora, Tittensor, Adl, Simpson, & Worm, 2011). They are the most successful animals, whether in abundance, species diversity, biomass or ecosystem function (Berenbaum, 2017; Mora et al., 2011; Stork, 1993; Whiting, 2004). According to the extent of metamorphic change, insects can be classified

into two major categories: hemimetabolous (e.g. grasshoppers, true bugs, and dragonflies) and holometabolous insects (e.g. beetles, butterflies, flies and bees). More than 80% of all insect species are holometabolous (Grimaldi & Engel, 2005; Trautwein, Wiegmann, Beutel, Kjer, & Yeates, 2012). Eleven of the 29 insect orders belong to the holometabolous insects that undergo complete metamorphosis (see figure 1) a monophyletic group that evolved about 344 million years ago (Misof et al., 2014). Holometaboly is considered an evolutionary key innovation explaining insect diversity (Mayhew, 2007; Rainford, Hofreiter, Nicholson, & Mayhew, 2014); but see (Condamine, Clapham, & Kergoat, 2016), and holometabolous insects have lower extinction rates than other groups without this innovation (Nicholson, Ross, & Mayhew, 2014).

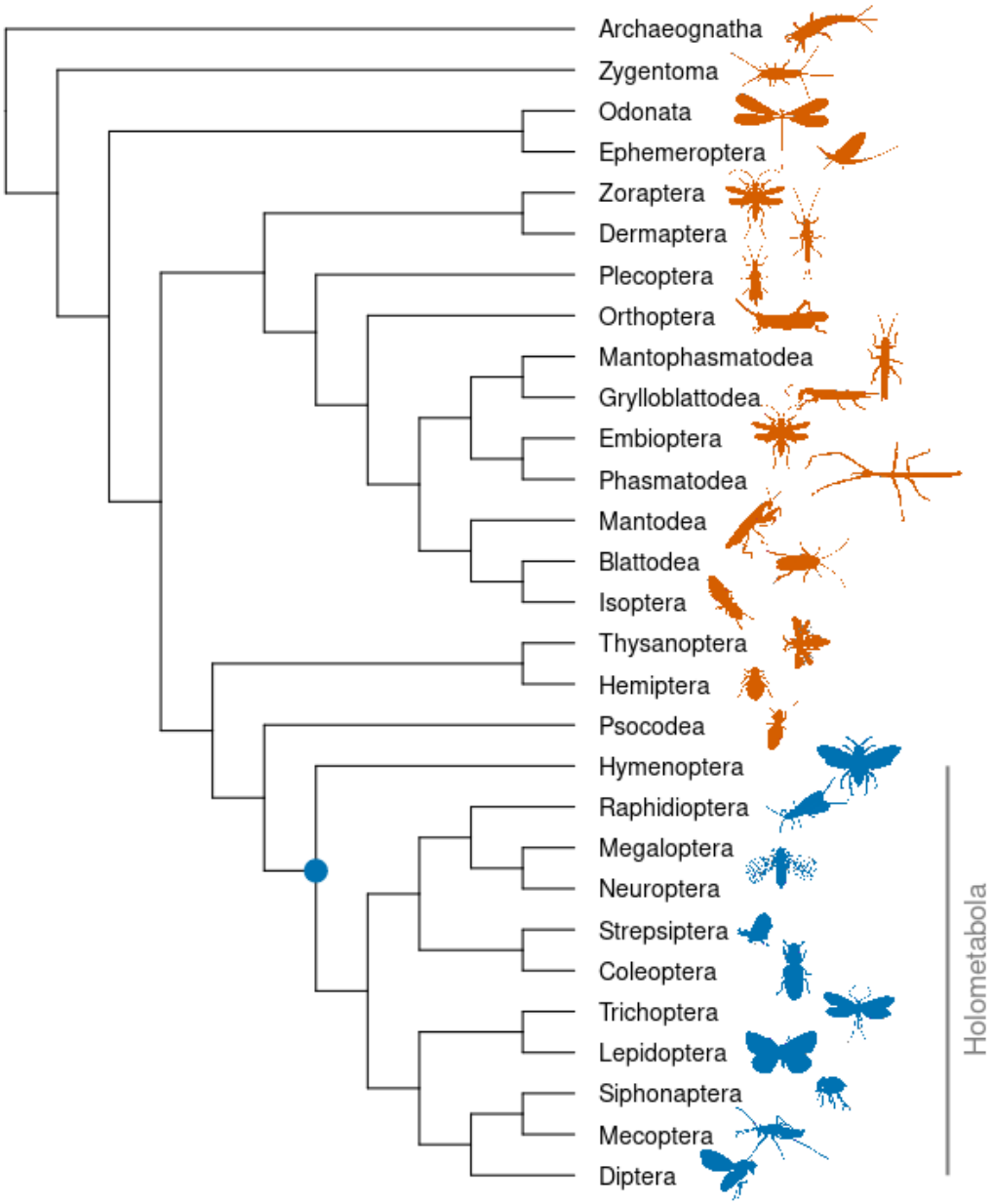

Figure 1: Phylogenetic tree of insect relationships redrawn after Misof et al. (2014). The coloured blue node indicates the origin of complete metamorphosis, which gave rise to the eleven orders of holometabolous insects. Examples of the Holometabola are presented in the blue pictures. The orange pictures are examples of the second major group of insects, the hemimetabolous insects.

GENERAL INTRODUCTION

The holometabolous life cycle comprises embryonic, immature (larval), pupal and adult stages (see figure 2), where growth occurs exclusively during larval development. As one example of complete metamorphosis, the caterpillar-butterfly transition mentioned at the beginning is an easily observable transformation and one of the most popular among amateur and professional entomologists. Lepidoptera (butterflies and moths), the second-largest order of insects (Grimaldi & Engel, 2005), are easy to follow when occurring on flowering plants throughout development (Menken, Boomsma, & Van Nieukerken, 2010). They were also central to the work by Sybilla Maria Merian in the 17th century (Merian & Knibbeler, 2017) and the development of coevolutionary hypotheses (Ehrlich & Raven, 1964). The caterpillar hatches from the egg and spends most time eating. Like other typical holometabolous larvae, the caterpillar has a cylindrical shape with only short (others no) appendages (Maddrell, 2018). Most caterpillars feed on plant material using biting-chewing mouthparts (Forbes, 1910; Krenn, 2010). They grow intensely, except for the outer skin, the exoskeleton with a limited capacity to expand (Grunert, Clarke, Ahuja, Eswaran, & Nijhout, 2015). If the caterpillar outgrows the exoskeleton, it moults and sheds the exoskeleton off and replaces it with another. Caterpillars develop through a variable number of moults that can double under adverse conditions (Esperk, Tammaru, & Nylin, 2007). The caterpillar's body is radically remodelled in the subsequent non-feeding pupal or chrysalis stage. The pupa is the defining feature of holometabolous insects. Like in other holometabola, the entire anatomy is reconstructed, including the digestive tract (Lowe, Garwood, Simonsen, Bradley, & Withers, 2013), which undergoes apoptosis (programmed cell death) and proliferation (Martín-Vega, Simonsen, & Hall, 2017). The chrysalis splits and emerges in the adult butterfly with many appendages such as wings, antennae, proboscis, and legs. Most adult butterflies are anthophilous;

they feed on nectar or other flower fluids using their proboscis, a tubular sucking organ (Krenn, 2010). In contrast, the second major group of insects, the hemimetabolous insects, undergo incomplete metamorphosis. The hemimetabolous life cycle comprises embryonic, immature (nymphal) and adult stages. A miniature version of the adult with legs, antennae, mouthparts, eyes and other structures emerges from the egg (Chapman, 2013; Lutz & Huebner, 1980; Truman, 2019) that increases in size throughout the succeeding nymphal stages. The post-embryonic changes appear more gradually than in Holometabola and without a pupal stage with incomplete metamorphosis. Unlike holometabolous insects, the digestive tract, for instance, does not undergo extensive remodelling. The gut increases in length throughout development; cell death rarely occurs, whereas cell proliferation frequently occurs (Teixeira, Fialho, Zanuncio, Ramalho, & Serrão, 2013). However, the nymphs lack wings and reproductive organs and are smaller than adults. The wings and genitalia emerge at the final adult moult. For some of the basal hemimetabolous insects, the stoneflies (Plecoptera), the damsel- and dragonflies (Odonata), and the mayflies (Ephemeroptera), the nymphs are sometimes called naiads (Chapman, 2013; Comstock, 1918). These three groups have immature aquatic stages that are more distinct from adults than in other hemimetabolous insects. Hence, they undergo a more conspicuous metamorphosis and lose, for instance, their larval gills at the final adult moult. In Ephemeroptera, the oldest group of winged insects (Misof et al., 2014), the legs change shape and are lengthened. The mouthparts are reduced, non-functional and sometimes even lost at the final adult moult (Cranston & Gullan, 2009; Kamsoi, Ventos-Alfonso, Almudi, Casares, & Belles, 2021). Ephemeroptera are also unique in having a subimago, a winged stage between the nymph and the adult (Chapman, 2013; Kamsoi et al., 2021). Nevertheless, the general immature body form in

Ephemeroptera, Plecoptera and Odonates resembles that of the adult, and they are considered hemimetabolous.

Fish and amphibians are also species-rich taxa that evolved metamorphosis in the animal kingdom but a less extreme. The extant amphibians consist of about 88% anurans (Wake & Koo, 2018; Wiens, 2015). Most anurans undergo profound changes throughout their development (Lofts, 1976), consisting of three successive stages: pre-metamorphic, pro-metamorphic, and climax (Miyata & Ose, 2012; Vitt & Caldwell, 2014). During anuran metamorphosis, they shift from aquatic life stages (eggs, tadpoles, and metamorphs) to terrestrial subadult (juvenile) and adult forms (see figure 2). The eggs develop underwater. Anurans hatch from the eggs as tadpoles, herbivorous feeders with gills for breathing and a tail for swimming — the pre-metamorphic stage. After a few weeks, the tadpole develops limbs — the pro-metamorphic period has started. In the subsequent metamorphic climax, the tadpole loses its gills and relies on newly developed lungs for respiration. The tail that was much longer than the trunk is absorbed within a few days (Yaoita, 2019). Internal organs, including the digestive tract, are transformed (Hourdry, L'Hermite, & Ferrand, 1996). The gut, for instance, is shortened, and its coils are rearranged (Pretty, Naitoh, & Wassersug, 1995). The skin also transforms from a larval to an adult type (Ohmura & Wakahara, 1998; Regueira, Dávila, & Hermida, 2016). The adult frog is a predatory land-living form where more than 90% of its lifetime occurs (Earl E. Werner, 1986). Another species-rich vertebrate group that undergoes metamorphosis, the teleosts, are the most diverse group of living vertebrates in terms of species number and biomass (Faircloth, Sorenson, Santini, & Alfaro, 2013; Sallan, 2014; Wiens, 2015). Teleosts also undergo significant changes throughout development comparable to the metamorphosis of anurans but with less drastic morphological and habitat changes

(McMenamin & Parichy, 2013). Marine teleosts, for instance, usually shift from a pelagic (open water) dispersal larva to a benthic adult stage, which lives on the substrate or seafloor. The well-studied larvae of marine flatfish (flounder, halibut, plaice, sole, tonguefish, turbot), for example, resemble typical bilaterally symmetrical fish with eyes on each side of their body, and that swim upright in the water column (A. Schreiber, 2013). After a few weeks, the larvae metamorphose into their immature adult form and becomes asymmetrical. One eye translocates to the opposite head side, including a skull shift (McMenamin & Parichy, 2013; A. Schreiber, 2013). The gut becomes more complex and the number of coils increase (Gomes, Alves, Rønnestad, & Power, 2015). The skin colour changes with a newly developed pigmentation pattern on the body surface in the adult form (McMenamin & Parichy, 2013), which swims in a horizontally tilted posture (A. M. Schreiber, 2006).

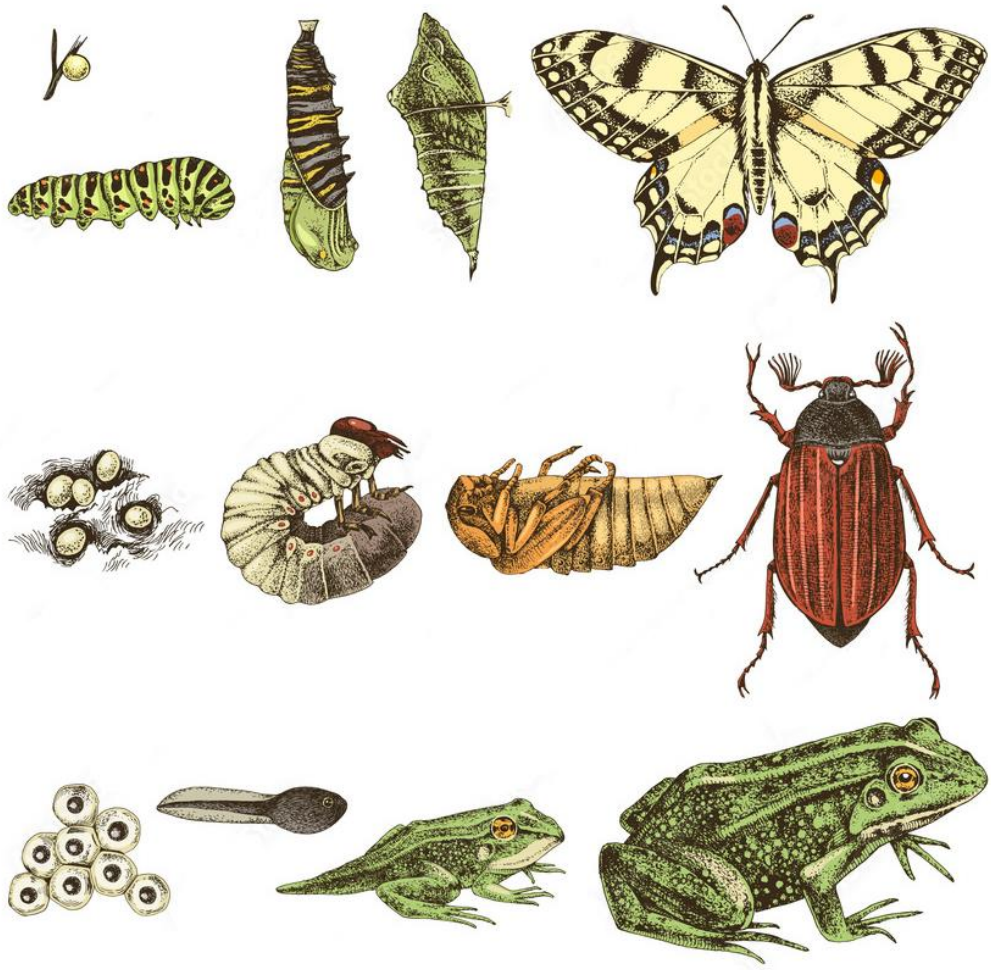

Figure 2: Examples from Lepidoptera and Coleoptera of complete metamorphosis in insects and anuran metamorphosis. The lepidopteran and coleopteran examples show the holometabolous development from an egg to the adult stage. The pupa, where complete metamorphosis occurs, is intercalated between the larval and adult life stages. The anuran example shows a less drastic metamorphosis that shifts the aquatic life stages (eggs and tadpole) to terrestrial juvenile and adult forms (Drawings: Adobe Stock, #284787037.)

Generally, holometabolous, teleost and anuran metamorphosis leads to an ontogenetic niche shift with distinct and specialised larval and adult life stages. All types of metamorphosis include drastic transformations of the internal and external anatomy. However, complete metamorphosis in insects is the most common yet dramatic, abrupt and striking developmental process within all the just-mentioned examples. In insects with complete metamorphosis, both autophagocytosis (degradation of cells) and apoptosis (programmed cell death) turn out to be important in remodelling the larval into adult organs, as reviewed by (Tettamanti & Casartelli, 2019). This transition to the adult is restricted to a unique stage, the pupa, intercalated between the larval and adult stages, leading to a more extreme and abrupt change than in fish and amphibians. The results of the morphological changes are visible at the final adult moult, such as when the butterfly emerges from its chrysalis. The transformation into a frog is also drastic and relatively rapid. It is easy to track how the tadpole develops limbs and absorbs the tail, but the changes are gradual in anurans compared to insects with complete metamorphosis. Each transformation step in anurans leads to the next level of transformation (Gosner, 1960). Some developmental processes in anurans also continue after the metamorphic climax, such as the maturation of gonads (Ogielska & Kotusz, 2004) and growth (Earl E. Werner, 1986). The pupa in holometabolous insects decouples growth and maturation. Growth is primarily confined to the larval stages, and maturation is reached at the final adult moult (Rewitz, Yamanaka, & O'Connor, 2013). Also, unlike insect pupae, metamorphosing tadpoles remain active; they can leap away from predators and adverse environmental conditions such as temporary ponds (Vitt & Caldwell, 2014; Earl E. Werner, 1986). These pressures lead to the shift from an aquatic to a terrestrial habitat in anurans enabled by metamorphosis. In contrast, in holometabolous insects, the drastic changes in the entire anatomy, including apoptosis and

proliferation of the gut, can have drastic consequences for the microbiota facilitating a niche shift. Though, immobile pupae are not defenceless. They have evolved a wide range of antipredator strategies, including cryptic colouration (camouflage, mimicry), hiding in vegetation or soil, chemical camouflage or bluffing (deimatic) movements and sounds (Lindstedt, Murphy, & Mappes, 2019).

Complete metamorphosis is one of the key evolutionary innovations explaining holometabolous insects' enormous and unique biodiversity (Nicholson et al., 2014). However, how the evolution of the pupal stage is related to the success of the holometabolous insects is unknown (Rolff, Johnston, & Reynolds, 2019). The dramatic and abrupt reconstruction of the larval body in the pupa includes the degradation and replacement of the gut inhabited by microbes. Therefore, gut remodelling gives holometabolous insects the unique opportunity to drive a change between the larval and adult microbiota (Hammer & Moran, 2019; Rolff et al., 2019) - one barely studied adaptive hypothesis explaining the success of holometabolous insects. Symbionts that inhabit insects provide nutrition, defence against infection or predation, and sometimes reproductive success and other services to the insect host (Brownlie & Johnson, 2009; Eleftherianos, Atri, Accetta, & Castillo, 2013; Engl & Kaltenpoth, 2018). Changing microbial composition throughout development facilitates niche shifts by allowing the insect to acquire specialised symbionts for a life-stage specific diet, ecology and physiology (Hammer & Moran, 2019; Rolff et al., 2019). For example, a caterpillar can feed on leaves, while the adult butterfly can feed on nectar.

It is also known that complete metamorphosis reduces microbes by several orders of magnitude, including growing populations of pathogens that would otherwise persist in the adult host (Hammer & Moran, 2019; Johnston & Rolff, 2015). Some studies have investigated changes in the gut

microbiota throughout host development in single species. For instance, (Sudakaran, Salem, Kost, & Kaltenpoth, 2012) found a very stable mid-gut microbial community with six predominant taxa consistently abundant throughout development in the hemimetabolous firebug (*Pyrrhocoris apterus*). In contrast, (Parmentier et al., 2018) found different gut microbial communities in larvae and adults of a wild bumblebee (*Bombus pascuorum*) nest, a holometabolous insect. The typical adult core gut microbes were absent in the larvae. Hammer, (Hammer, McMillan, & Fierer, 2014) also found distinct gut communities in the leaf-chewing larvae and nectar- and pollen-feeding adults of the red postman butterfly (*Heliconius erato*). The same pattern of distinct larval and adult microbiomes was also shown by (de Jonge et al., 2020) in a housefly (*Musca domestica*) and by (Wang, Xiang, & Wan, 2020) in the rainbow stag beetle (*Phalacrognathus muelleri*). However, if this is a generalisable pattern within holometabolous insects remains unclear.

The unique opportunity to change the microbial composition throughout insect development by gut remodelling during complete metamorphosis also puts the insect at a higher risk of infections. The physical barriers in the gut that avoid bacterial infections, like the peritrophic membrane in the midgut and the sclerotized cuticle of the fore- and hindgut, are broken down during complete metamorphosis. The insect must control its gut microbiota and initiate an immune response to avoid infectious diseases. (Johnston & Rolff, 2015) showed that complete eradication of the gut microbiota comes with the risk of losing beneficial symbionts. Hence complete metamorphosis creates a dilemma; either the insect host eradicates and reestablishes its gut microbes from the environment, or the insect maintains beneficial symbionts while fighting pathogens.

It is known that insects have a mixed-mode transmission of microbes (Ebert, 2013). Some beneficial symbionts are transmitted vertically and stored in specialised tissue during complete

metamorphosis, while others are horizontally transmitted and taken up from the environment later. Insects evolved various strategies to ensure the transmission of beneficial symbionts throughout development. (Stoll, Feldhaar, Fraunholz, & Gross, 2012) showed vertical transmission of microbes via bacteriocytes in ant species. The relative number of bacteria-filled bacteriocytes increased strongly during complete metamorphosis. (Maire et al., 2020) also showed a transmission of microbes via bacteriocytes in weevils by maintaining and relocating bacteriocytes during gut renewal in the pupa. Other specialised structures to transmit symbionts in insects are antennal glands (Kaltenpoth, Yildirim, Gürbüz, Herzner, & Strohm, 2012) and crypts (Kikuchi, Hosokawa, & Fukatsu, 2011).

It is also known that insects evolved strategies to control their microbes in the pupal gut as a prophylactic response to prevent infections during complete metamorphosis. (Russell & Dunn, 1991) found high lysozyme activity in the midgut lumen of the moth *Manduca sexta* during metamorphosis. Lysozyme, an antibacterial protein, accumulated before in the larval midgut epithelium and was released at the larval-pupal moult. Also, (Russell & Dunn, 1996) found that the pupal midgut of *M. sexta* contains a cocktail of antibacterial proteins, including at least lysozyme, bactericidal activity against *Escherichia coli*, hemolin, and phenoloxidase. Induction of antibacterial proteins in the gut prior to metamorphosis has also been described in the silkworm *Bombyx mori* and the tobacco cutworm *Spodoptera litura* (Mai et al., 2017). Mai et al. (2017) found up-regulated lebocin, a particular antimicrobial peptide (AMP) of Lepidoptera, in the midgut with a peak expression during the wandering stage. They also found that the ecdysteroid hormone, which is known to control metamorphosis, regulates lebocin expression in the midgut. In hemimetabolous insects, in contrast, the metamorphic changes are less drastic, and the gut microbiota seems to stay

relatively stable compared to holometabolous insects (Sudakaran et al., 2012). However, little is known about the regulation of immune genes during the nymphal–adult moult.

(Johnston, Paris, & Rolff, 2019) were the first to investigate the temporal dynamics of immune effector expression throughout the final larval moult as an adaptive response in holometabolous insects, which controls the microbiota during gut replacement. They used RNAseq to compare the expression of immune effector genes in the gut during metamorphosis in a holometabolous (*Galleria mellonella*) and a hemimetabolous insect (*Gryllus bimaculatus*). They found up-regulated immune effectors and the transcription factor GmEts in *G. mellonella* and no such up-regulation in the hemimetabolous *Gr. bimaculatus*. *G. mellonella* showed peak expression of lysozyme and three AMPs coinciding with delamination of the larval gut. Despite this new finding for one holometabolous species, it also remains unclear whether this finding reflects a general pattern within holometabolous insects.

Another barely studied and not mutually exclusive hypothesis explaining the success of holometabolous insects could be that intercalating the pupal stage decouples growth and differentiation (Arendt, 1997; Rolff et al., 2019). Arendt (1997) and Rolff et al. (2019) discuss that in holometabolous insects, most growth is confined to the larval stages, while most development occurs in the pupa allowing for fast larval growth. Insects only grow in the immature feeding stages with no marked change in body form; each successive stage is similar to the previous stage until metamorphosis (Chapman, 2013). The less mobile, soft-bodied, and worm-like shape larvae of holometabolous insects (Maddrell, 2018; Truman, 2019) allow them to exploit food resources better, which may benefit fast larval growth.

Fast growth allows for efficient and competitive exploitation of ephemeral resources, which appear patchily and have a short lifetime (Cole, 1980). Ephemeral habitats would be best exploited by insects that rapidly achieve adult size, mature, and disperse before the habitat disappears (Cole, 1980). (Day & Rowe, 2002) suggested an overhead threshold model for optimal size and age at a transition like the final juvenile moult. Their model predicts a developmental threshold of the minimum size or level of condition needed for the transition and an L-shaped reaction norm for size and age. Fast-growing organisms will reach the threshold earlier, resulting in a steep slope of the relationship between size and age at the final moult compared to slow-growing organisms. There is evidence for fast growth in holometabolous insects. Cole (1980) showed that holometabolous insects differ significantly in median growth ratios from hemimetabolous insects. However, the study by Cole (1980) comes with some weaknesses, given our current knowledge of statistical analysis. It was published prior to the invention of comparative methods by (Felsenstein, 1985). Cole (1980) used various size measurements to calculate growth ratios, did not include developmental times and used a median test based on non-parametric statistics (Siegel, 1957) that did not control phylogeny. Therefore, better evidence that most notably reduces type I error rates by including phylogeny is needed to support the decoupling growth and differentiation hypothesis.

Objectives

The pupal stage is one of the key traits of insects with complete metamorphosis (Nicholson et al., 2014). However, how the evolution of the pupal stage is related to the success of the holometabolous insects and why the pupa evolved is unknown (Rolff et al., 2019). My doctoral thesis aims to test two barely studied adaptive hypotheses explaining the evolution of the pupa (see

above). One explanation is that in holometabolous insects, the radical reconstruction of the larval body within the pupal stage clears the gut and provides the opportunity to drive a change between the larval and adult microbiota, facilitating niche shifts. The second and not mutually exclusive hypothesis is that intercalating the pupal stage decouples growth and differentiation in insects with complete metamorphosis, allowing for efficient and competitive exploitation of ephemeral resources (Arendt, 1997; Rolff et al., 2019).

In **chapters II** and **III** of this thesis, I investigated the hypothesis that in holometabolous insects, the radical reconstruction of the larval body within the pupal stage clears the gut and provides the opportunity to drive a change between the larval and adult microbiota and if the remodelling is associated with the induction of an immune response. In **chapter II**, using 16S rRNA gene metabarcoding, I systematically studied whether gut microbiota changes throughout host development differ distinctively between insects with and without a pupal stage. I compared alpha and beta diversities of larval and adult gut microbiomes of 18 systematically sampled different insect species from five orders of holometabolous and three orders of hemimetabolous insects throughout development. To reduce geographic variance, I collected all insect species in Northern Germany with two exceptions from Croatia and Finland, respectively. I sampled only herbivorous insects from terrestrial habitats and excluded social insects to reduce variance further.

Additionally, I collected a sub-sample of those species from laboratory-reared colonies, consisting of five species from four different insect orders as presumably, the gut microbiota differs in specimens from the field and laboratory (Martinson, Carpinteyro-Ponce, Moran, & Markow, 2017; Staudacher et al., 2016). Based on the reconstruction of the larval gut in the pupa of holometabolous insects, I predict to find significant changes in the beta diversity between larvae and adults of

holometabolous insects, but not in hemimetabolous insects. I also expect the alpha diversity to be higher in adult hemimetabolous than holometabolous insects as they build up their microbiota throughout development.

In **chapter III**, I investigated if the microbiota is under the control of host gut immunity during gut replacement using RNA-seq. I compared the expression of immune effector genes in the gut during metamorphosis in two holometabolous (*Calliphora vicina* and *Tenebrio molitor*) and a hemimetabolous insect (*Pyrrhocoris apterus*). I sampled six time points covering the final-instar larvae and beginning of pupation of the holometabolous insects and five time points covering the final-instar nymphs and freshly emerged adults of the hemimetabolous insects. Based on the previous finding by Johnston et al. (2019), I predict to find up-regulated immune gene effectors in the two holometabolous but not in the hemimetabolous insect.

In **chapter IV**, I investigated the second barely studied hypothesis explaining the evolution of the pupa in holometabolous insects; the decoupling of growth and differentiation. This hypothesis implies that growth and differentiation are decoupled in insects with complete metamorphosis, with most growth confined to the larval and most development confined to the pupal life stage. Based on a literature review, I calculated and compared growth rates and ratios of holometabolous versus hemimetabolous insects. I systematically searched for insect growth data on ZOBODAT (www.zobodat.at), the zoological-botanical database of Austria that contains digitised literature that traditionally relates to insect studies from Austria and, to a lesser extent, to Germany, reducing geographic variance. To reduce variance further, I exclusively used total body lengths as an estimate to study immature growth. I calculated the growth rates and ratio with and without development times, as body size and development time are essential life-history traits because they

are often highly correlated with fitness. To reduce type I error rates, I used phylogenetic mixed-effects models comparing hemi- versus holometabolous insects. I predict fast larval growth rates and a shorter growth period in holometabolous than hemimetabolous insects.

Figure 3 gives an overview of the three studies conducted within this thesis that aim to test the two adaptive hypotheses explaining the evolution of the pupa.

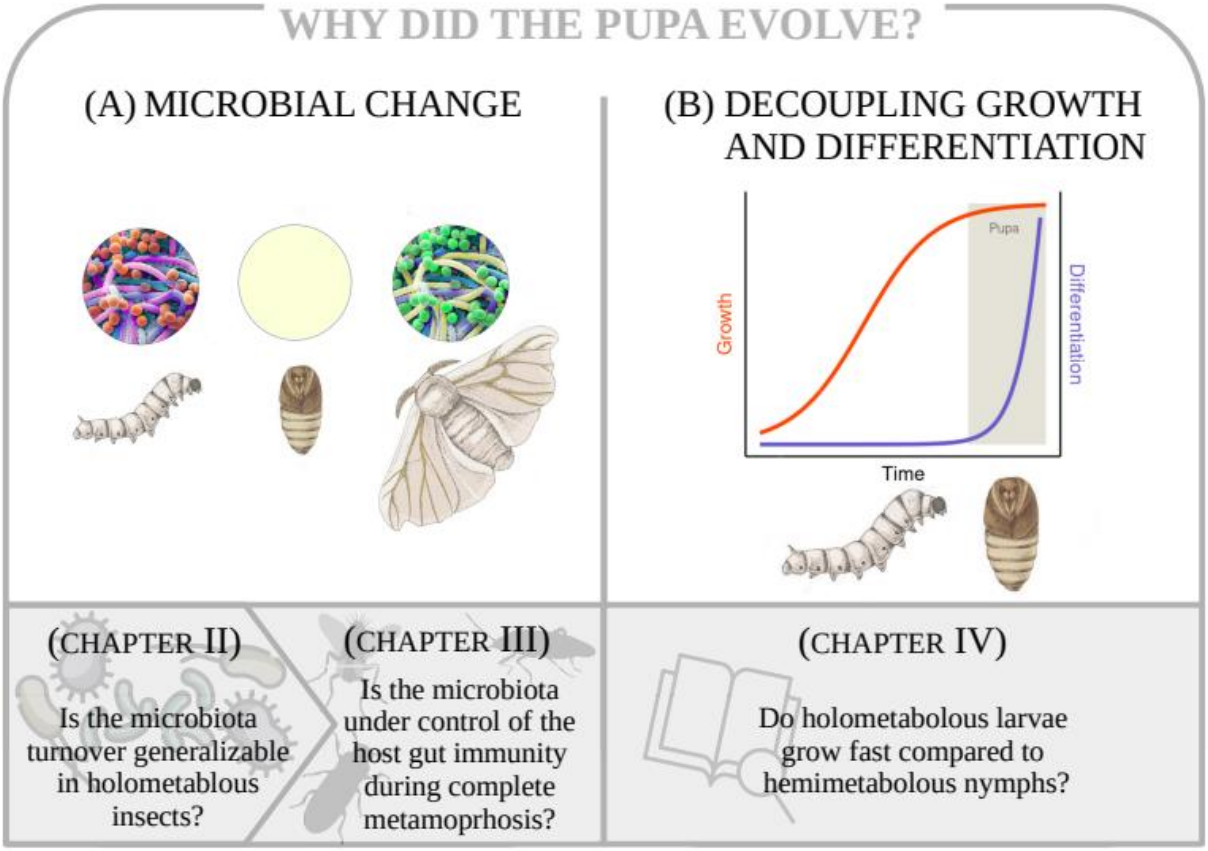

Figure 3: Overview of the three studies conducted within this thesis that aim to test two adaptive hypotheses explaining the evolution of the pupa: (A) Change between the larval and adult microbiota, facilitating niche shifts and (B) decoupling of growth and differentiation hypothesis. (CHAPTER II) Using 16s sequencing, I studied the gut microbiota throughout holometabolous compared to hemimetabolous development. (CHAPTER III) Using RNAseq, I investigated immune effectors' expression in the gut during metamorphosis (in the absence of infection) in two holometabolous and one hemimetabolous insect. (CHAPTER IV) I studied growth rates and ratios in insects in a literature-based study. (Butterfly drawings: Adobe Stock, #468809257.)

References

Arendt, J. D. (1997). Adaptive Intrinsic Growth Rates: An Integration Across Taxa. *The Quarterly Review of Biology*, *72*, 29.

Berenbaum, M. (2017). Insect Biodiversity – Millions and Millions. In *Insect Biodiversity* (pp. 783–792). John Wiley & Sons, Ltd. doi: 10.1002/9781118945568.ch25

Bishop, C. D., Erezyilmaz, D. F., Flatt, T., Georgiou, C. D., Hadfield, M. G., Heyland, A., … Youson, J. H. (2006). What is metamorphosis? *Integrative and Comparative Biology*, *46*(6), 655–661. doi: 10.1093/icb/icl004

Brownlie, J. C., & Johnson, K. N. (2009). Symbiont-mediated protection in insect hosts. *Trends in Microbiology*, *17*(8), 348–354. doi: 10.1016/j.tim.2009.05.005

Chapman, R. F. (2013). *The Insects—Structure and function* (5th ed.). Cambridge University Press.

Cole, B. J. (1980). Growth Ratios in Holometabolous and Hemimetabolous Insects. *Annals of the Entomological Society of America*, *73*(4), 489–491. doi: 10.1093/aesa/73.4.489

Comstock, J. H. (1918). Nymphs, Naiads, and Larvae. *Annals of the Entomological Society of America*, *11*(2), 222–224. doi: 10.1016/B978-012283245-1/50003-8

Condamine, F. L., Clapham, M. E., & Kergoat, G. J. (2016). Global patterns of insect diversification: Towards a reconciliation of fossil and molecular evidence? *Scientific Reports*, *6*(1), 19208. doi: 10.1038/srep19208

Cranston, P. S., & Gullan, P. J. (2009). Phylogeny of Insects. In *Encyclopedia of Insects* (Second, pp. 780–793). Elsevier. doi: 10.1016/B978-0-12-374144-8.00208-3

Day, T., & Rowe, L. (2002). *Developmental Thresholds and the Evolution of Reaction Norms for Age and Size at Life-History Transitions*. 13.

de Jonge, N., Michaelsen, T. Y., Ejbye-Ernst, R., Jensen, A., Nielsen, M. E., Bahrndorff, S., & Nielsen, J. L. (2020). Housefly (Musca domestica L.) associated microbiota across different life stages. *Scientific Reports*, *10*(1), 7842. doi: 10.1038/s41598-020-64704-y

Ebert, D. (2013). The Epidemiology and Evolution of Symbionts with Mixed-Mode Transmission. *Annual Review of Ecology, Evolution, and Systematics*, *44*(1), 623–643. doi: 10.1146/annurev-ecolsys-032513-100555

Ehrlich, P. R., & Raven, P. H. (1964). Butterflies and Plants: A Study in Coevolution. *Evolution*, *18*(4), 586–608.

Eleftherianos, I., Atri, J., Accetta, J., & Castillo, J. C. (2013). Endosymbiotic bacteria in insects: Guardians of the immune system? *Frontiers in Physiology*, *4*. doi: 10.3389/fphys.2013.00046

Engl, T., & Kaltenpoth, M. (2018). Influence of microbial symbionts on insect pheromones. *Natural Product Reports*, *35*(5), 386–397. doi: 10.1039/C7NP00068E

Esperk, T., Tammaru, T., & Nylin, S. R. (2007). Intraspecific Variability in Number of Larval Instars in Insects. *JOURNAL OF ECONOMIC ENTOMOLOGY*, *100*(3), 19.

Faircloth, B., Sorenson, L., Santini, F., & Alfaro, M. (2013). A Phylogenomic Perspective on the Radiation of Ray-Finned Fishes Based upon Targeted Sequencing of Ultraconserved Elements (UCEs). *PloS One*, *8*, e65923. doi: 10.1371/journal.pone.0065923

Felsenstein, J. (1985). Phylogenies and the Comparative Method. *The American Naturalist*, *125*(1), 115. doi: 10.1086/284325

Forbes, W. T. M. (1910). A Structural Study of Some Caterpillars.*. *Annals of the Entomological Society of America*, *3*(2), 94–132. doi: 10.1093/aesa/3.2.94

Gomes, A. S., Alves, R. N., Rønnestad, I., & Power, D. M. (2015). Orchestrating change: The thyroid hormones and GI-tract development in flatfish metamorphosis. *General and Comparative Endocrinology*, *220*, 2–12. doi: 10.1016/j.ygcen.2014.06.012

Gosner, K. L. (1960). A Simplified Table for Staging Anuran Embryos and Larvae with Notes on Identification. *Herpetologica*, *16*(3), 183–190.

Grimaldi, D., & Engel, M. S. (2005). *Evolution of the Insects*. Cambridge University Press.

Grunert, L. W., Clarke, J. W., Ahuja, C., Eswaran, H., & Nijhout, H. F. (2015). A Quantitative Analysis of Growth and Size Regulation in Manduca sexta: The Physiological Basis of Variation in Size and Age at Metamorphosis. *PLOS ONE*, *10*(5), e0127988. doi: 10.1371/journal.pone.0127988

Hammer, T. J., McMillan, W. O., & Fierer, N. (2014). Metamorphosis of a Butterfly-Associated Bacterial Community. *PLoS ONE*, *9*(1), e86995. doi: 10.1371/journal.pone.0086995

Hammer, T. J., & Moran, N. A. (2019). Links between metamorphosis and symbiosis in holometabolous insects. *Philosophical Transactions of the Royal Society B: Biological Sciences*, *374*(1783), 20190068. doi: 10.1098/rstb.2019.0068

Hourdry, J., L'Hermite, A., & Ferrand, R. (1996). Changes in the Digestive Tract and Feeding Behavior of Anuran Amphibians during Metamorphosis. *Physiological Zoology*, *69*(2), 219–251. doi: 10.1086/physzool.69.2.30164181

Johnston, P. R., Paris, V., & Rolff, J. (2019). Immune gene regulation in the gut during metamorphosis in a holo- versus a hemimetabolous insect. *Philosophical Transactions of the Royal Society B: Biological Sciences*, *374*(1783), 20190073. doi: 10.1098/rstb.2019.0073

Johnston, P. R., & Rolff, J. (2015). Host and Symbiont Jointly Control Gut Microbiota during Complete Metamorphosis. *PLOS Pathogens*, *11*(11), e1005246. doi: 10.1371/journal.ppat.1005246

Kaltenpoth, M., Yildirim, E., Gürbüz, M. F., Herzner, G., & Strohm, E. (2012). Refining the Roots of the Beewolf-Streptomyces Symbiosis: Antennal Symbionts in the Rare Genus Philanthinus (Hymenoptera, Crabronidae). *Applied and Environmental Microbiology*, *78*(3), 822–827. doi: 10.1128/AEM.06809-11

Kamsoi, O., Ventos-Alfonso, A., Almudi, I., Casares, F., & Belles, X. (2021, March 17). *The mayfly subimago explained. The regulation of metamorphosis in Ephemeroptera* (p. 2021.03.17.435759). p. 2021.03.17.435759. bioRxiv. doi: 10.1101/2021.03.17.435759

Kikuchi, Y., Hosokawa, T., & Fukatsu, T. (2011). An ancient but promiscuous host–symbiont association between Burkholderia gut symbionts and their heteropteran hosts. *The ISME Journal*, *5*(3), 446–460. doi: 10.1038/ismej.2010.150

Krenn, H. W. (2010). Feeding Mechanisms of Adult Lepidoptera: Structure, Function, and Evolution of the Mouthparts. *Annual Review of Entomology*, *55*(1), 307–327. doi: 10.1146/annurev-ento-112408-085338

Laudet, V. (2011). The Origins and Evolution of Vertebrate Metamorphosis | Elsevier Enhanced Reader. *Current Biology*, *21*(18), 727–737. doi: 10.1016/j.cub.2011.07.030

Lindstedt, C., Murphy, L., & Mappes, J. (2019). Antipredator strategies of pupae: How to avoid predation in an immobile life stage? *Philosophical Transactions of the Royal Society B: Biological Sciences*, *374*(1783). doi: 10.1098/rstb.2019.0069

Lofts, B. (1976). *Physiology of the Amphibia* (Vol. 3). Elsevier.

Lowe, T., Garwood, R. J., Simonsen, T. J., Bradley, R. S., & Withers, P. J. (2013). Metamorphosis revealed: Time-lapse three-dimensional imaging inside a living chrysalis. *Journal of The Royal Society Interface*, *10*(84), 20130304. doi: 10.1098/rsif.2013.0304

Lutz, D. A., & Huebner, E. (1980). *Development and cellular differentiation of an insect teleotrophic ovary (Rhodnius prolixus)*. *12*(4), 773–794. doi: 10.1016/0040-8166(80)90029-4

Maddrell, S. H. P. (2018). How the simple shape and soft body of the larvae might explain the success of endopterygote insects. *The Journal of Experimental Biology*, *221*(11), jeb177535. doi: 10.1242/jeb.177535

Mai, T., Chen, S., Lin, X., Zhang, X., Zou, X., Feng, Q., & Zheng, S. (2017). 20-hydroxyecdysone positively regulates the transcription of the antimicrobial peptide, lebocin, via BmEts and BmBR-C Z4 in the midgut of Bombyx mori during metamorphosis. *Developmental & Comparative Immunology*, *74*, 10–18. doi: 10.1016/j.dci.2017.04.002

Maire, J., Parisot, N., Ferrarini, M. G., Vallier, A., Gillet, B., Hughes, S., … Heddi, A. (2020). Spatial and morphological reorganization of endosymbiosis during metamorphosis accommodates adult metabolic requirements in a weevil. *Proceedings of the National Academy of Sciences*, *117*(32), 19347–19358. doi: 10.1073/pnas.2007151117

Martín-Vega, D., Simonsen, T. J., & Hall, M. J. R. (2017). Looking into the puparium: Micro-CT visualization of the internal morphological changes during metamorphosis of the blow fly, Calliphora vicina, with the first quantitative analysis of organ development in cyclorrhaphous dipterans. *Journal of Morphology*, *278*(5), 629–651. doi: 10.1002/jmor.20660

Mayhew, P. J. (2007). Why are there so many insect species? Perspectives from fossils and phylogenies. *Biological Reviews*, *82*(3), 425–454. doi: 10.1111/j.1469-185X.2007.00018.x

McMenamin, S., & Parichy, D. (2013). Metamorphosis in Teleosts. In *Current topics in developmental biology* (Vol. 103, pp. 127–165).

Menken, S. B. J., Boomsma, J. J., & Van Nieukerken, E. J. (2010). Large-scale evolutionary patterns of host plant associations in the Lepidoptera. *International Journal of Organic Evolution*, *64*(4), 1098–1119. doi: 10.1111/j.1558-5646.2009.00889.x

Merian, M. S., & Knibbeler, L. (2017). *Metamorphosis insectorum Surinamensium: 1705* (M. van Delft & H. Mulder, Eds.). Darmstadt: Lambert Schneider.

Misof, B., Liu, S., Meusemann, K., Peters, R. S., Donath, A., Mayer, C., … Zhou, X. (2014). Phylogenomics resolves the timing and pattern of insect evolution. *Science*, *346*(6210), 763–767. doi: 10.1126/science.1257570

Miyata, K., & Ose, K. (2012). Thyroid Hormone-disrupting Effects and the Amphibian Metamorphosis Assay. *Journal of Toxicologic Pathology*, *25*(1), 1–9. doi: 10.1293/tox.25.1

Mora, C., Tittensor, D. P., Adl, S., Simpson, A. G. B., & Worm, B. (2011). How Many Species Are There on Earth and in the Ocean? *PLoS Biology*, *9*(8), e1001127. doi: 10.1371/journal.pbio.1001127

Nicholson, D. B., Ross, A. J., & Mayhew, P. J. (2014). Fossil evidence for key innovations in the evolution of insect diversity. *Proceedings of the Royal Society B: Biological Sciences*, *281*(1793), 20141823–20141823. doi: 10.1098/rspb.2014.1823

Ogielska, M., & Kotusz, A. (2004). Pattern and rate of ovary differentiation with reference to somatic development in anuran amphibians. *Journal of Morphology*, *259*(1), 41–54. doi: 10.1002/jmor.10162

Ohmura, H., & Wakahara, M. (1998). Transformation of skin from larval to adult types in normally metamorphosing and metamorphosis-arrested salamander, Hynobius retardatus. *Differentiation*, *63*(5), 237–246. doi: 10.1046/j.1432-0436.1998.6350237.x

Parmentier, A., Meeus, I., Nieuwerburgh, F. V., Deforce, D., Vandamme, P., & Smagghe, G. (2018). A different gut microbial community between larvae and adults of a wild bumblebee nest (Bombus pascuorum). *Insect Science*, *25*(1), 66–74. doi: 10.1111/1744-7917.12381

Pretty, R., Naitoh, T., & Wassersug, R. J. (1995). Metamorphic shortening of the alimentary tract in anuran larvae (Rana catesbeiana). *The Anatomical Record*, *242*(3), 417–423. doi: 10.1002/ar.1092420314

Rainford, J. L., Hofreiter, M., Nicholson, D. B., & Mayhew, P. J. (2014). Phylogenetic Distribution of Extant Richness Suggests Metamorphosis Is a Key Innovation Driving Diversification in Insects. *PLoS ONE*, *9*(10), e109085. doi: 10.1371/journal.pone.0109085

Regueira, E., Dávila, C., & Hermida, G. N. (2016). Morphological Changes in Skin Glands During Development in Rhinella Arenarum (Anura: Bufonidae). *The Anatomical Record*, *299*(1), 141–156. doi: 10.1002/ar.23284

Rewitz, K. F., Yamanaka, N., & O'Connor, M. B. (2013). Developmental Checkpoints and Feedback Circuits Time Insect Maturation. In *Current topics in developmental biology* (Vol. 103, pp. 1–33). Retrieved from https://www.ncbi.nlm.nih.gov/pmc/articles/PMC4060521/

Rolff, J., Johnston, P. R., & Reynolds, S. (2019). Complete metamorphosis of insects. *Philosophical Transactions of the Royal Society B: Biological Sciences*, (374). doi: 10.1098/rstb.2019.0063

Russell, V. W., & Dunn, P. E. (1991). Lysozyme in the midgut of Manduca sexta during metamorphosis. *Archives of Insect Biochemistry and Physiology*, *17*(2–3), 67–80. doi: https://doi.org/10.1002/arch.940170202

Russell, V. W., & Dunn, P. E. (1996). Antibacterial Proteins in the Midgut of Manduca sexta During Metamorphosis. *Journal of Insect Physiology*, *42*(1), 65–71. doi: 10.1016/0022-1910(95)00083-6

Sallan, L. (2014). Major issues in the origin of ray-finned fish (Actinopterygii) biodiversity. *Biological Reviews of the Cambridge Philosophical Society*, *89*. doi: 10.1111/brv.12086

Schreiber, A. (2013). Flatfish: An Asymmetric Perspective on Metamorphosis. In *Current topics in developmental biology* (Vol. 103, pp. 167–194).

Schreiber, A. M. (2006). Asymmetric craniofacial remodeling and lateralized behavior in larval flatfish. *Journal of Experimental Biology*, *209*(4), 610–621. doi: 10.1242/jeb.02056

Siegel, S. (1957). Nonparametric Statistics. *The American Statistician*, *11*(3), 13–19. doi: 10.1080/00031305.1957.10501091

Stoll, S., Feldhaar, H., Fraunholz, M., & Gross, R. (2012). Bacteriocyte dynamics during development of a holometabolous insect, the carpenter ant Camponotus floridanus. *BMC Microbiology*.

Stork, N. E. (1993). How many species are there? *Biodiversity & Conservation*, *2*(3), 215–232. doi: 10.1007/BF00056669

Sudakaran, S., Salem, H., Kost, C., & Kaltenpoth, M. (2012). Geographical and ecological stability of the symbiotic mid-gut microbiota in European firebugs, *Pyrrhocoris apterus* (Hemiptera, Pyrrhocoridae). *Molecular Ecology*, *21*(24), 6134–6151. doi: 10.1111/mec.12027

Teixeira, A. das D., Fialho, M. do C. Q., Zanuncio, J. C., Ramalho, F. de S., & Serrão, J. E. (2013). Degeneration and cell regeneration in the midgut of Podisus nigrispinus (Heteroptera: Pentatomidae) during post-embryonic development. *Arthropod Structure & Development*, *42*(3), 237–246. doi: 10.1016/j.asd.2013.02.004

Tettamanti, G., & Casartelli, M. (2019). Cell death during complete metamorphosis. *Philosophical Transactions of the Royal Society B: Biological Sciences*, *374*(1783). doi: 10.1098/rstb.2019.0065

Trautwein, M. D., Wiegmann, B. M., Beutel, R., Kjer, K. M., & Yeates, D. K. (2012). Advances in Insect Phylogeny at the Dawn of the Postgenomic Era. *Annual Review of Entomology*, *57*(1), 449–468. doi: 10.1146/annurev-ento-120710-100538

Truman, J. W. (2019). The Evolution of Insect Metamorphosis. *Current Biology*, *29*(23), R1252–R1268. doi: 10.1016/j.cub.2019.10.009

Vitt, L. J., & Caldwell, J. P. (2014). Chapter 2—Anatomy of Amphibians and Reptiles. In *Herpetology (Fourth Edition)* (pp. 35–82). San Diego: Academic Press. doi: 10.1016/B978-0-12-386919-7.00002-2

Wake, D. B., & Koo, M. S. (2018). Amphibians. *Current Biology*, *28*(21), R1237–R1241. doi: 10.1016/j.cub.2018.09.028

Wang, M., Xiang, X., & Wan, X. (2020). Divergence in Gut Bacterial Community Among Life Stages of the Rainbow Stag Beetle Phalacrognathus muelleri (Coleptera: Lucanidae). *Insects*, *11*(10), 719. doi: 10.3390/insects11100719

Werner, E. E. (1988). Size, Scaling, and the Evolution of Complex Life Cycles. In B. Ebenman & L. Persson (Eds.), *Size-Structured Populations* (pp. 60–81). Berlin, Heidelberg: Springer. doi: 10.1007/978-3-642-74001-5_6

Werner, Earl E. (1986). Amphibian Metamorphosis: Growth Rate, Predation Risk, and the Optimal Size at Transformation. *The American Naturalist*, *128*(3), 319–341.

Whiting, M. F. (2004). Phylogeny of the holometabolous insects. In *Assembling the tree of life* (pp. 345–359).

Wiens, J. J. (2015). Explaining large-scale pattern of vertebrate diversity. *Biology Letters*, *11*. doi: http://dx.doi.org/10.1098/rsbl.2015.0506

Yaoita, Y. (2019). Tail Resorption During Metamorphosis in Xenopus Tadpoles. *Frontiers in Endocrinology*, *10*. Retrieved from https://www.frontiersin.org/article/10.3389/fendo.2019.00143

CHAPTER II: COMPLETE METAMORPHOSIS AND MICROBIOTA TURNOVER IN INSECTS

Christin Manthey[1], Paul Johnston[2,3,4], Shinichi Nakagawa[5], Jens Rolff[1,2,4]

1. Freie Universität Berlin, Institut für Biologie, Evolutionary Biology, Königin-Luise-Strasse 1-3, 14195 Berlin, Germany.
2. Berlin Center for Genomics in Biodiversity Research, Berlin, Germany.
3. Leibniz-Institute of Freshwater Ecology and Inland Fisheries (IGB), Berlin, Germany.
4. Berlin-Brandenburg Institute of Advanced Biodiversity Research (BBIB), Berlin, Germany.
5. Evolution & Ecology Research Centre and School of Biological, Earth and Environmental Sciences, University of New South Wales, Sydney, NSW, Australia

Abstract

The insects constitute the majority of animal diversity. Most insects are holometabolous: during complete metamorphosis their bodies are radically re-organized. This re-organization poses a significant challenge to the gut microbiota, as the gut is replaced during pupation, a process that does not occur in hemimetabolous insects. In holometabolous hosts, it offers the opportunity to decouple the gut microbiota between the larval and adult life stages resulting in high beta diversity whilst limiting alpha diversity. Here we studied 18 different herbivorous insect species from 5 orders of holometabolous and 3 orders of hemimetabolous insects. Comparing larval and adult specimens, we find a much higher beta-diversity and hence microbiota turnover in holometabolous insects compared to hemimetabolous insects. Alpha diversity did not differ between holo- and hemimetabolous insects nor between developmental stages within these groups. Our results support the idea that pupation offers the opportunity to change the gut microbiota and hence facilitates

ecological niche shifts. This possible effect of niche shift facilitation could explain a selective advantage of the evolution of complete metamorphosis, which is a defining trait of the most speciose insect taxon, the holometabola

Introduction

Insects are the most diverse animal taxon on earth (Berenbaum, 2017; Mora, Tittensor, Adl, Simpson, & Worm, 2011) and collectively comprise 50 to 70% of all living animal species (Grimaldi & Engel, 2005; Mora et al., 2011). More than 80% of all described insect species are holometabolous - they undergo complete metamorphosis (Grimaldi & Engel, 2005) that includes a pupal stage intercalated between the larva and the adult. In the pupa, the insect body is radically remodeled. All larval organs, including the gut, are broken down and reconstructed, resulting in distinct and specialized larval and adult life stages (Hall & Martín-Vega, 2019; Hinton, 1948; Rolff, Johnston, & Reynolds, 2019; Truman, 2019). Complete metamorphosis is considered a key trait explaining insect diversity (Mayhew, 2007; Rainford, Hofreiter, Nicholson, & Mayhew, 2014, but see Condamine, Clapham, & Kergoat, 2016) and only evolved once, hence the holometabola are a monophyletic group (Misof et al., 2014). The diversification of the speciose orders of the holometabolous insects coincides with the diversification of the land plants (Condamine et al., 2016; Misof et al., 2014).

How this radical re-organization of the insect body is related to the astounding radiation of the holometabolous insects is not known (Rolff et al., 2019), but it is one of the key traits of holometabolous insects (Nicholson, Ross, & Mayhew, 2014) One possible explanation could be that intercalating the pupal stage decouples growth and differentiation (Arendt, 1997; Rolff et al.,

2019), allowing for efficient and competitive exploitation of ephemeral resources. Another, not mutually exclusive explanation is, that larvae and adults can occupy distinct niches (Hammer & Moran, 2019). If the niche shift also includes a diet shift, a change in gut microbiota could possibly facilitate such niche shifts (Hammer & Moran, 2019).

One of the major internal reconstructions during the pupal stage includes the replacement of the gut epithelium. From the perspective of the microbes in the gut, the epithelial replacement constitutes a dramatic habitat change. The gut microbiota, that can provide nutrition, defense and other services to the insect host, changes in density and community structure, including the elimination of particular microbes during pupation (Hammer & Moran, 2019; Johnston & Rolff, 2015). These changes may result from a combination of factors including the drastic anatomical and physiological transformations in the replacement gut, host immune effector induction in the metamorphic gut, bacterial competition for continued occupancy of the pupal gut, and ontogenetic habitat and diet shifts of the host. In the lepidopteran *Galleria mellonella*, the absolute abundance of the microbiota can be reduced by several orders of magnitude during metamorphosis, including the elimination of pathogenic bacteria that would otherwise persist in the adult host (Johnston & Rolff, 2015). In *G. mellonella*, the host immune system and the symbionts interact with the microbial community in the gut through complete metamorphosis. Observations in other taxa of the Lepidoptera (Rolff et al., 2019 and refs therein) as well as in some Coleoptera (Critchlow, Norris, & Tate, 2019) are consistent with partial host control of the microbiota. The replacement of the gut epithelium potentially offers the insect a unique opportunity to significantly alter the gut microbiota, allowing an insect to acquire life stage-specific microbes (Hammer & Moran, 2019;

Johnston & Rolff, 2015). Such gut microbiota changes during the pupal stage increase the opportunity of niche shifts (Engel & Moran, 2013).

Some studies have investigated changes in the gut microbiota at different stages of host development. For example, the hemimetabolous insect *Pyrrhocoris apterus* (Sudakaran, Salem, Kost, & Kaltenpoth, 2012) hosts a very stable mid-gut community composition with six predominant taxa being consistently abundant throughout development. By contrast in a holometabolous insect, the hymenopteran *Bombus pascuorum*, Parmentier et al. (2018) reported different gut microbial communities within larval and adult specimens of a wild nest. The typical core gut bacteria in the adults were absent in the larvae. Hammer, McMillan, & Fierer (2014) also found distinct gut microbiota communities in the leaf-chewing larvae and nectar- and pollen-feeding adults in the lepidopteran *Heliconius erato*. Studies of the dipteran *Musca domestica* (de Jonge et al., 2020) and the coleopteran *Phalacrognathus muelleri* (Wang, Xiang, & Wan, 2020) have found a similar pattern.

The high microbiota turnover observed in some holometabolous species poses the risk of losing beneficial microbes which would result in a cost to both, host and symbiont. Hammer & Moran (2019) suggest that holometabolous insects may be less likely to evolve strictly vertically transmitted symbioses than hemimetabolous insects. To overcome this hurdle a number of strategies have evolved to ensure transmission of obligate symbiont between life stages in holometabolous insects. Stoll, Feldhaar, Fraunholz, & Gross (2012) showed vertical transmission of microbes via bacteriocytes in ant species. The relative number of bacteria-filled bacteriocytes increased strongly during complete metamorphosis. Maire et al. (2020) also showed a transmission of microbes via bacteriocytes in weevils by maintaining and relocating bacteriocytes during gut

renewal in the pupa. Other specialized structures to transmit symbionts in insects are antennal glands (Kaltenpoth, Yildirim, Gürbüz, Herzner, & Strohm, 2012) or crypts (Kikuchi, Hosokawa, & Fukatsu, 2011).

An alternative, and not mutually exclusive view, is that the differences in the gut microbiota between larval and adult holometabolous insects is influenced by the diet and the environment. Though not studied specifically in the context of metamorphosis, the influence of diet on gut microbiota composition has been demonstrated in arthropods. Chandler, Morgan Lang, Bhatnagar, Eisen, & Kopp (2011) found that diet in a range of *Drosophila* species, comprising cactus, flower, fruit and mushroom feeding species, shapes the adult gut microbiota within a taxonomically restricted selection of microbes. In the spider *Badumna longinqua*, the gut microbiota composition is strongly influenced by the microbiota of the prey species.

Here, we investigated whether gut microbiota changes during the adult moult, which includes pupation in the holometabolous insects, differ between hemi- and holometabolous insects. Because of the re-organization of the gut in the pupal stage we expect (a) a significant change in bacterial composition resulting in much greater beta-diversity in holometabolous than in hemimetabolous insects. The diversity of gut microbes can be strongly reduced during pupation (Hammer et al., 2014; Johnston & Rolff, 2015). (b) We therefore speculated that greater alpha diversity would be observed in the gut microbiota of hemimetabolous insects, given the lack of gut epithelial replacement and associate host immunity. Also, as the diversity of the gut microbiota scales positively with size across species (Sherrill-Mix et al., 2018), it is possible that alpha diversity is higher in adult than larval insects, especially in hemimetabolous species.

To address these questions, we sampled 18 different species from seven major insect orders across the life stages. To reduce geographic variance, we collected all insect species in Central and Northern Europe. To further reduce variance, we sampled only herbivorous insects from terrestrial habitats and excluded social insects. Additionally, we collected a sub-sample of those species from laboratory-reared colonies, consisting of five species from four different insect orders (figure 1) as the gut microbiota may differ between specimens from the field and laboratory (Martinson, Carpinteyro-Ponce, Moran, & Markow, 2017; Staudacher et al., 2016).

Materials and Methods

Insect Sampling and Preparation

Larval and adult specimens of 18 insect species from seven different insect orders, including Orthoptera, Thysanoptera, Hemiptera, Hymenoptera, Coleoptera, Lepidoptera and Diptera, were sampled in Central and Northern Europe between April and October 2018 (see figure 1 and supplementary table 1). Pupae were additionally sampled for the three hymenopteran species. In total, sixteen species across development were collected in Northern Germany, *Tenebrio molitor* in Croatia and *Neodiprion sertifer* in Finland. Additionally, a sub-sample of those species was sampled, consisting of five species from four different insect orders, which originated from laboratory-reared colonies (supplementary table 2). Figure 1 gives an overview of all insect species collected in the field and the subset of those species from laboratory-reared colonies. A total of 643 individual insects were sampled. All species were identified using common identification keys and were confirmed by specialists.

After collection, the insects were stored individually in 50 ml centrifuge tubes (Falcon tubes) with holes for ventilation. In two very small species, *Frankliniella occidentalis* and *Aleyrodes proletella*, individuals were pooled (tables 1 and 2). These pools were kept and used as a biological replicate later. After a 24-hour starvation period, the insects were sacrificed, and preserved by freezing (-80°C), except two field-collected species which were preserved in ethanol (95%): *Frankliniella occidentalis* and *Neodiprion sertifer*. Hammer, Dickerson, & Fierer (2015) compared two different storage methods, freezing and ethanol, amongst others, and found that the storage method did not affect microbiota composition assessments. In accordance with the study by Hammer et al. (2015) and other studies on arthropod microbiota (De Cock et al., 2019; Kennedy, Tsau, Gillespie, & Krehenwinkel, 2020) we assume that our data are a robust representation of the gut microbiota.

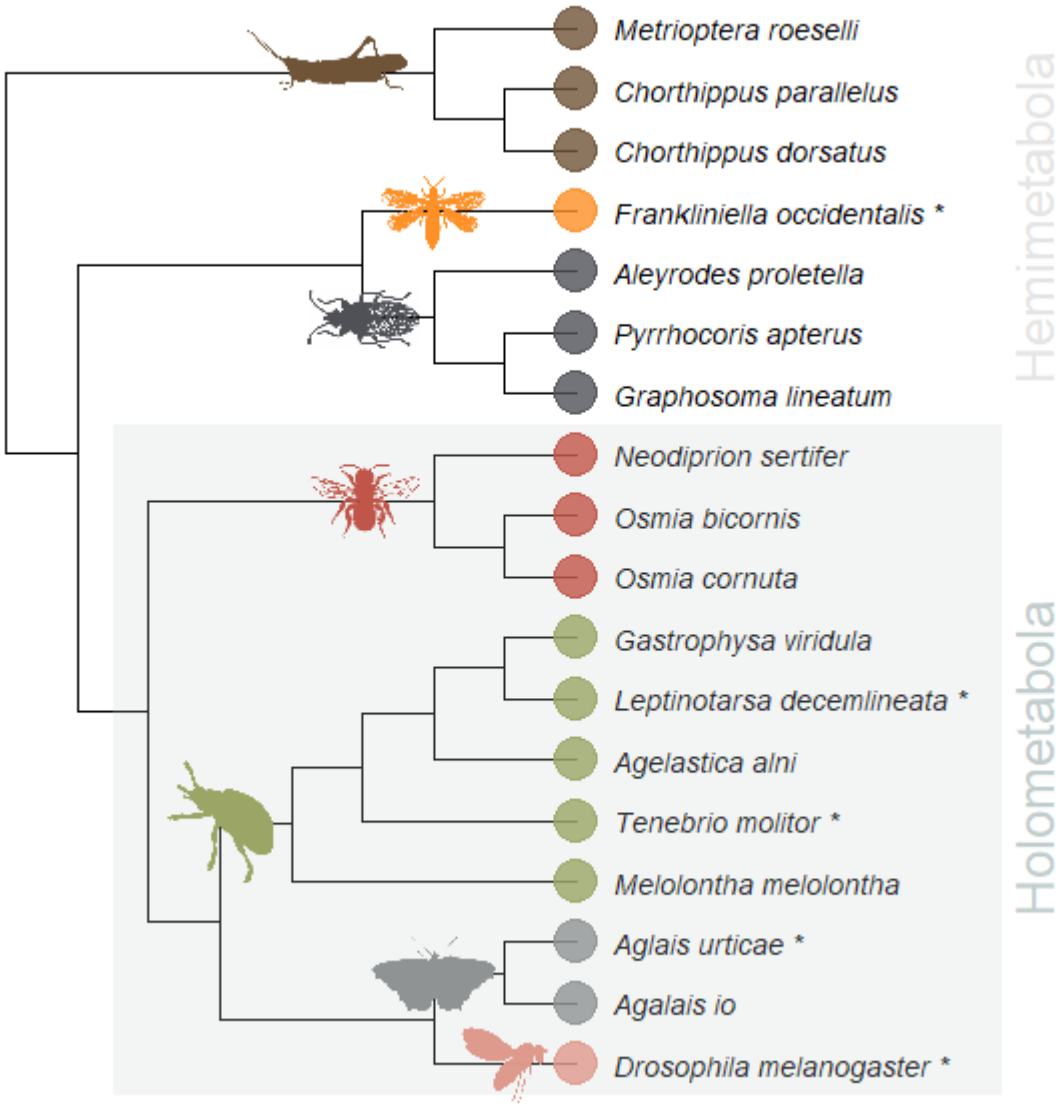

Figure 1: Phylogenetic tree of the 18 field-collected species. The five species marked with a star were additionally sampled from laboratory-reared colonies. The 11 highlighted species represent the monophyletic group of the holometabolous insects. The other seven species are hemimetabolous.

DNA Extraction

Samples of the sacrificed insects were processed on ice under sterile conditions. A biological replicate was an individual insect sample, except for samples of three small species: a replicate of *Frankliniella occidentalis* was pooled from 30 individuals, a replicate of *Aleyrodes proletella* from 40 and a replicate of *Drosophila melanogaster* from 10 individuals. The exact number of biological replicates per species and life stage are shown in tables 1 and 2 (supplement). After removing the legs and wings off (adults only) using sterilised forceps and dissecting scissors, the samples were placed in 2-ml microcentrifuge tubes (Eppendorf Safe-Lock Tubes). Then samples were bead-ground using TCBeads and C1 solution from the PowerSoil DNA Isolation Kit (Qiagen) three times for 30 sec at 30 Hz in a tissue homogenizer. The insects were not dissected before homogenization in order to process all samples under standardized methods as the Thrips and Whiteflies were too small to dissect guts. Insects were not sterilised prior to homogenisation. Hammer et al. (2015) found no effect on the bacterial communities of not surface sterilised insect species (butterfly, grasshopper, bee and beetle) compared to control specimens that were surface sterilized: samples clustered by species independent of surface sterilisation and relative abundances of bacterial genera were similar between sterilised and non-sterilised specimens. Also, surface contaminants derived from handling the specimens were extremely rare in non-sterilised and surface sterilised specimens. As it remains possible that surface sterilisation could affect internal bacterial communities, Hammer et al. (2015) recommend omitting surface sterilisation from insect microbiota studies.

Total DNA was extracted from 60 µl of tissue homogenate using the PowerSoil DNA extraction kit (Qiagen) under sterile conditions. Tissue homogenates were pretreated with 10 µl Proteinase K

and 500 µl Power soil bead solution at 56 °C overnight. Subsequent DNA isolation was continued as indicated in the manufacturer‘s instruction.

Negative extraction controls were included to detect and filter contamination. The negative controls consisted of mock samples, which contained no insect tissue.

Primers and PCR amplification of the 16S rRNA gene fragment

PCR amplification of the 16S rRNA gene fragments was performed with MyTaqTM HS DNA Polymerase and the forward and reverse 515f-806r primer sequence pairs, targeting the V3 – V4 region of the 16S rRNA gene (Thompson et al., 2017). The PCR reaction was conducted using 1 µl sample in a total volume of 25 µl. The PCR amplification program was as follows: 94 °C for 1 min, 95 °C for 15 sec, 50 °C for 15 sec, two cycles of 72 °C for 45 sec and 2 min, followed by a final extension step to 4 °C. A volume of 5 µl of the PCR product was run on a 1.5% agarose gel stained with Sybr Gold at 160 V for 40 min.

PCR products were purified with CleanNGS CNGS-0050 (GC biotech B.V., Leidse Schouw 2, 2408 AE Alpen aan den Rijn, Netherlands) and dual indices and Illumina sequencing adapters were attached by limited-cycle PCR amplification (initial denaturation at 95°C for 2 min followed by eight cycles of denaturation at 95°C for 20 s, annealing at 52°C for 30 s, extension at 72°C for 30 s, and a final extension cycle at 72°C for 3 min). The enzymes used were Herculase II Fusion DNA Polymerase (Agilent Technologies Sales & Services GmbH & Co. Hewlett-Packard-Str. 831, 76337 Waldbronn, Germany). PCR products were quantified with Quant-iT™ PicoGreen™ dsDNA Assay Kit (Life Technologies GmbH Thermo Fisher Scientific,Frankfurter Straße 129b,

64319 Darmstadt, Germany), measured with Optima Fluostar (BMG LABTECH GmbH, Allmendgrün 8,77799 Ortenberg, Germany).

Sequencing of bacterial community

Amplicon libraries were sequenced for 600 cycles using an Illumina MiSeq (Illumina, San Diego, California, USA) at the Berlin Center for Genomics in Biodiversity Research (BeGenDiv). The resulting 300-bp paired end reads were analysed using a full-stack R (R Core Team, 2020) pipeline incorporating dada2 (Callahan et al., 2016, p. 2) and phyloseq (Mcmurdie & Holmes, 2013). Forward reads were trimmed to 240 bp and reverse reads to 160 bp. The reads were truncated at the first instance of a quality score less than two and filtered to a maximum amount of estimated errors of two per truncated read. The remaining forward and reverse reads were dereplicated, and error rate estimates were computed. The developed error model was used to infer exact amplicon sequence variants (ASVs) from the amplicon sequencing data. The resulting denoised read pairs were merged. A sequencing table was constructed with the denoised and merged reads and chimeras were removed. Taxonomy was assigned to the sequence table using the Ribosomal Database Project (Cole et al., 2014) training set, version 16. Contaminant taxa were identified using prevalence-based filtering from the decontam package (Davis, Proctor, Holmes, Relman, & Callahan, 2018). Remaining unknown sequences were identified using the Basic Local Alignment Search Tool (BLAST) (Altschul, Gish, Miller, Myers, & Lipman, 1990) and taxonomy was assigned using TaxonKit (Shen & Xiong, 2019). Further remaining unknown sequences were renamed with higher taxonomic ranks and eukaryota were removed. See R script for more details on the dada2 pipeline.

Statistical Analysis

All statistical analyses were performed in R (version 3.6.3; R Core Team, 2020). Shannon indices were calculated per developmental stage and species using the microbiome package (Lathi et al., 2019). To adjust for differences in library sizes, Willis (2019) suggests accounting for unobserved taxa instead of rarefying the data. The breakaway estimator (Willis & Bunge, 2016) was used but did not differ from an estimator that does not account for unobserved taxa. Therefore, the simpler approach using proportions was used. The number of reads can be found in the supplementary material (figure S19, table 23). After generating a distance matrix for each species, mean differences in alpha-diversity between life stages using the Shannon index were computed using the *meandist* function from the R package vegan (Oksanen et al., 2008). The generated distance matrix tests each larval specimen against each adult specimen in Shannon diversity by calculating absolute difference values. Shannon means for larvae and adults within each species were computed using the *summarySE* function from the Rmisc package (Hope, 2013). Bray-Curtis dissimilarity matrices were computed for each species with the *distance* function from the phyloseq package (Mcmurdie & Holmes, 2013) and used to calculate mean beta-diversities comparing life stages using the *meandist* function from the R package vegan (Oksanen et al., 2008). The data were normalised to proportions to control for read depth prior to ordination. Differences in beta-diversity, Shannon life-stage difference, and the larval and adult Shannon estimates were tested between holo- and hemimetabolous insects. Regression analyses controlled for phylogeny were performed to reduce type I error rates. Grafen's branch lengths were generated before modelling the phylogenetic correlation matrix for the models (Grafen, 1989). The models were phylogenetic linear mixed-effects models using the *rma.mv* function from the R package metafor (Cinar,

Nakagawa, & Viechtbauer, 2021) that incorporates sampling variance (the square of SE). First, an intercept model with two random effects (species ID and phylogeny) was fitted. The total amount of heterogeneity (I^2) and the heterogeneity explained by differences between species and phylogeny was calculated. I^2 describes the percentage of total variation across samples that is due to heterogeneity rather than sampling variance (Higgins, 2003; Senior et al., 2016). Then a model with the two random effects (species ID and phylogeny) and the type of metamorphosis as a fixed effect that looked at the contrast between hemi- and holometabolous insects was fitted, and the amount of variation in the response attributed to the type of metamorphosis was calculated as marginal R^2 (Nakagawa & Schielzeth, 2013). A third model that specified the variance structure of the two insect groups by modelling heteroscedasticity was fitted and used to visualise the results using the orchaRd package (Nakagawa et al., 2020). The orchard plots display 95% confidence intervals and 95% prediction intervals of the group means for hemi- and holometabolous insects. The prediction interval displays the 95% probability that the response estimate of an insect species in a new study lies within this interval. Further absolute abundances were plotted for all species and life stages using the R package microbiome (Lathi et al., 2019) (see supplement, figures S1 – S18). The sequences were agglomerated at the genus level for the relative abundance plots. Rare bacterial taxa present less than 1% of all taxa per species are not shown in the figures. The larval and adult Shannon means per species were compared, according to test assumptions, with a Two-sample t-test, Wilcoxon rank-sum test and Welch-test, respectively. See tables 18 and 19 (supplement) and figures S1 – S18 for more details. To meet the assumption of normally distributed data for the Two-sample t-test, the response variable was transformed before testing for group differences using logarithm transformation for *Chorthippus parallelus* and *Chorthippus dorsatus*

and via reciprocal 1/x6 transformation for the dataset of *Graphosoma lineatum*. The effect sizes were calculated using the effsize package (Torchiano, 2020). The beta dissimilarity data per species and for all data pooled was analysed by perMANOVA with life stage as a predictor variable, and a dispersion test was fitted using the vegan package (Oksanen et al., 2008) (see supplementary tables 13 and 14). Principle coordinate analysis (PCoA) on Bray-Curtis dissimilarity was used to display the beta diversities per species with life stage as a grouping factor using the phyloseq package (Mcmurdie & Holmes, 2013) (see figures S1 – S18) and for all data pooled with species and life stage as a grouping factor (see figures S20 and S21, and table 15).

Results

We obtained 18 insect species covering seven major orders, including three hemimetabolous (Orthoptera, Thysanoptera, Hemiptera) and four holometabolous insect orders (Hymenoptera, Coleoptera, Lepidoptera and Diptera). We sampled larval and adult life stages for all of them. We collected a sub-sample of those 18 species from laboratory-reared colonies that covered five insect species from four different orders, including one hemimetabolous (Thysanoptera) and four holometabolous insect orders (Coleoptera, Lepidoptera and Diptera) (figure 1). Using 16S rRNA gene metabarcoding (see supplement for more details), we determined the gut microbial compositions per life stage and species and plotted the data. All relative abundance plots can be found in the supplementary material. The data from *Pyrrhocoris apterus* and *Melolontha melolontha*, which originated from two different locations, were pooled as population did not affect alpha diversity (see supplement, table 16) nor beta diversity (table 13).

Microbiota turnover at the larval-adult transition

Microbial beta diversity of holometabolous insects was significantly greater than that of hemimetabolous insects when comparing larval and adult life stages of each species (Beta = 0.3123; 95% CI = 0.0432, 0.5814; figure 2; see supplement for more details). The heterogeneity was high (I^2 = 87.41%), with 52.42% of the variance explained by phylogeny and 34.99% explained by differences between species. The amount of variation in beta-diversity attributed to the type of metamorphosis was 46.29% (R^2). With the exception of *Leptinotarsa decemlineata*, all field-collected holometabolous insect species showed significant differences in beta diversity between larval and adult life stages (supplementary table 13). Within the hemimetabolous species collected in the field, two species differed significantly in beta diversity: *Chorthippus dorsatus* and *Pyrrhocoris apterus*. The other five Hemimetabola did not differ in beta-diversity between life stages. This pattern was consistent in the subset of five laboratory-reared species. To display the differences in beta diversity between life stages for each species, we used Principal Coordinate Analysis (PCoA) ordination (see supplement, figures S1 – S18, PCoA plots per species).

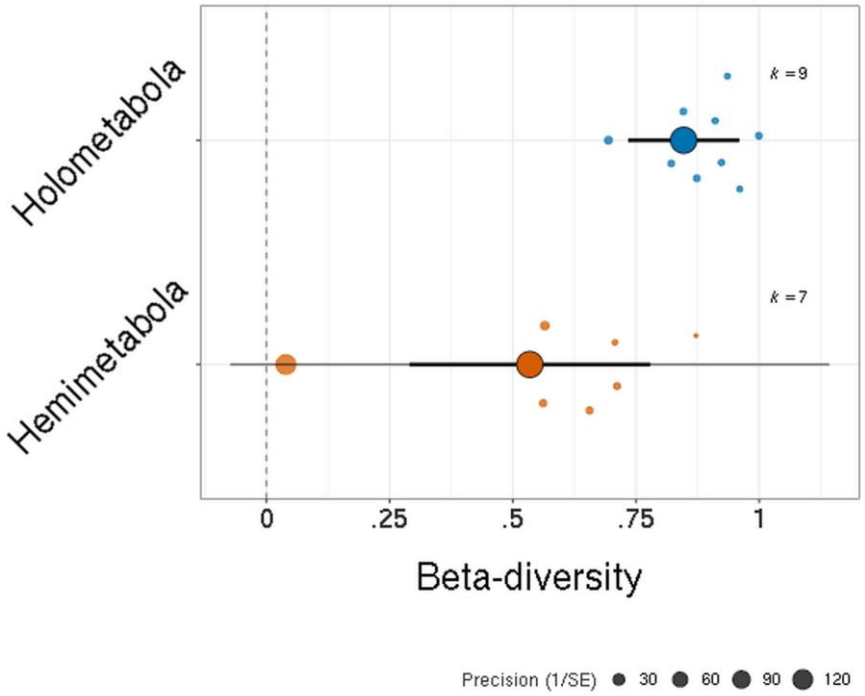

Figure 2: The average beta diversity (Bray-Curtis dissimilarity) in larval and adult bacterial communities among hemi- versus holometabolous insects (Beta = 0.3123; 95% CI = 0.0432, 0.5814) with 95% confidence (bold error bars) and prediction intervals (thin error bars). Each point represents the beta diversity between life stages of a particular insect.

Alpha-diversity

We calculated Shannon diversity indices per life stage and species and calculated the difference in alpha diversities between life stages per species. Alpha diversity differences between larval and adult life stages did not differ between holo- and hemimetabolous insects (Shannon-difference = 0.2786; 95% CI = -0.4827, 1.04; figure 3; see supplement for more details). The heterogeneity was high (I^2 = 94.68%), with 89.32% of the variance explained by phylogeny and 5.36% explained by differences between species. The amount of variation in Shannon-difference attributed to the type of metamorphosis was 12.61% (R^2). The microbial alpha diversity was also not different between

holo- versus hemimetabolous larvae (Shannon_Larvae = 0.1586; 95% CI = -0.4614, 0.7787; figure 4; see supplement for more details) and adults (Shannon_Adults = 0.1803; 95% CI = -0.6152, 0.9758; figure 4; see supplement for more details), respectively. The heterogeneity was high in larval (I^2 = 98.8%) and adult (I^2 = 97.28%) Shannon indices. 46.48% of the variance is explained by phylogeny in the model testing larval Shannon and 36.26% in the model testing adult Shannon group differences. Five species did differ significantly in alpha diversity between life stages within the holometabolous insects. Within the hemimetabolous insects, one species differed significantly in alpha diversity between life stages. See supplementary table 18 and 19 for more details.

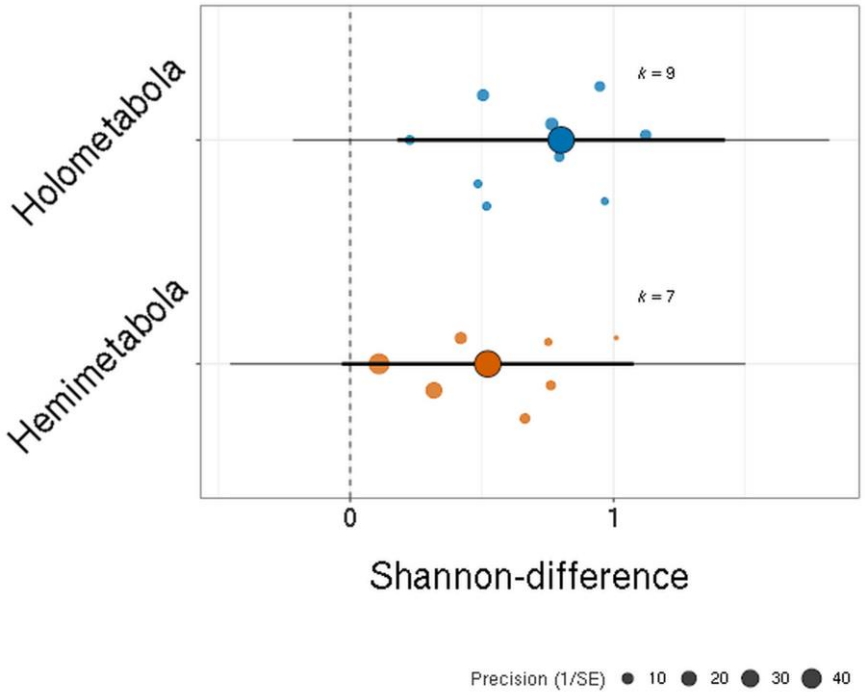

Figure 3: Average Shannon-difference of larval and adult bacterial communities with 95% confidence (bold error bars) and prediction intervals (thin error bars) among hemi- and holometabolous insects (Shannon-difference = 0.2786; 95% CI = -0.4827, 1.04). Each point represents Shannon-difference between life stages of a particular insect.

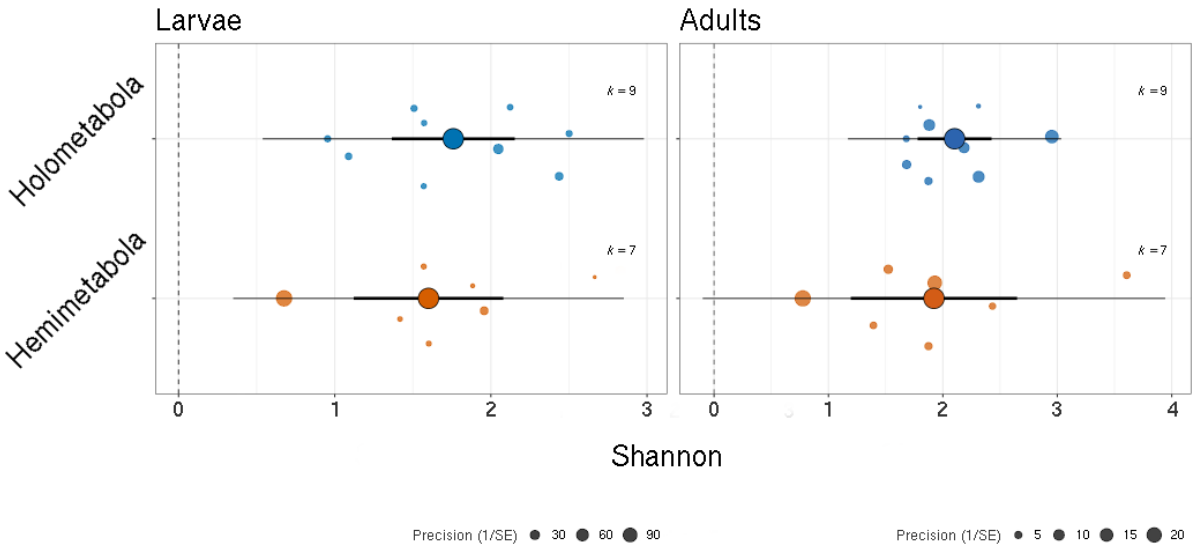

Figure 4: Average larval alpha diversity between hemi- and holometabolous insects (Shannon_Larvae = 0.1586; 95% CI = -0.4614, 0.7787, left graph), and of adults (Shannon_Adults = 0.1803; 95% CI = -0.6152, 0.9758, right graph). Each point represents the alpha diversity, measured as Shannon difference, of larvae (left graph) or adults (right graph).

Discussion

We investigated beta and alpha diversity throughout development, comparing 18 insect species from four holo- and three hemimetabolous insect orders. We find a clear pattern: holometabolous insects show a strong microbial turnover between larvae and adults, while this is not found in hemimetabolous insects.

Almost all examined holometabolous insect species showed significantly different gut microbial communities between larval and adult specimens as reflected by the differences in beta diversity. The overall pattern we report is well supported: hemimetabolous insects do not show changes in beta diversity during development. The remaining variation in beta diversity within the holometabolous insects may be partly explained by different ecologies which warrants further

investigation. *Neodiprion sertifer*, the European pine sawfly, displayed the lowest beta diversity in our sample of holometabolous insects but still a higher beta diversity than many hemimetabolous insects. Larval and adult generations overlap in *N. sertifer*, and larvae feed pine needles, while adults usually do not feed. The three most abundant bacterial taxa (see supplementary table S22) are *Enterobacteriacae*, *Pseudomonas* and *Yersinia*. Despite the fact that *N. sertifer* as a forest pest is relatively well studied, the role of the microbiota has rarely been studied. A previous paper on a closely related species also found a high abundance of *Yersinia* (Whittome, Graham, & Levin, 2007).

The flour beetle *Tenebrio molitor* also showed a very low beta diversity between larvae and adults. Larval and adult *T. molitor* have overlapping populations, and unusually for holometabolous insects they share the same habitat throughout development, and they are cannibalistic (Staudacher et al., 2016) and could obtain microbes via feeding on conspecifics. Both laboratory- and field-collected individuals were dominated by either *Lactobacillales* or *Enterobacterales* with a small population of *Actinobacteria*. The highest microbiota turnover in the holometabolous insects was found in the cockchafer (*Melolontha melolontha*). This is the only species in our selection that has a soil-dwelling larval stage, which almost certainly exposes the larvae to a high diversity of soil bacterial during its very long development time that lasts several years. The adults feed on plant leaves. Many of the anaerobic taxa observed in *M. melolontha* are also described from the forest cockchafer *Melolontha hippocastani*, where they inhabit an expanded midgut organ that resembles the termite paunch, which is specialized for anaerobic fermentation (Arias-Cordero et al., 2012). A similar reduction of bacterial diversity also occurs in adult *M. hippocastani*, which may relate to the drastic reduction in size and content of the anaerobic compartment in the adult (Arias-Cordero

et al., 2012). Interestingly, the highest beta diversity in hemimetabolous species was recorded in thrips. They have evolved a neometabolous life-style with two partly quiescent stages between the larva and the adult (Truman, 2019). The stages are also called pupae but their development does not entail the dramatic change in morphology as in holometabolous insects (Truman, 2019). The lowest beta diversity was found in the striped shield bug *Graphasoma lineatum*. *G. lineatum* harbour beneficial symbionts in midgut crypts, including *Pantoea* (Karamipour, Fathipour, & Mehrabadi, 2016), a genus of gram-negative bacteria and the most abundant bacterial taxon in both larval and adult specimens. *Pantoea* is consistently present throughout insect development and accounts for the vast majority of reads in all *G. lineatum* samples.

Microbiota turnover seems to be a general pattern within holometabolous, but not hemimetabolous insects, independent of the insects' field and laboratory origin and we did not find any consistent patterns of the most abundant bacterial taxa between larvae and adults or holo- and hemimetabolous insects (supplementary table S22). The microbial composition changes are presumably driven by the intercalated pupal stage in holometabolous insects, which allows a radical remodeling of the hosts' gut, but often is also accompanied by different diet choices of larvae and adults. Prior to pupation a cessation of feeding and purging of the gut contents takes place (Johnston & Rolff, 2015). After that, immune effectors such as lysozyme and AMPs are secreted into the gut (Johnston & Rolff, 2015) followed by anatomical and physiological changes resulting in the replacement of the gut. Competition of the remaining bacteria with possible new colonizers of the adult gut then shapes the adult microbiota. The role of the host immune system is illustrated by a study in *Galleria mellonella*, a species where the stage of gut replacement can be precisely determined in vivo (Johnston, Paris, & Rolff, 2019). This study revealed that pupal gut delamination coincides

with peak immune gene expression in the gut. This is consistent with other observations in other holometabolous insects with lower temporal resolution (Johnston et al., 2019; Russell & Dunn, 1991; Xu et al., 2012). In contrast, no such effect was observed for the hemimetabolous *Gryllus bimaculatus* (Johnston et al., 2019). The up-regulation of immune genes during gut renewal is therefore a candidate mechanism contributing to the patterns reported in our study. In principal, the insect host can establish a completely new and distinct adult gut microbiome by this reduction of the gut microbiota and a subsequent change in diet of the emerging adult. A different diet will expose the insects to new microbes that can colonize the gut and potentially also facilitate better digestion of the new diet.

Alpha diversity did not display a pattern related to holo- vs. hemimetabolous development. Complete metamorphosis results in a reduction of the microbial absolute abundance by orders of magnitude (Johnston & Rolff, 2015, and refs therein) which can be recovered in the adults. In the light of Hammer et al. (2014) this could be explained by a recovery of the microbiota upon adult feeding. They reported that the richness of the microbiota was recovered in the feeding adults of *Helioconus*, though the composition had changed, strongly suggesting that the new members of the microbiota have been acquired from the diet. Therefore, the gut microbiota is shaped by a niche modification, in which early arriving species change the types of niches available within the local sites (Fukami, 2015).

It has been suggested that microbiota turnover would allow insects to occupy different niches throughout development (Hammer & Moran, 2019), which most likely contributed to the success of holometabolous insects. Our data are consistent with this hypothesis, the clearance of the gut provides the opportunity for a microbiota turnover, an effect not observed in hemimetabolous

insects. It seems possible that this observation is directly related to the decoupling hypothesis, which proposes that growth is confined to the larval stage, while most differentiation occurs in the pupa (Arendt, 1997; Rolff et al., 2019). A facilitation of niche shifts by changes in the gut microbiota, if confirmed by experimental studies, could be considered as an important driver of the evolution of complete metamorphosis. Alternatively, the advent of complete metamorphosis, driven by other selective factors such as growth rate (Rolff et al., 2019), facilitated the gut microbiota turnover.

Acknowledgements

We are grateful to Olivia Judson and Dino McMahon for comments on the manuscript and Elisa Bittermann, Sarah Sparmann and Susan Mbedi for support in the lab. This research was funded by the DFG (Deutsche Forschungsgemeinschaft).

References

Altschul, S. F., Gish, W., Miller, W., Myers, E. W., & Lipman, D. J. (1990). Basic Local Alignment Search Tool. J. Mol. Biol., 403–410.

Arendt, J. D. (1997). Adaptive Intrinsic Growth Rates: An Integration Across Taxa. The Quarterly Review of Biology, 72, 29.

Arias-Cordero, E., Ping, L., Reichwald, K., Delb, H., Platzer, M., & Boland, W. (2012). Comparative Evaluation of the Gut Microbiota Associated with the Below- and Above-Ground Life Stages (Larvae and Beetles) of the Forest Cockchafer, Melolontha hippocastani. PLoS ONE, 7(12), e51557. doi: 10.1371/journal.pone.0051557

Berenbaum, M. (2017). Insect Biodiversity – Millions and Millions. In Insect Biodiversity (pp. 783–792). John Wiley & Sons, Ltd. doi: 10.1002/9781118945568.ch25

Callahan, B. J., McMurdie, P. J., Rosen, M. J., Han, A. W., Johnson, A. J. A., & Holmes, S. P. (2016). DADA2: High-resolution sample inference from Illumina amplicon data. Nature Methods, 13(7), 581–583. doi: 10.1038/nmeth.3869

Chandler, J. A., Morgan Lang, J., Bhatnagar, S., Eisen, J. A., & Kopp, A. (2011). Bacterial Communities of Diverse Drosophila Species: Ecological Context of a Host–Microbe Model System. PLoS Genetics, 7(9), e1002272. doi: 10.1371/journal.pgen.1002272

Cinar, O., Nakagawa, S., & Viechtbauer, W. (2021). Phylogenetic multilevel meta-analysis: A simulation study on the importance of modelling the phylogeny. Methods in Ecology and Evolution, 12(1), 4–12. doi: 10.1111/2041-210X.13760

Cole, J. R., Wang, Q., Fish, J. A., Chai, B., McGarrell, D. M., Sun, Y., … Tiedje, J. M. (2014). Ribosomal Database Project: Data and tools for high throughput rRNA analysis. Nucleic Acids Research, 42(D1), D633–D642. doi: 10.1093/nar/gkt1244

Condamine, F. L., Clapham, M. E., & Kergoat, G. J. (2016). Global patterns of insect diversification: Towards a reconciliation of fossil and molecular evidence? Scientific Reports, 6(1), 19208. doi: 10.1038/srep19208

Critchlow, J. T., Norris, A., & Tate, A. T. (2019). The legacy of larval infection on immunological dynamics over metamorphosis. Philosophical Transactions of the Royal Society B: Biological Sciences, 374(1783), 20190066. doi: 10.1098/rstb.2019.0066

Davis, N. M., Proctor, D. M., Holmes, S. P., Relman, D. A., & Callahan, B. J. (2018). Simple statistical identification and removal of contaminant sequences in marker-gene and metagenomics data. Microbiome, 6(1), 226. doi: 10.1186/s40168-018-0605-2

De Cock, M., Virgilio, M., Vandamme, P., Augustinos, A., Bourtzis, K., Willems, A., & De Meyer, M. (2019). Impact of Sample Preservation and Manipulation on Insect Gut Microbiome

Profiling. A Test Case With Fruit Flies (Diptera, Tephritidae). Frontiers in Microbiology, 10, 2833. doi: 10.3389/fmicb.2019.02833

de Jonge, N., Michaelsen, T. Y., Ejbye-Ernst, R., Jensen, A., Nielsen, M. E., Bahrndorff, S., & Nielsen, J. L. (2020). Housefly (Musca domestica L.) associated microbiota across different life stages. Scientific Reports, 10(1), 7842. doi: 10.1038/s41598-020-64704-y

Engel, P., & Moran, N. A. (2013). The gut microbiota of insects – diversity in structure and function. FEMS Microbiology Reviews, 37(5), 699–735. doi: 10.1111/1574-6976.12025

Fukami, T. (2015). Historical Contingency in Community Assembly: Integrating Niches, Species Pools, and Priority Effects. Annual Review of Ecology, Evolution, and Systematics, 46(1), 1–23. doi: 10.1146/annurev-ecolsys-110411-160340

Grafen, A. (1989). The Phylogenetic Regression. Philosophical Transactions of the Royal Society of London. B, Biological Sciences, 326(1233), 119–157.

Grimaldi, D., & Engel, M. S. (2005). Evolution of the Insects. Cambridge University Press.

Hall, M. J. R., & Martín-Vega, D. (2019). Visualization of insect metamorphosis. Philosophical Transactions of the Royal Society B: Biological Sciences, 374(1783), 20190071. doi: 10.1098/rstb.2019.0071

Hammer, T. J., Dickerson, J. C., & Fierer, N. (2015). Evidence-based recommendations on storing and handling specimens for analyses of insect microbiota. PeerJ, 3, e1190. doi: 10.7717/peerj.1190

Hammer, T. J., McMillan, W. O., & Fierer, N. (2014). Metamorphosis of a Butterfly-Associated Bacterial Community. PLoS ONE, 9(1), e86995. doi: 10.1371/journal.pone.0086995

Hammer, T. J., & Moran, N. A. (2019). Links between metamorphosis and symbiosis in holometabolous insects. Philosophical Transactions of the Royal Society B: Biological Sciences, 374(1783), 20190068. doi: 10.1098/rstb.2019.0068

Higgins, J. P. T. (2003). Measuring inconsistency in meta-analyses. BMJ, 327(7414), 557–560. doi: 10.1136/bmj.327.7414.557

Hinton, H. E. (1948). On the Origin and Function of the Pupal Stage. Transactions of the Royal Entomological Society of London, 99(12), 395–409. doi: https://doi.org/10.1111/j.1365-2311.1948.tb01227.x

Hope, R. M. (2013). Rmisc: Ryan Miscellaneous (Version 1.5).

Johnston, P. R., Paris, V., & Rolff, J. (2019). Immune gene regulation in the gut during metamorphosis in a holo- versus a hemimetabolous insect. Philosophical Transactions of the Royal Society B: Biological Sciences, 374(1783), 20190073. doi: 10.1098/rstb.2019.0073

Johnston, P. R., & Rolff, J. (2015). Host and Symbiont Jointly Control Gut Microbiota during Complete Metamorphosis. PLOS Pathogens, 11(11), e1005246. doi: 10.1371/journal.ppat.1005246

Kaltenpoth, M., Yildirim, E., Gürbüz, M. F., Herzner, G., & Strohm, E. (2012). Refining the Roots of the Beewolf-Streptomyces Symbiosis: Antennal Symbionts in the Rare Genus Philanthinus (Hymenoptera, Crabronidae). Applied and Environmental Microbiology, 78(3), 822–827. doi: 10.1128/AEM.06809-11

Karamipour, N., Fathipour, Y., & Mehrabadi, M. (2016). Gammaproteobacteria as essential primary symbionts in the striped shield bug, Graphosoma Lineatum (Hemiptera: Pentatomidae). Scientific Reports, 6(1), 33168. doi: 10.1038/srep33168

Kennedy, S. R., Tsau, S., Gillespie, R., & Krehenwinkel, H. (2020). Are you what you eat? A highly transient and prey-influenced gut microbiome in the grey house spider Badumna longinqua. Molecular Ecology, 29(5), 1001–1015. doi: 10.1111/mec.15370

Kikuchi, Y., Hosokawa, T., & Fukatsu, T. (2011). An ancient but promiscuous host–symbiont association between Burkholderia gut symbionts and their heteropteran hosts. The ISME Journal, 5(3), 446–460. doi: 10.1038/ismej.2010.150

Lathi, L., Ernst, F. G. M., Braccia, D. C., Huang, R., Borman, T., Corrada Bravo, H., … Shetty, S. (2019). Microbiome R package (Version 2.1.26) [R]. Retrieved from http://microbiome.github.io

Maire, J., Parisot, N., Ferrarini, M. G., Vallier, A., Gillet, B., Hughes, S., … Heddi, A. (2020). Spatial and morphological reorganization of endosymbiosis during metamorphosis accommodates adult metabolic requirements in a weevil. Proceedings of the National Academy of Sciences, 117(32), 19347–19358. doi: 10.1073/pnas.2007151117

Martinson, V. G., Carpinteyro-Ponce, J., Moran, N. A., & Markow, T. A. (2017). A Distinctive and Host-Restricted Gut Microbiota in Populations of a Cactophilic Drosophila Species. Applied and Environmental Microbiology, 83(23). doi: 10.1128/AEM.01551-17

Mayhew, P. J. (2007). Why are there so many insect species? Perspectives from fossils and phylogenies. Biological Reviews, 82(3), 425–454. doi: 10.1111/j.1469-185X.2007.00018.x

Mcmurdie, P., & Holmes, S. (2013). Phyloseq: An R Package for Reproducible Interactive Analysis and Graphics of Microbiome Census Data (Version 1.30.0).

Misof, B., Liu, S., Meusemann, K., Peters, R. S., Donath, A., Mayer, C., … Zhou, X. (2014). Phylogenomics resolves the timing and pattern of insect evolution. Science, 346(6210), 763–767. doi: 10.1126/science.1257570

Mora, C., Tittensor, D. P., Adl, S., Simpson, A. G. B., & Worm, B. (2011). How Many Species Are There on Earth and in the Ocean? PLoS Biology, 9(8), e1001127. doi: 10.1371/journal.pbio.1001127

Nakagawa, S., Lagisz, M., O'Dea, R. E., Rutkowska, J., Yang, Y., Noble, D. W. A., & Senior, A. M. (2020). The orchard plot: Cultivating a forest plot for use in ecology, evolution, and beyond. Research Synthesis Methods, 12(1), 4–12. doi: 10.1002/jrsm.1424

Nakagawa, S., & Schielzeth, H. (2013). A general and simple method for obtaining R2 from generalized linear mixed-effects models. Methods in Ecology and Evolution, 4(2), 133–142. doi: 10.1111/j.2041-210x.2012.00261.x

Nicholson, D. B., Ross, A. J., & Mayhew, P. J. (2014). Fossil evidence for key innovations in the evolution of insect diversity. Proceedings of the Royal Society B: Biological Sciences, 281(1793), 20141823–20141823. doi: 10.1098/rspb.2014.1823

Oksanen, J., Guillaume Blanchet, F., Friendly, M., Kindt, R., Legendre, P., McGlinn, D., & Wagner, H. (2008). Vegan: Community ecology package (Version 2.5-7). Retrieved from http://cran.r-project.org/, http://vegan.r-forge.r-project.org/

Parmentier, A., Meeus, I., Nieuwerburgh, F. V., Deforce, D., Vandamme, P., & Smagghe, G. (2018). A different gut microbial community between larvae and adults of a wild bumblebee nest (Bombus pascuorum). Insect Science, 25(1), 66–74. doi: 10.1111/1744-7917.12381

R Core Team. (2020). R: A language and environment for statistical computing. Vienna, Austria: R Foundation for Statistical Computing. Retrieved from https://www.R-project.org/

Rainford, J. L., Hofreiter, M., Nicholson, D. B., & Mayhew, P. J. (2014). Phylogenetic Distribution of Extant Richness Suggests Metamorphosis Is a Key Innovation Driving Diversification in Insects. PLoS ONE, 9(10), e109085. doi: 10.1371/journal.pone.0109085

Rolff, J., Johnston, P. R., & Reynolds, S. (2019). Complete metamorphosis of insects. Philosophical Transactions of the Royal Society B: Biological Sciences, (374). doi: 10.1098/rstb.2019.0063

Russell, V. W., & Dunn, P. E. (1991). Lysozyme in the midgut of Manduca sexta during metamorphosis. Archives of Insect Biochemistry and Physiology, 17(2–3), 67–80. doi: https://doi.org/10.1002/arch.940170202

Senior, A. M., Grueber, C. E., Kamiya, T., Lagisz, M., O'Dwyer, K., Santos, E. S. A., & Nakagawa, S. (2016). Heterogeneity in ecological and evolutionary meta-analyses: Its magnitude and implications. Ecology, 97(12), 3293–3299. doi: 10.1002/ecy.1591

Shen, W., & Xiong, J. (2019). TaxonKit: A cross-platform and efficient NCBI taxonomy toolkit. BioRxiv. doi: 10.1101/513523

Sherrill-Mix, S., McCormick, K., Lauder, A., Bailey, A., Zimmerman, L., Li, Y., … Bushman, F. D. (2018). Allometry and Ecology of the Bilaterian Gut Microbiome. MBio, 9(2). doi: 10.1128/mBio.00319-18

Staudacher, H., Kaltenpoth, M., Breeuwer, J. A. J., Menken, S. B. J., Heckel, D. G., & Groot, A. T. (2016). Variability of Bacterial Communities in the Moth Heliothis virescens Indicates Transient Association with the Host. PLOS ONE, 11(5), e0154514. doi: 10.1371/journal.pone.0154514

Stoll, S., Feldhaar, H., Fraunholz, M., & Gross, R. (2012). Bacteriocyte dynamics during development of a holometabolous insect, the carpenter ant Camponotus floridanus. BMC Microbiology.

Sudakaran, S., Salem, H., Kost, C., & Kaltenpoth, M. (2012). Geographical and ecological stability of the symbiotic mid-gut microbiota in European firebugs, Pyrrhocoris apterus (Hemiptera, Pyrrhocoridae). Molecular Ecology, 21(24), 6134–6151. doi: 10.1111/mec.12027

Thompson, L. R., Sanders, J. G., McDonald, D., Amir, A., Ladau, J., Locey, K. J., … Knight, R. (2017). A communal catalogue reveals Earth's multiscale microbial diversity. Nature, 551(7681), 457–463. doi: 10.1038/nature24621

Torchiano, M. (2020). effsize: Efficient Effect Size Computation (Version 0.8.1). Retrieved from https://CRAN.R-project.org/package=effsize

Truman, J. W. (2019). The Evolution of Insect Metamorphosis. Current Biology, 29(23), R1252–R1268. doi: 10.1016/j.cub.2019.10.009

Wang, M., Xiang, X., & Wan, X. (2020). Divergence in Gut Bacterial Community Among Life Stages of the Rainbow Stag Beetle Phalacrognathus muelleri (Coleptera: Lucanidae). Insects, 11(10), 719. doi: 10.3390/insects11100719

Whittome, B., Graham, R. I., & Levin, D. B. (2007). Preliminary Examination of Gut Bacteria from Neodiprion Abietis (hymenoptera: Diprionidae) Larvae. J. ent. Soc. Ont., 138, 49-63.

Willis, A. D. (2019). Rarefaction, Alpha Diversity, and Statistics. Frontiers in Microbiology, 10. doi: 10.3389/fmicb.2019.02407

Willis, A. D., & Bunge, J. (2016). Species Richness Estimation and Modeling (Version 3.0) [R].

Xu, Q., Lu, A., Xiao, G., Yang, B., Zhang, J., Li, X., … Ling, E. (2012). Transcriptional Profiling of Midgut Immunity Response and Degeneration in the Wandering Silkworm, Bombyx mori. PLoS ONE, 7(8), e43769. doi: 10.1371/journal.pone.0043769

CHAPTER III: IMMUNE GENE REGULATION IN THE GUT DURING METAMORPHOSIS IN TWO HOLO- VERSUS A HEMIMETABOLOUS INSECT

Christin Manthey 1, Paul R. Johnston [12,3], Jens Rolff [1,4]

1. Freie Universität Berlin, Institut für Biologie, Evolutionary Biology, Königin-Luise-Strasse 1-3, 14195 Berlin, Germany.
2. Berlin Center for Genomics in Biodiversity Research, Berlin, Germany.
3. Leibniz-Institute of Freshwater Ecology and Inland Fisheries (IGB), Berlin, Germany.
4. Berlin-Brandenburg Institute of Advanced Biodiversity Research (BBIB), Berlin, Germany.

Abstract

During complete metamorphosis, holometabolous insects remodel their entire anatomy, including the gut and must control their microbiota to avoid infectious disease. High activity of antimicrobial peptides and proteins in the gut during metamorphosis has been best described in several Lepidoptera. The immune system of the dipteran *Drosophila melanogaster* also controls the number of bacteria during metamorphosis. However, little is known about the regulation of immune genes during the nymphal–adult moult in Hemimetabola which undergo less drastic metamorphic changes. Different patterns of immune effector expression during metamorphosis were shown in a study comparing the lepidopteran *Galleria mellonela* and the orthopteran *Gryllus bimaculatus*. *G. mellonella* showed a strong up-regulation of antimicrobial proteins and peptides in the gut at the larval-pupal moult. No such up-regulation was detected at the nymphal-adult moult in *G. bimaculatus.* Whether these findings reflect general patterns within holometabolous versus

hemimetabolous insects remains unclear. Using RNAseq, we compare the expression of immune effector genes in the gut during metamorphosis in two holometabolous (*Calliphora vicina* and *Tenebrio molitor*) and a hemimetabolous insect (*Pyrrhocoris apterus*). We found high read count abundances of differentially expressed immune effectors in the gut at the larval-pupal moult in *C. vicina* and *T. molitor*; no such high abundances were observed at the nymphal-adult moult in *P. apterus*. Our findings confirm that only complete metamorphosis elicits a prophylactic immune response as an adaptive response in holometabolous insects, which controls the microbiota during gut replacement.

Introduction

Complete metamorphosis is considered a key trait that explains the incredible diversity of insects (Nicholson, Ross, & Mayhew, 2014). The drastic reconstructions in the pupal stage in insects with complete metamorphosis (Holometabola) (Hall & Martín-Vega, 2019) allow for decoupling of growth and differentiation (Arendt, 1997). It also gives the insect the unique opportunity to change the microbial composition throughout insect development (Manthey, Johnston, & Rolff, 2021), facilitating niche shifts between the larval and adult life stages (Hammer & Moran, 2019; Rolff, Johnston, & Reynolds, 2019).

However, the drastic reconstruction during complete metamorphosis puts the insect at a higher risk of infections. The physical barriers in the gut that avoid bacterial infections, like the peritrophic membrane in the midgut and the sclerotised cuticle of the fore- and hindgut, are broken down during complete metamorphosis. Hence, the insect must control its gut microbiota to avoid infectious disease, creating a dilemma; either the insect host eradicates and reestablishes its gut

microbes from the environment, or the insect maintains beneficial symbionts while fighting pathogens. Johnston & Rolff (2015) showed that complete eradication of the gut microbiota comes with the risk of losing beneficial symbionts. It is known that insects have a mixed-mode transmission of microbes (Ebert, 2013). Some beneficial symbionts are transmitted vertically and stored in specialised tissues during complete metamorphosis, while others are horizontally transmitted and taken up from the environment later. Insects evolved various strategies to ensure the transmission of beneficial symbionts throughout development. Stoll, Feldhaar, Fraunholz, & Gross (2012) showed vertical transmission of microbes via bacteriocytes in ant species. The relative number of bacteria-filled bacteriocytes increased strongly during complete metamorphosis. Maire et al. (2020) also showed a transmission of microbes via bacteriocytes in weevils by maintaining and relocating bacteriocytes during gut renewal in the pupa. Other specialised structures to transmit symbionts in insects are antennal glands (Kaltenpoth, Yildirim, Gürbüz, Herzner, & Strohm, 2012) and crypts (Kikuchi, Hosokawa, & Fukatsu, 2011).

Also, insects initiate immune responses to control their gut microbiota and avoid infectious diseases. When in contact with a pathogen, insects defend themselves using cellular and humoral immunity (Du Pasquier, 2001; Hultmark, 1993). Immediate reactions include the induction of proteolytic cascades, such as activating phenoloxidase that affects melanin formation (Zhao, Li, Wang, & Jiang, 2007). Among the induced effector molecules are antimicrobial proteins and peptides (AMPs). However, holometabolous insects must control their gut microbiota to avoid infectious disease during complete metamorphosis.

It is likely that holometabolous insects evolved strategies to pre-emptively activate immune processes in the pupal gut to prevent infections during complete metamorphosis. Russell & Dunn

(1991) described high activity of the antimicrobial protein lysozyme in the midgut lumen of the moth *Manduca sexta* (Lepidoptera) during complete metamorphosis. Lysozyme accumulated in the larval midgut epithelium and was subsequently released into to the gut lumen at the larval-pupal moult. Also, Russell & Dunn (1996) found that the pupal midgut of *M. sexta* contains a cocktail of antimicrobial proteins, including at least lysozyme, bactericidal activity against *Escherichia coli*, hemolin, and phenoloxidase. Induction of antimicrobial peptides in the gut prior to complete metamorphosis has also been described in other Lepidoptera, the silkworm *Bombyx mori* and the tobacco cutworm *Spodoptera litura* (Mai et al., 2017). Mai et al. (2017) found up-regulated lebocin, an AMP specific to Lepidoptera, in the midgut with a peak expression during the wandering stage. They also found that the ecdysteroid hormone 20-hydroxyecdysone (20E), which is known to control metamorphosis, regulates lebocin expression in the midgut. Nunes, Koyama, & Sucena (2021) confirm the link between the endocrine and immune systems to control the number of bacteria in the pupa of the fruit fly *Drosophila melanogaster* (Diptera). They found three AMPs (*drosomycin*, *drosomycin-like 2* and *drosomycin-like 5*) differentially expressed at pupation irrespective of the presence of bacteria and regulated by 20E. This shows that co-option of immune effector gene expression by the 20E moulting pathway is not restricted to the Lepidoptera and may be a general phenomenon in the Holometabola.

In contrast, in insects with incomplete metamorphosis (Hemimetabola), the metamorphic changes are less drastic, and the gut microbiota stays relatively stable compared to holometabolous insects (Manthey et al., 2021). However, little is known about the regulation of immune genes during the nymphal–adult moult. Johnston, Paris, & Rolff (2019) were the first to show that hemimetabolous and holometabolous insects have different patterns of immune effector expression. They found a

strong up-regulation of antimicrobial proteins and peptides and the transcription factor GmEts at the onset of pupation in the greater wax moth *Galleria mellonella* (Lepidoptera), but no such up-regulation at the nymphal–adult moult in the cricket *Gryllus bimaculatus* (Orthoptera). *G. mellonella* showed peak expression of lysozymes and three AMPs coinciding with delamination of the larval gut. However, whether these findings reflect general patterns within holometabolous and hemimetabolous insects remains unclear.

Here we use RNA-seq to compare the temporal dynamics of immune effectors expression in the gut at the larval-pupal moult in two holometabolous, the blow fly *Calliphora vicina* (Diptera) and the mealworm beetle *Tenebrio molitor* (Coleoptera) and at the nymphal–adult moult in a hemimetabolous insect, the firebug *Pyrrhocoris apterus* (Hemiptera). According to Johnston et al. (2019), we hypothesized an induction of immune effector expression at the onset of complete metamorphosis in the two holometabolous insects. By contrast, given that the gut does not undergo drastic reconstruction during incomplete metamorphosis and in the absence of infection, we expect no immune effector induction in the hemimetabolous insect.

Material and Methods

Tenebrio molitor rearing and sampling

Tenebrio molitor (mealworm beetle) larvae were purchased from a commercial supplier (Der Terraristikladen, Düsseldorf, Germany) and used to establish a laboratory colony at the Freie Universität Berlin. The mealworm beetles were held in faunaboxes (Reptilienkosmos, Viersen, Germany) with a 14 L: 10 D cycle and 60 ± 5% humidity at 25 ± 1°C. They were fed wheat bran

supplemented with carrot and water ad libitum. The mealworm beetles were sampled in the final instar larva and pupa. The six sampling stages were specified as follows:

(I) Final moult stage, a freshly moulted, large last instar larva with a still translucent white cuticle maximum of one hour after the final moult.

(II) Little movement stage, a larva 1-2 d before puparation resting on the substrate, but responding to pinch grips.

(III) No movement stage, a larva 12 h before puparation resting on the substrate and not responding to pinch grips.

(IV) Pupa after 1 - 6 h, a white soft pupa 1-6 h after pupation.

(V) Pupa after 12-20 h, a light brown beige pupa 12-20 h after pupation.

(VI) Pupa after 24-48 h, a light brown beige pupa with clearly black eyes 24-48 h after pupation.

RNA was isolated from dissected guts as described below and used to create three independent replicate pools per stage, each representing five individual insects, resulting in 18 sample pools.

Calliphora vicina rearing and sampling

A laboratory colony of *Calliphora vicina* (urban bluebottle blowfly) was established with insects purchased from a commercial supplier (Reptilienkosmos, Viersen, Germany) and reared at the Freie Universität Berlin. The blowflies were held in insect gauze cages (BugDorm, Taichung, Taiwan) in an incubator with a 14 L: 10 D cycle and 60 ± 5% humidity at 25 ± 1°C. They were fed a diet of milk powder, sugar (ratio 3:1) and water ad libitum. Additionally, calf's liver was offered for oviposition. Blowflies were checked daily to determine their development. The larvae developed over three larval stages, with the third larval instar being divided into the feeding and

post-feeding stages. The first and second larval stages lasted one day, and the final instar larva lasted five to seven days. The blowflies were sampled at the onset of complete metamorphosis in the post-feeding and pupal stages. The sampling stages in the post-feeding and pupa were specified as follows:

(I) Post-feeding larval stage, a still actively crawling but non-feeding third instar larva.

(II) Pre-pupal stage, a white, contracted larva responding to pinch grips; just before the transition to white puparium; shiny white and soft cuticle.

(III) Pupal stage at the onset, a white and motionless puparium ready for pupariation; cuticle was dull white and dried (unlike stage II).

(IV) Pupa after 1 h, a medium brown tubule emerged one hour after stage III; the cuticle was slightly more hardened than in stage III.

(V) Pupa after 4-6 h, a reddish-brown cryptocephalous pupa, 4-6 h after stage III; the puparium was fully hardened; beginning of larval-pupal apolysis.

(VI) Pupa after 8-12 h, a blackish-brown pupa 8-12 h after stage III; larval pupal apolysis.

RNA was isolated from dissected guts and used to create three independent replicate pools per stage, each representing five individual insects, resulting in 18 sample pools.

Pyrrhocoris apterus rearing and sampling

A laboratory culture of *Pyrrhocoris apterus* (firebug) was established with insects collected from *Tilia cordata* (small-leaved linden) trees at three locations in Berlin (see table 1) in April 2021. Only firebugs not parasitized by mites were collected. The firebugs were reared in faunaboxes

(Reptilienkosmos, Viersen, Germany) at the Freie Universität Berlin with a 14 L: 10 D cycle at room temperature (21 ± 1°C). They were fed *T. cordata* seeds and water ad libitum via cotton plugged tube. After oviposition, the eggs were held in plastic boxes covered with a gauze until hatching. Firebugs were reared individually from the fourth instar in small plastic boxes covered with gauze and checked daily to determine their development. The nymphs developed over five instars within a maximum of 40 days. The fifth instar lasted ten days. Five stages in the last instar larva and the adult were sampled from the F1-generation and specified as follows:

(I) Final instar nymph, a freshly moulted, fifth instar nymph that is still decoloured and entirely reddish-orange.

(II) Final instar after 4-5 days, a fifth instar nymph four to five days after stage I.

(III) Final instar after 9 days, a last instar nymph nine days after stage I.

(IV) Final instar after 9.5 days, a last instar nymph nine and a half days after stage I.

(V) Adult, a freshly eclosed adult maximum four hours after the imaginal moult.

Isolated RNA from guts was used to create three independent replicate pools per stage, each representing five individual insects, resulting in 18 sample pools.

Table 1: Sampling locations (coordinates) of the *Pyrrhocoris apterus* from *Tilia cordata* trees in Berlin.

Location	Lon	Lat
Wilmersdorfer Volkspark, Berlin	13.3345748	52.4810068
Gustav-Mahler-Platz, Berlin	13.3056438	52.4618606
Lansstraße, Berlin	13.2919478	52.4569725

RNA isolation and library preparation

Insect guts were dissected with dissecting utensils sterilised with ethanol. The dissected guts were rinsed in distilled water, and RNA was extracted from the guts with Trizol. They were homogenized in 1ml Trizol (Sigma, Taufkirchen, Germany) with two sterile 3 mm beads (Qiagen, Hilden, Germany) and a bead device at 20 Hz for 3 min. According to the manufacturers' instructions, total RNA was recovered using chloroform phase separation and isopropyl alcohol precipitation. RNA concentrations were measured using the Qubit™ RNA High Sensitivity Kit and a Qubit 4 fluorometer (ThermoFisher, Schwerte, Germany). Equal quantities of the samples were used to create independent replicate pools for each stage. RNA pools were purified by incubating the samples with TurboDNase (© Ambion) for 30 min at 37°C and cleaned up with the RNeasy MiniElute cleanup kit (Qiagen, Hilden, Germany) following the manufacturers' instructions. The concentrations of the pooled RNA samples were measured using the Qubit™ RNA HS Assay Kit and a Qubit™ 4 fluorometer (ThermoFisher, Schwerte, Germany). Samples from *Tenebrio molitor* and *Calliphora vicina* were qualified with the High Sensitivity RNA ScreenTape Assay Kit and the Agilent 4200 TapeStation system (Agilent, Santa Clara, United States) and *Pyrrhocoris apterus* samples with the Agilent RNA 6000 Pico Kit on a BioAnalyzer 2100 (Agilent, Santa Clara, United States). *T. molitor*, *C. vicina* and *P. apterus* libraries were prepared using the NEBNext® Ultra II Directional RNA Library Prep Kit (New England Biolabs, Ipswich, United States) at the Berlin Center for Genomics in Biodiversity Research (BeGenDiv). Library qualities were assessed with the High Sensitivity D1000 ScreenTape Assay Kit and the Agilent 4200 TapeStation system (Agilent, Santa Clara, United States). The libraries of all three insect species were sequenced on

NovaSeq 6000 at the Institute of Clinical Molecular Biology (IKMB) in Kiel for 300 cycles to yield 15–41 million 150-bp read pairs per library (mean 28 million).

De novo assembly and anotation

Assemblies for both species were produced using Trinity v. 2.8.4 (Haas et al., 2013), incorporating quality and adapter filtering via Trimmomatic (Bolger, Lohse, & Usadel, 2014) and subsequent in silico normalization. Assemblies were annotated with the Trinotate annotation pipeline (Grabherr et al., 2011).

Immune effector gene identification

Orthofinder 2.5.4 (Emms & Kelly, 2016) was used was to infer *T. molitor*, *C. vicina* and *P. apterus* orthologs of annotated immune genes from previously published insect genome projects (Benoit et al., 2016; dos Santos et al., 2015; Herndon et al., 2020; International Aphid Genomics Consortium, 2010; International Silkworm Genome Consortium, 2008). Additionally, blast and HMM homology searches were performed using previously described insect immune effector proteins as queries against each *de novo* assembly.

Differential gene expression

Differential gene expression was determined using the R Bioconductor package DESeq2 v. 1.26.0 (Love, Huber, & Anders, 2014). For all three insect species, transcript abundances were quantified by pseudo-aligning RNAseq reads to *de novo* assemblies using Salmon v. 1.8.0 (Patro, Duggal, Love, Irizarry, & Kingsford, 2017). The R package tximport (Soneson, Love, & Robinson, 2015) was used to import salmons transcript-level quantifications into R v. 3.6.3 (R Core Team, 2020).

The tximport object was used in conjunction with the sample metadata to make a DESeqDataSet object using the *DESeqDataSetFromTximport* function from the R package DESeq2 (Love et al., 2014). The DESeqDataSet object was used to identify differential expression as a function of developmental stage using the *DESeq* function. A likelihood-ratio test was used to compare a full model containing developmental stage as term to a reduced (intercept-only) negative binomial GLM to identify differentially expressed genes. All genes with a false discovery rate (FDR) corrected p-value less than 0.05 were considered differentially expressed genes. The mean of the normalised counts for each gene was used as the informative covariate for independent hypothesis weighting (Ignatiadis, Klaus, Zaugg, & Huber, 2016) to optimise the power of multiple testing. The normalised counts were regularised log-transformed (rlog) for the PCA plots. The R package ggplot2 (Wickham, 2011) was used for plotting.

Results

Tenebrio molitor

A total of 13 differentially expressed immune effectors, including three lysozymes, nine AMPs and *prophenoloxidase*, a type-3 copper innate immunity protein, were identified in *Tenebrio molitor* during pupation. The AMPs included attacins (*attacin 1*, *attacin 2*, *tenecin 4*), one cecropin, coleoptericins (*coleoptericin A*, *coleoptericin B*, *tenecin 2*), the defensin *tenecin 1*, and the antifungal thaumatin *tenecin 3*. These immune effectors have been previously described by Johnston, Makarova, & Rolff (2014). Throughout *T. molitor* development, attacins and coleoptericins showed peak expressions at the onset of pupation (stage IV). The expressions of the immune effector at the six defined developmental stages in the last instar larva and pupa of *T.*

molitor are shown in figure 1. The read count abundances, averaged over all developmental stages, of these differentially expressed immune effectors ranged from 60.53 (*I-type lysozyme 1*) to 19,962.58 (*Tenecin 1*) and had an overall mean of 8,509.60 (± 1,844.99 SE) read counts. A 14th identified immune effector, an attacin, was not differentially expressed (corrected p-value > 0.05) and had a mean read count of 158.44 (± 76.18 SE). The normalized read counts for the differentially and the non-differentially expressed immune effectors are shown in table 2 (supplement).

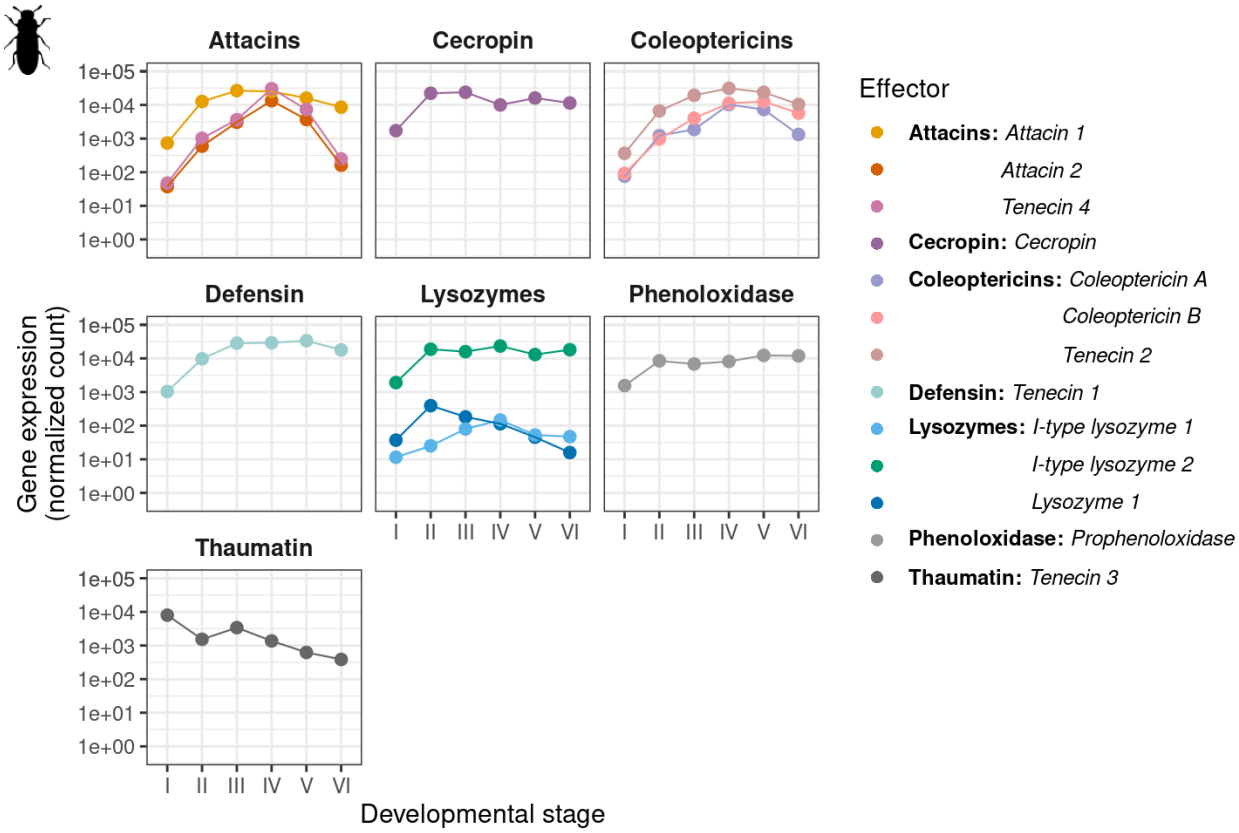

Figure 1: Differentially expressed immune effectors (corrected p-value <= 0.05) in the gut during the larval–pupal moult of *Tenebrio molitor*. Roman numerals correspond to specified developmental stages: (I) Last instar larvae, (II) little movement, (III) no movement, (IV) pupation after 1-6 h, (V) 12-20 h, and (VI) 24-48 h (see Material and Methods for more details). Plotted values represent the coefficients and 95% confidence intervals from negative binomial generalized linear models.

Calliphora vicina

We identified six differentially expressed immune effector genes, which encoded two lysozymes and four AMPs, including two attacins and two diptericins. One lysozyme (lysozyme b) first increased in normalized read counts with peak read counts one hour after pupation in the fourth developmental stage and then decreased (see figure 2). The attacins also showed peak expressions one hour after pupation (stage IV). Figure 2 shows all six differentially expressed immune effectors of *C. vicina* at the six defined developmental stages in the last instar larva and pupa. The read count abundances, averaged over all developmental stages, of these differentially expressed immune effectors ranged from 17.45 (*diptericin a*) to 1,290.21 (*attacin a*). They had an overall mean of 668.21 (± 183.58 SE) read counts. Lysozymes, attacins and diptericins have been previously described in *C. vicina*. Diptericin has been shown to be released by the blowflies' hemocytes (Gordya et al., 2017; Yakovlev et al., 2017). Yoon et al. (2022) showed high expression levels of attacin c, diptericins and lysozymes in the final instar larvae of *C.vicina*.

A total of 30 identified immune genes had a corrected p-value greater than 0.05 and were not differentially expressed. These genes encoded six types of immune effectors: lysozymes, attacins, coleoptericins, diptericins, cecropins and defensins. The read count abundances, averaged over all six developmental stages, of these non-differentially expressed immune effectors ranged from 0.27 (attacin j) to 691.35 (attacin a) and had an overall mean of 72.22 (± 28.71 SE) read counts. Table 3 in the supplement gives an overview of the normalized count means for the differentially and non-differentially expressed immune effectors and the number of unique immune effectors within each effector group.

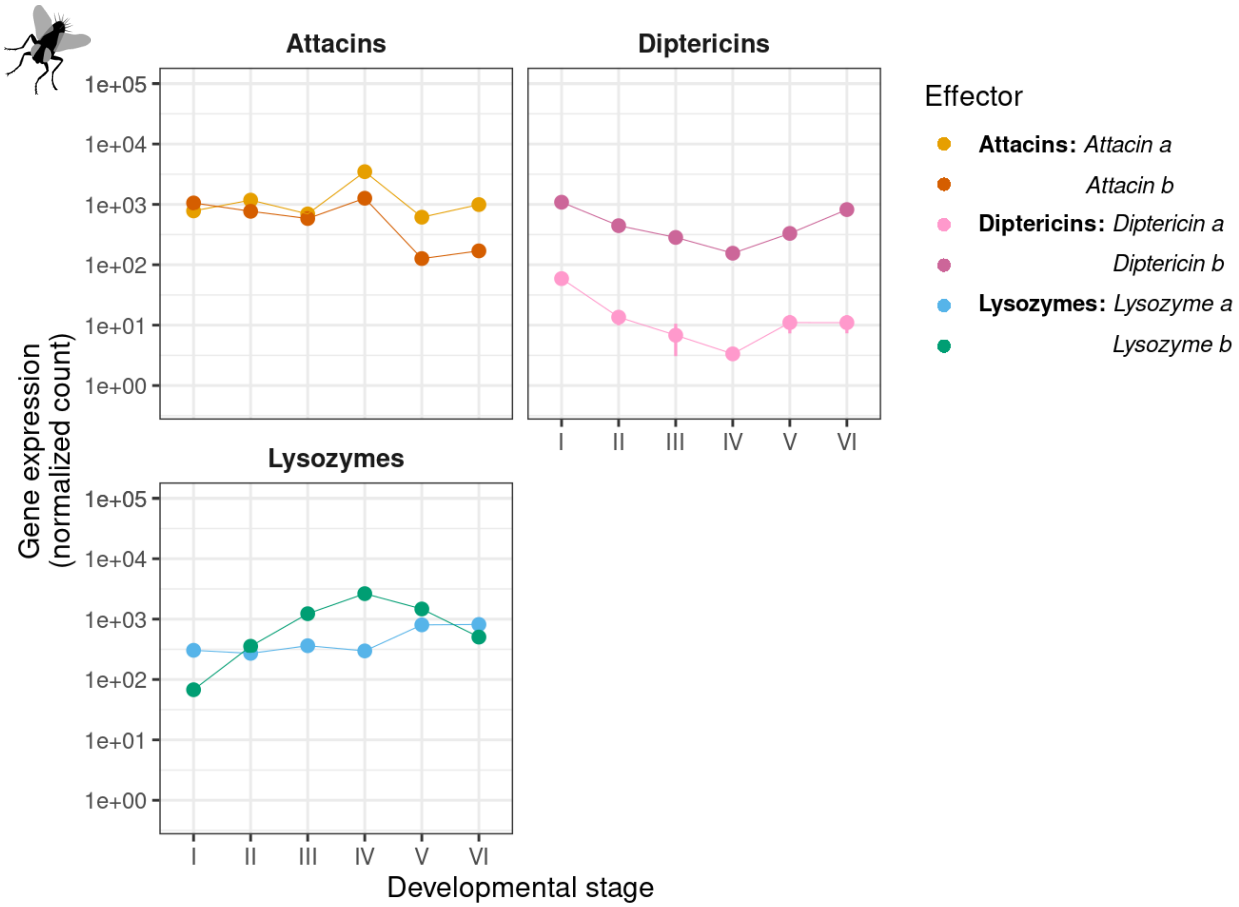

Figure 2: Differentially expressed immune effectors (corrected p-value <= 0.05) in the gut during the larval–pupal moult of *Calliphora vicina*. Roman numerals correspond to specified developmental stages: (I) Post feeding larvae, (II) pre-pupal stage, (III) pupal stage at the onset, (IV) pupae after 1 h, (V) 4-6 h, and (VI) 8-12 h (see Material and Methods for more details). Plotted values represent the coefficients and 95% confidence intervals from negative binomial generalized linear models.

Pyrrhocoris apterus

A total of nine immune effectors were identified in the *P. apterus de novo* assembly, of which three (*lysozyme*, *c-type lysozyme* and *phenoloxidase*) were differentially expressed at very low normalised read count abundances ranging from 8.15 (*Lysozyme*) to 41.21 (*C-type lysozyme*) and with an overall mean of 26.20 (± 9.66 SE) read counts (averaged over all five developmental stages). The lysozymes showed highest expressions one day before the nymphal-adult moult (stage

III) and phenoloxidase four to five days after the moult into the final instar (stage II). Figure 3 shows the expressions of these immune effectors throughout the five defined developmental stages in the last instar nymph and adult. The other immune effectors consisted of three I-type and two C-type lysozymes. Supplementary table 4 gives an overview of the normalised read count abundances for the differentially and non-differentially expressed immune effectors.

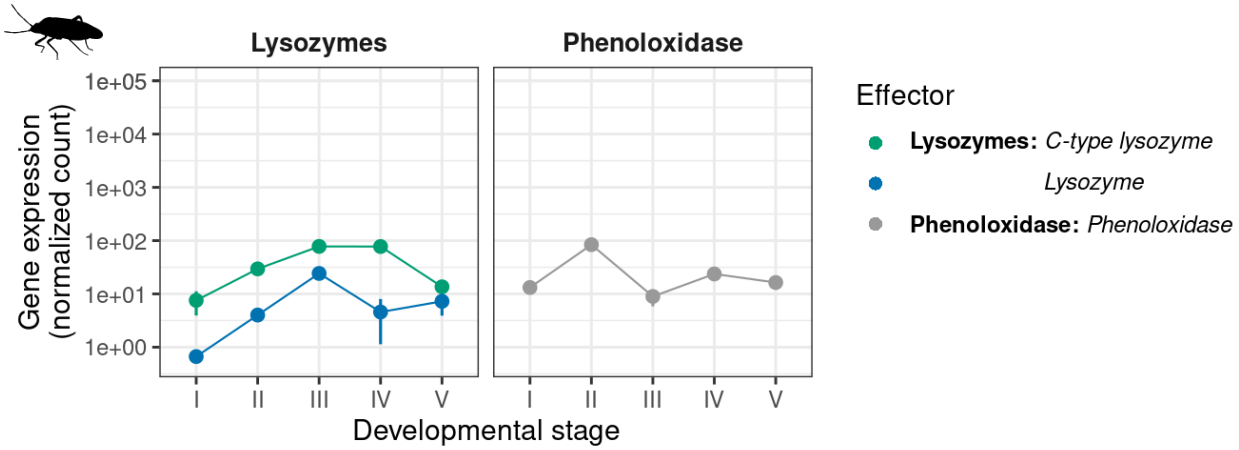

Figure 3: Differentially expressed immune effectors (corrected p-value <= 0.05) in the gut during the nymphal-adult moult of *Pyrrhocoris apterus*. Roman numerals correspond to specified developmental stages: (I) Freshly moulted last instar nymphs, (II) last instar nymphs after 4-5 d, (III) 9 d and (IV) 9.5 d, and (V) freshly eclosed adults (see Material and Methods for more details). Plotted values represent the coefficients and 95% confidence intervals from negative binomial generalized linear models.

Discussion

We found high read count abundances of differentially expressed immune effectors in the gut at the larval-pupal moult of the two holometabolous insects, *Tenebrio molitor* and *Calliphora vicina*; no such high abundances were observed at the nymphal-adult moult in the hemimetabolous insect *Pyrrhocoris apterus*. We also found peak expressions of immune effectors at the onset of pupation of the two holometabolous insects. *P.apterus* showed the highest expressions of immune

effectors before the nymphal-adult moult. Our findings of high immune effector expressions in holometabolous but not hemimetabolous insects during metamorphosis are consistent with Johnston et al. (2019) and confirm that only complete metamorphosis elicits a prophylactic gut immune response as an adaptive response in holometabolous insects, which controls the microbiota during gut replacement (Russell & Dunn, 1991, 1996).

The immune effectors identified in the mealworm beetle *T. molitor* have been previously described by Johnston et al. (2014) as components of the mealworm beetle's immune system. They identified immediate and long-lasting immune responses in the course of seven days after an immune challenge with heat-killed bacteria. The immediate response included the upregulation of phenoloxidase, which produces cytotoxic melanin and oxidative intermediates with broad-spectrum antibacterial activity (Zhao et al., 2007). In our study, phenoloxidase was differentially expressed and increased in the level of expression from the first (freshly moulted final instar larvae) to the second developmental stage (little movement stage, 1-2 d before puparation). It then did not change in the expression level throughout the remaining developmental stages of our study. The long-lasting induced immune effectors identified by Johnston et al. (2014) were antibacterial peptides and the iron-sequestering protein ferritin. These AMPs included attacins, coleoptericins and the defensin *tenecin 1*. Other AMPs, including cecropins, the attacin *tenecin 4,* the coleoptericin *tenecin 2* and the antifungal thaumatin *tenecin 3*, as well as lysozymes, were not upregulated after the immune challenge. We found peak expressions of *tenecin 2* and *tenecin 4* at the onset of pupation, indicating a prophylactic gut immune response.

The blowfly *C. vicina* showed peak expressions of antimicrobial proteins and peptides in the brown pupa one hour after puparation (stage IV). Nunes et al. (2021) found in another dipteran species,

the fruit fly *Drosophila melanogaster*, peak expressions of three AMPs (*drosomycin*, *drosomycin-like 2* and *drosomycin-like 5*) in the motionless white pre-pupa and discussed these AMP peaks as a prophylactic immune response. The AMP *drosomycin-like 2* was recruited in the midgut (Nunes et al., 2021), which undergoes extensive remodelling at complete metamorphosis (Martín-Vega, Simonsen, & Hall, 2017).

In the firebug *P. apterus*, we found lysozymes and phenoloxidase upregulated with very low read count abundances compared to the peak expressions of the two holometabolous insect species. The less drastic changes of the gut of hemimetabolous insects during metamorphosis, which does not entail gut replacement (Teixeira, Fialho, Zanuncio, Ramalho, & Serrão, 2013), are likely to explain the differences. The more minor changes during incomplete metamorphosis seem not to necessitate prophylaxis. The lysozymes in *P. apterus* were strongest upregulated one day (stage III) and 12 hours before adult eclosion (stage IV) and phenoloxidase four to five days after the moult in the final instar (stage II). Phenoloxidase is a central enzyme secreted by the salivary glands of phytophagous Hemiptera, including Pyrrhocoridae (Hori, 2000). Insect salvia has numerous functions, including digestion and antimicrobial activity. According to Miles (1969), polyphenol oxidase seems to be an invariable component of the watery salvia of phytophagous Hemiptera. It serves as a counter to defensive toxins in the insects' food (Miles, 1969). Also, the immune system of insects controls beneficial symbionts (Login et al., 2011). In another species from the Pyrrhocoridae family, the cotton stainer bug *Dysdercus fasciatus*, beneficial and heritable gut bacterial symbionts induce an immune response with an upregulation of *c-type lysozyme* and the AMP *pyrrhocoricin* (Bauer, Salem, Marz, Vogel, & Kaltenpoth, 2014).

However, experimental support for a prophylactic effect in holometabolous insects is lacking. We also cannot exclude the possibility that in either species, there may be true differentially expressed immune genes that were not successfully annotated . (Johnston et al., 2019) discuss that alternatively to a prophylactic effect, immune induction may serve to control the proliferation of the microbiota as they observed that the upregulation of immune effectors persisted into the pupa when the gut of their studied greater wax moth *Galleria mellonella* undergoes apoptosis and necrosis to release breakdown products that are recycled by the replacement gut. This indicates the possibility that immune induction may suppress bacterial growth that otherwise disrupts the complex trophic relationship between the autolytic larval and the replacement adult gut. A second alternative explanation, Johnston et al. (2019) discuss, is that the observed immune induction drives changes in microbial community composition, facilitating ontogenetic habitat and/or diet shifts.

Acknowledgements

We are grateful to Elisa Bittermann, Luisa Linke, Jia Clara Kim and Marlene Finger for support in the lab. This research was funded by the DFG (Deutsche Forschungsgemeinschaft).

References

Arendt, J. D. (1997). Adaptive Intrinsic Growth Rates: An Integration Across Taxa. *The Quarterly Review of Biology*, *72*, 29.

Bauer, E., Salem, H., Marz, M., Vogel, H., & Kaltenpoth, M. (2014). Transcriptomic Immune Response of the Cotton Stainer Dysdercus fasciatus to Experimental Elimination of

Vitamin-Supplementing Intestinal Symbionts. *PLoS ONE*, *e114865*. doi: 10.1371/journal.pone.0114865

Benoit, J. B., Adelman, Z. N., Reinhardt, K., Dolan, A., Poelchau, M., Jennings, E. C., … Richards, S. (2016). Unique features of a global human ectoparasite identified through sequencing of the bed bug genome. *Nature Communications*, *7*(1), 1–10. doi: 10.1038/ncomms10165

Bolger, A. M., Lohse, M., & Usadel, B. (2014). Trimmomatic: A flexible trimmer for Illumina sequence data. *Bioinformatics*, *30*(15), 2114–2120. doi: 10.1093/bioinformatics/btu170

dos Santos, G., Schroeder, A. J., Goodman, J. L., Strelets, V. B., Crosby, M. A., Thurmond, J., … the FlyBase Consortium. (2015). FlyBase: Introduction of the Drosophila melanogaster Release 6 reference genome assembly and large-scale migration of genome annotations. *Nucleic Acids Research*, *43*(D1), D690–D697. doi: 10.1093/nar/gku1099

Du Pasquier, L. (2001). The immune system of invertebrates and vertebrates. *Comparative Biochemistry and Physiology Part B: Biochemistry & Molecular Biology*, *129*(1), 1–15. doi: 10.1016/S1096-4959(01)00306-2

Ebert, D. (2013). The Epidemiology and Evolution of Symbionts with Mixed-Mode Transmission. *Annual Review of Ecology, Evolution, and Systematics*, *44*(1), 623–643. doi: 10.1146/annurev-ecolsys-032513-100555

Emms, D., & Kelly, S. (2016). OrthoFinder: Solving fundamental biases in whole genome comparisons dramatically improves orthogroup inference accuracy. *Genome Biology*, *16*. doi: 10.1186/s13059-015-0721-2

Gordya, N., Yakovlev, A., Kruglikova, A., Tulin, D., Potolitsina, E., Suborova, T., … Chernysh, S. (2017). Natural antimicrobial peptide complexes in the fighting of antibiotic resistant biofilms: Calliphora vicina medicinal maggots. *PLOS ONE*, *12*(3), e0173559. doi: 10.1371/journal.pone.0173559

Grabherr, M. G., Haas, B. J., Yassour, M., Levin, J. Z., Thompson, D. A., Amit, I., … Regev, A. (2011). Full-length transcriptome assembly from RNA-Seq data without a reference genome. *Nature Biotechnology*, *29*(7), 644–652. doi: 10.1038/nbt.1883

Haas, B. J., Papanicolaou, A., Yassour, M., Grabherr, M., Blood, P. D., Bowden, J., … Regev, A. (2013). De novo transcript sequence reconstruction from RNA-seq using the Trinity platform for reference generation and analysis. *Nature Protocols*, *8*(8), 1494–1512. doi: 10.1038/nprot.2013.084

Hall, M. J. R., & Martín-Vega, D. (2019). Visualization of insect metamorphosis. *Philosophical Transactions of the Royal Society B: Biological Sciences*, *374*(1783), 20190071. doi: 10.1098/rstb.2019.0071

Herndon, N., Shelton, J., Gerischer, L., Ioannidis, P., Ninova, M., Dönitz, J., … Bucher, G. (2020). Enhanced genome assembly and a new official gene set for Tribolium castaneum. *BMC Genomics*, *21*(1), 47. doi: 10.1186/s12864-019-6394-6

Hammer, T. J., & Moran, N. A. (2019). Links between metamorphosis and symbiosis in holometabolous insects. *Philosophical Transactions of the Royal Society B: Biological Sciences*, *374*(1783), 20190068. doi: 10.1098/rstb.2019.0068

Hori, K. (2000). Possible causes of disease symptoms resulting from the feeding of phytophagous Heteraoptera. In *Heteroptera of Economic Importance* (Schaefer, Carl W. & Panizzi, Antônio Ricardo, pp. 11–35). CRC Press.

Hultmark, D. (1993). Immune reactions in Drosophila and other insects: A model for innate immunity. *Trends in Genetics*, *9*(5), 178–183. doi: 10.1016/0168-9525(93)90165-E

Ignatiadis, N., Klaus, B., Zaugg, J. B., & Huber, W. (2016). Data-driven hypothesis weighting increases detection power in genome-scale multiple testing. *Nature Methods*, *13*(7), 577–580. doi: 10.1038/nmeth.3885

International Aphid Genomics Consortium. (2010). Genome Sequence of the Pea Aphid Acyrthosiphon pisum. *PLoS Biology*, *8*(2), e1000313. doi: 10.1371/journal.pbio.1000313

International Silkworm Genome Consortium. (2008). The genome of a lepidopteran model insect, the silkworm Bombyx mori. *Insect Biochemistry and Molecular Biology*, *38*(12), 1036–1045. doi: 10.1016/j.ibmb.2008.11.004

Johnston, P. R., Makarova, O., & Rolff, J. (2014). Inducible Defenses Stay Up Late: Temporal Patterns of Immune Gene Expression in *Tenebrio molitor*. *G3 Genes|Genomes|Genetics*, *4*(6), 947–955. doi: 10.1534/g3.113.008516

Johnston, P. R., Paris, V., & Rolff, J. (2019). Immune gene regulation in the gut during metamorphosis in a holo- versus a hemimetabolous insect. *Philosophical Transactions of the Royal Society B: Biological Sciences*, *374*(1783), 20190073. doi: 10.1098/rstb.2019.0073

Johnston, P. R., & Rolff, J. (2015). Host and Symbiont Jointly Control Gut Microbiota during Complete Metamorphosis. *PLOS Pathogens*, *11*(11), e1005246. doi: 10.1371/journal.ppat.1005246

Kaltenpoth, M., Yildirim, E., Gürbüz, M. F., Herzner, G., & Strohm, E. (2012). Refining the Roots of the Beewolf-Streptomyces Symbiosis: Antennal Symbionts in the Rare Genus Philanthinus (Hymenoptera, Crabronidae). *Applied and Environmental Microbiology*, *78*(3), 822–827. doi: 10.1128/AEM.06809-11

Kikuchi, Y., Hosokawa, T., & Fukatsu, T. (2011). An ancient but promiscuous host–symbiont association between Burkholderia gut symbionts and their heteropteran hosts. *The ISME Journal*, *5*(3), 446–460. doi: 10.1038/ismej.2010.150

Login, F. H., Balmand, S., Vallier, A., Vincent-Monégat, C., Vigneron, A., Weiss-Gayet, M., … Heddi, A. (2011). Antimicrobial Peptides Keep Insect Endosymbionts Under Control. *Science*, *334*(6054), 362–365. doi: 10.1126/science.1209728

Love, M. I., Huber, W., & Anders, S. (2014). Moderated estimation of fold change and dispersion for RNA-seq data with DESeq2. *Genome Biology*, *15*(12), 550. doi: 10.1186/s13059-014-0550-8

Mai, T., Chen, S., Lin, X., Zhang, X., Zou, X., Feng, Q., & Zheng, S. (2017). 20-hydroxyecdysone positively regulates the transcription of the antimicrobial peptide, lebocin, via BmEts and BmBR-C Z4 in the midgut of Bombyx mori during metamorphosis. *Developmental & Comparative Immunology*, *74*, 10–18. doi: 10.1016/j.dci.2017.04.002

Maire, J., Parisot, N., Ferrarini, M. G., Vallier, A., Gillet, B., Hughes, S., … Heddi, A. (2020). Spatial and morphological reorganization of endosymbiosis during metamorphosis accommodates adult metabolic requirements in a weevil. *Proceedings of the National Academy of Sciences*, *117*(32), 19347–19358. doi: 10.1073/pnas.2007151117

Manthey, C., Johnston, P., & Rolff, J. (2021). *Complete metamorphosis and microbiota turnover in insects* [Preprint]. Evolutionary Biology. doi: 10.1101/2021.06.15.448481

Martín-Vega, D., Simonsen, T. J., & Hall, M. J. R. (2017). Looking into the puparium: Micro-CT visualization of the internal morphological changes during metamorphosis of the blow fly, Calliphora vicina, with the first quantitative analysis of organ development in cyclorrhaphous dipterans. *Journal of Morphology*, *278*(5), 629–651. doi: 10.1002/jmor.20660

Miles, P. W. (1969). Interaction of plant phenols and salivary phenolases in the relationship between plants and Hemiptera. *Entomologia Experimentalis et Applicata*, *12*(5), 736–744.

Nicholson, D. B., Ross, A. J., & Mayhew, P. J. (2014). Fossil evidence for key innovations in the evolution of insect diversity. *Proceedings of the Royal Society B: Biological Sciences*, *281*(1793), 20141823–20141823. doi: 10.1098/rspb.2014.1823

Nunes, C., Koyama, T., & Sucena, É. (2021). Co-option of immune effectors by the hormonal signalling system triggering metamorphosis in Drosophila melanogaster. *PLOS Genetics*, *17*(11), e1009916. doi: 10.1371/journal.pgen.1009916

Patro, R., Duggal, G., Love, M. I., Irizarry, R. A., & Kingsford, C. (2017). Salmon provides fast and bias-aware quantification of transcript expression. *Nature Methods*, *14*(4), 417–419. doi: 10.1038/nmeth.4197

R Core Team. (2020). *R: A language and environment for statistical computing.* Vienna, Austria: R Foundation for Statistical Computing. Retrieved from https://www.R-project.org/

Rolff, J., Johnston, P. R., & Reynolds, S. (2019). Complete metamorphosis of insects. *Philosophical Transactions of the Royal Society B: Biological Sciences*, (374). doi: 10.1098/rstb.2019.0063

Russell, V. W., & Dunn, P. E. (1991). Lysozyme in the midgut of Manduca sexta during metamorphosis. *Archives of Insect Biochemistry and Physiology*, *17*(2–3), 67–80. doi: https://doi.org/10.1002/arch.940170202

Russell, V. W., & Dunn, P. E. (1996). Antibacterial Proteins in the Midgut of Manduca sexta During Metamorphosis. *Journal of Insect Physiology*, *42*(1), 65–71. doi: 10.1016/0022-1910(95)00083-6

Soneson, C., Love, M. I., & Robinson, M. D. (2015). *Differential analyses for RNA-seq: Transcript-level estimates improve gene-level inferences Supplementary Material*. 27.

Stoll, S., Feldhaar, H., Fraunholz, M., & Gross, R. (2012). Bacteriocyte dynamics during development of a holometabolous insect, the carpenter ant Camponotus floridanus. *BMC Microbiology*.

Teixeira, A. das D., Fialho, M. do C. Q., Zanuncio, J. C., Ramalho, F. de S., & Serrão, J. E. (2013). Degeneration and cell regeneration in the midgut of Podisus nigrispinus (Heteroptera:

Pentatomidae) during post-embryonic development. *Arthropod Structure & Development*, *42*(3), 237–246. doi: 10.1016/j.asd.2013.02.004

Wickham, H. (2011). Ggplot2. WIREs Computational Statistics, 3(2), 180–185. doi: 10.1002/wics.147

Yakovlev, A. Y., Nesin, A. P., Simonenko, N. P., Gordya, N. A., Tulin, D. V., Kruglikova, A. A., & Chernysh, S. I. (2017). Fat body and hemocyte contribution to the antimicrobial peptide synthesis in Calliphora vicina R.-D. (Diptera: Calliphoridae) larvae. In Vitro Cellular & Developmental Biology - Animal, 53(1), 33–42. doi: 10.1007/s11626-016-0078-1

Yoon, K. A., Kim, W.-J., Cho, H., Yoon, H., Ahn, N.-H., Lee, B.-H., & Lee, S. H. (2022). Characterization of Anti-Microbial Peptides and Proteins from Maggots of Calliphoridae and Sarcophagidae Fly Species (Diptera). SSRN Electronic Journal. doi: 10.2139/ssrn.4079553

Zhao, P., Li, J., Wang, Y., & Jiang, H. (2007). Broad-spectrum antimicrobial activity of the reactive compounds generated in vitro by Manduca sexta phenoloxidase. Insect Biochemistry and Molecular Biology, 37(9), 952–959. doi: 10.1016/j.ibmb.2007.05.001

CHAPTER IV: COMPLETE METAMORPHOSIS AND FAST LARVAL GROWTH IN INSECTS

Christin Manthey [1], Michael Monaghan [1,2,3], Ulrich Steiner [1], Jens Rolff [1,4]

1. Freie Universität Berlin, Institut für Biologie, Evolutionary Biology, Königin-Luise-Strasse 1-3, 14195 Berlin, Germany.
2. Berlin Center for Genomics in Biodiversity Research, Berlin, Germany.
3. Leibniz-Institute of Freshwater Ecology and Inland Fisheries (IGB), Berlin, Germany.
4. Berlin-Brandenburg Institute of Advanced Biodiversity Research (BBIB), Berlin, Germany.

Abstract

The insects constitute the majority of animal diversity. Most insects are holometabolous and undergo complete metamorphosis. The holometabolous larva produces little to no resemblance to the adult and hatches in an intercalated pupal life stage. A distinct adult life form emerges from the pupa after the larval organs are broken down and reconstructed. In contrast, hemimetabolous insects undergo incomplete metamorphosis. The hemimetabolous nymph hatches directly in the adult form that generally resembles the instars. Intercalating the pupal stage decouples growth and differentiation. In Holometabola, most growth is confined to the larval, while most development occurs in the pupa allowing for fast larval growth in holometabolous insects. We compared 33 species from three holo- and seven hemimetabolous insect orders and calculated growth ratios, rates and periods. We found faster larval growth, higher growth ratios and much higher variances for those traits in holometabolous than hemimetabolous insects. We also found much shorter

growth periods of the larval stages in holometabolous than hemimetabolous insects. Our results support the decoupling of growth and differentiation hypothesis, allowing fast larval growth.

Introduction

More than 60% of all living animals are insects (Grimaldi & Engel, 2005; Mora, Tittensor, Adl, Simpson, & Worm, 2011). According to the extent of change at metamorphosis, insects can be classified into two major categories: hemimetabolous and holometabolous insects. Today more than 80% of all insects have a holometabolous lifestyle and undergo a complete metamorphosis (Grimaldi & Engel, 2005). Holometaboly in insects evolved once, about 344 million years ago (Misof et al., 2014). The hemimetabolous insects arose some 100 million years earlier. Though the holometabolous insects are the much younger group of insects on an evolutionary time scale, they are the more successful group of insects whether in terms of abundance, species diversity, biomass or ecosystem function (Berenbaum, 2017; Mora et al., 2011; Whiting, 2004). The holometabolous insects undergo a complete metamorphosis. In holometabolous insects, only part of the embryonic tissue, organized into primordia, is utilized to make a reduced larval structure. The rest are set aside to pass through the larval stages in a determined but not differentiated state as imaginal disc primordia (Aldaz & Escudero, 2010; Chapman, 2013; Sehnal, 1985). The larva produces little to no resemblance to the adult and hatches in an intercalated pupal life stage. The imaginal discs differentiate during complete metamorphosis under the influence of hormonal changes to form pupal and adult organs, respectively, which were absent in larvae or replaced specific larval organs. A distinct adult life form emerges from the pupa after the larval organs are broken down and reconstructed (Hall & Martín-Vega, 2019; Hinton, 1948; Rolff, Johnston, & Reynolds, 2019;

Truman, 2019). In contrast, hemimetabolous insects undergo incomplete metamorphosis. In hemimetabolous insects, legs, wings, antennae, mouthparts, eyes, and other structures form during embryogenesis. The embryonic primordia grow and differentiate as they form miniature versions of the adult structures (Truman, 2019). The nymph hatches directly in the adult form that generally resembles the instars except for its smaller size and lack of wings and genitalia (Chapman, 2013; Lutz & Huebner, 1980; Truman, 2019).

The pupal stage is one of the key traits of holometabolous insects (Nicholson, Ross, & Mayhew, 2014). However, how it is related to the success of the holometabolous insects is not known (Rolff et al., 2019). There are two main adaptive hypotheses explaining the evolution of the pupal stage. One explanation is that in holometabolous insects, the radical reconstruction of the larval body within the pupal stage clears the gut and provides the opportunity to drive a change between the larval and adult microbiota. A microbial change was observed in holometabolous but not in hemimetabolous insects (Manthey, Johnston, & Rolff, 2021) and may allow the insect to acquire life stage-specific symbionts, facilitating niche shifts (Hammer & Moran, 2019; Moran, 1994). It further reduces growing populations of pathogens that would otherwise persist in the adult host (Johnston & Rolff, 2015). The second barely studied and not a mutually exclusive hypothesis is that intercalating the pupal stage decouples growth and differentiation (Arendt, 1997; Rolff et al., 2019). Arendt (1997) and Rolff et al. (2019) discuss that in holometabolous insects, most growth is confined mainly to the larval stages, while most development occurs in the pupal life stage allowing for fast larval growth in holometabolous insects.

Growth in insects only occurs in the immature feeding stages, which usually grow with no marked change in body form; each successive stage is similar to the previous stage until metamorphosis

(Chapman, 2013). The larval and adult holometabolous life stages are distinct developmental and evolvable modules compared to the highly correlated stages of hemimetabolous insects allowing the divergent evolution of stage-specific morphological and life-history specialisations in larvae and adults (Yang, 2001 and references therein). Holometabolous insects usually have soft-bodied and worm-like shape larvae with less motility than hemimetabolous insects (Maddrell, 2018; Truman, 2019), allowing them to exploit food resources better, which may benefit fast larval growth. The adults are specialised for dispersal and reproduction. Fast growth allows for efficient and competitive exploitation of ephemeral resources, which appear patchily and have a short lifetime (Cole, 1980). Ephemeral habitats would be best exploited by insects that rapidly achieve adult size, mature, and disperse before the habitat disappears (Cole, 1980). Day and Rowe (2002) suggested an overhead threshold model for optimal size and age at a transition like the final juvenile moult, for instance. Their model predicts a developmental threshold of the minimum size or level of condition needed for the transition and an L-shaped reaction norm for size and age. Fast-growing organisms will reach the threshold earlier, resulting in a steep slope of the relationship between size and age at the final moult compared to slow-growing organisms. There is evidence for fast growth in holometabolous insects. Cole (1980) showed that holometabolous insects differ significantly in median growth ratios from hemimetabolous insects. However, the study by Cole (1980) comes with some weaknesses given our current knowledge on statistical analysis. It was published prior to the invention of comparative methods by Felsenstein (1985). In his study, Cole (1980) studied growth ratios, calculated as the size of one instar to the previous instar, averaged over all immature stages. He did not include developmental times and compared the two groups of insects with a median test based on non-parametric statistics (Siegel, 1957) that did not control for

phylogeny. Cole (1980) further used studies that provided a wide variety of size measurements for head widths (e.g. head capsule and head width across eyes) and measurements of the trophic apparatus of immature insects (e.g. labium, cepahlopharyngeal skeleton or siphon length). Regarding the findings of Cole (1980), we predict that holometabolous compared to hemimetabolous insects reach the developmental threshold earlier due to fast larval growth and hence a steep slope on the L-shaped reaction norm for age and size at the final juvenile moult. Fecundity correlates positively with size (Alois Honěk, 1993), and adult body size is determined by the size the larva and nymph, respectively, has reached when it stops feeding and begins metamorphosis. Hence size at the final moult determines how much an insect can reproduce. Therefore, fast growth may benefit fecundity. It further shortens the growth period.

To investigate growth in hemi- versus holometabolous insects, we conducted a literature review like Cole (1980). For insect growth data, we systematically searched ZOBODAT, the Zoological-Botanical Database (Malicky & Aubrecht, 2001) database. ZOBODATs data collection contains digitised literature that traditionally relates to insect studies from Austria and, to a lesser extent, to Germany, reducing geographic variance. To further reduce variance, we exclusively used total body lengths as an estimate to study immature growth. Total body lengths can be accurately measured under laboratory and field conditions (Costa & Gomes-Filho, 2002). However, we calculated growth rates with and without development times as body size and development time are essential life-history traits because they are often highly correlated with fitness. To reduce type I error rates, we controlled for phylogeny in our model to compare hemi- versus holometabolous insects. We predict fast larval growth rates and a shorter growth period in holometabolous compared to hemimetabolous insects.

Methods

Literature search

Publications were collected that reported total body lengths and developmental times for immature stages of insects. Literature was systematically searched on ZOBODAT, the Zoological-Botanical Database (www.zobodat.at), which contains digitised literature on insect studies from Austria and, to a lesser extent, Germany, reducing geographic variance. Titles were searched exclusively with a single keyword used as search terms. The search terms included all 29 order names of insects shown in Misof et al. (2014) and their respective German names and corresponding synonyms. Search results were refined to publications with an existing PDF file on ZOBODAT. Publications dates ranged from 1763 to 2021. Publications with the following words or phrases in their titles were not further reviewed and excluded for reading: Aufzählung (enumeration/list); Verzeichnis (index); Classification; neue Arten (new species)/ neue exotische (new exotic) / neue Formen (new forms); Bemerkungen über (remarks about) / Bemerkungen zur (remarks on); Beiträge zur Kenntnis (contributions to knowledge); Bestimmungsschüssel (identification key); Ergebnisse zoologischer Reise (results of zoological trip); Forschungsreise (research trip); Beschreibung einiger (description of some); Zur Verbreitung von (on the distribution of). The remaining publications were included in the final dataset if they met the following criteria:

(i) Living animals or exuviae were measured

(ii) Total body lengths from most immature stages were taken

(iii)Developmental times from all collected immature stages were reported.

Table 1 in the supplement lists all search terms, the number of generated publications from the initial search, the number of publications that fit all criteria, and the species numbers for each insect order.

Growth estimates

Three growth estimates were calculated: Growth ratios (GR), relative growth rates (RGR) and percentage growth per day (PGR). GR is a standardised measure of growth, which is the ratio of the size of one instar to the size of the previous instar, averaged over all immature moults and was used in the study by Cole (1980). The RGR is the growth rate relative to size - that takes into account the differences in initial sizes and, therefore, can be used to compare the growth of different species. It controls for developmental times and is also called the exponential growth rate. The PGR is also a rate of growth per unit time that controls for differences in initial sizes between species. It is the percentage increase over time. GR, RGR and PGR were calculated as follows:

$$\mathrm{GR} = \frac{1}{n}\sum_{i=1}^{n}(\text{size instar}_{n} \div \text{size instar}_{n-1}) \quad (1)$$

$$\mathrm{RGR} = \frac{1}{n}\sum_{i=1}^{n}\left(\frac{ln(\text{size instar}_{n}/\text{size instar}_{n-1})}{\Delta t}\right) = \left(\frac{ln(\text{size instar}_{n}) - ln(\text{size instar}_{n-1})}{\Delta t}\right) \quad (2)$$

$$\mathrm{PGR} = \frac{1}{n}\sum_{i=1}^{n}\left(\left(\frac{\text{size instar}_{n} - \text{size instar}_{n-1}}{\text{size instar}_{n-1}/100}\right)/\Delta\, t\right) \quad (3)$$

Where *n* is the number of instars for a species of concern, and *t* is the developmental time for an instar. Instar development times were the individual instar lengths. Larval stages in which larvae stopped feeding and entered a wandering stage were not included. The peak larval length was taken

as the final length for an instar. Growth ratios were calculated like in Cole (1980) and a more recent publication by Tammaru, Nylin, Ruohomäki, and Gotthard (2004). The total body lengths for three Odonates, *Erythemis simplicicollis*, *Anax junius* and *Nasiaeshna pentacantha*, based on exuviae length measures. The GR, RGR and PGR for *Eucorydia yasumatsui*, *Tenebrio molitor*, *Zophobas atratus* and *Lasiocampa pini* were weighted growth estimates depending on the number of instars because of their variation in the number of instars (see supplementary table 4 for more details). The lengths of the three Gryllidae species were measured every ten days, and therefore the growth estimates were not calculated per instar but in ten-day intervals.

Growth period

Total and mean durations of the growth period for each species were calculated as follows:

$$\text{Total GP} = \sum_{i=1}^{n} \text{time period instar}_i \quad (4)$$

$$\text{Mean GR} = \frac{1}{n} \sum_{i=1}^{n} \text{time period instar}_i \quad (5)$$

Where *n* is the number of instars for a species of concern. The total growth period (Total GP) was determined as the time from egg hatching to pupation for holometabolous insects and from egg hatching to adult eclosion for hemimetabolous insects, respectively. The mean growth period (Mean GP) is the sum of the growth period for each instar averaged over all immature stages. The three *Gryllidae* species were excluded from the growth period calculations because they were measured every ten days and not for each instar. For the Total GP, three holometabolous species, *Cucujus cinnaberinus*, *Epilobophora sabinata teriolensis*, and *Saturnia pyri*, and one

hemimetabolous species, *Nasiaeschna pentacantha*, were excluded because the developmental time of either the first or last larval stage was not reported.

Statistical Analysis

All statistical analyses were performed in R (version 3.6.3; R Core Team, 2020). Differences in the GR, RGR and PGR were tested between holo- and hemimetabolous insects. The variance heterogeneity (Dutilleul & Legendre, 1993) across the two groups was tested with the Breusch-Pegan test using the *ncvTest* function from the R package car (Fox, Weisberg, & Price, 2021). Regression analyses controlled for phylogeny were performed to reduce type I error rates. Grafen's branch lengths were generated before modelling the phylogenetic correlation matrix for the models (Grafen, 1989). The models were phylogenetic linear mixed-effects models using the *rma.mv* function from the R package metafor (Cinar, Nakagawa, & Viechtbauer, 2021) that incorporates sampling variance (the square of SE). First, an intercept model with two random effects (species ID and phylogeny) was fitted. The percentage of total variation (I^2) due to heterogeneity rather than chance (sampling variance) was calculated (Higgins, 2003; Senior et al., 2016) and separated into the heterogeneity explained by phylogeny and differences between observation points (species ID) using the *i2_ml* function from the R package orchaRd (Nakagawa et al., 2020). A second model with the two random effects (species ID and phylogeny) and the type of metamorphosis as a fixed effect that looked at the contrast between hemi- and holometabolous insects was fitted. The percentage of variation in the growth estimates attributed to the type of metamorphosis was calculated as marginal R^2 (Nakagawa & Schielzeth, 2013) using the *r2_ml* function from the orchaRd package (Nakagawa et al., 2020). A third model that specified the variance structure of the two insect groups by modelling heteroscedasticity (heterogeneity of variances) was fitted and

used to visualise the results using the orchaRd package (Nakagawa et al., 2020). The orchard plots display 95% confidence intervals and 95% prediction intervals of the group means for hemi- and holometabolous insects. The prediction interval displays the 95% probability that the response estimate of an insect species in a new study lies within this interval. Also, the differences in the growth periods were tested between holo- and hemimetabolous insects. The Mean GP was tested with phylogenetic linear mixed-effects models. First, an intercept model with two random effects (species ID and phylogeny) and a second model with an additional fixed effect (type of metamorphosis) were fitted, and the I^2 and R^2 were computed. The Total GP was tested using a two-sample t-test. They were the sum of the growth period durations without variability needed for the phylogenetic linear mixed-effects models. To meet the assumption of normally distributed data, the Total GP variable was transformed before testing for group differences using logarithm transformation. Further, growth trajectories were plotted for each insect species (see supplement).

Results

In total, we calculated growth ratios and rates for 33 insect species, including 21 hemimetabolous and 12 holometabolous insects. The hemimetabolous insects cover seven orders of insects, including Odonata, Zoraptera, Orthoptera, Phasmatodea, Blattodea, Hemiptera and Psocodea. The holometabolous insects cover three insect orders: Coleoptera, Lepidoptera, and Diptera. See figure 1 for details. The growth trajectories for each species can be found in the supplementary material.

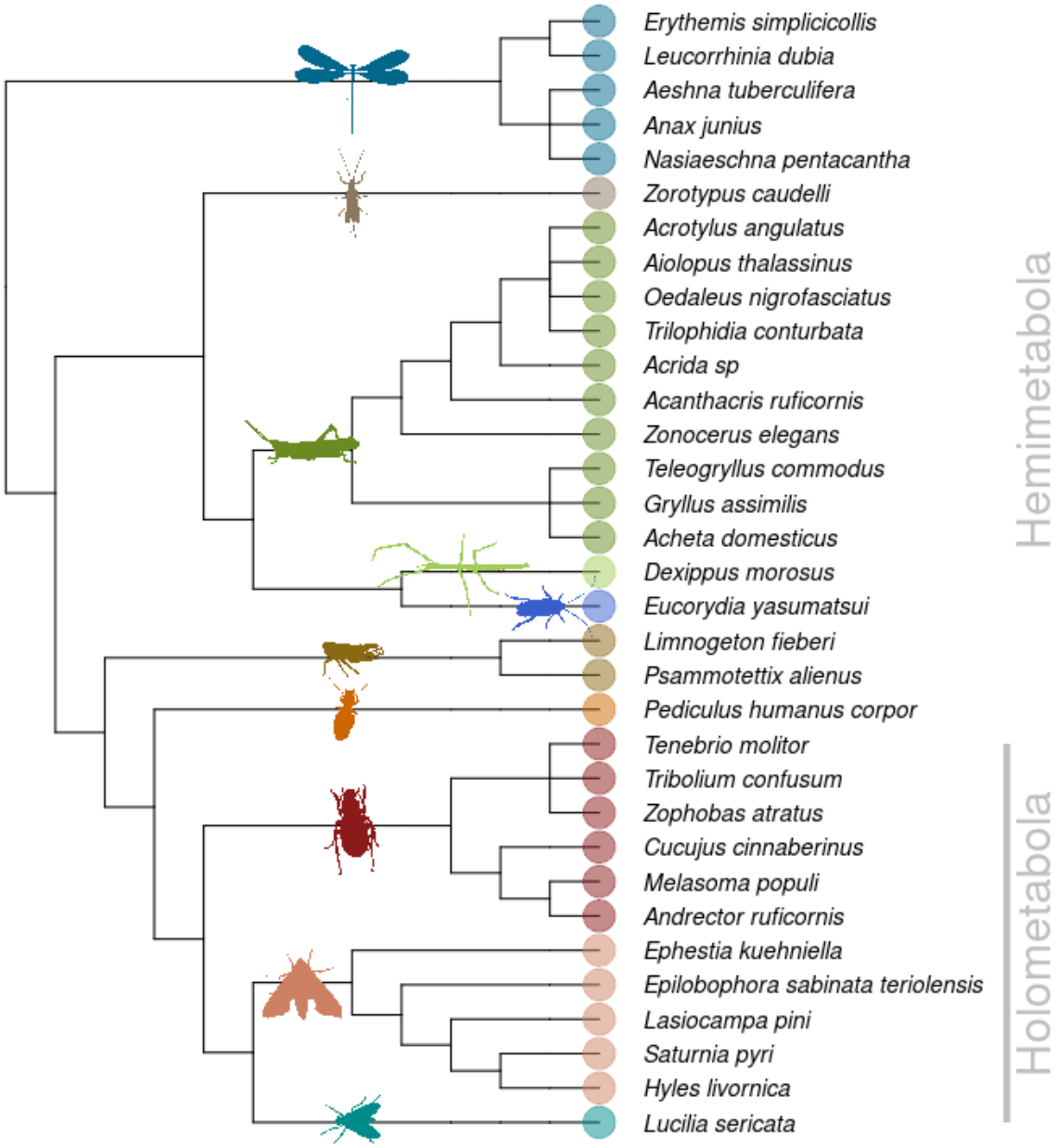

Figure 1: Phylogenetic tree of the 33 insect species including 21 hemimetabolous and 12 holometabolous insects.

Growth estimates

Our results show significantly greater GR, RGR and PGR in holometabolous than hemimetabolous insects (see figure 2 and table 2 for the model results). The difference was not affected when running the models without the three *Gryllidae* species measured in ten-day intervals (see supplementary table 5). The variance heterogeneity was significant for all growth estimates indicating unequal variances when comparing hemimetabolous and holometabolous insects (see table 3). The total heterogeneities (I^2) for GR, RGR and PGR were high, with about half of the variance explained by phylogeny and the remaining half explained by differences between species for each estimate (see table 3). The maximum growth estimates of holometabolous insects were much higher than those of hemimetabolous insects for all three growth estimates (see figure 1 and supplementary table 9). The percentage of variation attributed to the type of metamorphosis (R^2) was 23.64% in GR, 20.79% in RGR and 35.70% in PGR.

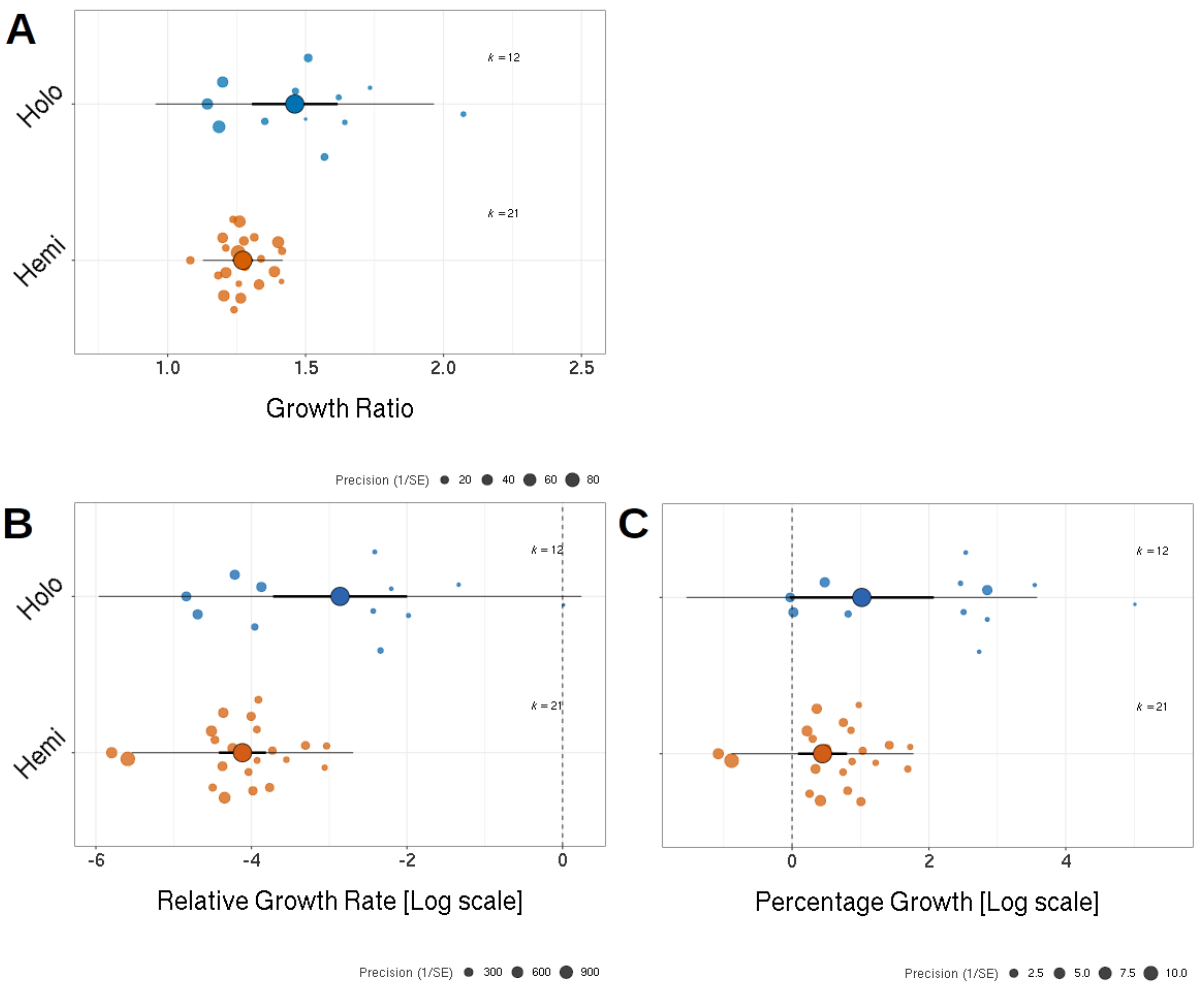

Figure 2: The mean growth estimates among hemi- versus holometabolous insects calculated as (A) Growth Ratio (GR = 0.1883; 95% CI = 0.0286, 0.3480), (B) Relative Growth Rate per day (RGR = 0.0548; 95% CI = 0.0109, 0.0986) and (C) Percentage Growth per day (RGR = 7.9303; 95% CI = 2.4871, 13.3734). The point position on the x-axis corresponds to the mean growth estimate with 95% confidence (bold error bars) and prediction intervals (thin error bars). Each point without a black border represents the values of a particular insect (scaled by their precision). **Note**: The Relative Growth Rate and the Percentage Growth per day are plotted on a log scale.

Table 2: The regression analysis results controlled for phylogeny (phylogenetic linear mixed-effects models with specified variance structure by modelling heteroscedasticity) testing differences in GR, RGR and PGR between hemi- and holometabolous insects.

Growth estimate		Estimate	SE	T-value	Df	P-value	Lower CI	Upper CI	
GR	Intercept	1.272	0.018	70.276	31	<.0001	1.236	1.309	***
	Hemi_Holo	0.188	0.078	2.404	31	0.022	0.029	0.348	*
RGR	Intercept	0.018	0.002	7.922	31	<.0001	0.013	0.022	***
	Hemi_Holo	0.055	0.022	2.548	31	0.016	0.011	0.099	*
PGR	Intercept	2.074	0.265	7.813	31	<.0001	1.532	2.615	***
	Hemi_Holo	7.930	2.669	2.971	31	0.006	2.487	13.373	**

Table 3: Results of the Breusch-Pagan test for heteroscedasticity (heterogeneity of variances) using the *ncvTest* function from the R package car and the percentage of total variation due to heterogeneity from the phylogenetic intercept models using the *i2_ml* function from the orchaRd package.

Growth estimate	Breusch-Pegan test				Extent of heterogeneity (I^2)		
	X^2	Df	P-value		Total I^2 [%]	I^2 due to phylogeny [%]	I^2 due to species ID [%]
GR	16.247	1	5.5601e-05	***	93.63	46.82	46.82
RGR	28.572	1	9.0266e-08	***	96.57	48.28	48.28
PGR	28.685	1	8.5155e-08	***	99.17	49.59	49.59

Growth periods

Mean GP per day of holometabolous insects was significantly greater than of hemimetabolous insects (Mean GP = -11.0502; 95% CI = -16.8393, -5.2611; figure 3; see supplementary table 6). The heterogeneity was high (I^2 = 98.99%), with 49.49% of the variance explained by phylogeny and differences between species. The amount of variation in beta-diversity attributed to the type of

metamorphosis was 40.31% (R^2). The Total GP were not significantly different when comparing hemi- and holometabolous insects (Two-sample t-test, t = 2.1163, df = 10.805, p-value = 0.05838; figure 3), but showed a trend of shorter Total GP in holometabolous than hemimetabolous insects. The five fastest species were all holometabolous (see supplementary table 10).

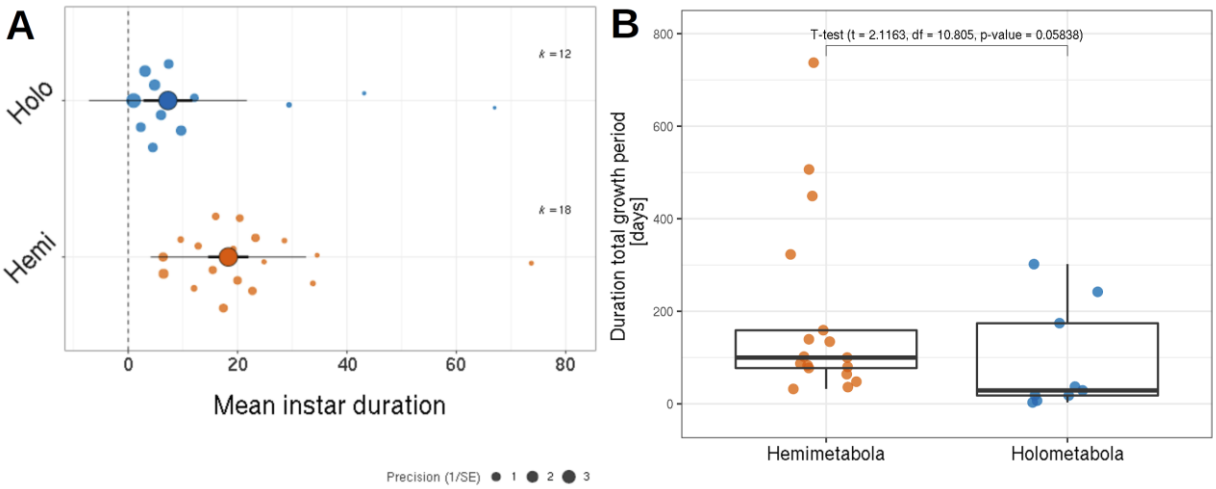

Figure 3: Developmental times for hemi- versus holometabolous insects calculated as (A) Mean Instar Durations (Mean GP = -11.0502; 95% CI = -16.8393, -5.2611) with 95% confidence (bold error bars) and prediction intervals (thin error bars) and (B) Total Instar Durations (Total GP; Two-sample t-test, t = 2.1163, df = 10.805, p-value = 0.05838). Each point represents a particular insect species. **Note**: The orchard plot (panel A) is generally used to visualize the results of a model that incorporates sampling variance (the square of SE) and is, therefore, not used for visualizing the Total Instar Durations, which is the sum of all instar durations (first to the last instar) for each species without variability. The variability was not reported in the reviewed literature most of the time.

Discussion

We investigated growth ratios and rates, comparing 33 species from three holo- and seven hemimetabolous insect orders. We found a clear pattern: holometabolous insects show faster larval growth and much higher growth estimates variability than hemimetabolous insects. We also found

much shorter growth periods of the immature stages in holometabolous than hemimetabolous insects.

Our results show that the five fastest species are all holometabolous. We found the highest growth in all three growth estimates and the shortest mean instar duration in the blowfly *Lucilia sericata*. *L. sericata* belongs to the Diptera, the youngest order of insects (Misof et al., 2014) that evolved a worm-like larva that can exploit food resources by burrowing into foods reducing the energy costs involved in finding food (Maddrell, 2018). In addition, *L. sericata* larvae feed on a nutrient-rich meat diet facilitating fast growth (Clark, Evans, & Wall, 2006; Green, Simmonds, & Blaney, 2003). The rates of most physiological processes in insects are highly dependent on environmental conditions such as temperature. We found the lowest RGR and PGR and the most prolonged mean instar duration in the geometrid moth *Epilobophora sabinata teriolensis*, the only species reared under shady and cold conditions. In a study of a lepidopteran species from the same family, *Epimecis hortaria*, Niesenbaum & Kluger (2006) found lower leaf consumption in larvae that feed in cold conditions compared to larvae feed at warmer temperatures in a laboratory experiment. *E. hortaria* larvae in the field that consumed leaves from shade environments had lower conversion efficiencies than their counterparts feeding on leaves in the sunlight. In a study on another geometrid moth, *Ascotis selenaria*, (San Choi & Kim, 2014) identified a decrease in total development times of larvae with increasing temperature.

Within hemimetabolous insects, we found the lowest growth ratio and rates in the walkingstick *Dixippus morosus* (Phasmatodea). The longest insect known, *Phobaeticus chani* from Borneo, which reaches 567 mm, belongs to Phasmatodea (Whitman, 2008). Phasmids can be several times longer than their closely related Orthoptera of the same body weight. Nentwig (1990) identified a

three-fold body length in stick insects, including *D. morosus*, compared to *Acheta domesticus*, a cricket of the same body weight. *A. domesticus,* like all other orthopteran species in our study, showed median growth rates and ratios. The giant waterbug *Limnogeton fieberi* (Hemiptera) showed the greatest PGR, and the dragonfly *Erythemis simplicicollis* (Odonata) had the greatest RGR, second greatest PGR, and shortest mean instar duration. Both are aquatic insects that finish post-embryonic growth within one summer season. They are therefore time constrained.

Fast larval growth seems to be a general pattern within holometabolous but not hemimetabolous insects. One possible explanation for the great variability in growth ratio and rates in holometabolous larvae is that they may respond more plastic to suboptimal environmental conditions than hemimetabolous instars. Lepidopteran larvae compensated for starvation by increasing their relative growth rates (Tammaru et al., 2004). The bean weevil *Bruchidius atrolineatus* underwent a facultative diapause when the pods of their host plant were unavailable and remained in diapause when the relative humidity was low (Lenga, Glitho, & Huignard, 1993). The fruit fly *Drosophila suzukii* can lay eggs and thrive at temperatures more than half as low as their optimum at 26-28°C (Little, Chapman, & Hillier, 2020; Tonina, Mori, Giomi, & Battisti, 2016). *D. suzukii* has a high developmental success at a temperature range from 13 to 30°C and decreased their larval duration from 30 to 10 days in this temperature range (Winkler, Jung, Kleinhenz, & Racca, 2020). A species that is able to adapt to a range of environmental conditions can more readily become established in novel habitats.

Also, shorter mean instar duration and shorter total developmental time of the immature stages within holometabolous but not hemimetabolous insects seem to be a general pattern. Honěk and Kocourek (1990) found that relative durations of developmental stages were typical in orders of

holometabolous insects. Shorter embryonic and larval stages compensated for longer pupal durations. They discuss that the relative length of the larval stage may differ according to the trophic specialization. Insects which feed on low energy content take a more considerable proportion of the total development for the larval stage. The second cause they discuss is the degree of morphological change within a developmental stage. A greater amount of morphogenesis requires relatively longer development. Honěk and Kocourek (1990) also found more extended embryonic development in hemimetabolous than holometabolous insects. The greater amount of morphogenesis may require longer embryonic development in hemimetabolous insects. Shorter developmental times may reduce predation risk and benefit the exploitation of ephemeral habitats. Lindstedt et al. (2019) discuss that holometabolous insect's trade-off predation risk by wandering less when the pupal stage is shorter. They also discuss that the immobile pupae are not defenceless. They have evolved a wide range of antipredator strategies, including cryptic colouration (camouflage, mimicry), hiding in vegetation or soil, chemical camouflage or bluffing (deimatic) movements and sounds (Lindstedt et al., 2019).

Body size and development time are essential life-history traits. Fecundity, for example, correlates positively with adult size (Alois Honěk, 1993). As growth in insects only occurs in the immature stages, the final size of the last instar determines adult size. Due to decoupled growth and differentiation, the decreased morphogenesis in the immature stages of holometabolous insects increases allocation to growth, facilitating fast larval growth. Fast growth allows for efficient and competitive exploitation of ephemeral resources. It allows reaching the developmental threshold, predicted by Day and Rowe (2002), for the minimum size or level of condition needed for the transition, such as the final juvenile moult, earlier. That allows organisms to reach a steeper point

on Day and Rowes (2002) predicted L-shaped reaction norm for size and age at the final moult, which predicts adult size. Support that insects trade-off growth and differentiation comes from the Diptera, *Drosophila melanogaster*. The body size of *D. melanogaster* increases as temperature decreases due to increased cell size rather than cell number (Partridge, Barrie, Fowler, & French, 1994).

Our results align with the findings of fast larval growth in holometabolous compared to hemimetabolous insects by Cole (1980) and improve the findings by implementing a rigorous phylogeny to the analysis. We further identified higher variability and shorter instar durations in holometabolous than hemimetabolous insects. Our results support the decoupling hypothesis, which proposes that growth is confined to the larval stage, while most differentiation occurs in the pupa (Arendt, 1997; Rolff et al., 2019), facilitating fast larval growth and short larval durations, an effect observed in holometabolous but not in hemimetabolous insects. Fast larval growth could be a selective factor for decoupling growth and differentiation, ultimately resulting in the evolution of the pupa in holometabolous insects.

Acknowledgements

We are grateful to Mathias Franz for feedback. This research was funded by the DFG (Deutsche Forschungsgemeinschaft).

References

Aldaz, S., & Escudero, L. M. (2010). Imaginal discs. *Current Biology, 20*(10), R429-31. doi: 10.1016/j.cub.2010.03.010

Arendt, J. D. (1997). Adaptive Intrinsic Growth Rates: An Integration Across Taxa. *The Quarterly Review of Biology*, *72*, 29.

Berenbaum, M. (2017). Insect Biodiversity – Millions and Millions. In *Insect Biodiversity* (pp. 783–792). John Wiley & Sons, Ltd. doi: 10.1002/9781118945568.ch25

Chapman, R. F. (2013). *The Insects—Structure and function* (5th ed.). Cambridge University Press.

Cinar, O., Nakagawa, S., & Viechtbauer, W. (2021). Phylogenetic multilevel meta-analysis: A simulation study on the importance of modelling the phylogeny. *Methods in Ecology and Evolution*, *12*(1), 4–12. doi: 10.1111/2041-210X.13760

Clark, K., Evans, L., & Wall, R. (2006). Growth rates of the blowfly, Lucilia sericata, on different body tissues. *Forensic Science International*, *156*(2), 145–149. doi: 10.1016/j.forsciint.2004.12.025

Cole, B. J. (1980). Growth Ratios in Holometabolous and Hemimetabolous Insects. *Annals of the Entomological Society of America*, *73*(4), 489–491. doi: 10.1093/aesa/73.4.489

Costa, F. A. P. L., & Gomes-Filho, A. (2002). Using body length measurements to study larval growth: A lepidopteran example. *Neotropical Entomology*, *31*(2), 177–180. doi: 10.1590/S1519-566X2002000200002

Day, T., & Rowe, L. (2002). *Developmental Thresholds and the Evolution of Reaction Norms for Age and Size at Life-History Transitions*. 13.

Dutilleul, P., & Legendre, P. (1993). Spatial Heterogeneity against Heteroscedasticity: An Ecological Paradigm versus a Statistical Concept. *Oikos*, *66*(1), 152–171. doi: 10.2307/3545210

Fox, J., Weisberg, S., & Price, B. (2021). Companion to Applied Regression (Version 3.0-12).

Grafen, A. (1989). The Phylogenetic Regression. *Philosophical Transactions of the Royal Society of London. B, Biological Sciences*, *326*(1233), 119–157.

Green, P. W. C., Simmonds, M. S. J., & Blaney, W. M. (2003). Diet nutriment and rearing density affect the growth of black blowfly larvae, Phormia regina (Diptera: Calliphoridae). *European Journal of Entomology*, *100*(1), 39–42. doi: 10.14411/eje.2003.008

Grimaldi, D., & Engel, M. S. (2005). *Evolution of the Insects*. Cambridge University Press.

Hall, M. J. R., & Martín-Vega, D. (2019). Visualization of insect metamorphosis. *Philosophical Transactions of the Royal Society B: Biological Sciences*, *374*(1783), 20190071. doi: 10.1098/rstb.2019.0071

Hammer, T. J., & Moran, N. A. (2019). Links between metamorphosis and symbiosis in holometabolous insects. *Philosophical Transactions of the Royal Society B: Biological Sciences*, *374*(1783), 20190068. doi: 10.1098/rstb.2019.0068

Higgins, J. P. T. (2003). Measuring inconsistency in meta-analyses. *BMJ*, *327*(7414), 557–560. doi: 10.1136/bmj.327.7414.557

Hinton, H. E. (1948). On the Origin and Function of the Pupal Stage. *Transactions of the Royal Entomological Society of London*, *99*(12), 395–409. doi: https://doi.org/10.1111/j.1365-2311.1948.tb01227.x

Honěk, A., & Kocourek, F. (1990). Temperature and development time in insects: A general relationship between thermal constants. *Zoologische Jahrbücher, Abteilung Für Systematik, Ökologie Und Geographie Der Tiere*, *117*(4), 401–439.

Honěk, Alois. (1993). Intraspecific Variation in Body Size and Fecundity in Insects: A General Relationship. *Oikos*, *66*(3), 483–492. doi: 10.2307/3544943

Johnston, P. R., & Rolff, J. (2015). Host and Symbiont Jointly Control Gut Microbiota during Complete Metamorphosis. *PLOS Pathogens*, *11*(11), e1005246. doi: 10.1371/journal.ppat.1005246

Lenga, A., Glitho, I., & Huignard, J. (1993). Interactions between photoperiod, relative humidity and host-plant cues on the reproductive diapause termination in Bruchidius atrolineatus Pic

(Coleoptera Bruchidae). *Invertebrate Reproduction & Development*, *24*(2), 87–96. doi: 10.1080/07924259.1993.9672337

Little, C. M., Chapman, T. W., & Hillier, N. K. (2020). Plasticity Is Key to Success of Drosophila suzukii (Diptera: Drosophilidae) Invasion. *Journal of Insect Science*, *20*(3), 5. doi: 10.1093/jisesa/ieaa034

Lutz, D. A., & Huebner, E. (1980). *Development and cellular differentiation of an insect teleotrophic ovary (Rhodnius prolixus)*. *12*(4), 773–794. doi: 10.1016/0040-8166(80)90029-4

Maddrell, S. H. P. (2018). How the simple shape and soft body of the larvae might explain the success of endopterygote insects. *The Journal of Experimental Biology*, *221*(11), jeb177535. doi: 10.1242/jeb.177535

Manthey, C., Johnston, P., & Rolff, J. (2021). *Complete metamorphosis and microbiota turnover in insects* [Preprint]. Evolutionary Biology. doi: 10.1101/2021.06.15.448481

Misof, B., Liu, S., Meusemann, K., Peters, R. S., Donath, A., Mayer, C., … Zhou, X. (2014). Phylogenomics resolves the timing and pattern of insect evolution. *Science*, *346*(6210), 763–767. doi: 10.1126/science.1257570

Mora, C., Tittensor, D. P., Adl, S., Simpson, A. G. B., & Worm, B. (2011). How Many Species Are There on Earth and in the Ocean? *PLoS Biology*, *9*(8), e1001127. doi: 10.1371/journal.pbio.1001127

Nakagawa, S., Lagisz, M., O'Dea, R. E., Rutkowska, J., Yang, Y., Noble, D. W. A., & Senior, A. M. (2020). The orchard plot: Cultivating a forest plot for use in ecology, evolution, and beyond. *Research Synthesis Methods*, *12*(1), 4–12. doi: 10.1002/jrsm.1424

Nakagawa, S., & Schielzeth, H. (2013). A general and simple method for obtaining R2 from generalized linear mixed-effects models. *Methods in Ecology and Evolution*, *4*(2), 133–142. doi: 10.1111/j.2041-210x.2012.00261.x

Nentwig, W. (1990). Stick insects (Phasmida) as prey of spiders: Size, palatability and defence mechanisms in feeding tests. *Oecologia*, *82*(4), 446–449. doi: 10.1007/BF00319784

Nicholson, D. B., Ross, A. J., & Mayhew, P. J. (2014). Fossil evidence for key innovations in the evolution of insect diversity. *Proceedings of the Royal Society B: Biological Sciences*, *281*(1793), 20141823–20141823. doi: 10.1098/rspb.2014.1823

Niesenbaum, R. A., & Kluger, E. C. (2006). When Studying the Effects of Light on Herbivory, Should One Consider Temperature? The Case of <I>Epimecis hortaria</I> F. (Lepidoptera: Geometridae) Feeding on <I>Lindera benzoin</I> L. (Lauraceae). *Environmental Entomology*, *35*(3), 600–606. doi: 10.1603/0046-225X-35.3.600

Partridge, L., Barrie, B., Fowler, K., & French, V. (1994). Evolution and development of body size and cell size in Drosophila melanogaster in response to temperature. *Evolution*, *48*(4), 1269–1277.

R Core Team. (2020). *R: A language and environment for statistical computing.* Vienna, Austria: R Foundation for Statistical Computing. Retrieved from https://www.R-project.org/

Rolff, J., Johnston, P. R., & Reynolds, S. (2019). Complete metamorphosis of insects. *Philosophical Transactions of the Royal Society B: Biological Sciences*, (374). doi: 10.1098/rstb.2019.0063

San Choi, K., & Kim, D.-S. (2014). Temperature-dependent development of Ascotis selenaria (Lepidoptera: Geometridae) and its stage emergence models with field validation. 66, 72–79.

Sehnal, F. (1985). Morphology of Insect Development. *Annual Review of Entomology*, *30*(1), 89–109. doi: 10.1146/annurev.en.30.010185.000513

Senior, A. M., Grueber, C. E., Kamiya, T., Lagisz, M., O'Dwyer, K., Santos, E. S. A., & Nakagawa, S. (2016). Heterogeneity in ecological and evolutionary meta-analyses: Its magnitude and implications. *Ecology*, *97*(12), 3293–3299. doi: 10.1002/ecy.1591

Siegel, S. (1957). Nonparametric Statistics. *The American Statistician*, *11*(3), 13–19. doi: 10.1080/00031305.1957.10501091

Tammaru, T., Nylin, S., Ruohomäki, K., & Gotthard, K. (2004). Compensatory responses in lepidopteran larvae: A test of growth rate maximisation. *Oikos*, *107*(2), 352–362. doi: 10.1111/j.0030-1299.2004.13363.x

Tonina, L., Mori, N., Giomi, F., & Battisti, A. (2016). Development of Drosophila suzukii at low temperatures in mountain areas. *Journal of Pest Science*, *89*(3), 667–678. doi: 10.1007/s10340-016-0730-2

Truman, J. W. (2019). The Evolution of Insect Metamorphosis. *Current Biology*, *29*(23), R1252–R1268. doi: 10.1016/j.cub.2019.10.009

Whiting, M. F. (2004). Phylogeny of the holometabolous insects. In *Assembling the tree of life* (pp. 345–359).

Whitman, D. W. (2008). The significance of body size in the Orthoptera: A review. *Journal of Orthoptera Research*, *17*(2), 117–134. doi: 10.1665/1082-6467-17.2.117

Winkler, A., Jung, J., Kleinhenz, B., & Racca, P. (2020). A review on temperature and humidity effects on Drosophila suzukii population dynamics. *Agricultural and Forest Entomology*, *22*(3), 179–192. doi: 10.1111/afe.12381

Yang, A. S. (2001). Modularity, evolvability, and adaptive radiations: A comparison of the hemi- and holometabolous insects. *Evolution and Development*, *3*(2), 59–72. doi: 10.1046/j.1525-142x.2001.003002059.x

CHAPTER V: GENERAL DISCUSSION

In this thesis, I investigated two barely studied adaptive hypotheses explaining the evolution of the pupal stage in insects with complete metamorphosis. The first hypothesis I studied predicts a microbial change in insects with complete metamorphosis due to the pupa's drastic morphological changes that include the remodelling of the gut, facilitating niche shifts. I investigated beta and alpha diversity throughout development, comparing 18 insect species from four holo- and three hemimetabolous insect orders and found a clear pattern: holometabolous insects show a substantial microbial turnover between larvae and adults. In contrast, this is not found in hemimetabolous insects (**chapter II**). I also studied if the microbial turnover is under control of the host gut immunity and investigated the gut immune effector expression in two holo- and a hemimetabolous insect in the absence of an infection. I found high read count abundances of differentially expressed immune effectors at the larval-pupal moult of the holometabolous insects. No such high abundances were observed at the nymphal-adult moult in the hemimetabolous insect (**chapter III**). The second and not mutually exclusive hypothesis I investigated is the decoupling of growth and differentiation in holometabolous insects, which supposes that most growth is confined to the larval stage, while most differentiation occurs in the pupal stage, facilitating fast larval growth. I studied growth ratios and rates, comparing 33 species from three holo- and seven hemimetabolous insect orders and found a clear pattern: holometabolous insects showed fast larval growth and much higher growth estimates variability than hemimetabolous insects. I also found much shorter developmental times of the immature stages in holometabolous than hemimetabolous insects (**chapter IV**).

The pupa, intercalated between the holometabolous larva and adult, is a distinctive life stage in the animal kingdom of which almost nothing is known compared to larvae and adults. In the immobile,

non-feeding pupa, all larval organs, including the gut, are broken down and reconstructed (Hall & Martín-Vega, 2019; Hinton, 1948). The remodelling in the pupal stage includes both autophagocytosis (degradation of cells) and apoptosis (programmed cell death) (Tettamanti & Casartelli, 2019). This complete metamorphosis specified to the pupa leads to distinct larval (growing) and adult (dispersal and reproductive) life stages.

Microbiota Turnover

Complete metamorphosis allows holometabolous insects to drive an almost complete change between the larval and adult microbiota giving the insect the unique opportunity to acquire specialised symbionts for a life-stage specific diet, ecology and physiology (Hammer & Moran, 2019; Rolff et al., 2019).

A change in microbial composition throughout development was also reported in anurans, another group of animals that undergo profound changes throughout their development (Lofts, 1976). Chai et al. (2018) showed changes in the gut microbiota throughout the development of the asiatic toad *Bufo gargarizans*. The bacterial diversity was higher in the aquatic tadpole compared to the terrestrial juvenile toad. Chai et al. (2018) discussed that this decrease could be shaped by morphological, physiological, and even behavioural characteristics that evolved along with the varied feeding strategies in the various life stages. The tadpole of *B. gargarizans* is a plant-feeding stage, while the juvenile toad digests its tail and needs no extra food during the metamorphic climax. This finding coincides with Vences et al. (2016), who identified tadpoles' gut bacterial diversities as double that of adults in 12 tropical anuran species. They also found tadpole microbiomes from distinct geographic regions to be more similar than the microbiomes from aquatic tadpoles compared to terrestrial adults from the same region. During anuran metamorphosis, the gut is shortened, and its coils are rearranged (Pretty, Naitoh, & Wassersug,

1995). The gut structure in anurans seems to be strongly shaped by diet. Altig & Kelly (1974) found shorter and less voluminous guts in carnivorous than herbivorous tadpoles. In contrast, holometabolous insects can but do not necessarily change their habitat or diet throughout development yet still change their microbiota during complete metamorphosis (e.g. chapter II, all insects were terrestrial throughout the development). Diet changing Holometabola are Lepidoptera, for instance, with leave-feeding larvae and nectar-feeding adults. Several Lepidoptera species lack functional mouthparts and do not feed as adults (Altermann and Pearse, 2011). Both in insects and in anurans, hormonal systems play a very important role in these processes (Laudet, 2011). Unlike holometabolous insects, anurans remain active during metamorphosis and gradually metamorphose from omnivorous suspension (Altig and McDiarmid 1999) to carnivorous feeders.

Immune Gene Expression

Complete metamorphosis also induces the expression of immune effectors in the insect's gut as a prophylactic effect against bacterial infection. Findings by Johnston et al. (2019) of high immune effector expressions in holometabolous but not hemimetabolous insects during metamorphosis are consistent with the results of chapter III. This immune effector expression only induced by complete metamorphosis is an adaptive response in holometabolous insects that controls gut colonisation (Schmidt & Engel, 2021) and shapes the gut microbial composition.

Johnston & Rolff (2015) experimentally showed that pathogenic bacteria are reduced by several orders of magnitude during complete metamorphosis. It is also known that the remodelling of the gut eradicates viruses (Bird, 1953). Bird (1953) showed that the prepupal stage of the European spruce sawfly *Gilpinia hercyniae* is immune to infection by polyhedral (many-sided) viruses. The virus multiplies only in the nuclei of the digestive cells of the midgut epithelium. During complete metamorphosis, these are replaced by embryonic cells not susceptible to infection, although they

develop into digestive cells eventually. However, it is unknown if antiviral peptides (AVP) are also induced at the onset of complete metamorphosis as a prophylactic effect against viral infection. In a review, Feng et al. (2020) report on AVPs in holometabolous insects. Some AVPs were insect AMPs with antiviral activity, of which some were also identified in chapter III (e.g. cecropin and diptericin).

Complete eradication of the gut microbiota comes with the risk of losing beneficial symbionts (Johnston & Rolff, 2015), which would result in a cost to both the host and the symbiont. To overcome this hurdle, insects transmit some beneficial symbionts vertically and store them in specialised tissue during complete metamorphosis (Stoll, Feldhaar, Fraunholz, & Gross (2012); Maire et al. (2020); Kaltenpoth, Yildirim, Gürbüz, Herzner, & Strohm, 2012; Kikuchi, Hosokawa, & Fukatsu, 2011).

Other factors shaping the microbial composition

However, there is an alternative and not mutually exclusive view that the microbial gut composition does not solely result from drastic morphological transformations and heritable symbionts but rather from a combination of several factors. Engel & Moran (2013) also discussed host habitat, host diet and social interactions influencing insects' gut microbial composition. Yun et al. (2014), for instance, studied insect species of 21 taxonomic orders and found that the environmental habitat (underground, ground, aquatic, sky) in which the host lives as well as its diet (herbivore, carnivore, scavenger, omnivore) shape the gut microbiota. Nevertheless, their results would give a more robust pattern with higher numbers of within-species replication (305 insect specimens representing 218 species). Chandler, Morgan Lang, Bhatnagar, Eisen, & Kopp (2011) found that diet in a range of *Drosophila* species, comprising cactus, flower, fruit and mushroom feeding species, shapes the adult gut microbiota within a taxonomically restricted selection of microbes.

Fast larval growth

Another not mutually exclusive explanation for the evolution complete metamorphosis is the decoupling growth and differentiation hypothesis, which poses that intercalating the pupal stage confines most growth to the larval and most differentiation to the pupal life stage. Fast growth could be a selective factor for the evolution of this decoupling and hence the evolution of the pupa. The findings of fast larval growth in holometabolous compared to hemimetabolous insects in chapter IV support the hypothesis that growth and differentiation are decoupled in holometabolous insects (Arendt, 1997; Rolff et al., 2019). The worm-like larva (Maddrell, 2018) is a specialised feeding and growing life stage in holometabolous insects, facilitating fast larval growth (Rolff, 2019). The findings of chapter IV coincide with Cole (1980), who detected significantly greater median growth ratios in holometabolous than hemimetabolous insects and improved his findings by implementing a rigorous phylogeny to the analysis. Further, I included growth periods in the calculations of growth estimates. Body length as a measure of size was used exclusively and systematically searched on ZOBODAT, the Zoological-Botanical Database (www.zobodat.at; Malicky and Aubrecht, 2001), which contains digitised literature on insect studies from Austria, to a lesser extent, Germany, reducing geographic variance. Fast growth allows an organism to become larger (Day & Rowe; Rolff, 2019). Adult size correlates positively with fecundity (Honěk, 1993), a fitness advantage determined by the size at metamorphosis when holometabolous insects stop feeding. Also, maturation is reached at the final adult moult in insects (Rewitz, Yamanaka, & O'Connor, 2013)

In contrast to insects with complete metamorphosis and like hemimetabolous metamorphosis, anurans' metamorphosis consists of growth and differentiation at a time (Smith-Gill & Berven, 1979). In anurans, a group of animals that metamorphose gradually (Gosner, 1960), large larvae at metamorphosis turn mostly into large adults (Berven, 1990; Werner, 1996) but also examples of

an inverse relationship between size at metamorphosis and adult size are known (Pomeroy, 1981). However, growth (Werner, 1986) and the maturation of gonads (Ogielska & Kotusz, 2004) also continue after the metamorphic climax in anurans and are influenced by environmental factors such as low- and highland habitats (Miaud et al., 1998). Postmetamorphic growth in the terrestrial habitat accounts for at least 80% of the adult size (Werner, 1986). Werner (1996) suggests that fast larval growth in anurans is caused by size-specific predation on larval anurans. Faster-growing larvae spend less time in this more-vulnerable stage, decreasing the risk of death.

Metamorphosis

Since the symposium at the 2006 Society for Integrative and Comparative Biology (SICB) annual meeting in Orlando, FL (USA), there have been defined criteria for metamorphosis. Bishop et al. (2006) elaborated on similarities of various definitions of metamorphosis. The three main similarities across most of the definitions are that (i) metamorphosis includes a major morphological change, (ii) a change in the adaptive landscape, and (iii) the pre-metamorphic stage is post-embryonic (Bishop et al., 2006).

Metamorphosis is a widespread phenomenon in the animal kingdom that evolved several times independently (Laudet, 2011; E. E. Werner, 1988). Many evolutionary events in the diversification of life have been associated with the origin, persistence, or loss of metamorphosis (Moran, 1994). However, the extent to which the metamorphosis machinery is deployed separates the different animal taxa, with holometabolous insects having the most dramatic and abrupt transformation, which occurs in a unique stage: the pupa. Holometabolous insects are a monophyletic group (Misof, 2014) and Holometaboly is considered an evolutionary key innovation explaining insect diversity (Mayhew, 2007; Rainford, Hofreiter, Nicholson, & Mayhew, 2014; but see Condamine, Clapham, & Kergoat, 2016).

It is commonly thought that metamorphosis has evolved to decouple different life stages, such that larvae and adults can evolve independently of each other in response to different selection pressures (Werner 1988; Ebenman 1992; Moran 1994). Metamorphosis can be seen as an adaptation to different resources, particularly food and habitat (Truman & Riddiford, 1999). For instance, it enables an animal to exploit two different food resources throughout development. These adaptations allow for life-stage specific tasks (Moran 1994) such as feeding, growth, maturation and dispersal. The larva and adult of metamorphosing animals are distinct developmental and independently evolvable modules allowing the divergent evolution of stage-specific specialisations (Yang, 2001 and references therein). Also, metamorphosis can reduce niche overlap by shifts in diet, habitat, behaviour, and the timing of life-history events (Wilbur, 1980). The niches of two species may overlap in one stage of their life cycles but not in another. The facilitation of niche shifts by changes in the gut microbiota in Holometabola could be considered an essential driver of the evolution of complete metamorphosis. However, the microbiota turnover could also be driven by other selective factors such as growth rate (Rolff et al., 2019). Fast larval growth could be a selective factor for decoupling growth and differentiation, which ultimately results in the evolution of the pupal stage in holometabolous insects and, therefore, in distinct developmental and independently evolvable modules within one species.

In insects and amphibians, metamorphosis has persisted over long periods of evolutionary time. Ten Brink et el., (2019) showed that metamorphosis, once evolved, is a robust and hard-to-loss life-history strategy.

Outlook

Aquatic insects

Regarding the view that a combination of several factors influences the gut microbial composition of insects (Engel & Moran, 2013), selection for a microbiota turnover could be more extreme in insects that, additionally to complete metamorphosis, experience completely different ecological conditions over ontogeny. Moran & Engel (2013) discuss host habitat, host diet, heritable symbionts, and social interactions to influence the microbial composition. The insects studied in chapter II experienced similar environmental (terrestrial) challenges. Other insects, such as aquatic insects, shift from aquatic immature to terrestrial adult life stages, suggesting a more substantial microbial change than insects that do not experience such a habitat shift. To my knowledge, only very few studies investigated the temporal dynamics of the microbiota in aquatic insects. Nobles & Jackson (2020) showed that dragonfly species' aquatic larvae (sometimes called naiads) differ in gut microbial composition from their terrestrial adult stages. Larvae of different species were more similar than the larvae and adults of the same species. However, when comparing aquatic holometabolous versus aquatic hemimetabolous insects, the Holometabola presumably have a stronger change in the microbial composition due to the drastic reconstructions during complete metamorphosis, supporting the notion that complete metamorphosis alone drives a change in the microbial composition.

Testing the adaptive value of complete metamorphosis by reducing the microbiota turnover

The adaptive advantage of complete metamorphosis could be tested by experimentally lowering the gut microbiota changes over ontogeny using faecal transplantation. Transplanting the larval gut microbiome into the adult holometabolous life stage would mimic the temporal microbial dynamics of a hemimetabolous insect. When feeding on an adult diet, specimens with a larval microbiome

as adults would presumably have a reduced fitness than those with the adult microbiome transplanted. Such experimental studies could confirm the facilitation of niche shifts by gut microbial changes as an adaptive advantage of complete metamorphosis.

Cost of metamorphosis: heritable symbionts

As mentioned above, complete eradication of the gut microbiota comes with the risk of losing beneficial symbionts (Johnston & Rolff, 2015), resulting in a cost to the host and the symbiont. To overcome this hurdle, insects evolved various strategies to transmit beneficial symbionts vertically, a consequence of holometaboly. They store them in specialised tissue, such as bacteriocytes (Stoll, Feldhaar, Fraunholz, & Gross, 2012; Maire et al., 2020), antennal glands (Kaltenpoth, Yildirim, Gürbüz, Herzner, & Strohm, 2012) or crypts (Kikuchi, Hosokawa, & Fukatsu, 2011) during complete metamorphosis. Presumably, the transmission strategies of heritable symbionts between life stages are more diverse in holometabolous than hemimetabolous insects due to the radical remodelling of the larval anatomy during complete metamorphosis, causing higher costs of vertically transmitting heritable symbionts. In a comparative study (e.g. conducted as a literature review), such differences as a consequence of holometaboly could be demonstrated. Alternatively, Hammer & Moran (2019) suggest that holometabolous insects may be less likely to evolve strictly vertically transmitted symbioses than hemimetabolous insects.

Conclusion

2500 years ago, Aristotle was the first describing a notion about insect metamorphosis (Reynolds, 2019). More than 300 years ago, Maria Sybilla Merian was the first person who described complete metamorphosis using the transition from a caterpillar to a butterfly in detail (Merian, 2017). Compared to the larval and adult stages, the pupa seemed not well understood for a long time in history. Today, we know lots about the developmental biology of the pupal stage but still almost

nothing about its adaptive value. However, by investigating two adaptive hypotheses about the evolution of the pupal stage, this thesis puts more light on the adaptive value of complete metamorphosis. My thesis showed a microbiota turnover in holometabolous but not hemimetabolous insects during metamorphosis, facilitating niche shifts. Also, complete metamorphosis alone induced an immune response as an adaptive response. By decoupling growth and differentiation, the pupa allowed fast larval growth in holometabolous but not hemimetabolous insects. These results present a reasonable basis for further studying different aspects of the evolution of complete metamorphosis in insects, such as described above.

References

Altermatt, F., & Pearse, I. S. (2011). Similarity and specialization of the larval versus adult diet of European butterflies and moths. *The American Naturalist*, *178*(3), 372-382.

Altig, R., & Kelly, J. P. (1974). Indices of Feeding in Anuran Tadpoles as Indicated by Gut Characteristics. *Herpetologica*, *30*(2), 200–203.

Altig, R., & McDiarmid, R. (1999). Body plan: development and morphology.

Arendt, J. D. (1997). Adaptive Intrinsic Growth Rates: An Integration Across Taxa. *The Quarterly Review of Biology*, *72*, 29.

Berven, K. (1990). Factors Affecting Population Fluctuations in Larval and Adult Stages of the Wood Frog (Rana Sylvatica). *Ecology*, *71*(4), 1599–1608. doi: 10.2307/1938295

Bird, F. T. (1953). The effect of metamorphosis on the multiplication of an insect virus. *Canadian Journal of Zoology*, *31*(3), 300–303. doi: 10.1139/z53-023

Bishop, C. D., Erezyilmaz, D. F., Flatt, T., Georgiou, C. D., Hadfield, M. G., Heyland, A., … Youson, J. H. (2006). What is metamorphosis? *Integrative and Comparative Biology*, *46*(6), 655–661. doi: 10.1093/icb/icl004

Chai, L., Dong, Z., Chen, A., & Wang, H. (2018). Changes in intestinal microbiota of Bufo gargarizans and its association with body weight during metamorphosis. *Archives of microbiology*, *200*(7), 1087-1099.

Chandler, J. A., Morgan Lang, J., Bhatnagar, S., Eisen, J. A., & Kopp, A. (2011). Bacterial Communities of Diverse Drosophila Species: Ecological Context of a Host–Microbe Model System. *PLoS Genetics*, *7*(9), e1002272. doi: 10.1371/journal.pgen.1002272

Cole, B. J. (1980). Growth Ratios in Holometabolous and Hemimetabolous Insects. *Annals of the Entomological Society of America*, *73*(4), 489–491. doi: 10.1093/aesa/73.4.489

Condamine, F. L., Clapham, M. E., & Kergoat, G. J. (2016). Global patterns of insect diversification: Towards a reconciliation of fossil and molecular evidence? *Scientific Reports*, *6*(1), 19208. doi: 10.1038/srep19208

Day, T., & Rowe, L. (2002). *Developmental Thresholds and the Evolution of Reaction Norms for Age and Size at Life-History Transitions*. 13.

Ebenman, B. (1992). Evolution in organisms that change their niches during the life cycle. *The American Naturalist*, *139*(5), 990-1021.

Engel, P., & Moran, N. A. (2013). The gut microbiota of insects – diversity in structure and function. *FEMS Microbiology Reviews*, *37*(5), 699–735. doi: 10.1111/1574-6976.12025

Feng, M., Fei, S., Xia, J., Labropoulou, V., Swevers, L., & Sun, J. (2020). Antimicrobial Peptides as Potential Antiviral Factors in Insect Antiviral Immune Response. *Frontiers in Immunology*, *11*. Retrieved from https://www.frontiersin.org/article/10.3389/fimmu.2020.02030

Gosner, K. L. (1960). A Simplified Table for Staging Anuran Embryos and Larvae with Notes on Identification. *Herpetologica*, *16*(3), 183–190.

Hall, M. J. R., & Martín-Vega, D. (2019). Visualization of insect metamorphosis. *Philosophical Transactions of the Royal Society B: Biological Sciences*, *374*(1783), 20190071. doi: 10.1098/rstb.2019.0071

Hammer, T. J., & Moran, N. A. (2019). Links between metamorphosis and symbiosis in holometabolous insects. *Philosophical Transactions of the Royal Society B: Biological Sciences*, *374*(1783), 20190068. doi: 10.1098/rstb.2019.0068

Hinton, H. E. (1948). On the Origin and Function of the Pupal Stage. *Transactions of the Royal Entomological Society of London*, *99*(12), 395–409. doi: https://doi.org/10.1111/j.1365-2311.1948.tb01227.x

Honěk, A. (1993). Intraspecific Variation in Body Size and Fecundity in Insects: A General Relationship. *Oikos*, *66*(3), 483–492. doi: 10.2307/3544943

Johnston, P. R., Paris, V., & Rolff, J. (2019). Immune gene regulation in the gut during metamorphosis in a holo- versus a hemimetabolous insect. *Philosophical Transactions of the Royal Society B: Biological Sciences*, *374*(1783), 20190073. doi: 10.1098/rstb.2019.0073

Johnston, P. R., & Rolff, J. (2015). Host and Symbiont Jointly Control Gut Microbiota during Complete Metamorphosis. *PLOS Pathogens*, *11*(11), e1005246. doi: 10.1371/journal.ppat.1005246

Kaltenpoth, M., Yildirim, E., Gürbüz, M. F., Herzner, G., & Strohm, E. (2012). Refining the Roots of the Beewolf-Streptomyces Symbiosis: Antennal Symbionts in the Rare Genus Philanthinus (Hymenoptera, Crabronidae). *Applied and Environmental Microbiology*, *78*(3), 822–827. doi: 10.1128/AEM.06809-11

Kikuchi, Y., Hosokawa, T., & Fukatsu, T. (2011). An ancient but promiscuous host–symbiont association between Burkholderia gut symbionts and their heteropteran hosts. *The ISME Journal*, *5*(3), 446–460. doi: 10.1038/ismej.2010.150

Laudet, V. (2011). The Origins and Evolution of Vertebrate Metamorphosis | Elsevier Enhanced Reader. *Current Biology*, *21*(18), 727–737. doi: 10.1016/j.cub.2011.07.030

Lofts, B. (1976). *Physiology of the Amphibia* (Vol. 3). Elsevier.

Maddrell, S. H. P. (2018). How the simple shape and soft body of the larvae might explain the success of endopterygote insects. *The Journal of Experimental Biology*, *221*(11), jeb177535. doi: 10.1242/jeb.177535

Maire, J., Parisot, N., Ferrarini, M. G., Vallier, A., Gillet, B., Hughes, S., … Heddi, A. (2020). Spatial and morphological reorganization of endosymbiosis during metamorphosis accommodates adult metabolic requirements in a weevil. *Proceedings of the National Academy of Sciences*, *117*(32), 19347–19358. doi: 10.1073/pnas.2007151117

Malicky, M., & Aubrecht, G. (2001). Die biogeographische Datenbank ZOBODAT (ehemalige ZOODAT) am OÖ. Landesmuseum/Biologiezentrum in Linz, Oberösterreich - eine öffentliche Einrichtung für Wissenschaft und Naturschutz im Umfeld nationaler und internationaler Kooperationsmöglichkeiten. — Entomologica Austriaca 4/2001: 8-14. *Entomologica Austriaca*, *4*, 8–14.

Mayhew, P. J. (2007). Why are there so many insect species? Perspectives from fossils and phylogenies. *Biological Reviews*, *82*(3), 425–454. doi: 10.1111/j.1469-185X.2007.00018.x

Merian, M. S., & Knibbeler, L. (2017). *Metamorphosis insectorum Surinamensium: 1705* (M. van Delft & H. Mulder, Eds.). Darmstadt: Lambert Schneider.

Miaud, C., Guyétant, R., & Elmberg, J. (1999). Variations in life-history traits in the common frog Rana temporaria (Amphibia: Anura): A literature review and new data from the French Alps. *Journal of Zoology*, *249*, 61–73. doi: 10.1111/j.1469-7998.1999.tb01060.x

Misof, B., Liu, S., Meusemann, K., Peters, R. S., Donath, A., Mayer, C., … Zhou, X. (2014). Phylogenomics resolves the timing and pattern of insect evolution. *Science*, *346*(6210), 763–767. doi: 10.1126/science.1257570

Moran, N. A. (1994). Adaptation and Constraint in the Complex Life Cycles of Animals. *Annual Review of Ecology and Systematics*, *25*(1), 573–600. doi: 10.1146/annurev.es.25.110194.003041

Nobles, S., & Jackson, C. R. (2020). Effects of Life Stage, Site, and Species on the Dragonfly Gut Microbiome. *Microorganisms*, *8*(2), 183. doi: 10.3390/microorganisms8020183

Ogielska, M., & Kotusz, A. (2004). Pattern and rate of ovary differentiation with reference to somatic development in anuran amphibians. *Journal of Morphology*, *259*(1), 41–54. doi: 10.1002/jmor.10162

Pomeroy, L. V. (1981). *Developmental polymorphism in the tadpoles of the spadefoot toad Scaphiopus multiplicatus.* (Dissertation, University of California, Riverside). University of California, Riverside. Retrieved from https://www.proquest.com/openview/b1e156578aa497ca7fd41b867e7713bb/1?pq-origsite=gscholar&cbl=18750&diss=y

Pretty, R., Naitoh, T., & Wassersug, R. J. (1995). Metamorphic shortening of the alimentary tract in anuran larvae (Rana catesbeiana). *The Anatomical Record*, *242*(3), 417–423. doi: 10.1002/ar.1092420314

Rainford, J. L., Hofreiter, M., Nicholson, D. B., & Mayhew, P. J. (2014). Phylogenetic Distribution of Extant Richness Suggests Metamorphosis Is a Key Innovation Driving Diversification in Insects. *PLoS ONE*, *9*(10), e109085. doi: 10.1371/journal.pone.0109085

Rewitz, K. F., Yamanaka, N., & O'Connor, M. B. (2013). Developmental Checkpoints and Feedback Circuits Time Insect Maturation. In *Current topics in developmental biology* (Vol. 103, pp. 1–33). Retrieved from https://www.ncbi.nlm.nih.gov/pmc/articles/PMC4060521/

Reynolds, S. (2019). Cooking up the perfect insect: Aristotle's transformational idea about the complete metamorphosis of insects. *Philosophical Transactions of the Royal Society B: Biological Sciences*, *374*(1783), 20190074. doi: 10.1098/rstb.2019.0074

Rolff, J., Johnston, P. R., & Reynolds, S. (2019). Complete metamorphosis of insects. *Philosophical Transactions of the Royal Society B: Biological Sciences*, (374). doi: 10.1098/rstb.2019.0063

Schmidt, K., & Engel, P. (2021). Mechanisms underlying gut microbiota–host interactions in insects. *Journal of Experimental Biology*, *224*(2), jeb207696. doi: 10.1242/jeb.207696

Smith-Gill, S. J., & Berven, K. A. (1979). Predicting Amphibian Metamorphosis. *The American Naturalist*, *113*(4), 563–585. doi: 10.1086/283413

Stoll, S., Feldhaar, H., Fraunholz, M., & Gross, R. (2012). Bacteriocyte dynamics during development of a holometabolous insect, the carpenter ant Camponotus floridanus. *BMC Microbiology*.

ten Brink, H., de Roos, A. M., & Dieckmann, U. (2019). The Evolutionary Ecology of Metamorphosis. *The American Naturalist*, *193*(5), E116–E131. doi: 10.1086/701779

Tettamanti, G., & Casartelli, M. (2019). Cell death during complete metamorphosis. *Philosophical Transactions of the Royal Society B: Biological Sciences*, *374*(1783). doi: 10.1098/rstb.2019.0065

Truman, J. W., & Riddiford, L. M. (1999). *The origins of insect metamorphosis*. *401*, 6.

Vences, M., Lyra, M. L., Kueneman, J. G., Bletz, M. C., Archer, H. M., Canitz, J., … Glos, J. (2016). Gut bacterial communities across tadpole ecomorphs in two diverse tropical anuran faunas. *The Science of Nature*, *103*(3), 25. doi: 10.1007/s00114-016-1348-1

Werner, E. E. (1988). Size, Scaling, and the Evolution of Complex Life Cycles. In B. Ebenman & L. Persson (Eds.), *Size-Structured Populations* (pp. 60–81). Berlin, Heidelberg: Springer. doi: 10.1007/978-3-642-74001-5_6

Werner, Earl E. (1986). Amphibian Metamorphosis: Growth Rate, Predation Risk, and the Optimal Size at Transformation. *The American Naturalist*, *128*(3), 319–341.

Wilbur, H. M. (1980). Complex Life Cycles. *Annual Review of Ecology and Systematics*, *11*, 67–93.

Yang, A. S. (2001). Modularity, evolvability, and adaptive radiations: A comparison of the hemi- and holometabolous insects. *Evolution and Development*, *3*(2), 59–72. doi: 10.1046/j.1525-142x.2001.003002059.x

Yun, J.-H., Roh, S. W., Whon, T. W., Jung, M.-J., Kim, M.-S., Park, D.-S., … Bae, J.-W. (2014). Insect Gut Bacterial Diversity Determined by Environmental Habitat, Diet, Developmental

Stage, and Phylogeny of Host. *Applied and Environmental Microbiology*, *80*(17), 5254–5264. doi: 10.1128/AEM.01226-

APPENDICES

Appendix chapter II

Complete metamorphosis and microbiota turnover in insects

(**a**)

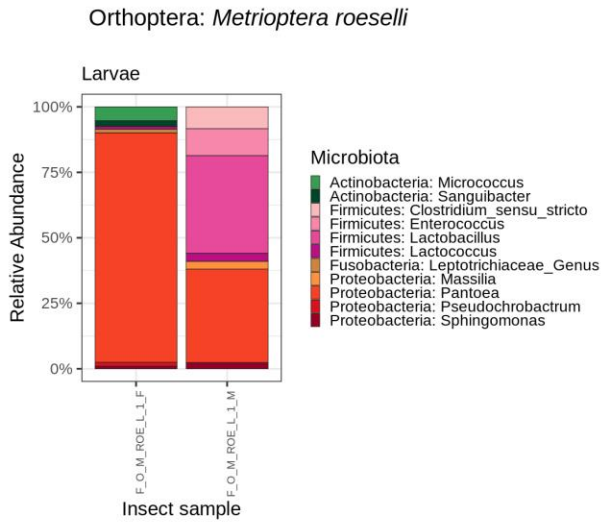
Orthoptera: Metrioptera roeselli
Larvae
100%
75%
50%
25%
0%
Relative Abundance
F_O_M_ROE_L_1_F
F_O_M_ROE_L_1_M
Insect sample
Microbiota
Actinobacteria: Micrococcus
Actinobacteria: Sanguibacter
Firmicutes: Clostridium_sensu_stricto
Firmicutes: Enterococcus
Firmicutes: Lactobacillus
Firmicutes: Lactococcus
Fusobacteria: Leptotrichiaceae_Genus
Proteobacteria: Massilia
Proteobacteria: Pantoea
Proteobacteria: Pseudochrobactrum
Proteobacteria: Sphingomonas

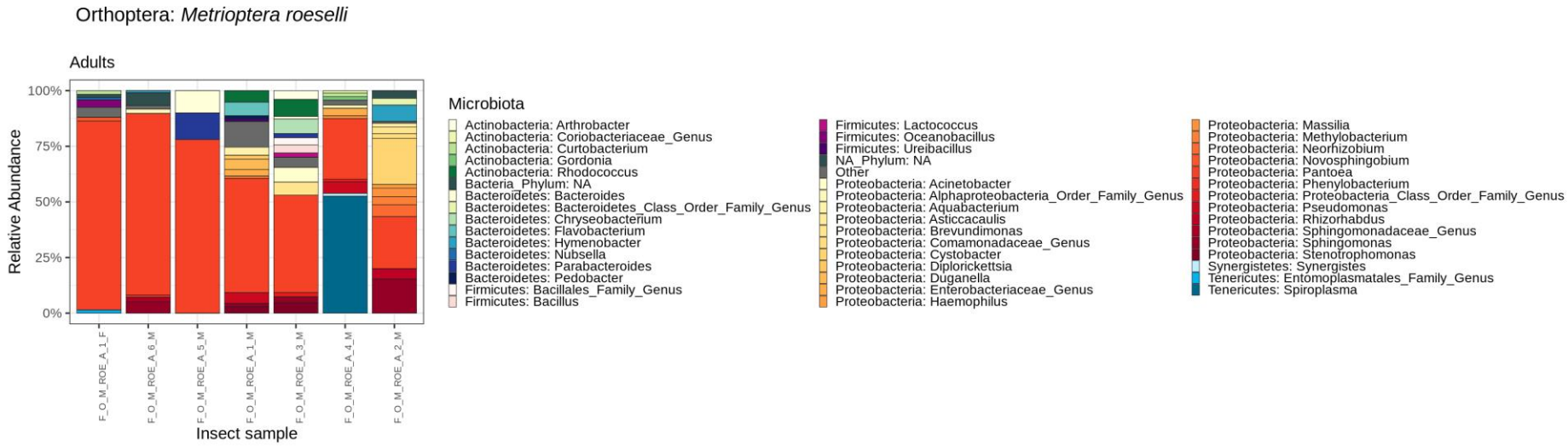
Orthoptera: Metrioptera roeselli
Adults
100%
75%
50%
25%
0%
Relative Abundance
F_O_M_ROE_A_1_F
F_O_M_ROE_A_6_M
F_O_M_ROE_A_5_M
F_O_M_ROE_A_1_M
F_O_M_ROE_A_3_M
F_O_M_ROE_A_4_M
F_O_M_ROE_A_2_M
Insect sample
Microbiota
Actinobacteria: Arthrobacter
Actinobacteria: Coriobacteriaceae_Genus
Actinobacteria: Curtobacterium
Actinobacteria: Gordonia
Actinobacteria: Rhodococcus
Bacteria_Phylum: NA
Bacteroidetes: Bacteroides
Bacteroidetes: Bacteroidetes_Class_Order_Family_Genus
Bacteroidetes: Chryseobacterium
Bacteroidetes: Flavobacterium
Bacteroidetes: Hymenobacter
Bacteroidetes: Nubsella
Bacteroidetes: Parabacteroides
Bacteroidetes: Pedobacter
Firmicutes: Bacillales_Family_Genus
Firmicutes: Bacillus
Firmicutes: Lactococcus
Firmicutes: Oceanobacillus
Firmicutes: Ureibacillus
NA_Phylum: NA
Other
Proteobacteria: Acinetobacter
Proteobacteria: Alphaproteobacteria_Order_Family_Genus
Proteobacteria: Aquabacterium
Proteobacteria: Asticcacaulis
Proteobacteria: Brevundimonas
Proteobacteria: Comamonadaceae_Genus
Proteobacteria: Cystobacter
Proteobacteria: Diplorickettsia
Proteobacteria: Duganella
Proteobacteria: Enterobacteriaceae_Genus
Proteobacteria: Haemophilus
Proteobacteria: Massilia
Proteobacteria: Methylobacterium
Proteobacteria: Neorhizobium
Proteobacteria: Novosphingobium
Proteobacteria: Pantoea
Proteobacteria: Phenylobacterium
Proteobacteria: Proteobacteria_Class_Order_Family_Genus
Proteobacteria: Pseudomonas
Proteobacteria: Rhizorhabdus
Proteobacteria: Sphingomonadaceae_Genus
Proteobacteria: Sphingomonas
Proteobacteria: Stenotrophomonas
Synergistetes: Synergistes
Tenericutes: Entomoplasmatales_Family_Genus
Tenericutes: Spiroplasma

(**b**)

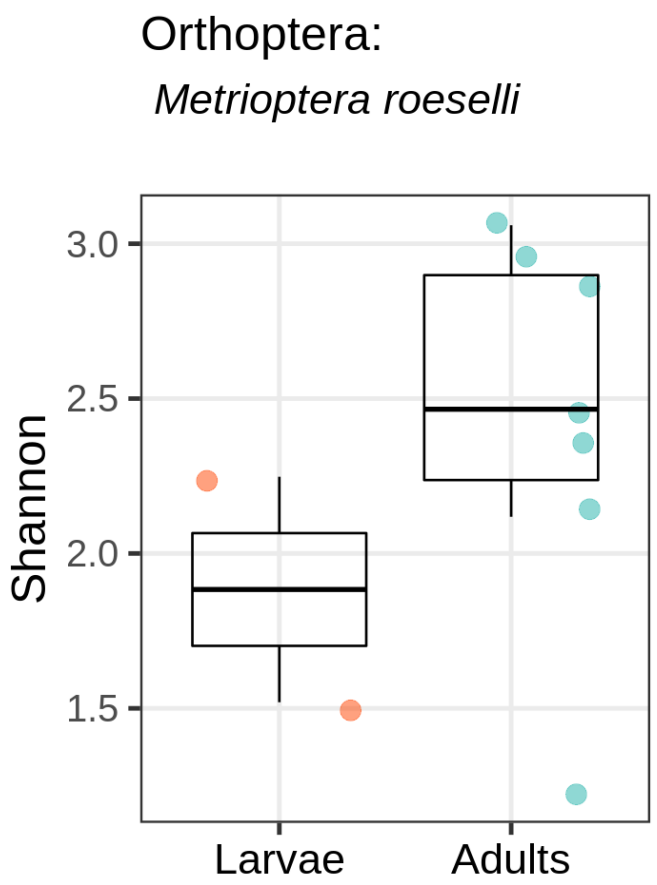

(**c**)

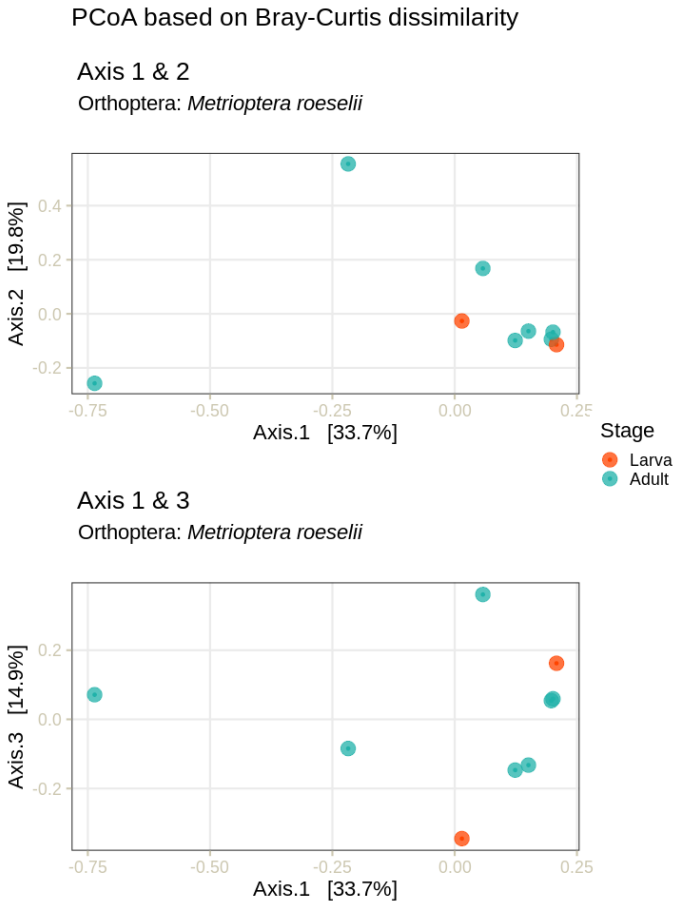

Figure S1: *Metrioptera roeselii* (Orthoptera) (a) microbiome composition assessed by 16S rRNA gene sequencing. Presented are the relative abundances of the bacterial genera for larval (top) and adult (bottom) samples. Shown are 99% of the genera. The remaining genera are shown as "Other." (b) Box plots of alpha-diversity indices (Shannon diversity) comparing larvae and adults. (c) Principal coordinate analysis (PCoA) plot based on bray-curtis distances. The percentage of the total variance explained by each PC is indicated in parentheses.

(**a**)

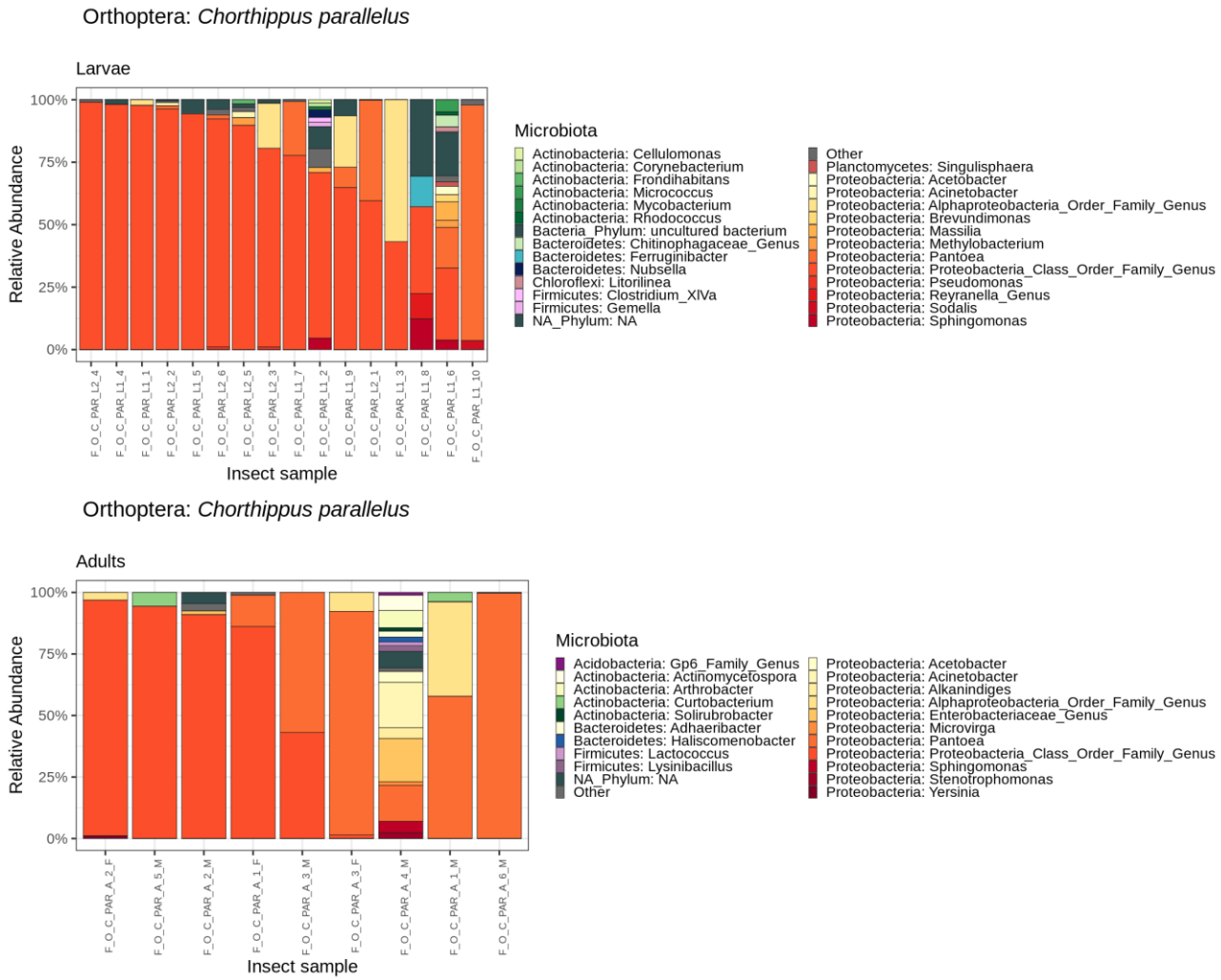
Orthoptera: Chorthippus parallelus
Larvae
Relative Abundance
100%
75%
50%
25%
0%
F_O_C_PAR_L2_4
F_O_C_PAR_L1_4
F_O_C_PAR_L1_1
F_O_C_PAR_L2_2
F_O_C_PAR_L1_5
F_O_C_PAR_L2_6
F_O_C_PAR_L2_5
F_O_C_PAR_L2_3
F_O_C_PAR_L1_7
F_O_C_PAR_L1_2
F_O_C_PAR_L1_9
F_O_C_PAR_L2_1
F_O_C_PAR_L1_3
F_O_C_PAR_L1_8
F_O_C_PAR_L1_6
F_O_C_PAR_L1_10
Insect sample
Microbiota
Actinobacteria: Cellulomonas
Actinobacteria: Corynebacterium
Actinobacteria: Frondihabitans
Actinobacteria: Micrococcus
Actinobacteria: Mycobacterium
Actinobacteria: Rhodococcus
Bacteria_Phylum: uncultured bacterium
Bacteroidetes: Chitinophagaceae_Genus
Bacteroidetes: Ferruginibacter
Bacteroidetes: Nubsella
Chloroflexi: Litorilinea
Firmicutes: Clostridium_XlVa
Firmicutes: Gemella
NA_Phylum: NA
Other
Planctomycetes: Singulisphaera
Proteobacteria: Acetobacter
Proteobacteria: Acinetobacter
Proteobacteria: Alphaproteobacteria_Order_Family_Genus
Proteobacteria: Brevundimonas
Proteobacteria: Massilia
Proteobacteria: Methylobacterium
Proteobacteria: Pantoea
Proteobacteria: Proteobacteria_Class_Order_Family_Genus
Proteobacteria: Pseudomonas
Proteobacteria: Reyranella_Genus
Proteobacteria: Sodalis
Proteobacteria: Sphingomonas

Orthoptera: Chorthippus parallelus
Adults
Relative Abundance
100%
75%
50%
25%
0%
F_O_C_PAR_A_2_F
F_O_C_PAR_A_5_M
F_O_C_PAR_A_2_M
F_O_C_PAR_A_1_F
F_O_C_PAR_A_3_M
F_O_C_PAR_A_3_F
F_O_C_PAR_A_4_M
F_O_C_PAR_A_1_M
F_O_C_PAR_A_6_M
Insect sample
Microbiota
Acidobacteria: Gp6_Family_Genus
Actinobacteria: Actinomycetospora
Actinobacteria: Arthrobacter
Actinobacteria: Curtobacterium
Actinobacteria: Solirubrobacter
Bacteroidetes: Adhaeribacter
Bacteroidetes: Haliscomenobacter
Firmicutes: Lactococcus
Firmicutes: Lysinibacillus
NA_Phylum: NA
Other
Proteobacteria: Acetobacter
Proteobacteria: Acinetobacter
Proteobacteria: Alkanindiges
Proteobacteria: Alphaproteobacteria_Order_Family_Genus
Proteobacteria: Enterobacteriaceae_Genus
Proteobacteria: Microvirga
Proteobacteria: Pantoea
Proteobacteria: Proteobacteria_Class_Order_Family_Genus
Proteobacteria: Sphingomonas
Proteobacteria: Stenotrophomonas
Proteobacteria: Yersinia

(**b**)

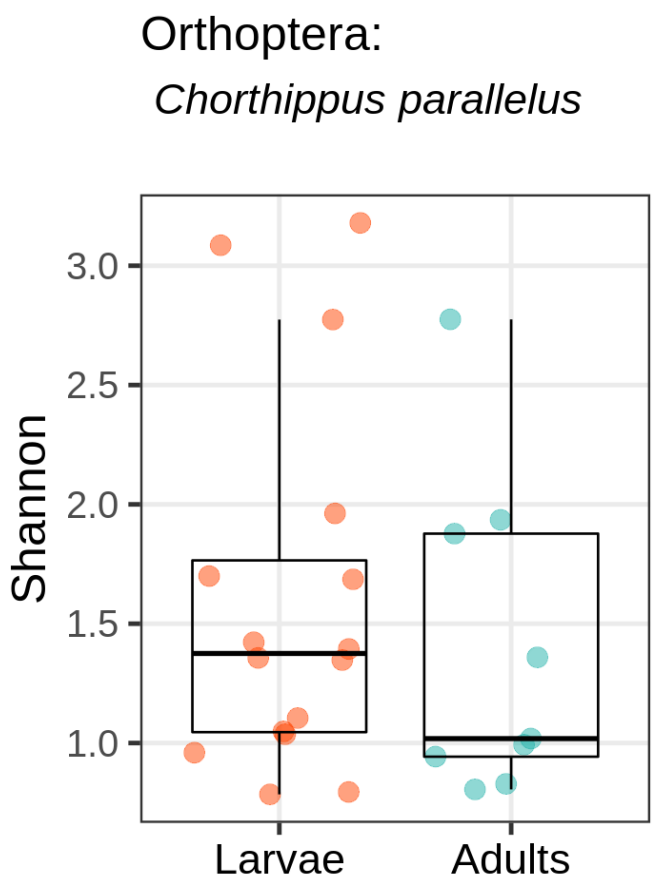

(**c**)

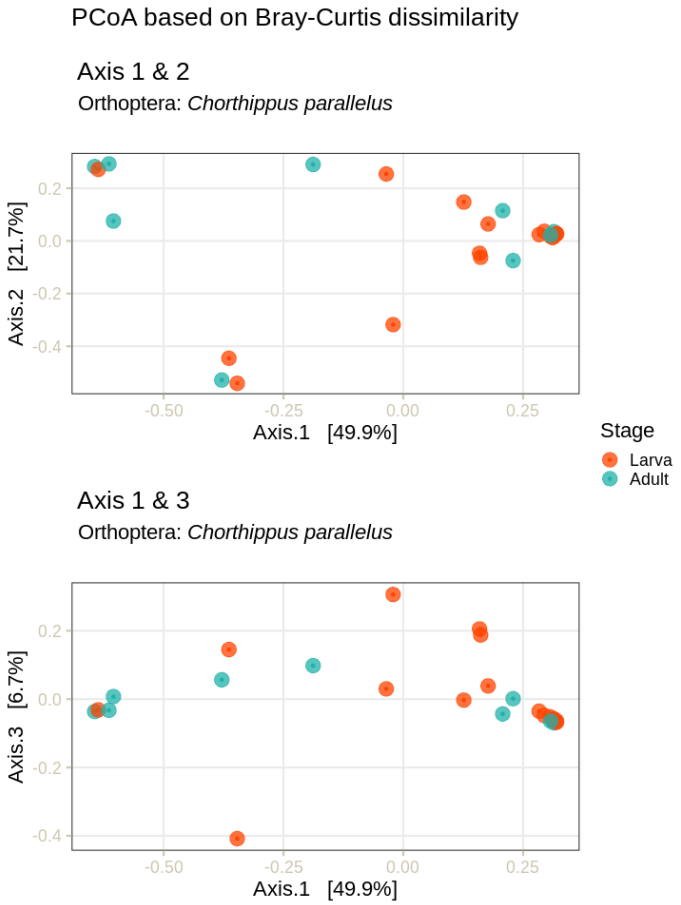

Figure S2: *Chorthippus parallelus* (Orthoptera) (a) microbiome composition assessed by 16S rRNA gene sequencing. Presented are the relative abundances of the bacterial genera for larval (top) and adult (bottom) samples. Shown are 99% of the genera. The remaining genera are shown as "Other." (b) Box plots of alpha-diversity indices (Shannon diversity) comparing larvae and adults. (c) Principal coordinate analysis (PCoA) plot based on bray-curtis distances. The percentage of the total variance explained by each PC is indicated in parentheses.

(a)

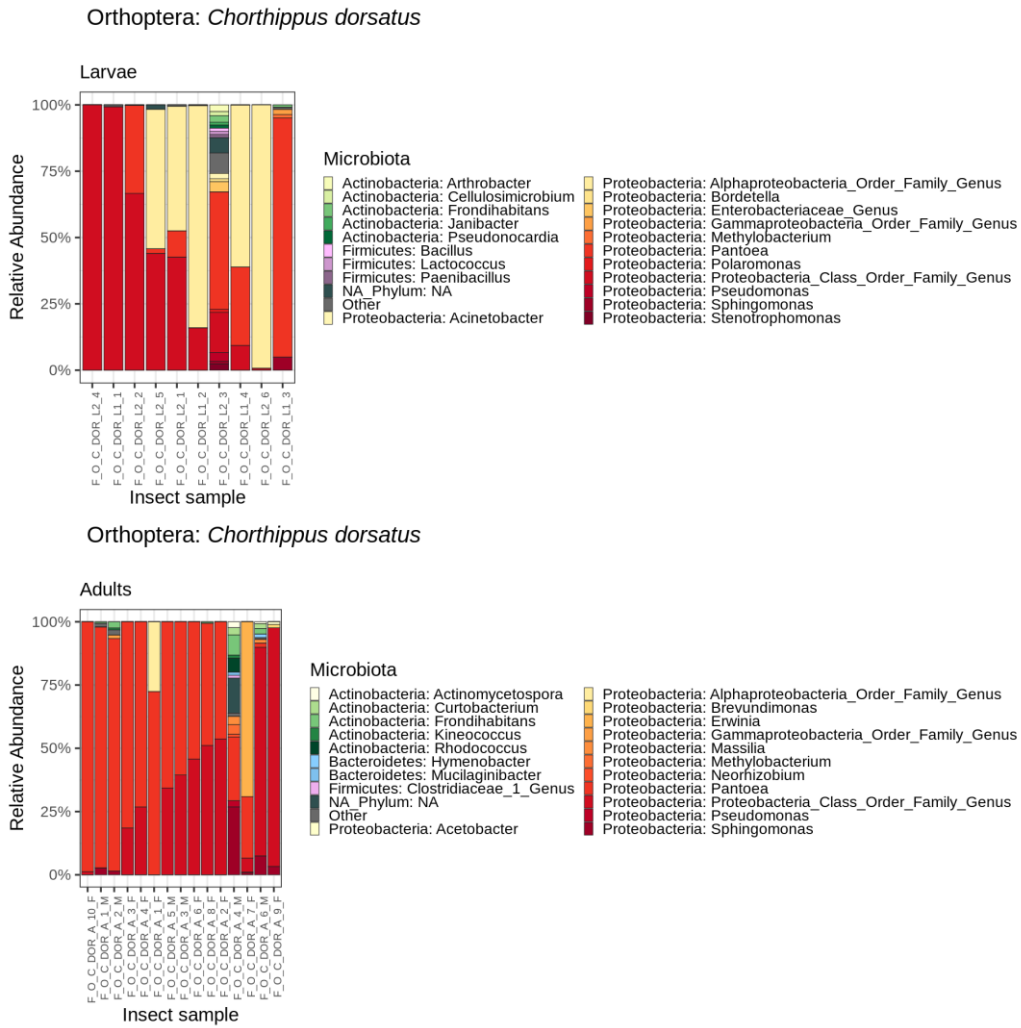
Orthoptera: Chorthippus dorsatus
Larvae
100%
75%
50%
25%
0%
Relative Abundance
F_O_C_DOR_L2_4
F_O_C_DOR_L1_1
F_O_C_DOR_L2_2
F_O_C_DOR_L2_5
F_O_C_DOR_L2_1
F_O_C_DOR_L1_2
F_O_C_DOR_L2_3
F_O_C_DOR_L1_4
F_O_C_DOR_L2_6
F_O_C_DOR_L1_3
Insect sample
Microbiota
Actinobacteria: Arthrobacter
Actinobacteria: Cellulosimicrobium
Actinobacteria: Frondihabitans
Actinobacteria: Janibacter
Actinobacteria: Pseudonocardia
Firmicutes: Bacillus
Firmicutes: Lactococcus
Firmicutes: Paenibacillus
NA_Phylum: NA
Other
Proteobacteria: Acinetobacter
Proteobacteria: Alphaproteobacteria_Order_Family_Genus
Proteobacteria: Bordetella
Proteobacteria: Enterobacteriaceae_Genus
Proteobacteria: Gammaproteobacteria_Order_Family_Genus
Proteobacteria: Methylobacterium
Proteobacteria: Pantoea
Proteobacteria: Polaromonas
Proteobacteria: Proteobacteria_Class_Order_Family_Genus
Proteobacteria: Pseudomonas
Proteobacteria: Sphingomonas
Proteobacteria: Stenotrophomonas

Orthoptera: Chorthippus dorsatus
Adults
100%
75%
50%
25%
0%
Relative Abundance
F_O_C_DOR_A_10_F
F_O_C_DOR_A_1_M
F_O_C_DOR_A_2_M
F_O_C_DOR_A_3_F
F_O_C_DOR_A_4_F
F_O_C_DOR_A_1_F
F_O_C_DOR_A_5_M
F_O_C_DOR_A_3_M
F_O_C_DOR_A_6_F
F_O_C_DOR_A_8_F
F_O_C_DOR_A_2_F
F_O_C_DOR_A_4_M
F_O_C_DOR_A_7_F
F_O_C_DOR_A_6_M
F_O_C_DOR_A_9_F
Insect sample
Microbiota
Actinobacteria: Actinomycetospora
Actinobacteria: Curtobacterium
Actinobacteria: Frondihabitans
Actinobacteria: Kineococcus
Actinobacteria: Rhodococcus
Bacteroidetes: Hymenobacter
Bacteroidetes: Mucilaginibacter
Firmicutes: Clostridiaceae_1_Genus
NA_Phylum: NA
Other
Proteobacteria: Acetobacter
Proteobacteria: Alphaproteobacteria_Order_Family_Genus
Proteobacteria: Brevundimonas
Proteobacteria: Erwinia
Proteobacteria: Gammaproteobacteria_Order_Family_Genus
Proteobacteria: Massilia
Proteobacteria: Methylobacterium
Proteobacteria: Neorhizobium
Proteobacteria: Pantoea
Proteobacteria: Proteobacteria_Class_Order_Family_Genus
Proteobacteria: Pseudomonas
Proteobacteria: Sphingomonas

(**b**)

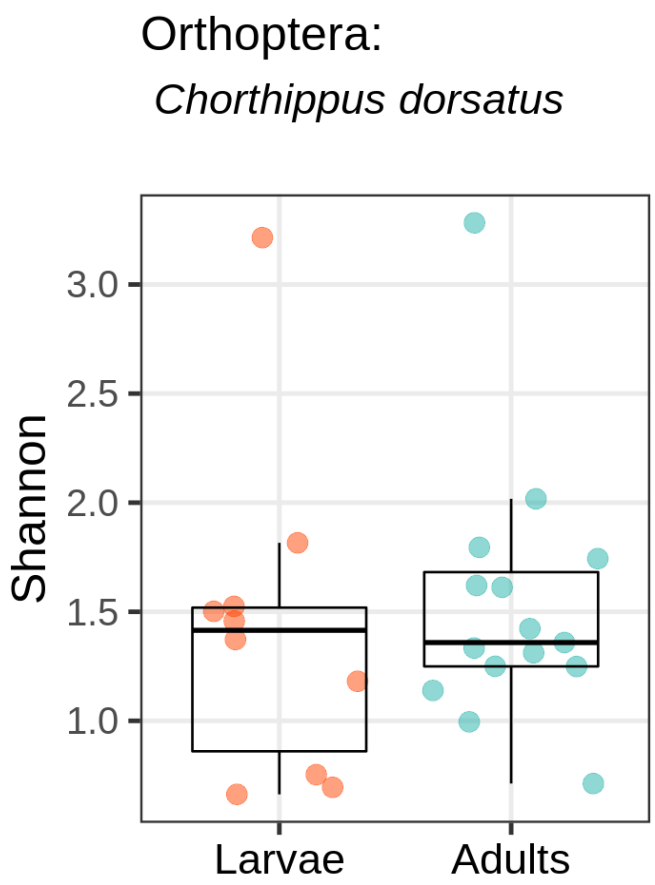

(**c**)

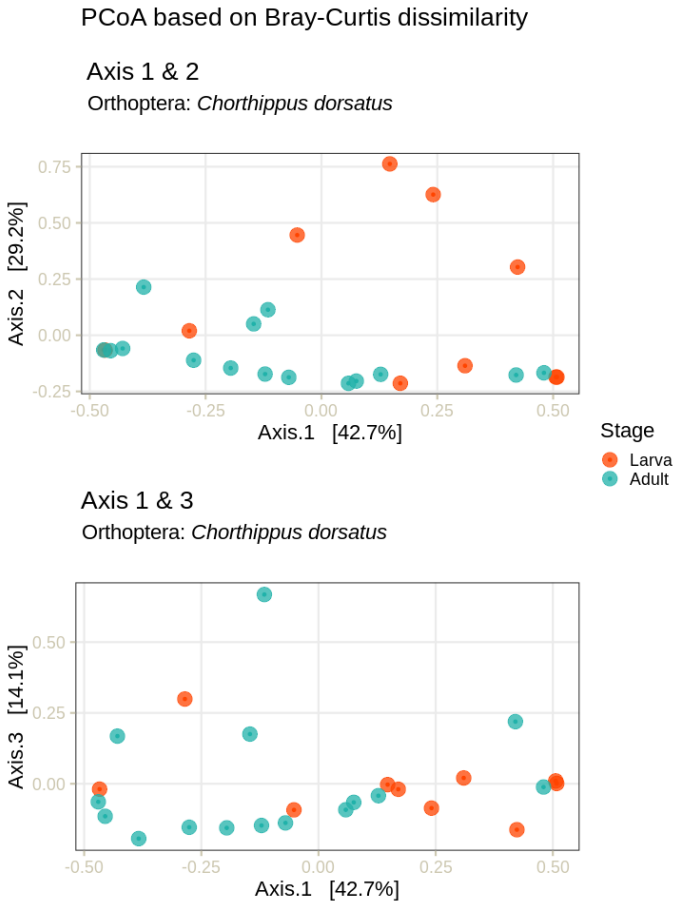

Figure S3: *Chorthippus dorsatus* (Orthoptera) (a) microbiome composition assessed by 16S rRNA gene sequencing. Presented are the relative abundances of the bacterial genera for larval (top) and adult (bottom) samples. Shown are 99% of the genera. The remaining genera are shown as "Other." (b) Box plots of alpha-diversity indices (Shannon diversity) comparing larvae and adults. (c) Principal coordinate analysis (PCoA) plot based on bray-curtis distances. The percentage of the total variance explained by each PC is indicated in parentheses.

(**a**)


Thysanoptera: Frankliniella occidentalis
Larvae
Relative Abundance
100%
75%
50%
25%
0%
F_T_F_OCC_L_9
F_T_F_OCC_L_3
F_T_F_OCC_L_8
Insect sample
Microbiota
Actinobacteria: Micrococcus
Bacteria_Phylum: Bacteria_Phylum_Class_Order_Family_Genus
Bacteroidetes: Alistipes
Bacteroidetes: Bacteroidales_Family_Genus
Bacteroidetes: Proteiniphilum
Bacteroidetes: Rikenellaceae_Genus
Bacteroidetes: Tannerella
Deferribacteres: Deferribacteraceae_Genus
Firmicutes: Bacillus
Firmicutes: Clostridiales_Family_Genus
Firmicutes: Clostridium_IV
Firmicutes: Clostridium_XIVb
Firmicutes: Firmicutes_Class_Order_Family_Genus
Firmicutes: Hydrogenoanaerobacterium
Firmicutes: Lachnospiraceae_Genus
Firmicutes: Lactococcus
Firmicutes: Ruminococcaceae_Genus
Firmicutes: Veillonellaceae_Genus
Other
Proteobacteria: Acetobacter
Proteobacteria: Acinetobacter
Proteobacteria: Alphaproteobacteria_Order_Family_Genus
Proteobacteria: Cronobacter
Proteobacteria: Desulfovibrionaceae_Genus
Proteobacteria: Enterobacter
Proteobacteria: Enterobacteriaceae_Genus
Proteobacteria: Mesorhizobium
Proteobacteria: Oxalobacter
Proteobacteria: Pantoea
Proteobacteria: Paracoccus
Proteobacteria: Proteobacteria_Class_Order_Family_Genus
Proteobacteria: Pseudomonadaceae_Genus
Proteobacteria: Pseudomonas
Proteobacteria: Rickettsia
Proteobacteria: Tepidimonas
Proteobacteria: Thauera
Synergistetes: Synergistaceae_Genus
Thysanoptera: Frankliniella occidentalis
Adults
Relative Abundance
100%
75%
50%
25%
0%
F_T_F_OCC_A_10
F_T_F_OCC_A_8
F_T_F_OCC_A_1
Insect sample
Microbiota
Acidobacteria: Granulicella_Family_Genus
Acidobacteria: Terriglobus_Family_Genus
Actinobacteria: Coriobacteriaceae_Genus
Actinobacteria: Corynebacterium
Actinobacteria: Micrococcus
Bacteroidetes: Bacteroidales_Family_Genus
Bacteroidetes: Proteiniphilum
Bacteroidetes: Rikenellaceae_Genus
Bacteroidetes: Tannerella
Firmicutes: Anaerotruncus
Firmicutes: Clostridiales_Family_Genus
Firmicutes: Clostridium_XIVa
Firmicutes: Clostridium_XIVb
Firmicutes: Firmicutes_Class_Order_Family_Genus
Firmicutes: Hungatella
Firmicutes: Intestinimonas
Firmicutes: Lachnospiraceae_Genus
Firmicutes: Lactococcus
Firmicutes: Ruminococcaceae_Genus
Firmicutes: Streptococcus
Other
Proteobacteria: Acetobacter
Proteobacteria: Acetobacteraceae_Genus
Proteobacteria: Acidicaldus
Proteobacteria: Acinetobacter
Proteobacteria: Alphaproteobacteria_Order_Family_Genus
Proteobacteria: Arsenophonus
Proteobacteria: Beijerinckiaceae_Genus
Proteobacteria: Campylobacter
Proteobacteria: Cronobacter
Proteobacteria: Desulfovibrionaceae_Genus
Proteobacteria: Enterobacter
Proteobacteria: Enterobacteriaceae_Genus
Proteobacteria: Escherichia/Shigella
Proteobacteria: Gluconobacter
Proteobacteria: Haemophilus
Proteobacteria: Janthinobacterium
Proteobacteria: Komagataeibacter
Proteobacteria: Mesorhizobium
Proteobacteria: Oxalobacter
Proteobacteria: Pantoea
Proteobacteria: Phenylobacterium
Proteobacteria: Proteobacteria_Class_Order_Family_Genus
Proteobacteria: Pseudomonadaceae_Genus
Proteobacteria: Pseudomonas
Proteobacteria: Rhizobiales_Family_Genus
Proteobacteria: Tepidimonas
Proteobacteria: Thauera
Proteobacteria: Vampirovibrio
Tenericutes: Spiroplasma
Verrucomicrobia: Opitutus
Verrucomicrobia: Spartobacteria_Order_Family_Genus

(**b**)

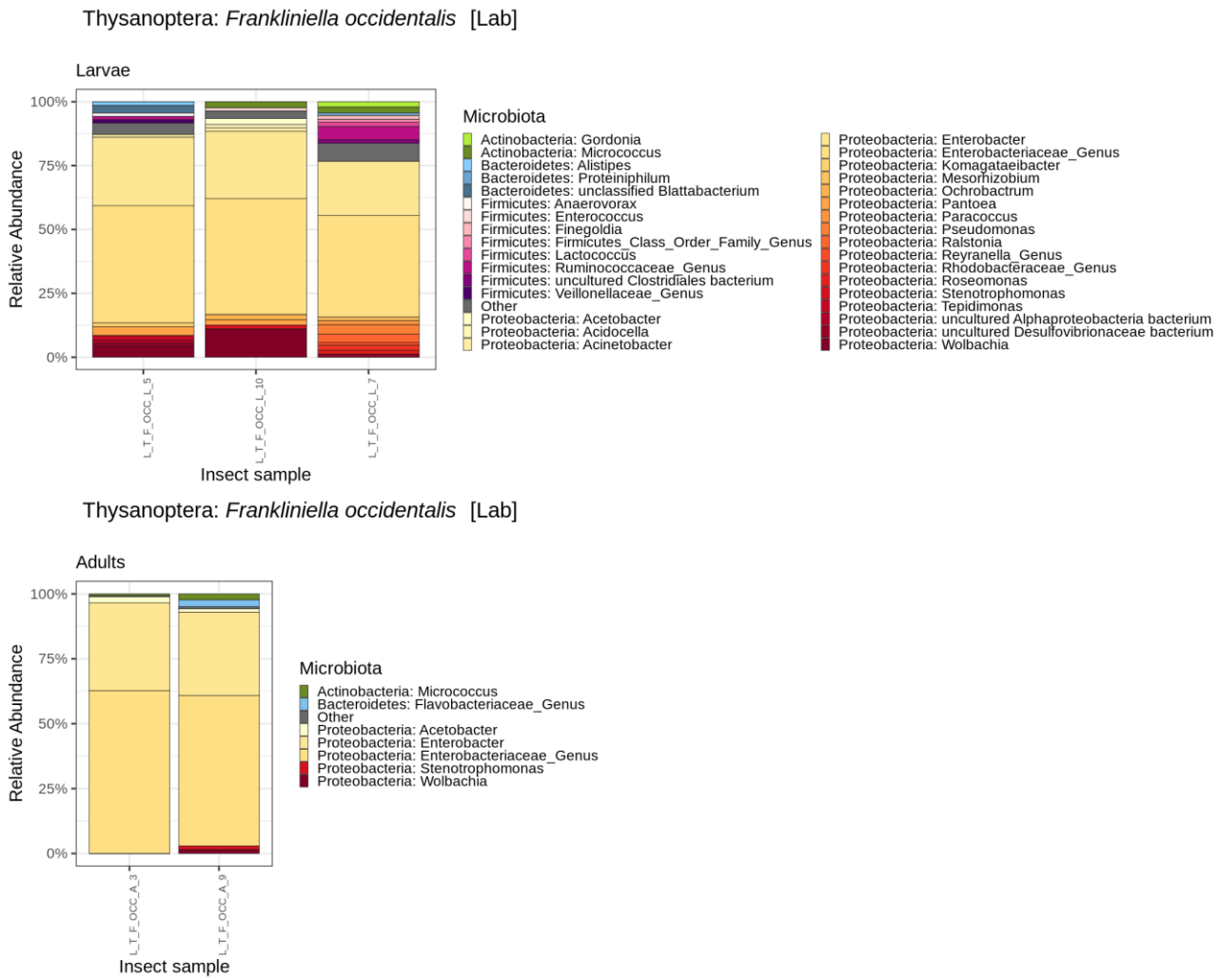
Thysanoptera: Frankliniella occidentalis [Lab]
Larvae
Relative Abundance
100%
75%
50%
25%
0%
L_T_F_OCC_L_5
L_T_F_OCC_L_10
L_T_F_OCC_L_7
Insect sample
Microbiota
Actinobacteria: Gordonia
Actinobacteria: Micrococcus
Bacteroidetes: Alistipes
Bacteroidetes: Proteiniphilum
Bacteroidetes: unclassified Blattabacterium
Firmicutes: Anaerovorax
Firmicutes: Enterococcus
Firmicutes: Finegoldia
Firmicutes: Firmicutes_Class_Order_Family_Genus
Firmicutes: Lactococcus
Firmicutes: Ruminococcaceae_Genus
Firmicutes: uncultured Clostridiales bacterium
Firmicutes: Veillonellaceae_Genus
Other
Proteobacteria: Acetobacter
Proteobacteria: Acidocella
Proteobacteria: Acinetobacter
Proteobacteria: Enterobacter
Proteobacteria: Enterobacteriaceae_Genus
Proteobacteria: Komagataeibacter
Proteobacteria: Mesorhizobium
Proteobacteria: Ochrobactrum
Proteobacteria: Pantoea
Proteobacteria: Paracoccus
Proteobacteria: Pseudomonas
Proteobacteria: Ralstonia
Proteobacteria: Reyranella_Genus
Proteobacteria: Rhodobacteraceae_Genus
Proteobacteria: Roseomonas
Proteobacteria: Stenotrophomonas
Proteobacteria: Tepidimonas
Proteobacteria: uncultured Alphaproteobacteria bacterium
Proteobacteria: uncultured Desulfovibrionaceae bacterium
Proteobacteria: Wolbachia
Thysanoptera: Frankliniella occidentalis [Lab]
Adults
Relative Abundance
100%
75%
50%
25%
0%
L_T_F_OCC_A_3
L_T_F_OCC_A_9
Insect sample
Microbiota
Actinobacteria: Micrococcus
Bacteroidetes: Flavobacteriaceae_Genus
Other
Proteobacteria: Acetobacter
Proteobacteria: Enterobacter
Proteobacteria: Enterobacteriaceae_Genus
Proteobacteria: Stenotrophomonas
Proteobacteria: Wolbachia

(c)

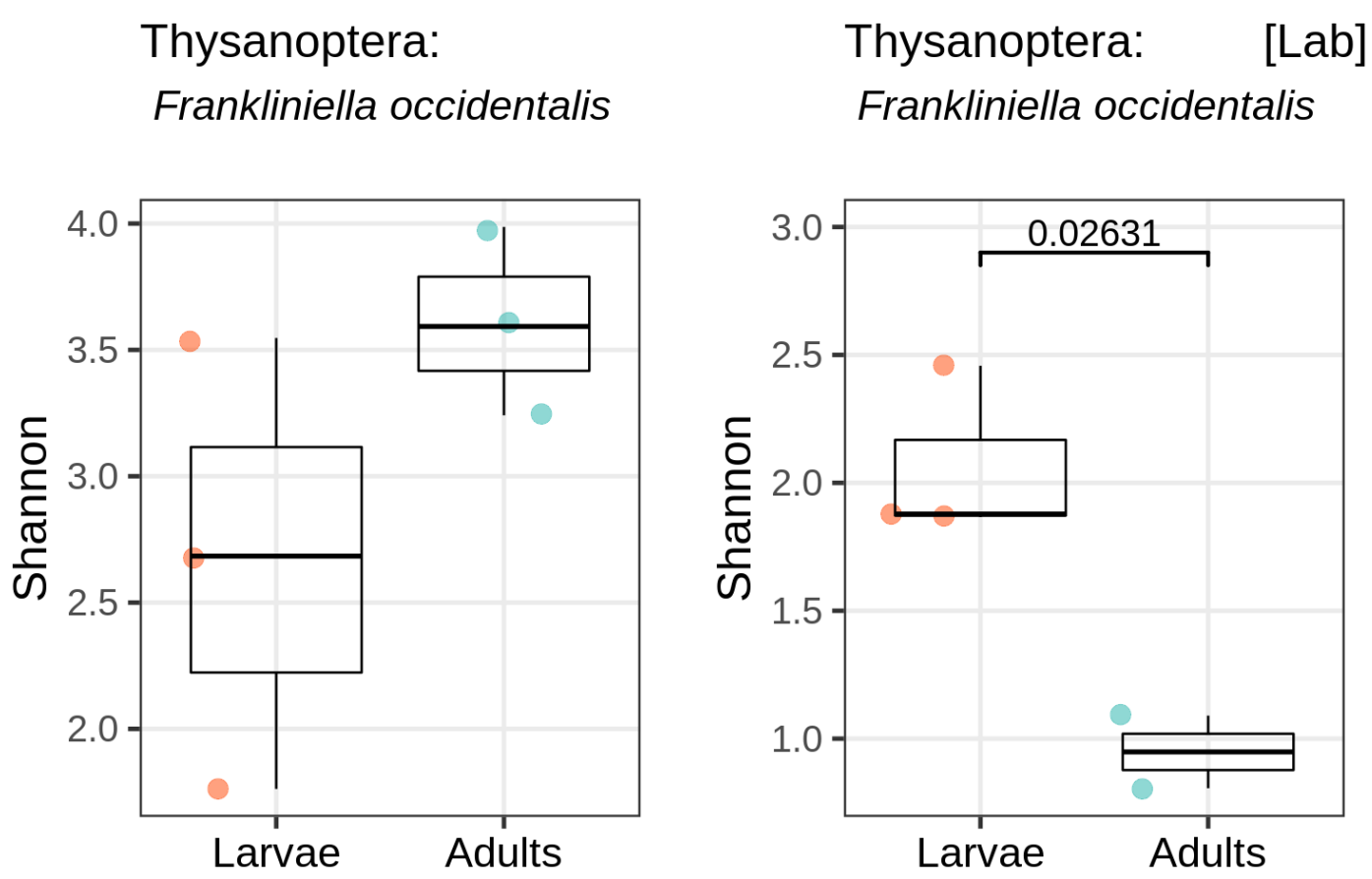
Thysanoptera:
Frankliniella occidentalis
Shannon
4.0
3.5
3.0
2.5
2.0
Larvae
Adults
Thysanoptera: [Lab]
Frankliniella occidentalis
0.02631
3.0
2.5
2.0
1.5
1.0
Shannon
Larvae
Adults

(d)

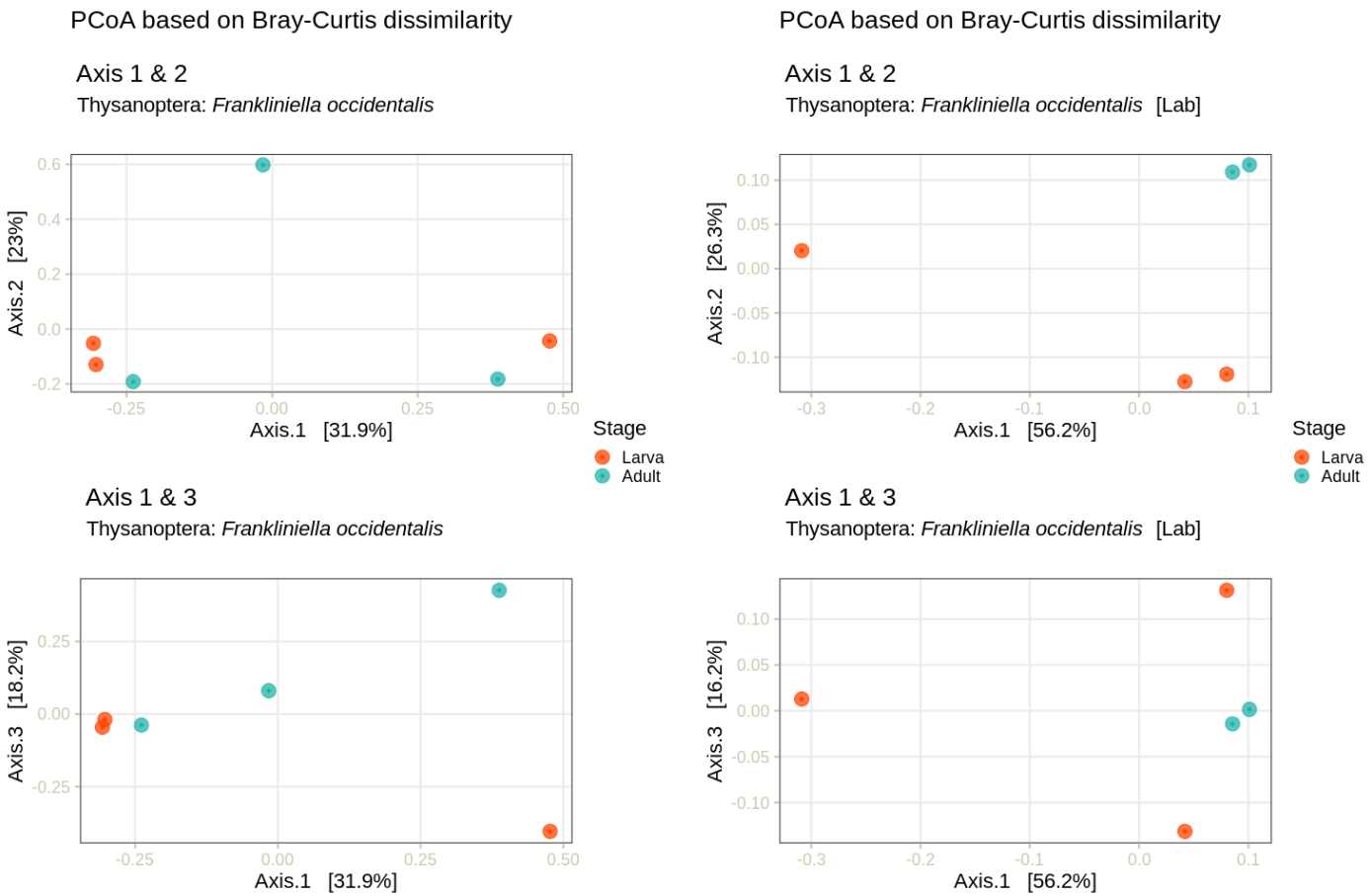

Figure S4: *Frankliniella occidentalis* (Thysanoptera) (a) microbiome composition assessed by 16S rRNA gene sequencing. Presented are the relative abundances of the bacterial genera for larval (top) and adult (bottom) samples. Shown are 99% of the genera. The remaining genera are shown as "Other." (b) Microbiome composition of laboratory-reared *Frankliniella occidentalis*. (c) Box plots of alpha-diversity indices (Shannon diversity) comparing larvae and adults for field-collected (left) and laboratory-reared *Frankliniella occidentalis* (right). (d) Principal coordinate analysis (PCoA) plot based on bray-curtis distances for field-collected (left) and laboratory-reared *Frankliniella occidentalis* (right; Two-sample t-test, t = -4.0962, df = 3, p-value = 0.02631). The percentage of the total variance explained by each PC is indicated in parentheses.

(**a**)

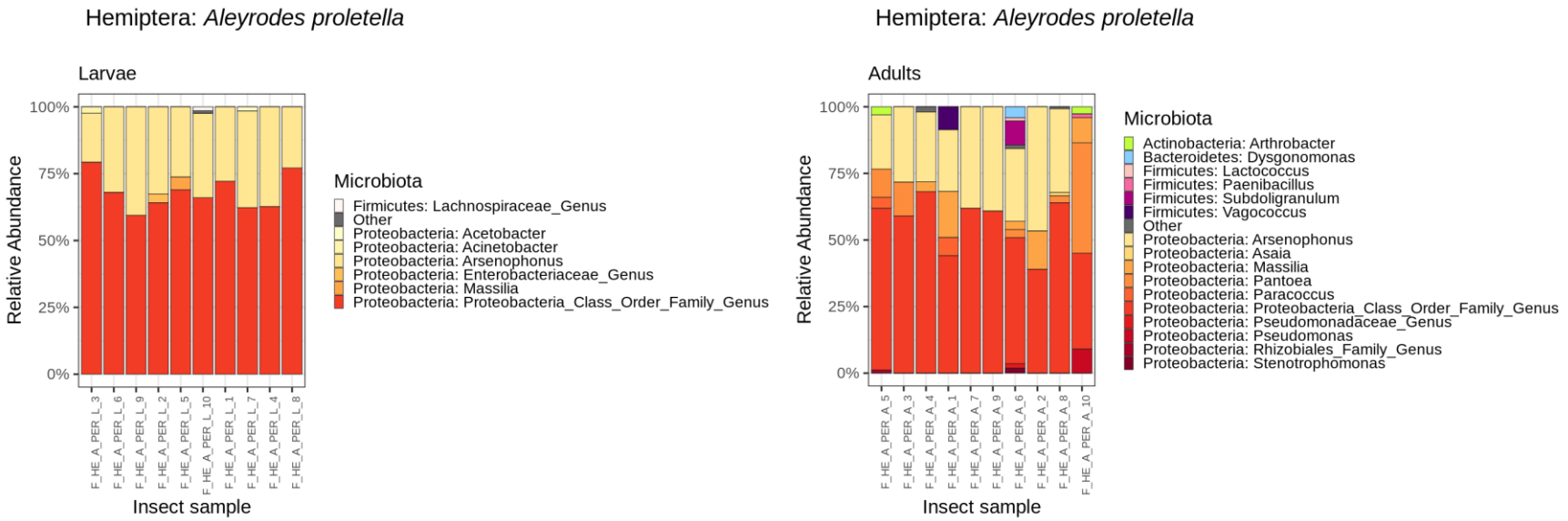
Hemiptera: Aleyrodes proletella
Larvae
Relative Abundance
100%
75%
50%
25%
0%
F_HE_A_PER_L_3
F_HE_A_PER_L_6
F_HE_A_PER_L_9
F_HE_A_PER_L_2
F_HE_A_PER_L_5
F_HE_A_PER_L_10
F_HE_A_PER_L_1
F_HE_A_PER_L_7
F_HE_A_PER_L_4
F_HE_A_PER_L_8
Insect sample
Microbiota
Firmicutes: Lachnospiraceae_Genus
Other
Proteobacteria: Acetobacter
Proteobacteria: Acinetobacter
Proteobacteria: Arsenophonus
Proteobacteria: Enterobacteriaceae_Genus
Proteobacteria: Massilia
Proteobacteria: Proteobacteria_Class_Order_Family_Genus
Hemiptera: Aleyrodes proletella
Adults
Relative Abundance
100%
75%
50%
25%
0%
F_HE_A_PER_A_5
F_HE_A_PER_A_3
F_HE_A_PER_A_4
F_HE_A_PER_A_1
F_HE_A_PER_A_7
F_HE_A_PER_A_9
F_HE_A_PER_A_6
F_HE_A_PER_A_2
F_HE_A_PER_A_8
F_HE_A_PER_A_10
Insect sample
Microbiota
Actinobacteria: Arthrobacter
Bacteroidetes: Dysgonomonas
Firmicutes: Lactococcus
Firmicutes: Paenibacillus
Firmicutes: Subdoligranulum
Firmicutes: Vagococcus
Other
Proteobacteria: Arsenophonus
Proteobacteria: Asaia
Proteobacteria: Massilia
Proteobacteria: Pantoea
Proteobacteria: Paracoccus
Proteobacteria: Proteobacteria_Class_Order_Family_Genus
Proteobacteria: Pseudomonadaceae_Genus
Proteobacteria: Pseudomonas
Proteobacteria: Rhizobiales_Family_Genus
Proteobacteria: Stenotrophomonas

(**b**)

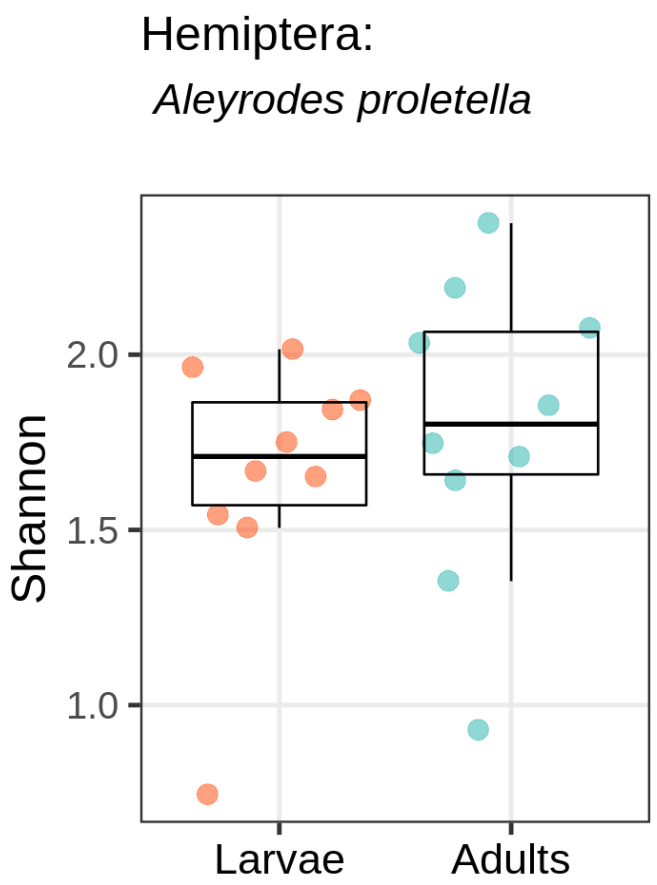

(**c**)

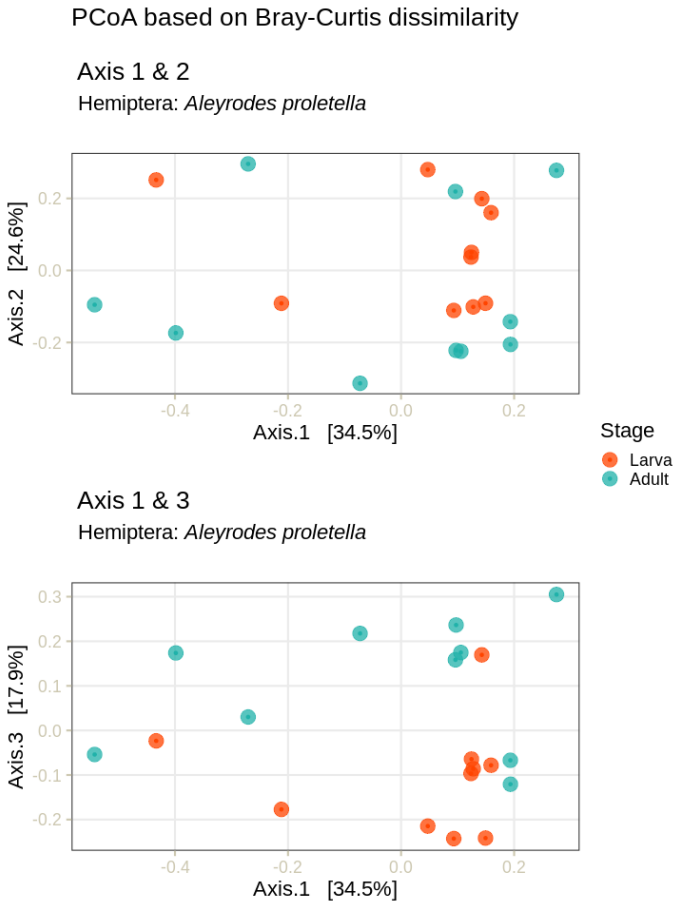

Figure S5: *Aleyrodes proletella* (Hemiptera) (a) microbiome composition assessed by 16S rRNA gene sequencing. Presented are the relative abundances of the bacterial genera for larval (left) and adult (right) samples. Shown are 99% of the genera. The remaining genera are shown as "Other." (b) Box plots of alpha-diversity indices (Shannon diversity) comparing larvae and adults. (c) Principal coordinate analysis (PCoA) plot based on bray-curtis distances. The percentage of the total variance explained by each PC is indicated in parentheses.

(**a**)

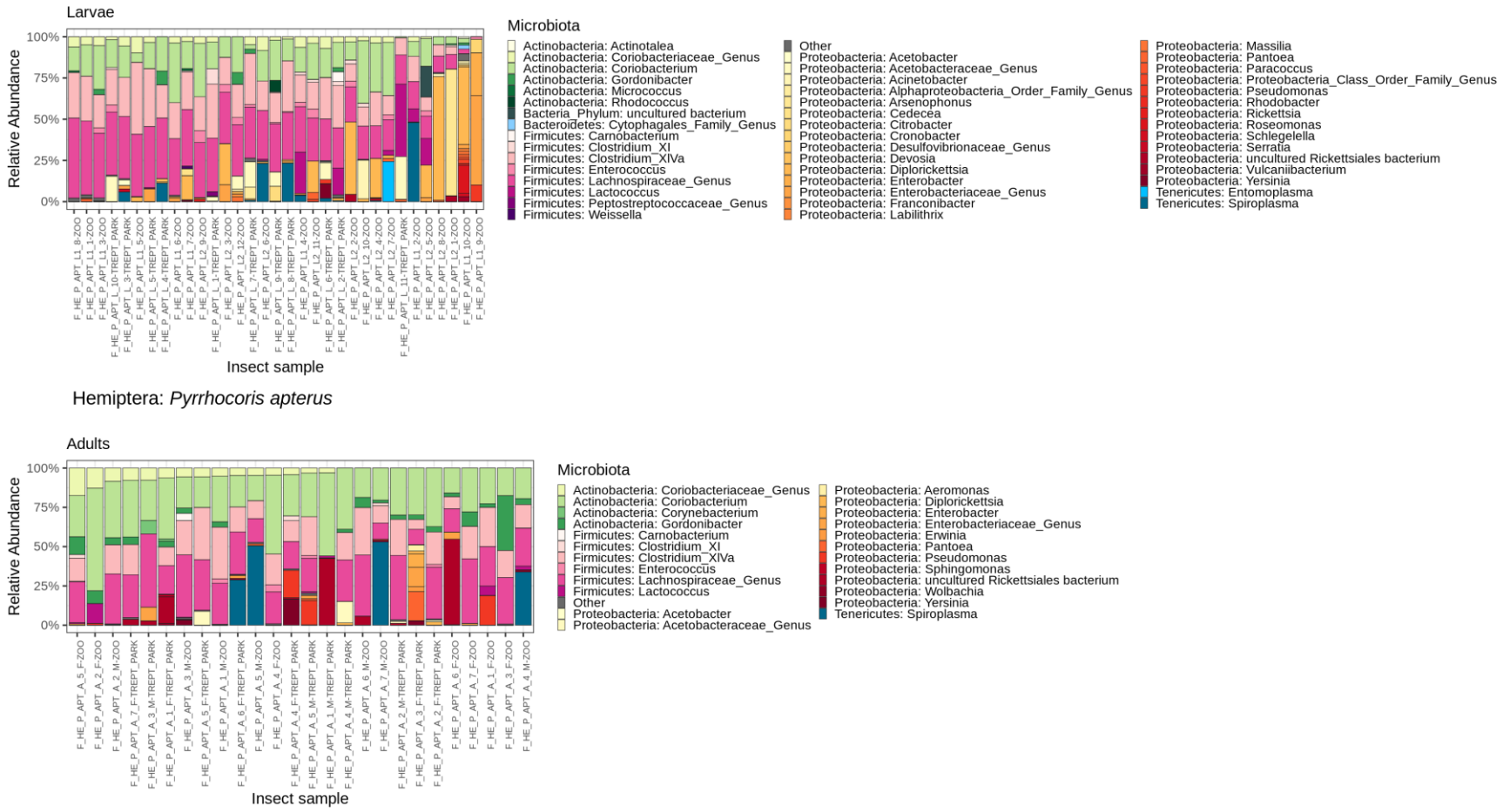
Hemiptera: *Pyrrhocoris apterus*
Larvae
Relative Abundance
100%
75%
50%
25%
0%
Insect sample
Microbiota
Actinobacteria: Actinotalea
Actinobacteria: Coriobacteriaceae_Genus
Actinobacteria: Coriobacterium
Actinobacteria: Gordonibacter
Actinobacteria: Micrococcus
Actinobacteria: Rhodococcus
Bacteria_Phylum: uncultured bacterium
Bacteroidetes: Cytophagales_Family_Genus
Firmicutes: Carnobacterium
Firmicutes: Clostridium_XI
Firmicutes: Clostridium_XlVa
Firmicutes: Enterococcus
Firmicutes: Lachnospiraceae_Genus
Firmicutes: Lactococcus
Firmicutes: Peptostreptococcaceae_Genus
Firmicutes: Weissella
Other
Proteobacteria: Acetobacter
Proteobacteria: Acetobacteraceae_Genus
Proteobacteria: Acinetobacter
Proteobacteria: Alphaproteobacteria_Order_Family_Genus
Proteobacteria: Arsenophonus
Proteobacteria: Cedecea
Proteobacteria: Citrobacter
Proteobacteria: Cronobacter
Proteobacteria: Desulfovibrionaceae_Genus
Proteobacteria: Devosia
Proteobacteria: Diplorickettsia
Proteobacteria: Enterobacter
Proteobacteria: Enterobacteriaceae_Genus
Proteobacteria: Franconibacter
Proteobacteria: Labilithrix
Proteobacteria: Massilia
Proteobacteria: Pantoea
Proteobacteria: Paracoccus
Proteobacteria: Proteobacteria_Class_Order_Family_Genus
Proteobacteria: Pseudomonas
Proteobacteria: Rhodobacter
Proteobacteria: Rickettsia
Proteobacteria: Roseomonas
Proteobacteria: Schlegelella
Proteobacteria: Serratia
Proteobacteria: uncultured Rickettsiales bacterium
Proteobacteria: Vulcaniibacterium
Proteobacteria: Yersinia
Tenericutes: Entomoplasma
Tenericutes: Spiroplasma
Hemiptera: *Pyrrhocoris apterus*
Adults
Relative Abundance
100%
75%
50%
25%
0%
Insect sample
Microbiota
Actinobacteria: Coriobacteriaceae_Genus
Actinobacteria: Coriobacterium
Actinobacteria: Corynebacterium
Actinobacteria: Gordonibacter
Firmicutes: Carnobacterium
Firmicutes: Clostridium_XI
Firmicutes: Clostridium_XlVa
Firmicutes: Enterococcus
Firmicutes: Lachnospiraceae_Genus
Firmicutes: Lactococcus
Other
Proteobacteria: Acetobacter
Proteobacteria: Acetobacteraceae_Genus
Proteobacteria: Aeromonas
Proteobacteria: Diplorickettsia
Proteobacteria: Enterobacter
Proteobacteria: Enterobacteriaceae_Genus
Proteobacteria: Erwinia
Proteobacteria: Pantoea
Proteobacteria: Pseudomonas
Proteobacteria: Sphingomonas
Proteobacteria: uncultured Rickettsiales bacterium
Proteobacteria: Wolbachia
Proteobacteria: Yersinia
Tenericutes: Spiroplasma

(**b**)

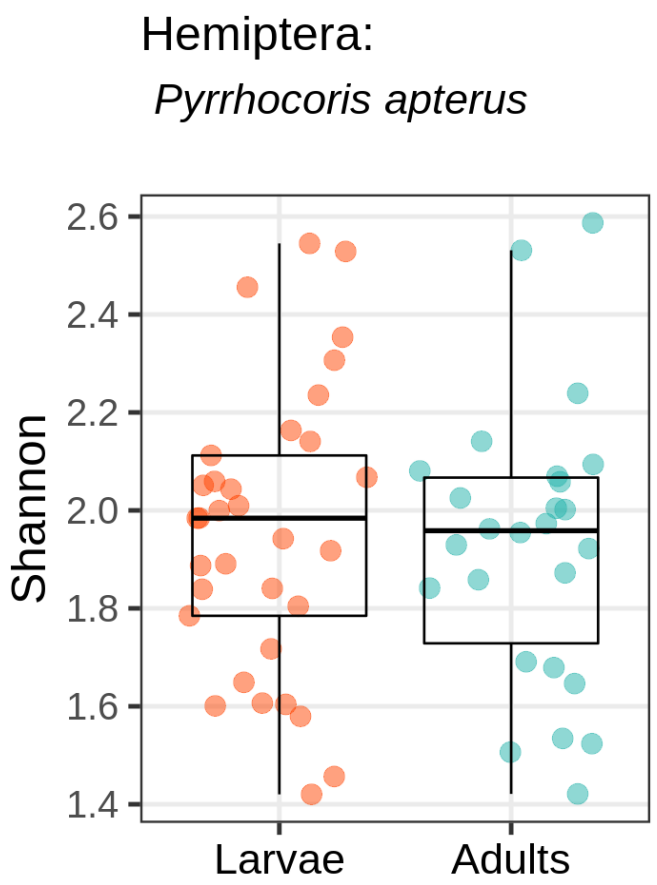

(**c**)

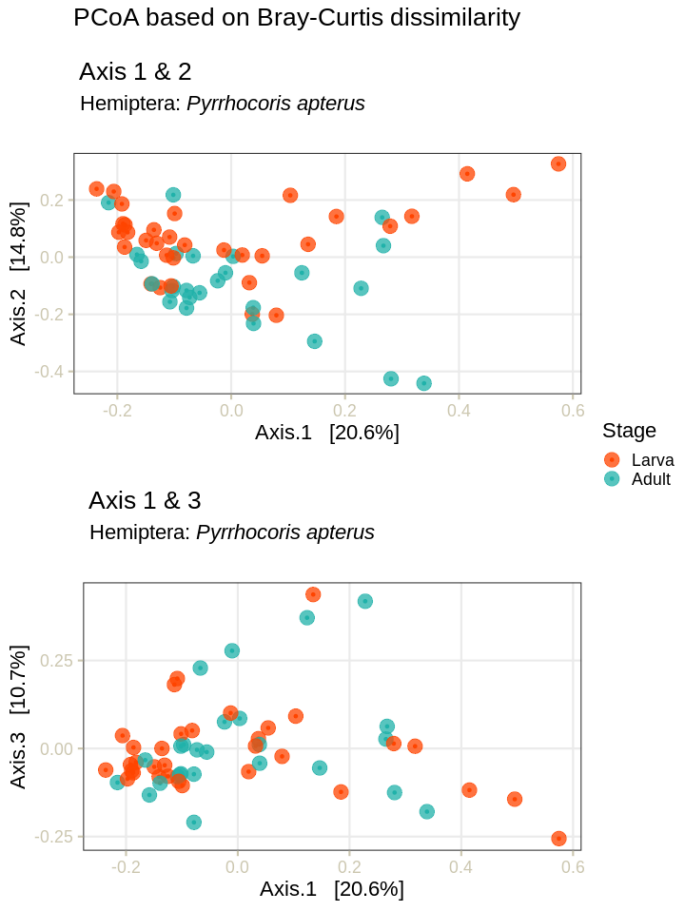

Figure S6: *Pyrrhocoris apterus* (Hemiptera) (a) microbiome composition assessed by 16S rRNA gene sequencing. Presented are the relative abundances of the bacterial genera for larval (top) and adult (bottom) samples. Shown are 99% of the genera. The remaining genera are shown as "Other." (b) Box plots of alpha-diversity indices (Shannon diversity) comparing larvae and adults. (c) Principal coordinate analysis (PCoA) plot based on bray-curtis distances. The percentage of the total variance explained by each PC is indicated in parentheses.

(**a**)

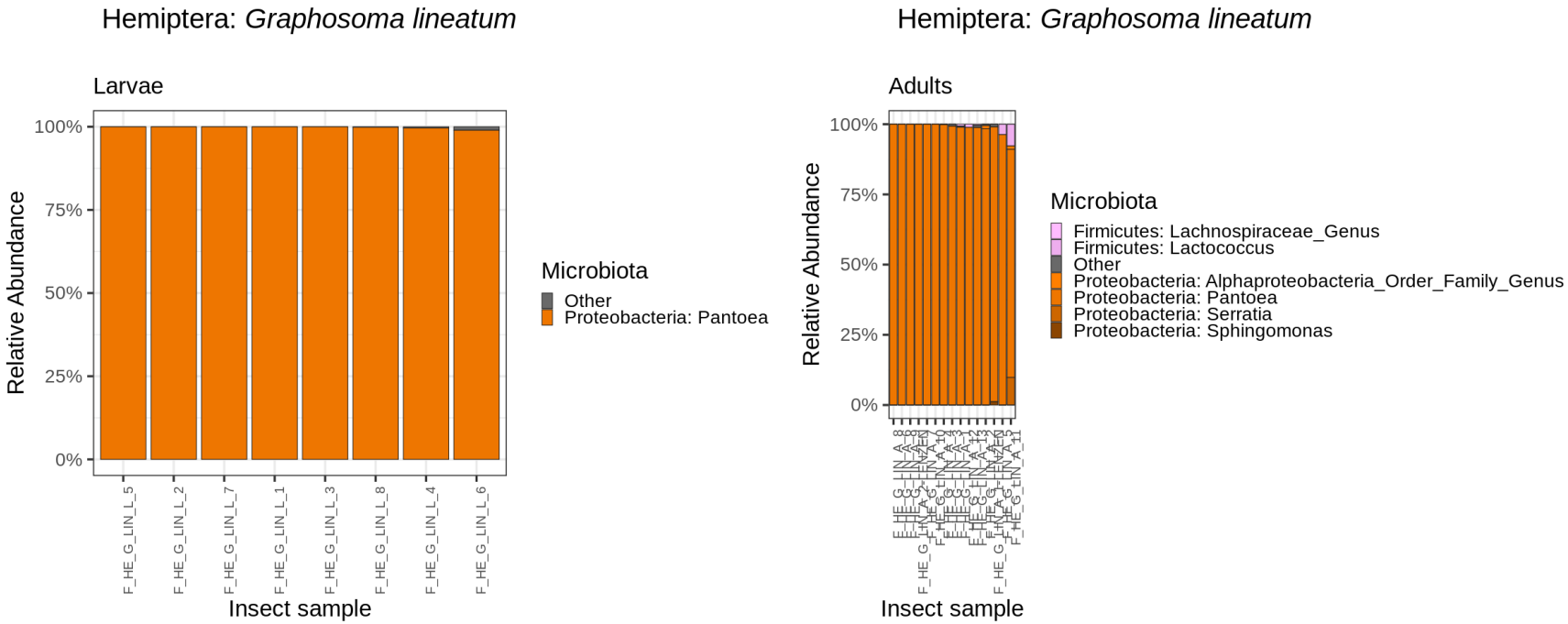
Hemiptera: *Graphosoma lineatum*
Larvae
Relative Abundance
100%
75%
50%
25%
0%
F_HE_G_LIN_L_5
F_HE_G_LIN_L_2
F_HE_G_LIN_L_7
F_HE_G_LIN_L_1
F_HE_G_LIN_L_3
F_HE_G_LIN_L_8
F_HE_G_LIN_L_4
F_HE_G_LIN_L_6
Insect sample
Microbiota
Other
Proteobacteria: Pantoea
Hemiptera: *Graphosoma lineatum*
Adults
Relative Abundance
100%
75%
50%
25%
0%
Insect sample
Microbiota
Firmicutes: Lachnospiraceae_Genus
Firmicutes: Lactococcus
Other
Proteobacteria: Alphaproteobacteria_Order_Family_Genus
Proteobacteria: Pantoea
Proteobacteria: Serratia
Proteobacteria: Sphingomonas

(**b**)

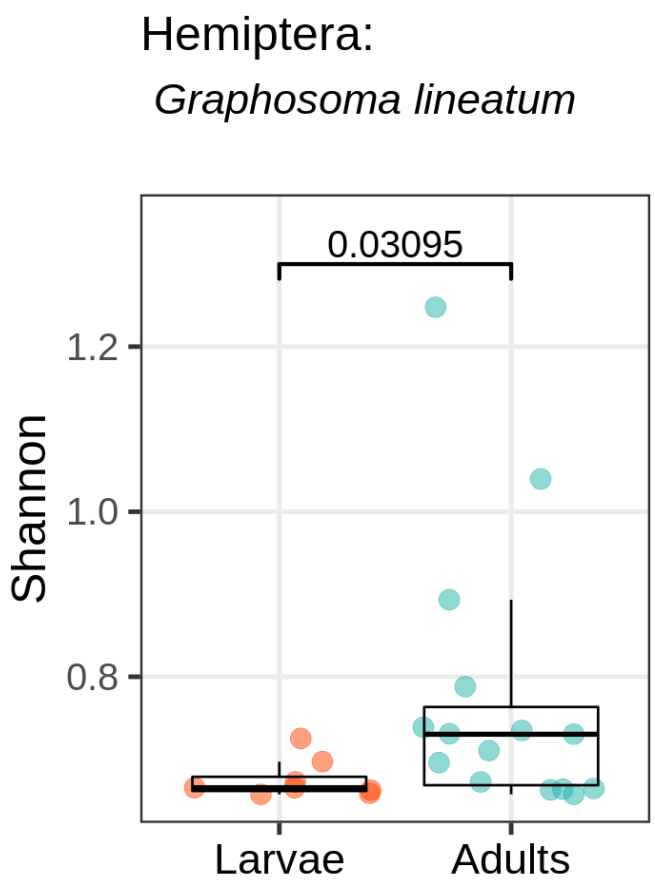

(**c**)

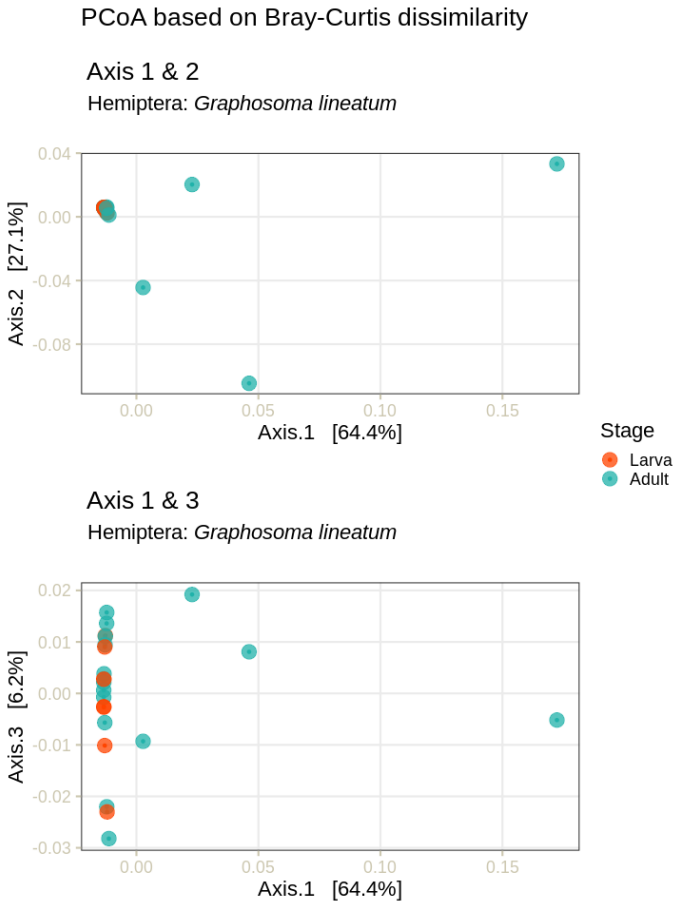

Figure S7: *Graphosoma lineatum* (Hemiptera) (a) microbiome composition assessed by 16S rRNA gene sequencing. Presented are the relative abundances of the bacterial genera for larval (left) and adult (right) samples. Shown are 99% of the genera. The remaining genera are shown as "Other." (b) Box plots of alpha-diversity indices (Shannon diversity) comparing larvae and adults (Two-sample t-test, t = -2.313, df = 21, p-value = 0.03095). (c) Principal coordinate analysis (PCoA) plot based on bray-curtis distances. The percentage of the total variance explained by each PC is indicated in parentheses.

(**a**)

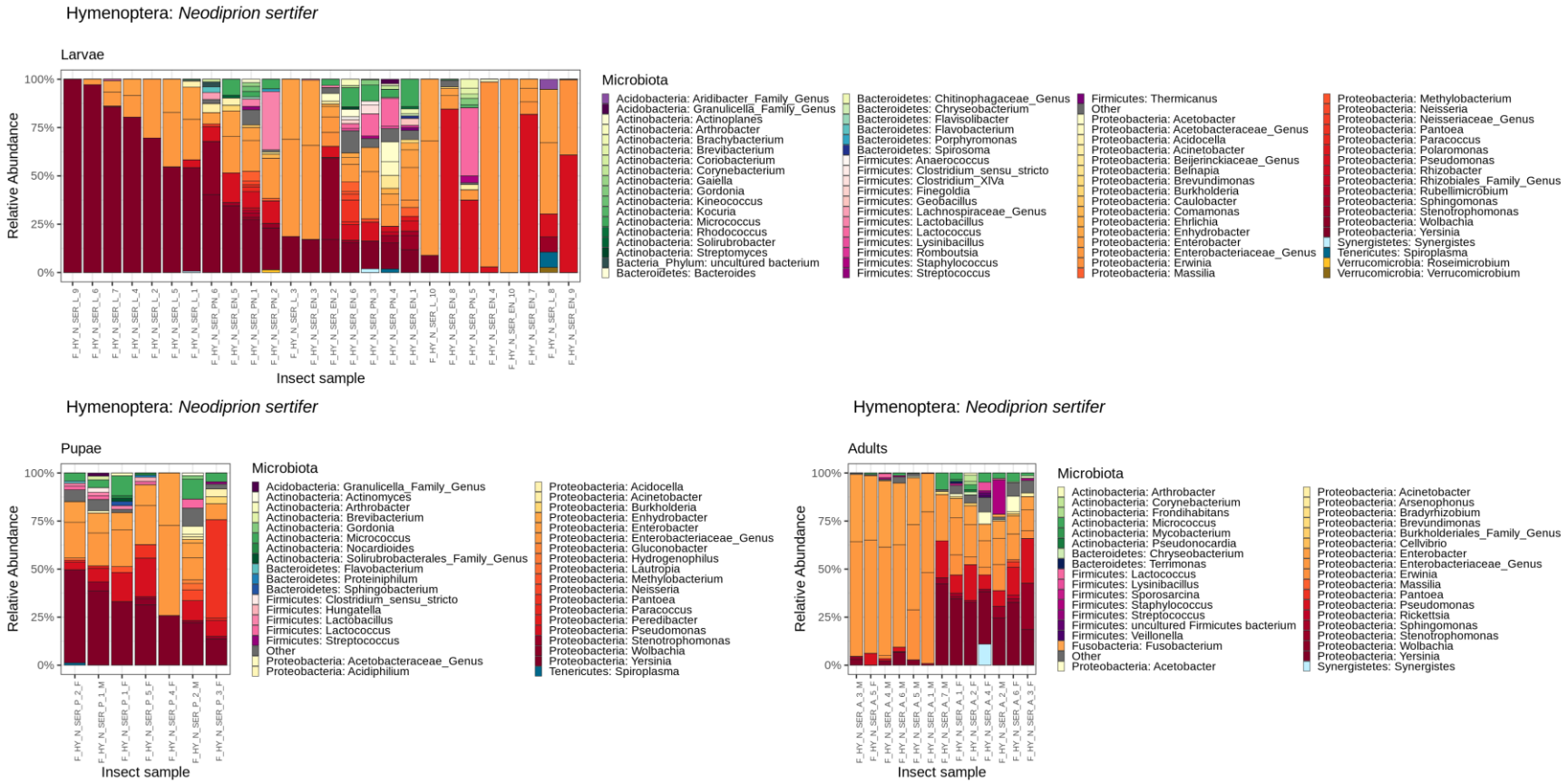
Hymenoptera: Neodiprion sertifer
Larvae
Relative Abundance
100%
75%
50%
25%
0%
Insect sample
Microbiota
Acidobacteria: Aridibacter_Family_Genus
Acidobacteria: Granulicella_Family_Genus
Actinobacteria: Actinoplanes
Actinobacteria: Arthrobacter
Actinobacteria: Brachybacterium
Actinobacteria: Brevibacterium
Actinobacteria: Coriobacterium
Actinobacteria: Corynebacterium
Actinobacteria: Gaiella
Actinobacteria: Gordonia
Actinobacteria: Kineococcus
Actinobacteria: Kocuria
Actinobacteria: Micrococcus
Actinobacteria: Rhodococcus
Actinobacteria: Solirubrobacter
Actinobacteria: Streptomyces
Bacteria_Phylum: uncultured bacterium
Bacteroidetes: Bacteroides
Bacteroidetes: Chitinophagaceae_Genus
Bacteroidetes: Chryseobacterium
Bacteroidetes: Flavisolibacter
Bacteroidetes: Flavobacterium
Bacteroidetes: Porphyromonas
Bacteroidetes: Spirosoma
Firmicutes: Anaerococcus
Firmicutes: Clostridium_sensu_stricto
Firmicutes: Clostridium_XlVa
Firmicutes: Finegoldia
Firmicutes: Geobacillus
Firmicutes: Lachnospiraceae_Genus
Firmicutes: Lactobacillus
Firmicutes: Lactococcus
Firmicutes: Lysinibacillus
Firmicutes: Romboutsia
Firmicutes: Staphylococcus
Firmicutes: Streptococcus
Firmicutes: Thermicanus
Other
Proteobacteria: Acetobacter
Proteobacteria: Acetobacteraceae_Genus
Proteobacteria: Acidocella
Proteobacteria: Acinetobacter
Proteobacteria: Beijerinckiaceae_Genus
Proteobacteria: Belnapia
Proteobacteria: Brevundimonas
Proteobacteria: Burkholderia
Proteobacteria: Caulobacter
Proteobacteria: Comamonas
Proteobacteria: Ehrlichia
Proteobacteria: Enhydrobacter
Proteobacteria: Enterobacter
Proteobacteria: Enterobacteriaceae_Genus
Proteobacteria: Erwinia
Proteobacteria: Massilia
Proteobacteria: Methylobacterium
Proteobacteria: Neisseria
Proteobacteria: Neisseriaceae_Genus
Proteobacteria: Pantoea
Proteobacteria: Paracoccus
Proteobacteria: Polaromonas
Proteobacteria: Pseudomonas
Proteobacteria: Rhizobacter
Proteobacteria: Rhizobiales_Family_Genus
Proteobacteria: Rubellimicrobium
Proteobacteria: Sphingomonas
Proteobacteria: Stenotrophomonas
Proteobacteria: Wolbachia
Proteobacteria: Yersinia
Synergistetes: Synergistes
Tenericutes: Spiroplasma
Verrucomicrobia: Roseimicrobium
Verrucomicrobia: Verrucomicrobium
Hymenoptera: Neodiprion sertifer
Pupae
Relative Abundance
100%
75%
50%
25%
0%
Insect sample
Microbiota
Acidobacteria: Granulicella_Family_Genus
Actinobacteria: Actinomyces
Actinobacteria: Arthrobacter
Actinobacteria: Brevibacterium
Actinobacteria: Gordonia
Actinobacteria: Micrococcus
Actinobacteria: Nocardioides
Actinobacteria: Solirubrobacterales_Family_Genus
Bacteroidetes: Flavobacterium
Bacteroidetes: Proteiniphilum
Bacteroidetes: Sphingobacterium
Firmicutes: Clostridium_sensu_stricto
Firmicutes: Hungatella
Firmicutes: Lactobacillus
Firmicutes: Lactococcus
Firmicutes: Streptococcus
Other
Proteobacteria: Acetobacteraceae_Genus
Proteobacteria: Acidiphilium
Proteobacteria: Acidocella
Proteobacteria: Acinetobacter
Proteobacteria: Burkholderia
Proteobacteria: Enhydrobacter
Proteobacteria: Enterobacter
Proteobacteria: Enterobacteriaceae_Genus
Proteobacteria: Gluconobacter
Proteobacteria: Hydrogenophilus
Proteobacteria: Lautropia
Proteobacteria: Methylobacterium
Proteobacteria: Neisseria
Proteobacteria: Pantoea
Proteobacteria: Paracoccus
Proteobacteria: Peredibacter
Proteobacteria: Pseudomonas
Proteobacteria: Stenotrophomonas
Proteobacteria: Wolbachia
Proteobacteria: Yersinia
Tenericutes: Spiroplasma
Hymenoptera: Neodiprion sertifer
Adults
Relative Abundance
100%
75%
50%
25%
0%
Insect sample
Microbiota
Actinobacteria: Arthrobacter
Actinobacteria: Corynebacterium
Actinobacteria: Frondihabitans
Actinobacteria: Micrococcus
Actinobacteria: Mycobacterium
Actinobacteria: Pseudonocardia
Bacteroidetes: Chryseobacterium
Bacteroidetes: Terrimonas
Firmicutes: Lactococcus
Firmicutes: Lysinibacillus
Firmicutes: Sporosarcina
Firmicutes: Staphylococcus
Firmicutes: Streptococcus
Firmicutes: uncultured Firmicutes bacterium
Firmicutes: Veillonella
Fusobacteria: Fusobacterium
Other
Proteobacteria: Acetobacter
Proteobacteria: Acinetobacter
Proteobacteria: Arsenophonus
Proteobacteria: Bradyrhizobium
Proteobacteria: Brevundimonas
Proteobacteria: Burkholderiales_Family_Genus
Proteobacteria: Cellvibrio
Proteobacteria: Enterobacter
Proteobacteria: Enterobacteriaceae_Genus
Proteobacteria: Erwinia
Proteobacteria: Massilia
Proteobacteria: Pantoea
Proteobacteria: Pseudomonas
Proteobacteria: Rickettsia
Proteobacteria: Sphingomonas
Proteobacteria: Stenotrophomonas
Proteobacteria: Wolbachia
Proteobacteria: Yersinia
Synergistetes: Synergistes

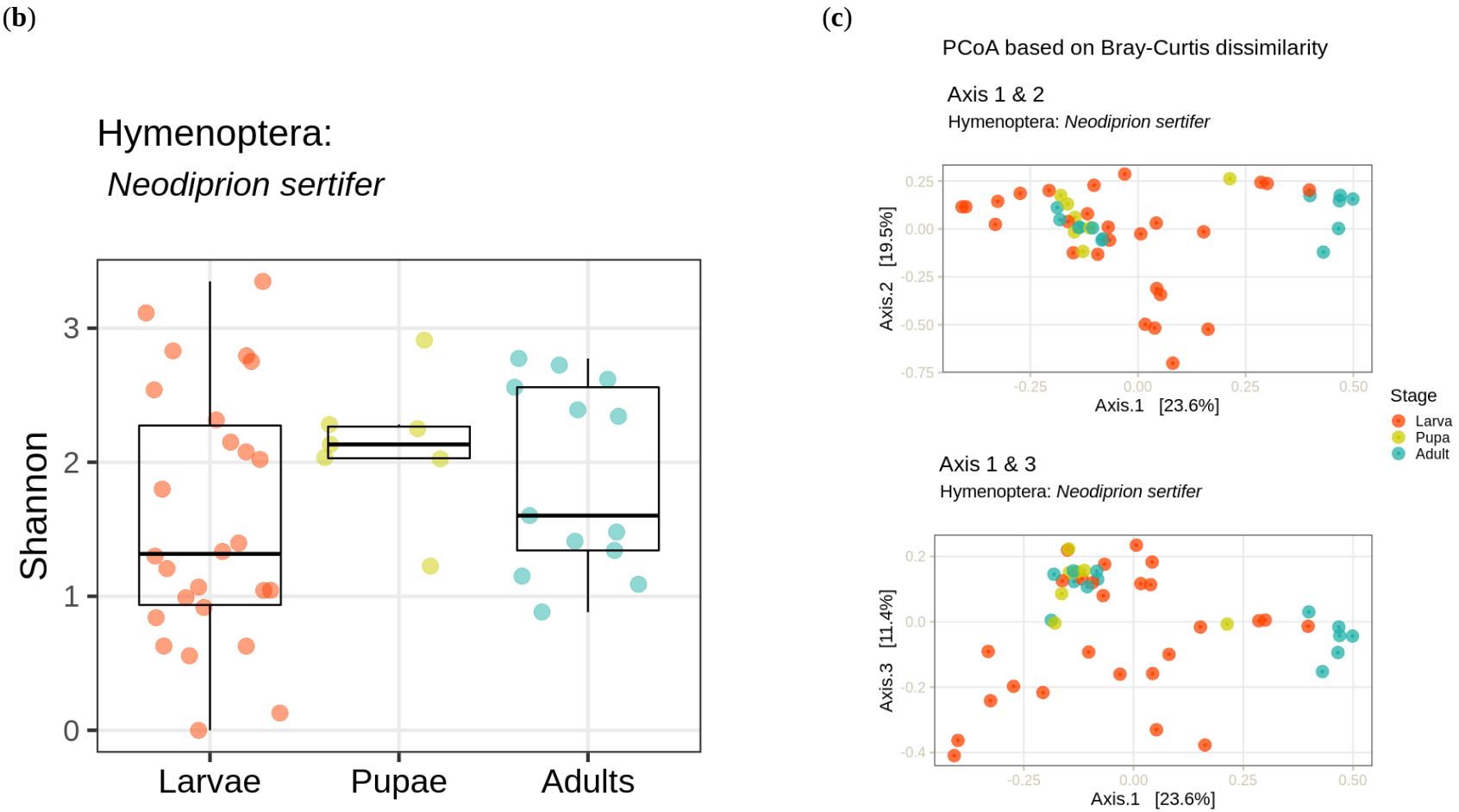

Figure S8: *Neodiprion sertifer* (Hymenoptera) (a) microbiome composition assessed by 16S rRNA gene sequencing. Presented are the relative abundances of the bacterial genera for larval (top), pupal (bottom left) and adult (bottom right) samples. Shown are 99% of the genera. The remaining genera are shown as "Other." (b) Box plots of alpha-diversity indices (Shannon diversity) comparing larvae, pupae and adults. (c) Principal coordinate analysis (PCoA) plot based on bray-curtis distances. The percentage of the total variance explained by each PC is indicated in parentheses.

(**a**)

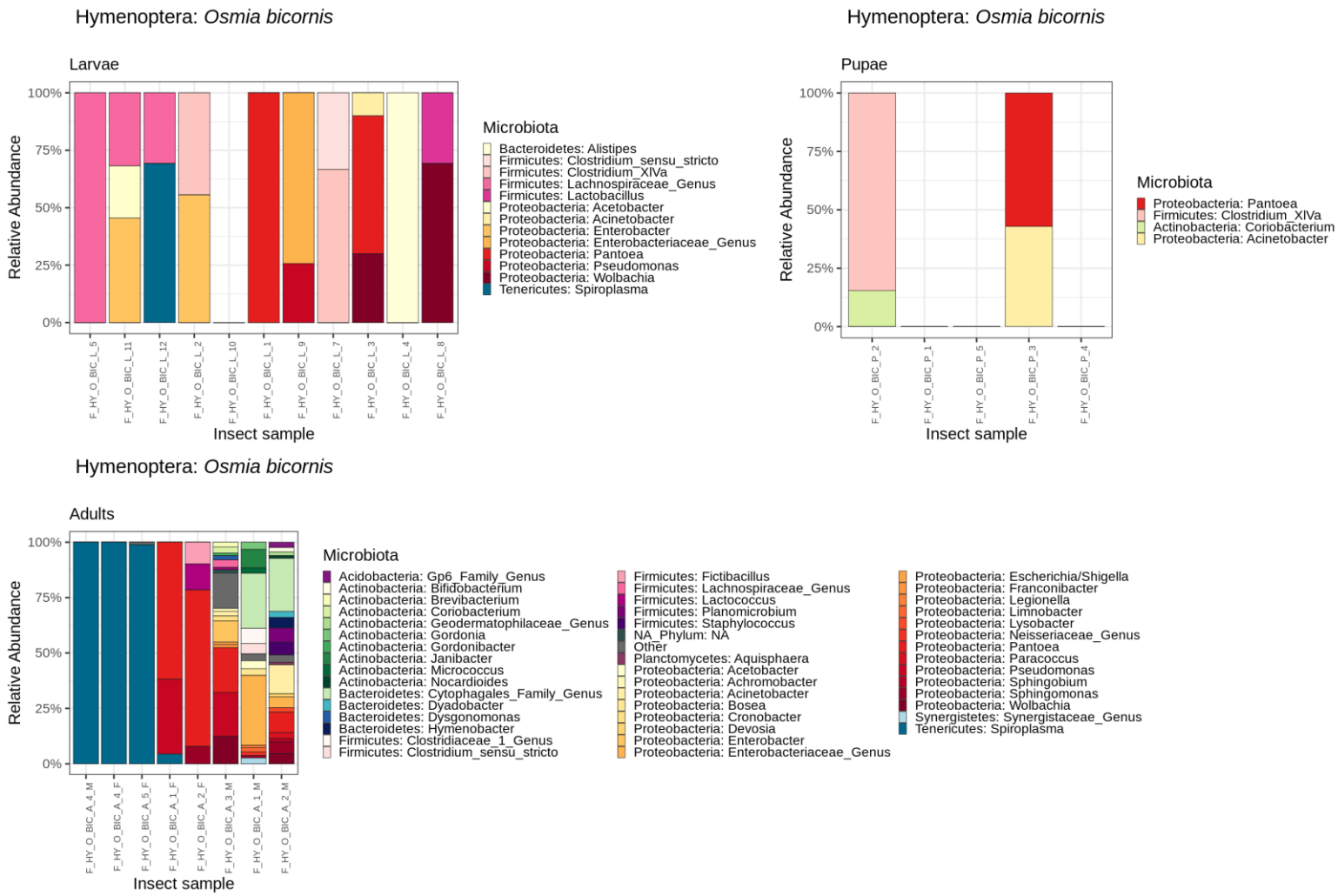
Hymenoptera: Osmia bicornis
Larvae
Relative Abundance
100%
75%
50%
25%
0%
F_HY_O_BIC_L_5
F_HY_O_BIC_L_11
F_HY_O_BIC_L_12
F_HY_O_BIC_L_2
F_HY_O_BIC_L_10
F_HY_O_BIC_L_1
F_HY_O_BIC_L_9
F_HY_O_BIC_L_7
F_HY_O_BIC_L_3
F_HY_O_BIC_L_4
F_HY_O_BIC_L_8
Insect sample
Microbiota
Bacteroidetes: Alistipes
Firmicutes: Clostridium_sensu_stricto
Firmicutes: Clostridium_XlVa
Firmicutes: Lachnospiraceae_Genus
Firmicutes: Lactobacillus
Proteobacteria: Acetobacter
Proteobacteria: Acinetobacter
Proteobacteria: Enterobacter
Proteobacteria: Enterobacteriaceae_Genus
Proteobacteria: Pantoea
Proteobacteria: Pseudomonas
Proteobacteria: Wolbachia
Tenericutes: Spiroplasma
Hymenoptera: Osmia bicornis
Pupae
Relative Abundance
100%
75%
50%
25%
0%
F_HY_O_BIC_P_2
F_HY_O_BIC_P_1
F_HY_O_BIC_P_5
F_HY_O_BIC_P_3
F_HY_O_BIC_P_4
Insect sample
Microbiota
Proteobacteria: Pantoea
Firmicutes: Clostridium_XlVa
Actinobacteria: Coriobacterium
Proteobacteria: Acinetobacter
Hymenoptera: Osmia bicornis
Adults
Relative Abundance
100%
75%
50%
25%
0%
F_HY_O_BIC_A_4_M
F_HY_O_BIC_A_4_F
F_HY_O_BIC_A_5_F
F_HY_O_BIC_A_1_F
F_HY_O_BIC_A_2_F
F_HY_O_BIC_A_3_M
F_HY_O_BIC_A_1_M
F_HY_O_BIC_A_2_M
Insect sample
Microbiota
Acidobacteria: Gp6_Family_Genus
Actinobacteria: Bifidobacterium
Actinobacteria: Brevibacterium
Actinobacteria: Coriobacterium
Actinobacteria: Geodermatophilaceae_Genus
Actinobacteria: Gordonia
Actinobacteria: Gordonibacter
Actinobacteria: Janibacter
Actinobacteria: Micrococcus
Actinobacteria: Nocardioides
Bacteroidetes: Cytophagales_Family_Genus
Bacteroidetes: Dyadobacter
Bacteroidetes: Dysgonomonas
Bacteroidetes: Hymenobacter
Firmicutes: Clostridiaceae_1_Genus
Firmicutes: Clostridium_sensu_stricto
Firmicutes: Fictibacillus
Firmicutes: Lachnospiraceae_Genus
Firmicutes: Lactococcus
Firmicutes: Planomicrobium
Firmicutes: Staphylococcus
NA_Phylum: NA
Other
Planctomycetes: Aquisphaera
Proteobacteria: Acetobacter
Proteobacteria: Achromobacter
Proteobacteria: Acinetobacter
Proteobacteria: Bosea
Proteobacteria: Cronobacter
Proteobacteria: Devosia
Proteobacteria: Enterobacter
Proteobacteria: Enterobacteriaceae_Genus
Proteobacteria: Escherichia/Shigella
Proteobacteria: Franconibacter
Proteobacteria: Legionella
Proteobacteria: Limnobacter
Proteobacteria: Lysobacter
Proteobacteria: Neisseriaceae_Genus
Proteobacteria: Pantoea
Proteobacteria: Paracoccus
Proteobacteria: Pseudomonas
Proteobacteria: Sphingobium
Proteobacteria: Sphingomonas
Proteobacteria: Wolbachia
Synergistetes: Synergistaceae_Genus
Tenericutes: Spiroplasma

(**b**)

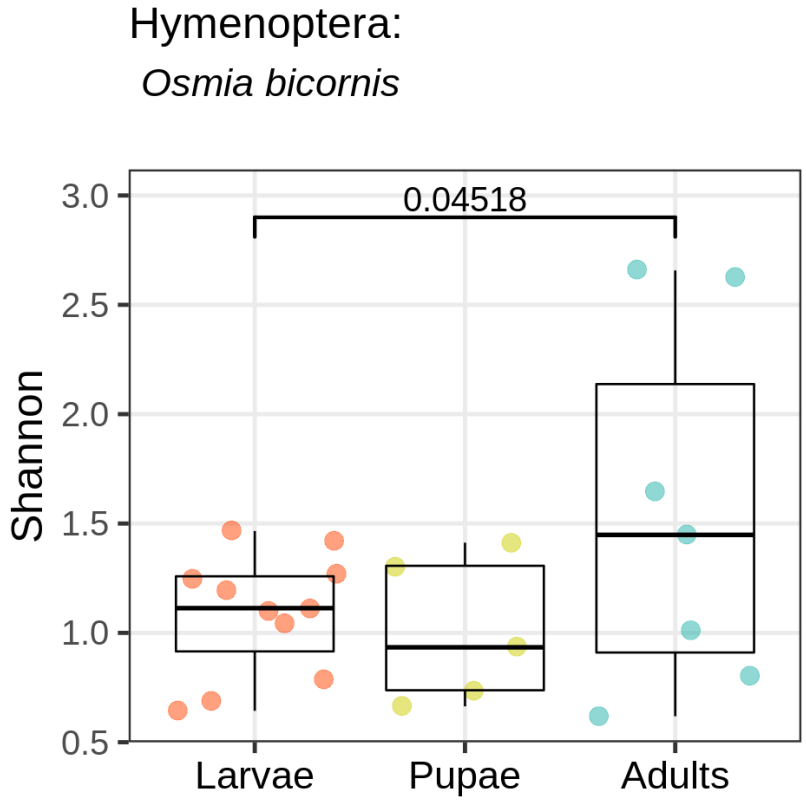

(**c**)

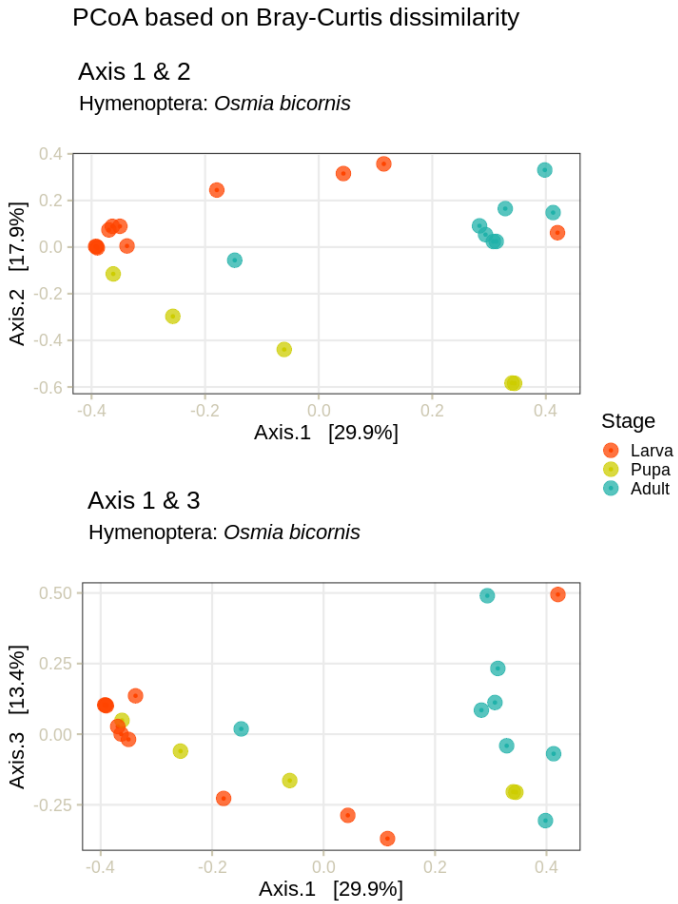

Figure S9: *Osmia bicornis* (Hymenoptera) (a) microbiome composition assessed by 16S rRNA gene sequencing. Presented are the relative abundances of the bacterial genera for larval (top left), pupal (top right) and adult (bottom) samples. Shown are 99% of the genera. The remaining genera are shown as "Other." (b) Box plots of alpha-diversity indices (Shannon diversity) comparing larvae, pupae and adults. (Two-sample t-test, t = 2.1619, df = 17, p-value = 0.04518) (c) Principal coordinate analysis (PCoA) plot based on bray-curtis distances. The percentage of the total variance explained by each PC is indicated in parentheses.

(**a**)

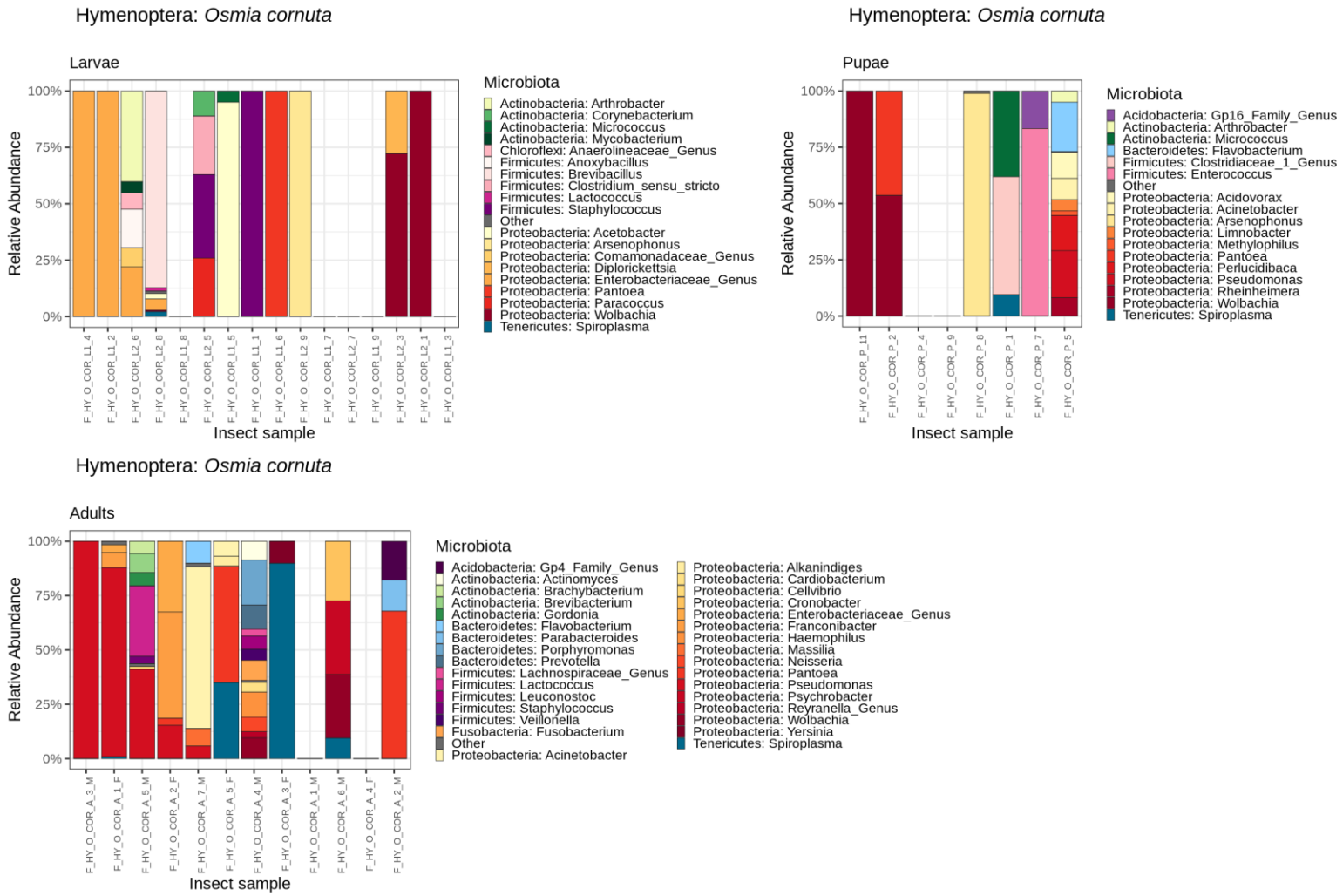
Hymenoptera: Osmia cornuta
Larvae
Relative Abundance
100%
75%
50%
25%
0%
F_HY_O_COR_L1_4
F_HY_O_COR_L1_2
F_HY_O_COR_L2_6
F_HY_O_COR_L2_8
F_HY_O_COR_L1_8
F_HY_O_COR_L2_5
F_HY_O_COR_L1_5
F_HY_O_COR_L1_1
F_HY_O_COR_L1_6
F_HY_O_COR_L2_9
F_HY_O_COR_L1_7
F_HY_O_COR_L2_7
F_HY_O_COR_L1_9
F_HY_O_COR_L2_3
F_HY_O_COR_L2_1
F_HY_O_COR_L1_3
Insect sample
Microbiota
Actinobacteria: Arthrobacter
Actinobacteria: Corynebacterium
Actinobacteria: Micrococcus
Actinobacteria: Mycobacterium
Chloroflexi: Anaerolineaceae_Genus
Firmicutes: Anoxybacillus
Firmicutes: Brevibacillus
Firmicutes: Clostridium_sensu_stricto
Firmicutes: Lactococcus
Firmicutes: Staphylococcus
Other
Proteobacteria: Acetobacter
Proteobacteria: Arsenophonus
Proteobacteria: Comamonadaceae_Genus
Proteobacteria: Diplorickettsia
Proteobacteria: Enterobacteriaceae_Genus
Proteobacteria: Pantoea
Proteobacteria: Paracoccus
Proteobacteria: Wolbachia
Tenericutes: Spiroplasma
Hymenoptera: Osmia cornuta
Pupae
Relative Abundance
100%
75%
50%
25%
0%
F_HY_O_COR_P_11
F_HY_O_COR_P_2
F_HY_O_COR_P_4
F_HY_O_COR_P_9
F_HY_O_COR_P_8
F_HY_O_COR_P_1
F_HY_O_COR_P_7
F_HY_O_COR_P_5
Insect sample
Microbiota
Acidobacteria: Gp16_Family_Genus
Actinobacteria: Arthrobacter
Actinobacteria: Micrococcus
Bacteroidetes: Flavobacterium
Firmicutes: Clostridiaceae_1_Genus
Firmicutes: Enterococcus
Other
Proteobacteria: Acidovorax
Proteobacteria: Acinetobacter
Proteobacteria: Arsenophonus
Proteobacteria: Limnobacter
Proteobacteria: Methylophilus
Proteobacteria: Pantoea
Proteobacteria: Perlucidibaca
Proteobacteria: Pseudomonas
Proteobacteria: Rheinheimera
Proteobacteria: Wolbachia
Tenericutes: Spiroplasma
Hymenoptera: Osmia cornuta
Adults
Relative Abundance
100%
75%
50%
25%
0%
F_HY_O_COR_A_3_M
F_HY_O_COR_A_1_F
F_HY_O_COR_A_5_M
F_HY_O_COR_A_2_F
F_HY_O_COR_A_7_M
F_HY_O_COR_A_5_F
F_HY_O_COR_A_4_M
F_HY_O_COR_A_3_F
F_HY_O_COR_A_1_M
F_HY_O_COR_A_6_M
F_HY_O_COR_A_4_F
F_HY_O_COR_A_2_M
Insect sample
Microbiota
Acidobacteria: Gp4_Family_Genus
Actinobacteria: Actinomyces
Actinobacteria: Brachybacterium
Actinobacteria: Brevibacterium
Actinobacteria: Gordonia
Bacteroidetes: Flavobacterium
Bacteroidetes: Parabacteroides
Bacteroidetes: Porphyromonas
Bacteroidetes: Prevotella
Firmicutes: Lachnospiraceae_Genus
Firmicutes: Lactococcus
Firmicutes: Leuconostoc
Firmicutes: Staphylococcus
Firmicutes: Veillonella
Fusobacteria: Fusobacterium
Other
Proteobacteria: Acinetobacter
Proteobacteria: Alkanindiges
Proteobacteria: Cardiobacterium
Proteobacteria: Cellvibrio
Proteobacteria: Cronobacter
Proteobacteria: Enterobacteriaceae_Genus
Proteobacteria: Franconibacter
Proteobacteria: Haemophilus
Proteobacteria: Massilia
Proteobacteria: Neisseria
Proteobacteria: Pantoea
Proteobacteria: Pseudomonas
Proteobacteria: Psychrobacter
Proteobacteria: Reyranella_Genus
Proteobacteria: Wolbachia
Proteobacteria: Yersinia
Tenericutes: Spiroplasma

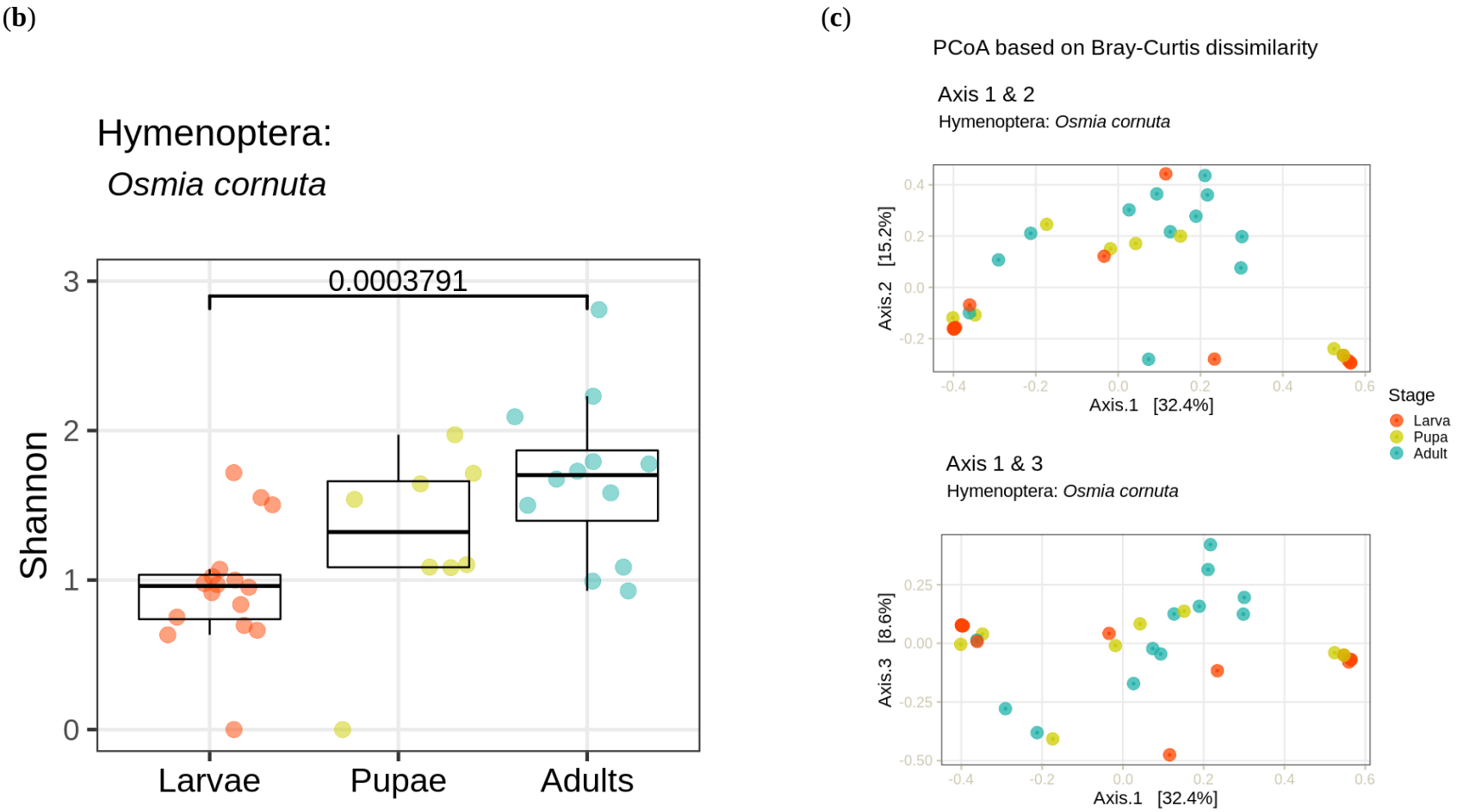

Figure S10: *Osmia cornuta* (Hymenoptera) (a) microbiome composition assessed by 16S rRNA gene sequencing. Presented are the relative abundances of the bacterial genera for larval (top left), pupal (top right) and adult (bottom) samples. Shown are 99% of the genera. The remaining genera are shown as "Other." (b) Box plots of alpha-diversity indices (Shannon diversity) comparing larvae, pupae and adults. (Two-sample t-test, t = 4.0803, df = 26, p-value = 0.0003791) (c) Principal coordinate analysis (PCoA) plot based on bray-curtis distances. The percentage of the total variance explained by each PC is indicated in parentheses.

APPENDIX CHAPTER II

(**a**)

Coleoptera: *Melolontha melolontha*

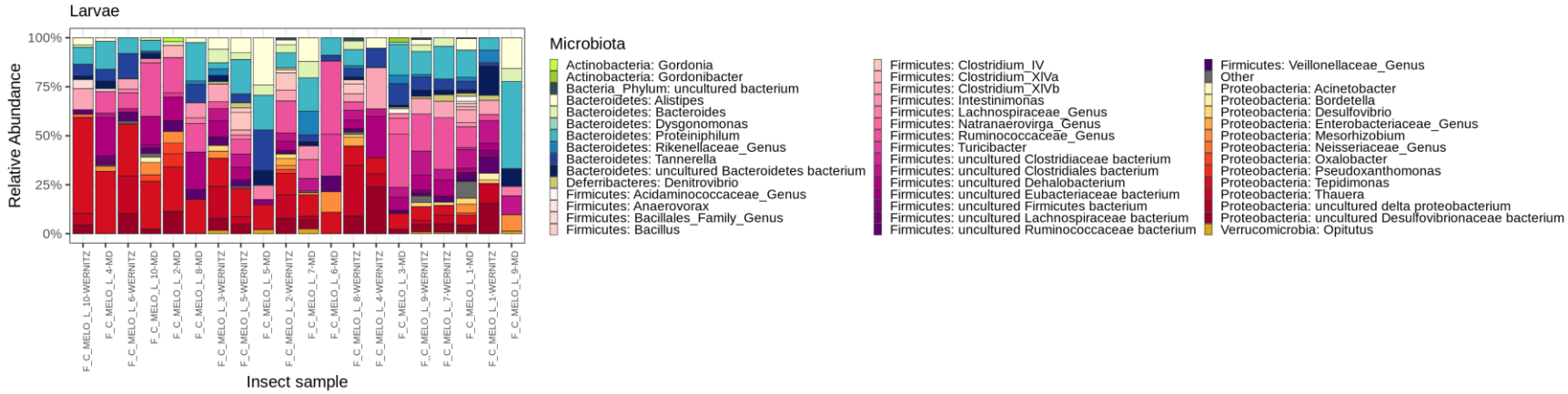

Coleoptera: *Melolontha melolontha*

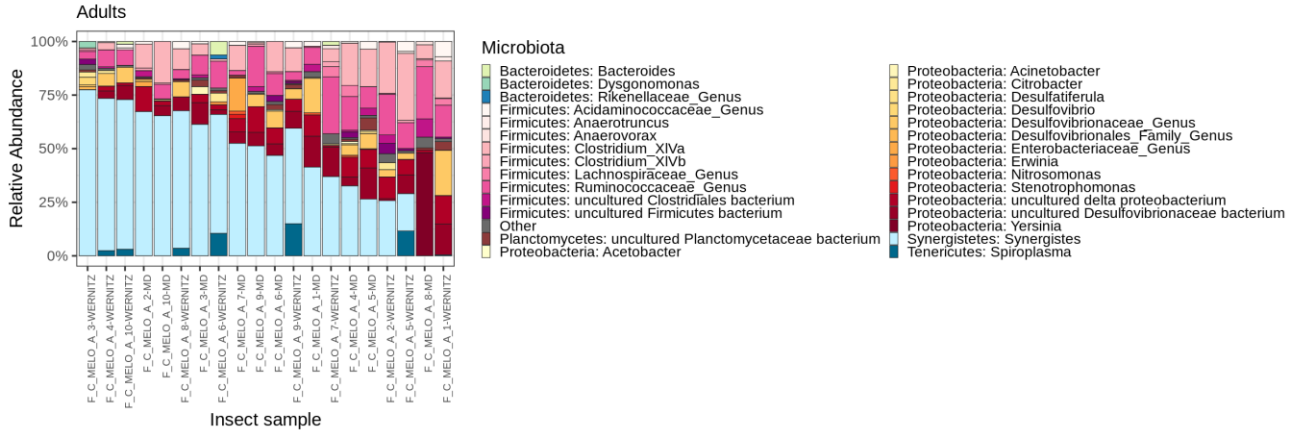

(**b**)

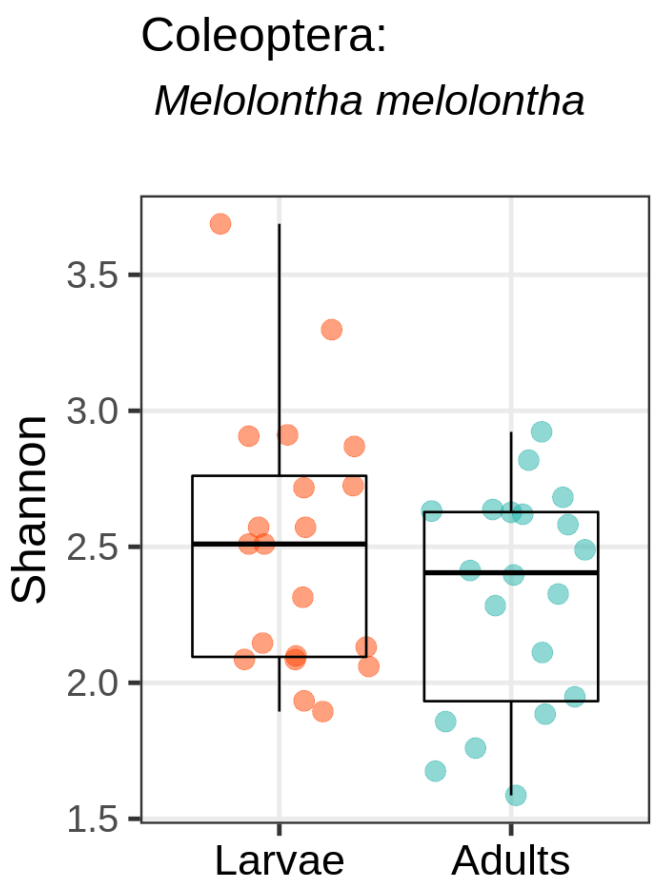

(**c**)

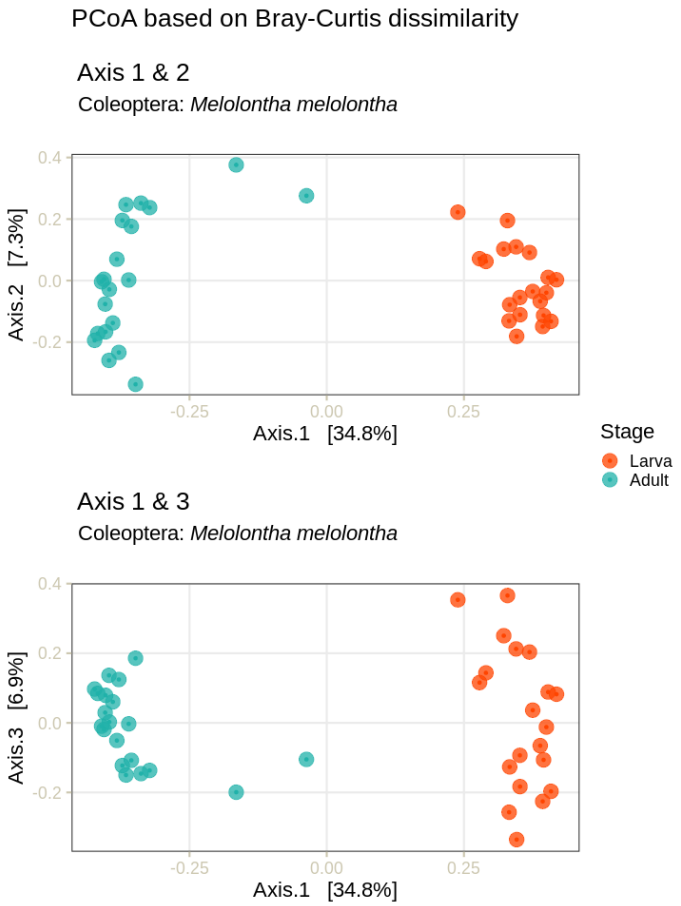

Figure S11: *Melolontha melolontha* (Coleoptera) (a) microbiome composition assessed by 16S rRNA gene sequencing. Presented are the relative abundances of the bacterial genera for larval (top) and adult (bottom) samples. Shown are 99% of the genera. The remaining genera are shown as "Other." (b) Box plots of alpha-diversity indices (Shannon diversity) comparing larvae and adults. (c) Principal coordinate analysis (PCoA) plot based on bray-curtis distances. The percentage of the total variance explained by each PC is indicated in parentheses.

(**a**)

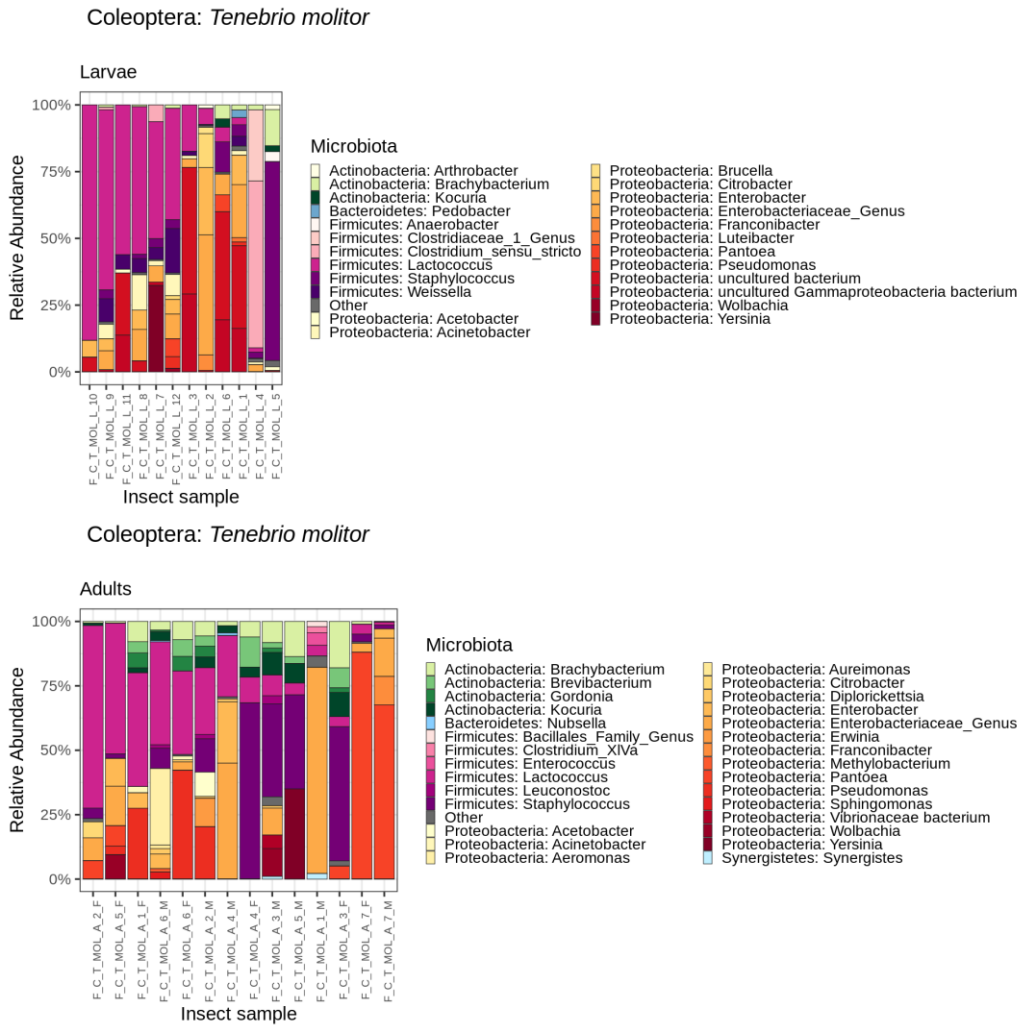
Coleoptera: Tenebrio molitor
Larvae
Relative Abundance
100%
75%
50%
25%
0%
F_C_T_MOL_L_10
F_C_T_MOL_L_9
F_C_T_MOL_L_11
F_C_T_MOL_L_8
F_C_T_MOL_L_7
F_C_T_MOL_L_12
F_C_T_MOL_L_3
F_C_T_MOL_L_2
F_C_T_MOL_L_6
F_C_T_MOL_L_1
F_C_T_MOL_L_4
F_C_T_MOL_L_5
Insect sample
Microbiota
Actinobacteria: Arthrobacter
Actinobacteria: Brachybacterium
Actinobacteria: Kocuria
Bacteroidetes: Pedobacter
Firmicutes: Anaerobacter
Firmicutes: Clostridiaceae_1_Genus
Firmicutes: Clostridium_sensu_stricto
Firmicutes: Lactococcus
Firmicutes: Staphylococcus
Firmicutes: Weissella
Other
Proteobacteria: Acetobacter
Proteobacteria: Acinetobacter
Proteobacteria: Brucella
Proteobacteria: Citrobacter
Proteobacteria: Enterobacter
Proteobacteria: Enterobacteriaceae_Genus
Proteobacteria: Franconibacter
Proteobacteria: Luteibacter
Proteobacteria: Pantoea
Proteobacteria: Pseudomonas
Proteobacteria: uncultured bacterium
Proteobacteria: uncultured Gammaproteobacteria bacterium
Proteobacteria: Wolbachia
Proteobacteria: Yersinia

Coleoptera: Tenebrio molitor
Adults
Relative Abundance
100%
75%
50%
25%
0%
F_C_T_MOL_A_2_F
F_C_T_MOL_A_5_F
F_C_T_MOL_A_1_F
F_C_T_MOL_A_6_M
F_C_T_MOL_A_6_F
F_C_T_MOL_A_2_M
F_C_T_MOL_A_4_M
F_C_T_MOL_A_4_F
F_C_T_MOL_A_3_M
F_C_T_MOL_A_5_M
F_C_T_MOL_A_1_M
F_C_T_MOL_A_3_F
F_C_T_MOL_A_7_F
F_C_T_MOL_A_7_M
Insect sample
Microbiota
Actinobacteria: Brachybacterium
Actinobacteria: Brevibacterium
Actinobacteria: Gordonia
Actinobacteria: Kocuria
Bacteroidetes: Nubsella
Firmicutes: Bacillales_Family_Genus
Firmicutes: Clostridium_XlVa
Firmicutes: Enterococcus
Firmicutes: Lactococcus
Firmicutes: Leuconostoc
Firmicutes: Staphylococcus
Other
Proteobacteria: Acetobacter
Proteobacteria: Acinetobacter
Proteobacteria: Aeromonas
Proteobacteria: Aureimonas
Proteobacteria: Citrobacter
Proteobacteria: Diplorickettsia
Proteobacteria: Enterobacter
Proteobacteria: Enterobacteriaceae_Genus
Proteobacteria: Erwinia
Proteobacteria: Franconibacter
Proteobacteria: Methylobacterium
Proteobacteria: Pantoea
Proteobacteria: Pseudomonas
Proteobacteria: Sphingomonas
Proteobacteria: Vibrionaceae bacterium
Proteobacteria: Wolbachia
Proteobacteria: Yersinia
Synergistetes: Synergistes

(b)

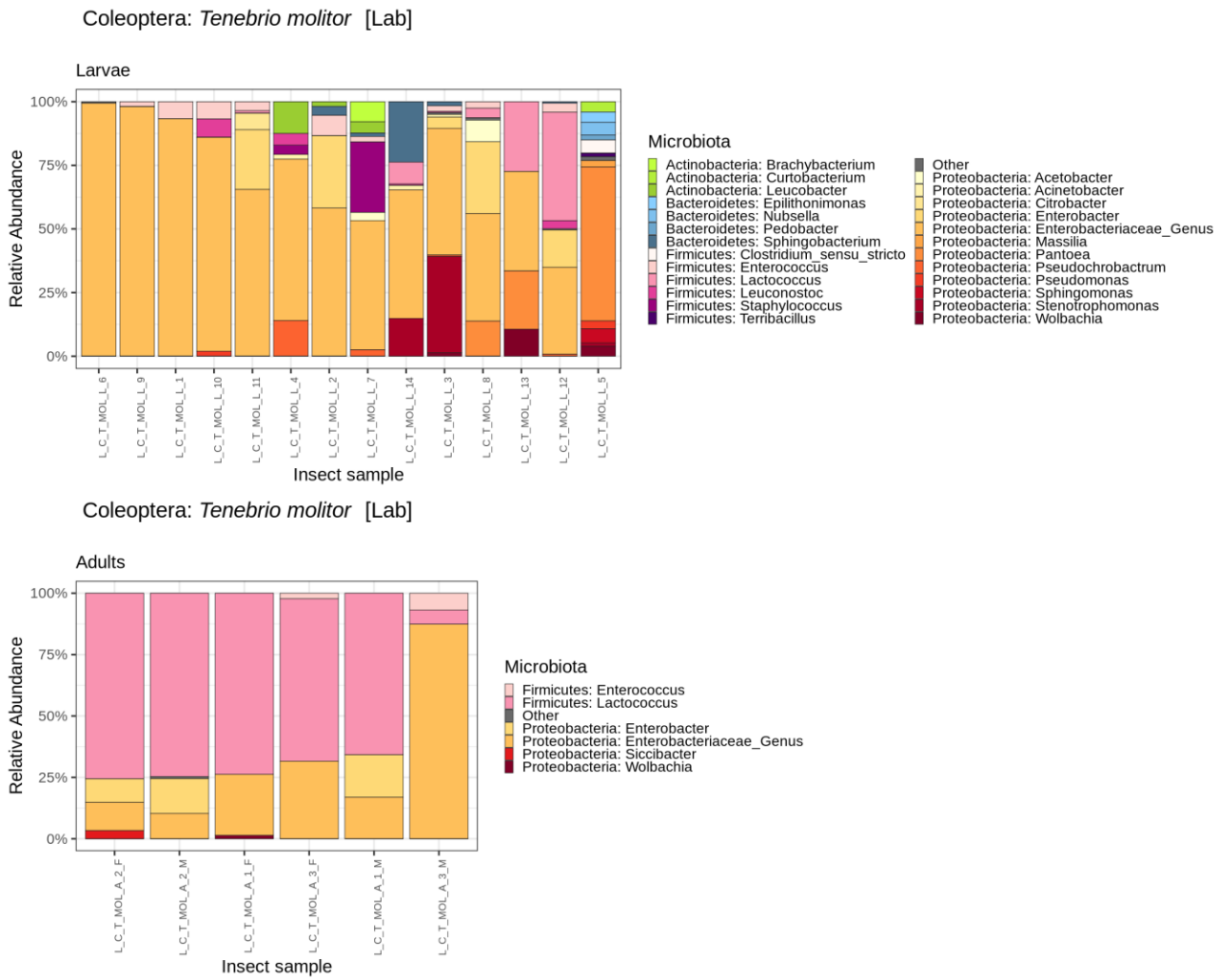
Coleoptera: Tenebrio molitor [Lab]
Larvae
Relative Abundance
100%
75%
50%
25%
0%
L_C_T_MOL_L_6
L_C_T_MOL_L_9
L_C_T_MOL_L_1
L_C_T_MOL_L_10
L_C_T_MOL_L_11
L_C_T_MOL_L_4
L_C_T_MOL_L_2
L_C_T_MOL_L_7
L_C_T_MOL_L_14
L_C_T_MOL_L_3
L_C_T_MOL_L_8
L_C_T_MOL_L_13
L_C_T_MOL_L_12
L_C_T_MOL_L_5
Insect sample
Microbiota
Actinobacteria: Brachybacterium
Actinobacteria: Curtobacterium
Actinobacteria: Leucobacter
Bacteroidetes: Epilithonimonas
Bacteroidetes: Nubsella
Bacteroidetes: Pedobacter
Bacteroidetes: Sphingobacterium
Firmicutes: Clostridium_sensu_stricto
Firmicutes: Enterococcus
Firmicutes: Lactococcus
Firmicutes: Leuconostoc
Firmicutes: Staphylococcus
Firmicutes: Terribacillus
Other
Proteobacteria: Acetobacter
Proteobacteria: Acinetobacter
Proteobacteria: Citrobacter
Proteobacteria: Enterobacter
Proteobacteria: Enterobacteriaceae_Genus
Proteobacteria: Massilia
Proteobacteria: Pantoea
Proteobacteria: Pseudochrobactrum
Proteobacteria: Pseudomonas
Proteobacteria: Sphingomonas
Proteobacteria: Stenotrophomonas
Proteobacteria: Wolbachia

Coleoptera: Tenebrio molitor [Lab]
Adults
Relative Abundance
100%
75%
50%
25%
0%
L_C_T_MOL_A_2_F
L_C_T_MOL_A_2_M
L_C_T_MOL_A_1_F
L_C_T_MOL_A_3_F
L_C_T_MOL_A_1_M
L_C_T_MOL_A_3_M
Insect sample
Microbiota
Firmicutes: Enterococcus
Firmicutes: Lactococcus
Other
Proteobacteria: Enterobacter
Proteobacteria: Enterobacteriaceae_Genus
Proteobacteria: Siccibacter
Proteobacteria: Wolbachia

(c)

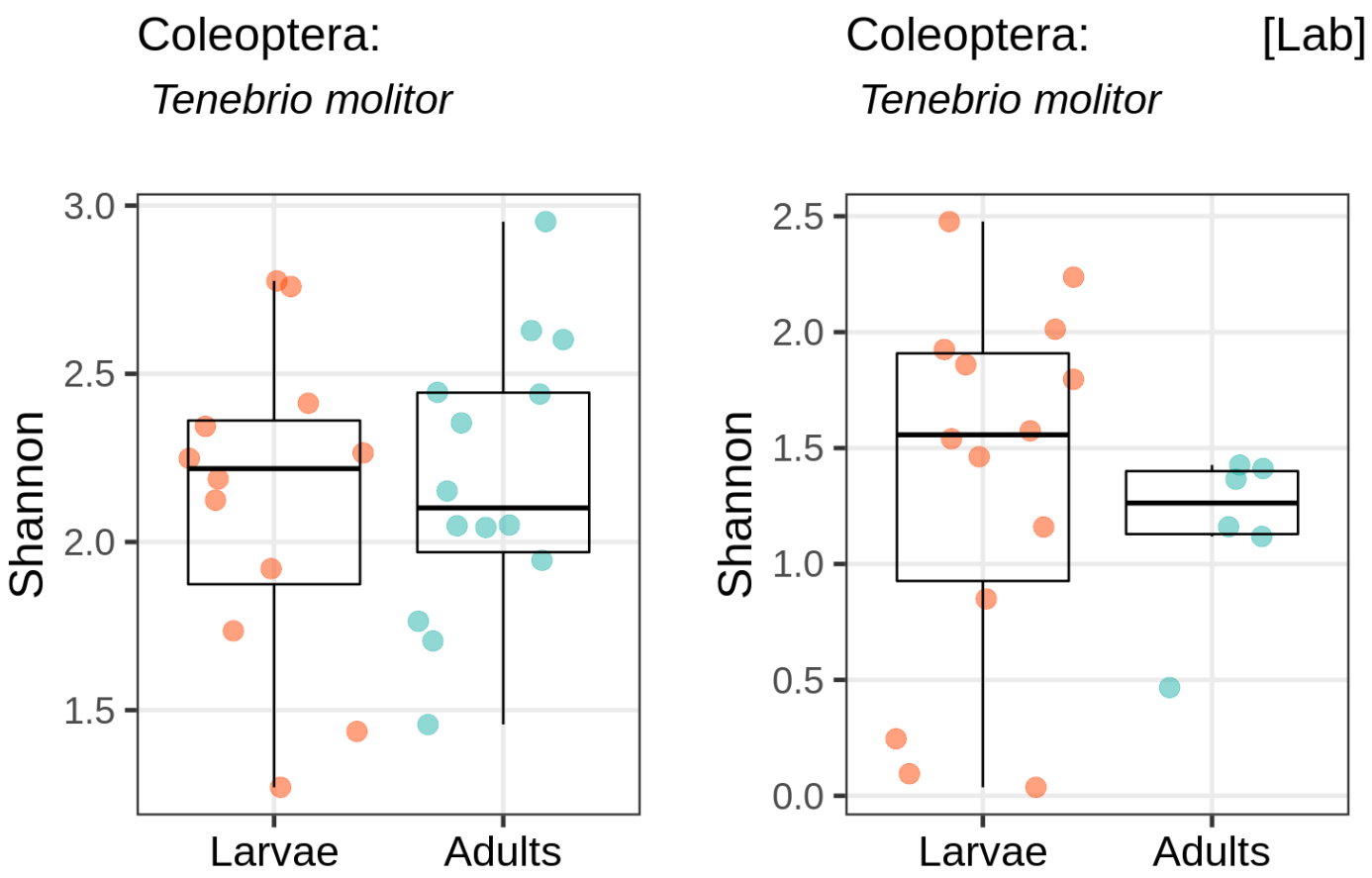
Coleoptera:
Tenebrio molitor
Shannon
3.0
2.5
2.0
1.5
Larvae
Adults
Coleoptera: [Lab]
Tenebrio molitor
Shannon
2.5
2.0
1.5
1.0
0.5
0.0
Larvae
Adults

(d)

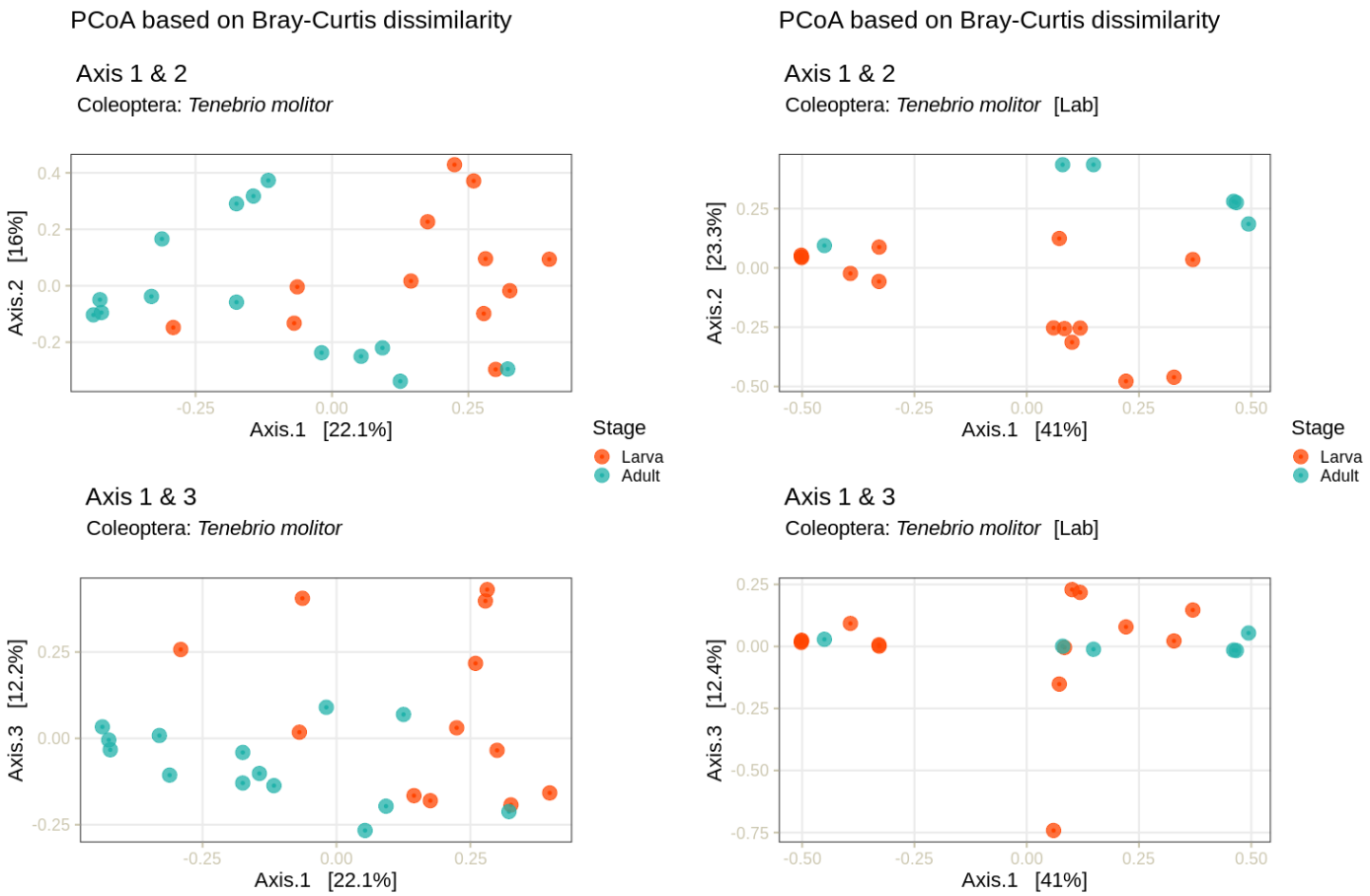

Figure S12: *Tenebrio molitor* (Coleoptera) (a) microbiome composition assessed by 16S rRNA gene sequencing. Presented are the relative abundances of the bacterial genera for larval (top) and adult (bottom) samples. Shown are 99% of the genera. The remaining genera are shown as "Other." (b) Microbiome composition of laboratory-reared *Tenebrio molitor*. (c) Box plots of alpha-diversity indices (Shannon diversity) comparing larvae and adults for field-collected (left) and laboratory-reared *Tenebrio molitor* (right). (d) Principal coordinate analysis (PCoA) plot based on bray-curtis distances for field-collected (left) and laboratory-reared *Tenebrio molitor* (right). The percentage of the total variance explained by each PC is indicated in parentheses.

(**a**)


Coleoptera: *Leptinotarsa decemlineata*
Larvae
Relative Abundance
100%
75%
50%
25%
0%
Insect sample
Microbiota
Acidobacteria: Gp16_Family_Genus
Acidobacteria: Gp17_Family_Genus
Acidobacteria: Gp6_Family_Genus
Actinobacteria: Agromyces
Actinobacteria: Arthrobacter
Actinobacteria: Blastococcus
Actinobacteria: Brachybacterium
Actinobacteria: Coriobacterium
Actinobacteria: Corynebacterium
Actinobacteria: Micrococcaceae_Genus
Actinobacteria: Micrococcus
Actinobacteria: Mycobacterium
Actinobacteria: Nocardia
Actinobacteria: Rhodococcus
Actinobacteria: Streptomyces
Bacteroidetes: Adhaeribacter
Bacteroidetes: Cloacibacterium
Bacteroidetes: Sphingobacterium
Firmicutes: Bacillaceae_2_Genus
Firmicutes: Bacillales_Family_Genus
Firmicutes: Bacillus
Firmicutes: Clostridiaceae_1_Genus
Firmicutes: Hungatella
Firmicutes: Lachnospiraceae_Genus
Firmicutes: Lactococcus
Firmicutes: Leuconostoc
Firmicutes: Lysinibacillus
Firmicutes: Planococcaceae_Genus
Firmicutes: Ruminococcaceae_Genus
Firmicutes: Sporosarcina
Firmicutes: Terribacillus
Other
Planctomycetes: Gemmata
Planctomycetes: Pirellula
Proteobacteria: Acetobacter
Proteobacteria: Achromobacter
Proteobacteria: Acinetobacter
Proteobacteria: Deltaproteobacteria_Order_Family_Genus
Proteobacteria: Ehrlichia
Proteobacteria: Enterobacter
Proteobacteria: Enterobacteriaceae_Genus
Proteobacteria: Erwinia
Proteobacteria: Franconibacter
Proteobacteria: Haemophilus
Proteobacteria: Haliangium
Proteobacteria: Hyphomicrobium
Proteobacteria: Lampropedia
Proteobacteria: Massilia
Proteobacteria: Myxococcales_Family_Genus
Proteobacteria: Ochrobactrum
Proteobacteria: Pantoea
Proteobacteria: Pseudomonas
Proteobacteria: Rhizobiaceae_Genus
Proteobacteria: Rhizobium
Proteobacteria: Sorangium
Proteobacteria: Stenotrophomonas
Proteobacteria: Tanticharoenia
Proteobacteria: Thauera
Proteobacteria: uncultured Alphaproteobacteria bacterium
Proteobacteria: Wolbachia
Synergistetes: Synergistaceae_Genus
Synergistetes: Synergistes
Coleoptera: *Leptinotarsa decemlineata*
Adults
Relative Abundance
100%
75%
50%
25%
0%
Insect sample
Microbiota
Acidobacteria: Gp2_Family_Genus
Acidobacteria: Gp4_Family_Genus
Acidobacteria: Gp6_Family_Genus
Actinobacteria: Arthrobacter
Actinobacteria: Bifidobacterium
Actinobacteria: Blastococcus
Actinobacteria: Brachybacterium
Actinobacteria: Brevibacterium
Actinobacteria: Gaiella
Actinobacteria: Geodermatophilaceae_Genus
Actinobacteria: Marmoricola
Actinobacteria: Mycobacterium
Bacteroidetes: Adhaeribacter
Bacteroidetes: Flavobacteriaceae_Genus
Bacteroidetes: Pontibacter
Bacteroidetes: Sphingobacterium
Firmicutes: Bacillales_Family_Genus
Firmicutes: Bacillus
Firmicutes: Domibacillus
Firmicutes: Geobacillus
Firmicutes: Lactococcus
Firmicutes: Lysinibacillus
Firmicutes: Sporosarcina
Firmicutes: Terribacillus
Other
Planctomycetes: Planctomycetaceae_Genus
Proteobacteria: Acetobacter
Proteobacteria: Acinetobacter
Proteobacteria: Burkholderiales_Family_Genus
Proteobacteria: Enterobacter
Proteobacteria: Enterobacteriaceae_Genus
Proteobacteria: Franconibacter
Proteobacteria: Janthinobacterium
Proteobacteria: Massilia
Proteobacteria: Neisseria
Proteobacteria: Pantoea
Proteobacteria: Paracoccus
Proteobacteria: Povalibacter
Proteobacteria: Pseudomonas
Proteobacteria: Rhizobiales_Family_Genus
Proteobacteria: Rhodobiaceae_Genus
Proteobacteria: Sphingomonadaceae_Genus
Proteobacteria: Sphingomonas
Proteobacteria: uncultured bacterium
Proteobacteria: uncultured Gammaproteobacteria bacterium
Proteobacteria: Wolbachia
Synergistetes: Synergistes
Verrucomicrobia: Spartobacteria_Order_Family_Genus
Verrucomicrobia: Terrimicrobium_Family_Genus

(**b**)

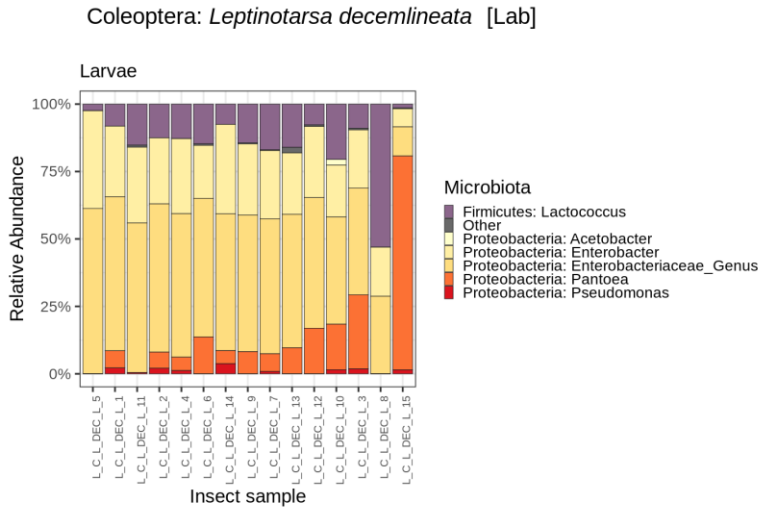
Coleoptera: Leptinotarsa decemlineata [Lab]
Larvae
100%
75%
50%
25%
0%
Relative Abundance
L_C_L_DEC_L_5
L_C_L_DEC_L_1
L_C_L_DEC_L_11
L_C_L_DEC_L_2
L_C_L_DEC_L_4
L_C_L_DEC_L_6
L_C_L_DEC_L_14
L_C_L_DEC_L_9
L_C_L_DEC_L_7
L_C_L_DEC_L_13
L_C_L_DEC_L_12
L_C_L_DEC_L_10
L_C_L_DEC_L_3
L_C_L_DEC_L_8
L_C_L_DEC_L_15
Insect sample
Microbiota
Firmicutes: Lactococcus
Other
Proteobacteria: Acetobacter
Proteobacteria: Enterobacter
Proteobacteria: Enterobacteriaceae_Genus
Proteobacteria: Pantoea
Proteobacteria: Pseudomonas

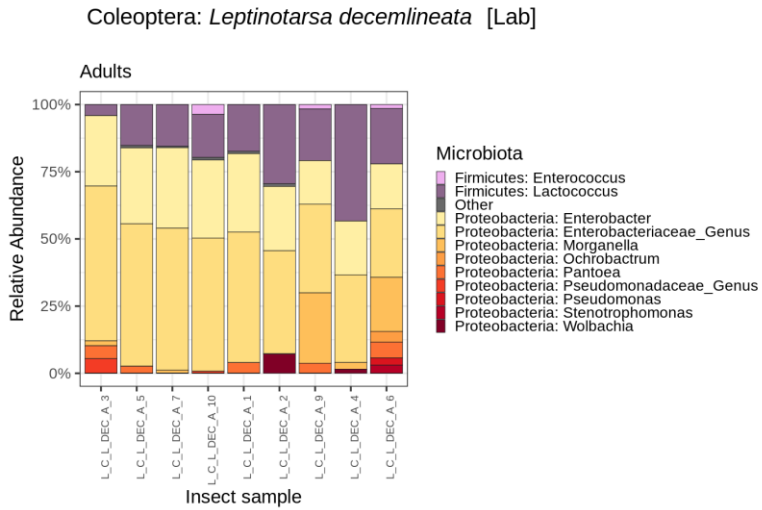
Coleoptera: Leptinotarsa decemlineata [Lab]
Adults
100%
75%
50%
25%
0%
Relative Abundance
L_C_L_DEC_A_3
L_C_L_DEC_A_5
L_C_L_DEC_A_7
L_C_L_DEC_A_10
L_C_L_DEC_A_1
L_C_L_DEC_A_2
L_C_L_DEC_A_9
L_C_L_DEC_A_4
L_C_L_DEC_A_6
Insect sample
Microbiota
Firmicutes: Enterococcus
Firmicutes: Lactococcus
Other
Proteobacteria: Enterobacter
Proteobacteria: Enterobacteriaceae_Genus
Proteobacteria: Morganella
Proteobacteria: Ochrobactrum
Proteobacteria: Pantoea
Proteobacteria: Pseudomonadaceae_Genus
Proteobacteria: Pseudomonas
Proteobacteria: Stenotrophomonas
Proteobacteria: Wolbachia

(c)

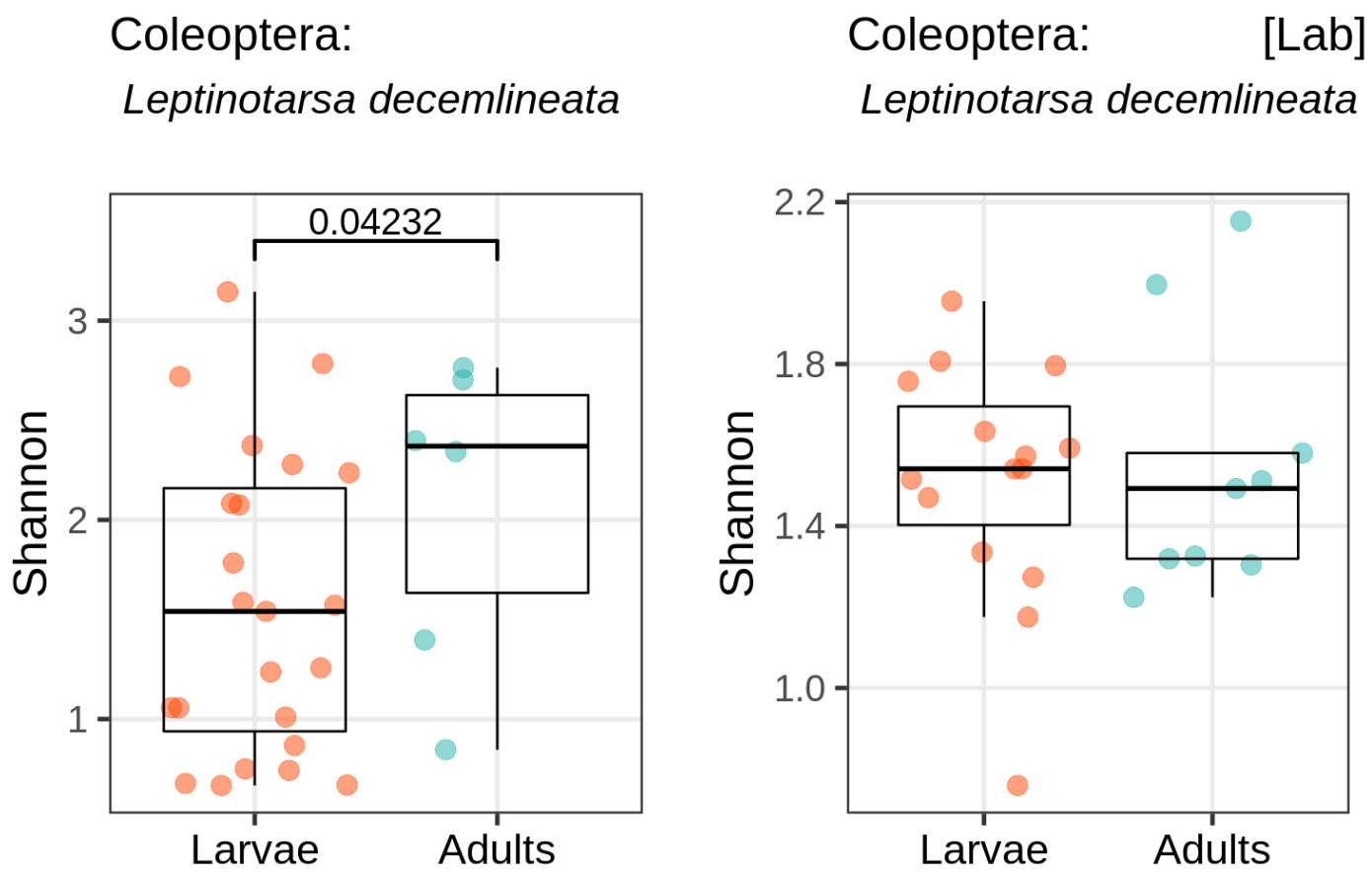
Coleoptera:
Leptinotarsa decemlineata
0.04232
Shannon
3
2
1
Larvae
Adults
Coleoptera: [Lab]
Leptinotarsa decemlineata
Shannon
2.2
1.8
1.4
1.0
Larvae
Adults

(d)

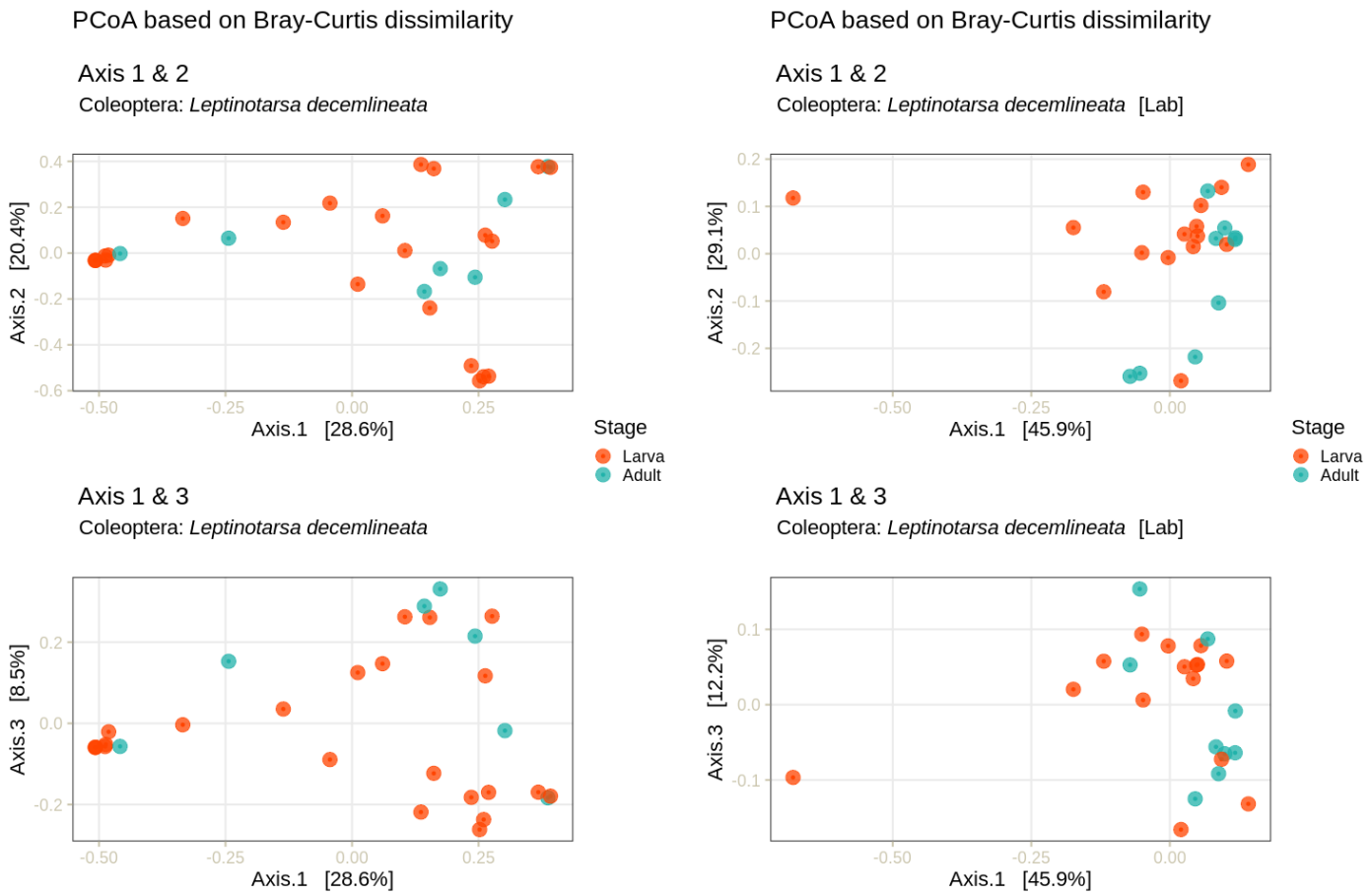

Figure S13: *Leptinotarsa decemlineata* (Coleoptera) (a) microbiome composition assessed by 16S rRNA gene sequencing. Presented are the relative abundances of the bacterial genera for larval (top) and adult (bottom) samples. Shown are 99% of the genera. The remaining genera are shown as "Other." (b) Microbiome composition of laboratory-reared *Leptinotarsa decemlineata.* (c) Box plots of alpha-diversity indices (Shannon diversity) comparing larvae and adults for field-collected (left) and laboratory-reared *Leptinotarsa decemlineata* (right; Two-sample t-test, t = 2.1276, df = 28, p-value = 0.04232). (d) Principal coordinate analysis (PCoA) plot based on bray-curtis distances for field-collected (left) and laboratory-reared *Leptinotarsa decemlineata* (right). The percentage of the total variance explained by each PC is indicated in parentheses.

(**a**)

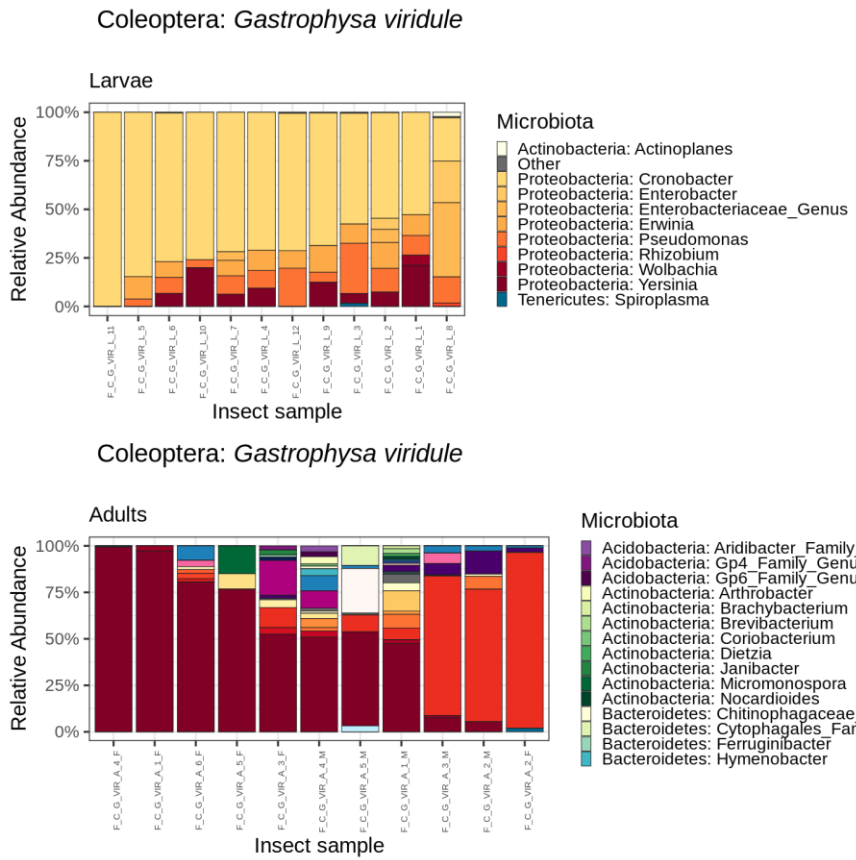
Coleoptera: Gastrophysa viridule
Larvae
Relative Abundance
100%
75%
50%
25%
0%
Insect sample
Microbiota
Actinobacteria: Actinoplanes
Other
Proteobacteria: Cronobacter
Proteobacteria: Enterobacter
Proteobacteria: Enterobacteriaceae_Genus
Proteobacteria: Erwinia
Proteobacteria: Pseudomonas
Proteobacteria: Rhizobium
Proteobacteria: Wolbachia
Proteobacteria: Yersinia
Tenericutes: Spiroplasma

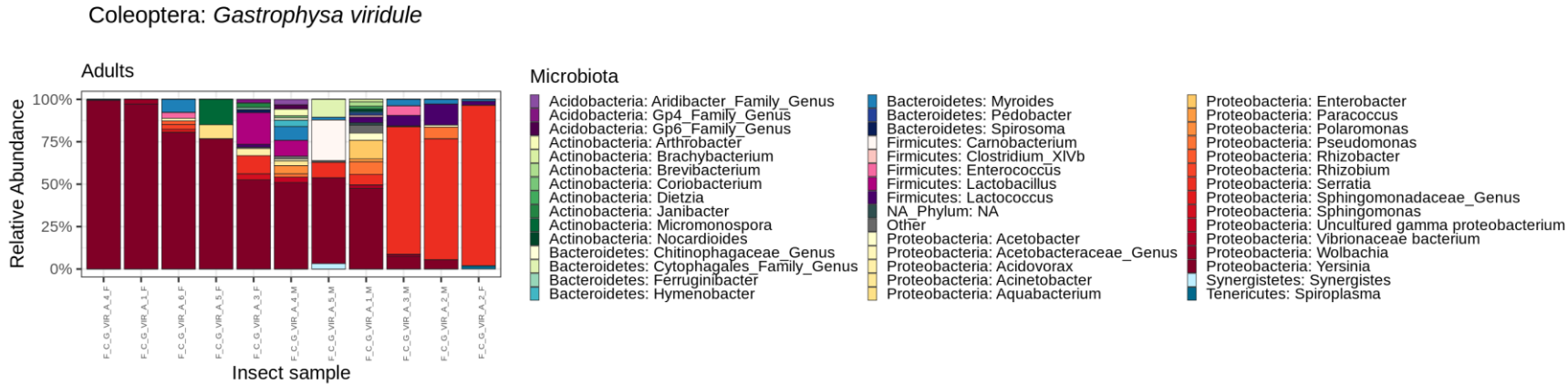
Coleoptera: Gastrophysa viridule
Adults
Relative Abundance
100%
75%
50%
25%
0%
Insect sample
Microbiota
Acidobacteria: Aridibacter_Family_Genus
Acidobacteria: Gp4_Family_Genus
Acidobacteria: Gp6_Family_Genus
Actinobacteria: Arthrobacter
Actinobacteria: Brachybacterium
Actinobacteria: Brevibacterium
Actinobacteria: Coriobacterium
Actinobacteria: Dietzia
Actinobacteria: Janibacter
Actinobacteria: Micromonospora
Actinobacteria: Nocardioides
Bacteroidetes: Chitinophagaceae_Genus
Bacteroidetes: Cytophagales_Family_Genus
Bacteroidetes: Ferruginibacter
Bacteroidetes: Hymenobacter
Bacteroidetes: Myroides
Bacteroidetes: Pedobacter
Bacteroidetes: Spirosoma
Firmicutes: Carnobacterium
Firmicutes: Clostridium_XlVb
Firmicutes: Enterococcus
Firmicutes: Lactobacillus
Firmicutes: Lactococcus
NA_Phylum: NA
Other
Proteobacteria: Acetobacter
Proteobacteria: Acetobacteraceae_Genus
Proteobacteria: Acidovorax
Proteobacteria: Acinetobacter
Proteobacteria: Aquabacterium
Proteobacteria: Enterobacter
Proteobacteria: Paracoccus
Proteobacteria: Polaromonas
Proteobacteria: Pseudomonas
Proteobacteria: Rhizobacter
Proteobacteria: Rhizobium
Proteobacteria: Serratia
Proteobacteria: Sphingomonadaceae_Genus
Proteobacteria: Sphingomonas
Proteobacteria: Uncultured gamma proteobacterium
Proteobacteria: Vibrionaceae bacterium
Proteobacteria: Wolbachia
Proteobacteria: Yersinia
Synergistetes: Synergistes
Tenericutes: Spiroplasma

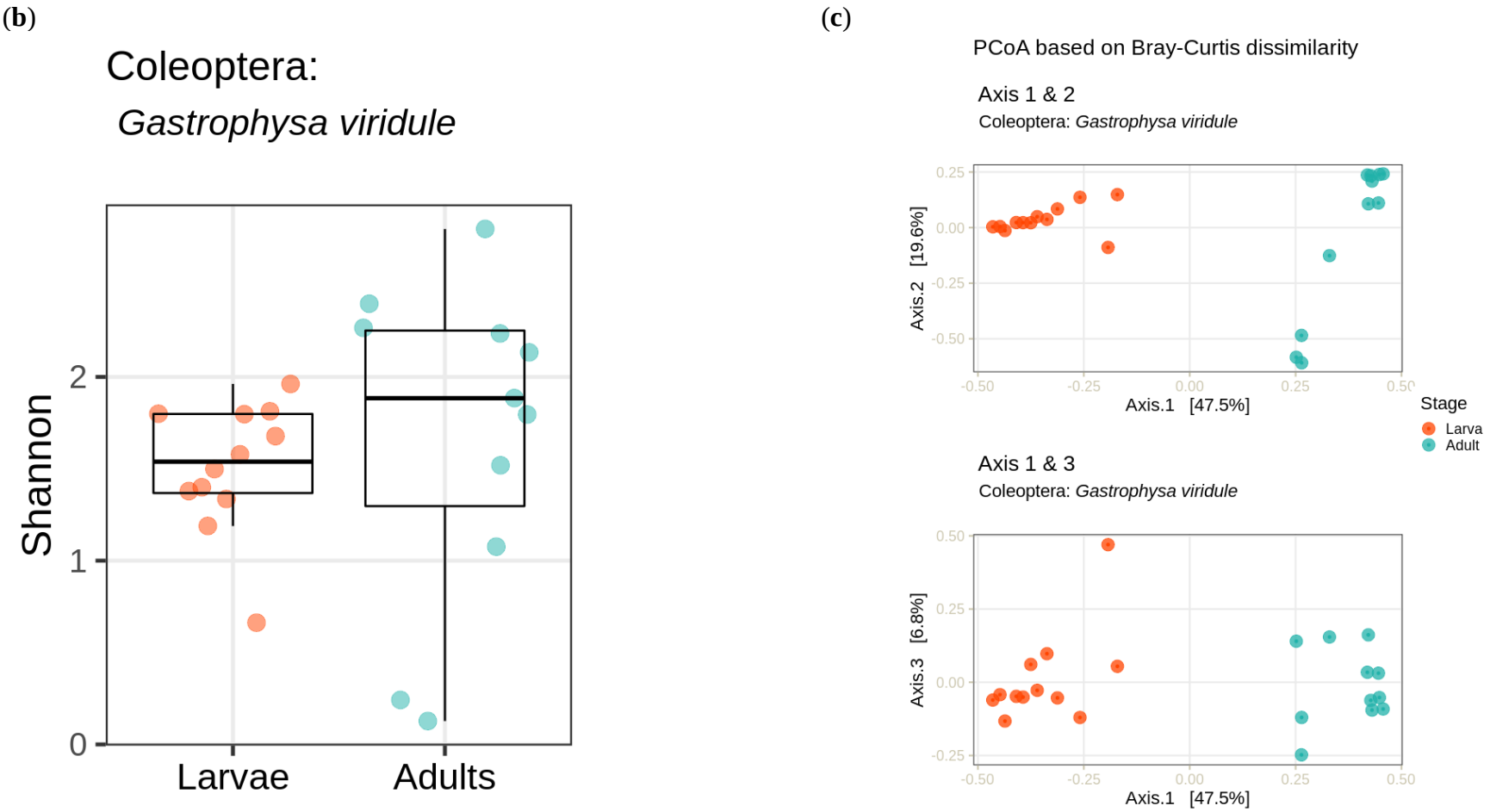

Figure S14: *Gastrophysa viridule* (Coleoptera) (a) microbiome composition assessed by 16S rRNA gene sequencing. Presented are the relative abundances of the bacterial genera for larval (top) and adult (bottom) samples. Shown are 99% of the genera. The remaining genera are shown as "Other." (b) Box plots of alpha-diversity indices (Shannon diversity) comparing larvae and adults. (c) Principal coordinate analysis (PCoA) plot based on bray-curtis distances. The percentage of the total variance explained by each PC is indicated in parentheses.

(**a**)

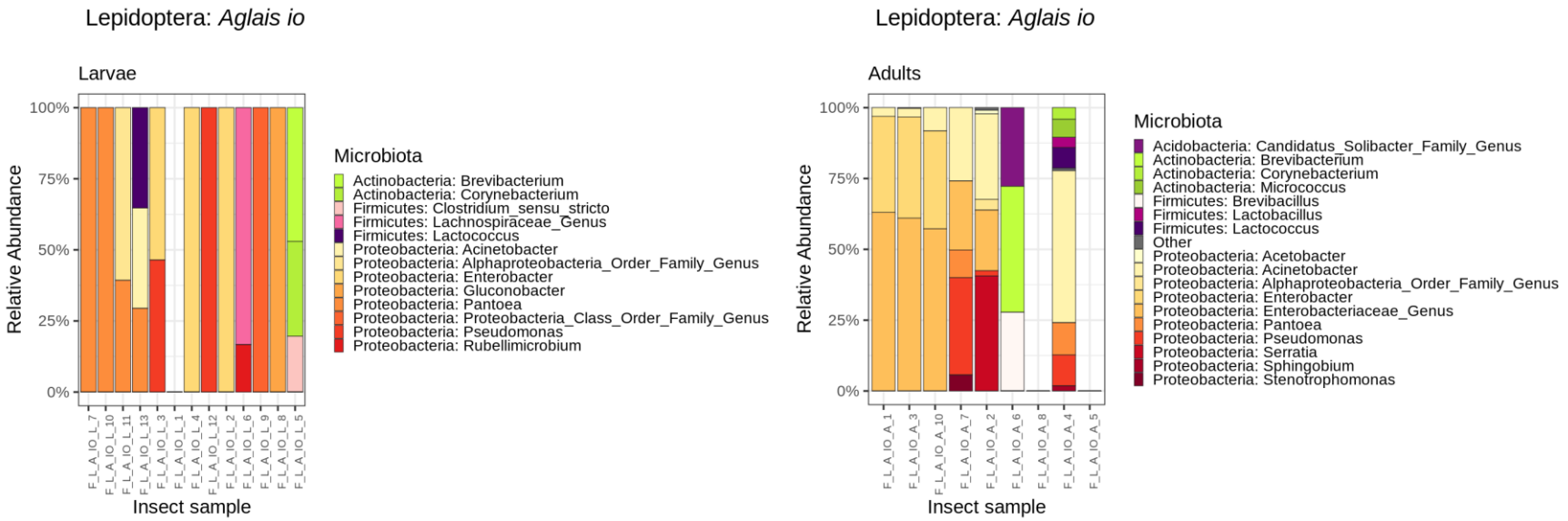
Lepidoptera: Aglais io
Larvae
Relative Abundance
100%
75%
50%
25%
0%
F_L_A_IO_L_7
F_L_A_IO_L_10
F_L_A_IO_L_11
F_L_A_IO_L_13
F_L_A_IO_L_3
F_L_A_IO_L_1
F_L_A_IO_L_4
F_L_A_IO_L_12
F_L_A_IO_L_2
F_L_A_IO_L_6
F_L_A_IO_L_9
F_L_A_IO_L_8
F_L_A_IO_L_5
Insect sample
Microbiota
Actinobacteria: Brevibacterium
Actinobacteria: Corynebacterium
Firmicutes: Clostridium_sensu_stricto
Firmicutes: Lachnospiraceae_Genus
Firmicutes: Lactococcus
Proteobacteria: Acinetobacter
Proteobacteria: Alphaproteobacteria_Order_Family_Genus
Proteobacteria: Enterobacter
Proteobacteria: Gluconobacter
Proteobacteria: Pantoea
Proteobacteria: Proteobacteria_Class_Order_Family_Genus
Proteobacteria: Pseudomonas
Proteobacteria: Rubellimicrobium
Lepidoptera: Aglais io
Adults
Relative Abundance
100%
75%
50%
25%
0%
F_L_A_IO_A_1
F_L_A_IO_A_3
F_L_A_IO_A_10
F_L_A_IO_A_7
F_L_A_IO_A_2
F_L_A_IO_A_6
F_L_A_IO_A_8
F_L_A_IO_A_4
F_L_A_IO_A_5
Insect sample
Microbiota
Acidobacteria: Candidatus_Solibacter_Family_Genus
Actinobacteria: Brevibacterium
Actinobacteria: Corynebacterium
Actinobacteria: Micrococcus
Firmicutes: Brevibacillus
Firmicutes: Lactobacillus
Firmicutes: Lactococcus
Other
Proteobacteria: Acetobacter
Proteobacteria: Acinetobacter
Proteobacteria: Alphaproteobacteria_Order_Family_Genus
Proteobacteria: Enterobacter
Proteobacteria: Enterobacteriaceae_Genus
Proteobacteria: Pantoea
Proteobacteria: Pseudomonas
Proteobacteria: Serratia
Proteobacteria: Sphingobium
Proteobacteria: Stenotrophomonas

(**b**)

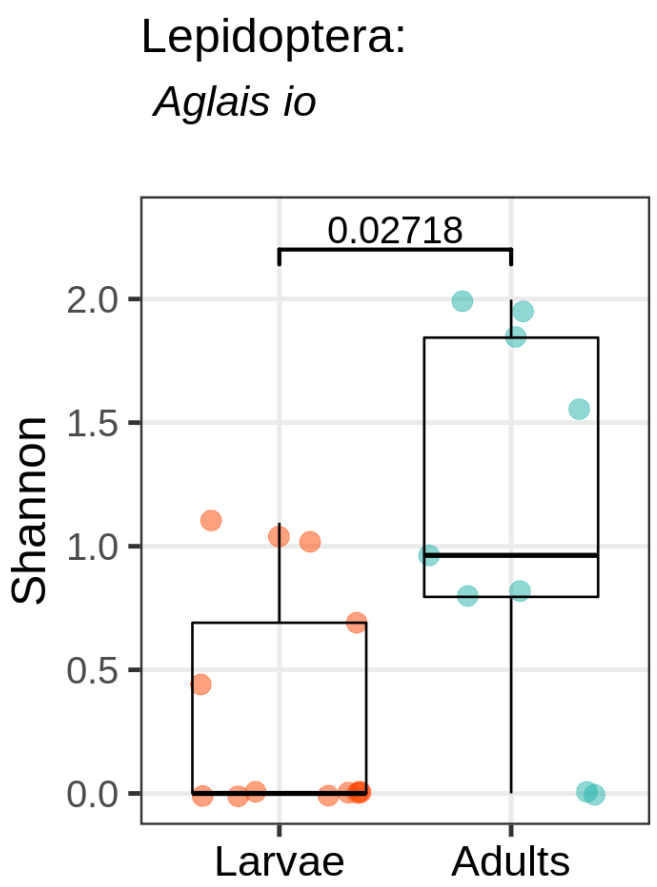

(**c**)

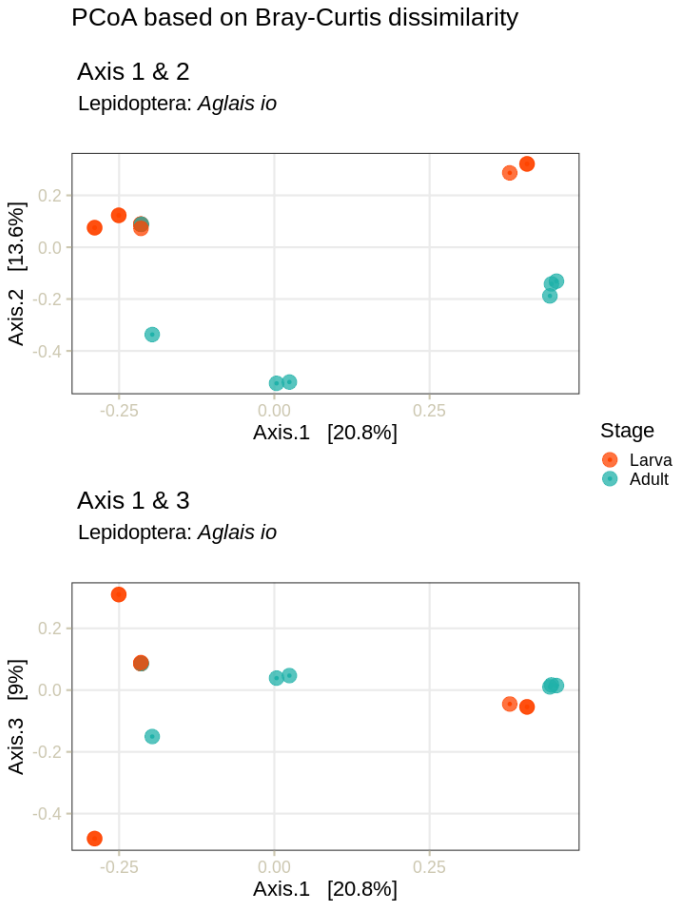

Figure S15: *Aglais io* (Lepidoptera) (a) microbiome composition assessed by 16S rRNA gene sequencing. Presented are the relative abundances of the bacterial genera for larval (left) and adult (right) samples. Shown are 99% of the genera. The remaining genera are shown as "Other." (b) Box plots of alpha-diversity indices (Shannon diversity) comparing larvae and adults (Wilcoxon rank-sum-test ,W = 90, p-value = 0.02718). (c) Principal coordinate analysis (PCoA) plot based on bray-curtis distances. The percentage of the total variance explained by each PC is indicated in parentheses

(**a**)

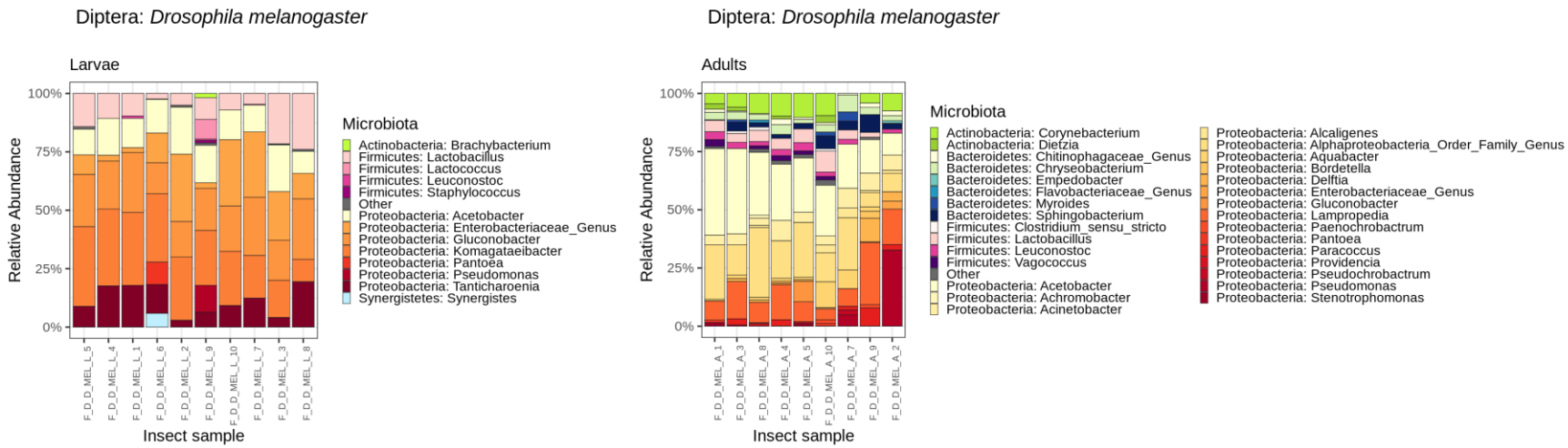
Diptera: Drosophila melanogaster
Larvae
Relative Abundance
100%
75%
50%
25%
0%
F_D_D_MEL_L_5
F_D_D_MEL_L_4
F_D_D_MEL_L_1
F_D_D_MEL_L_6
F_D_D_MEL_L_2
F_D_D_MEL_L_9
F_D_D_MEL_L_10
F_D_D_MEL_L_7
F_D_D_MEL_L_3
F_D_D_MEL_L_8
Insect sample
Microbiota
Actinobacteria: Brachybacterium
Firmicutes: Lactobacillus
Firmicutes: Lactococcus
Firmicutes: Leuconostoc
Firmicutes: Staphylococcus
Other
Proteobacteria: Acetobacter
Proteobacteria: Enterobacteriaceae_Genus
Proteobacteria: Gluconobacter
Proteobacteria: Komagataeibacter
Proteobacteria: Pantoea
Proteobacteria: Pseudomonas
Proteobacteria: Tanticharoenia
Synergistetes: Synergistes
Diptera: Drosophila melanogaster
Adults
Relative Abundance
100%
75%
50%
25%
0%
F_D_D_MEL_A_1
F_D_D_MEL_A_3
F_D_D_MEL_A_8
F_D_D_MEL_A_4
F_D_D_MEL_A_5
F_D_D_MEL_A_10
F_D_D_MEL_A_7
F_D_D_MEL_A_9
F_D_D_MEL_A_2
Insect sample
Microbiota
Actinobacteria: Corynebacterium
Actinobacteria: Dietzia
Bacteroidetes: Chitinophagaceae_Genus
Bacteroidetes: Chryseobacterium
Bacteroidetes: Empedobacter
Bacteroidetes: Flavobacteriaceae_Genus
Bacteroidetes: Myroides
Bacteroidetes: Sphingobacterium
Firmicutes: Clostridium_sensu_stricto
Firmicutes: Lactobacillus
Firmicutes: Leuconostoc
Firmicutes: Vagococcus
Other
Proteobacteria: Acetobacter
Proteobacteria: Achromobacter
Proteobacteria: Acinetobacter
Proteobacteria: Alcaligenes
Proteobacteria: Alphaproteobacteria_Order_Family_Genus
Proteobacteria: Aquabacter
Proteobacteria: Bordetella
Proteobacteria: Delftia
Proteobacteria: Enterobacteriaceae_Genus
Proteobacteria: Gluconobacter
Proteobacteria: Lampropedia
Proteobacteria: Paenochrobactrum
Proteobacteria: Pantoea
Proteobacteria: Paracoccus
Proteobacteria: Providencia
Proteobacteria: Pseudochrobactrum
Proteobacteria: Pseudomonas
Proteobacteria: Stenotrophomonas

(b)

Diptera: *Drosophila melanogaster* [Lab]

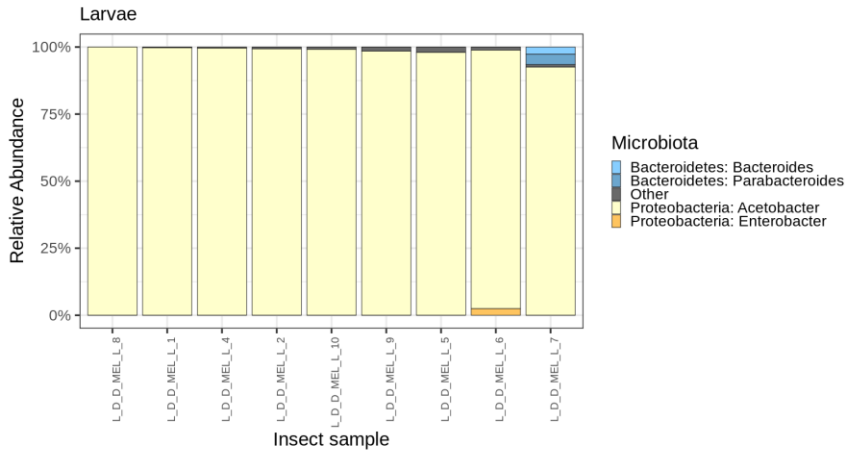

Diptera: *Drosophila melanogaster* [Lab]

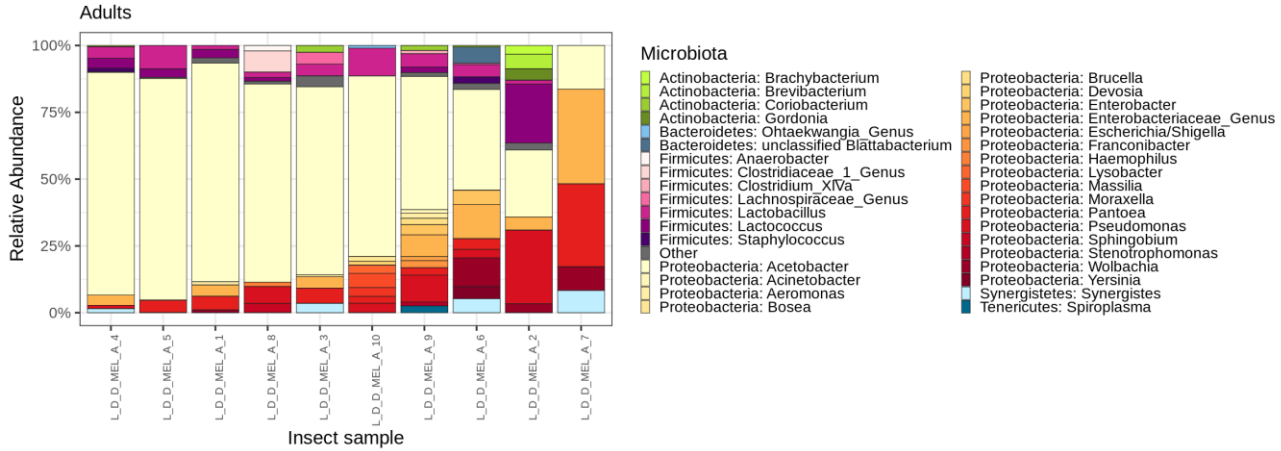

(c)

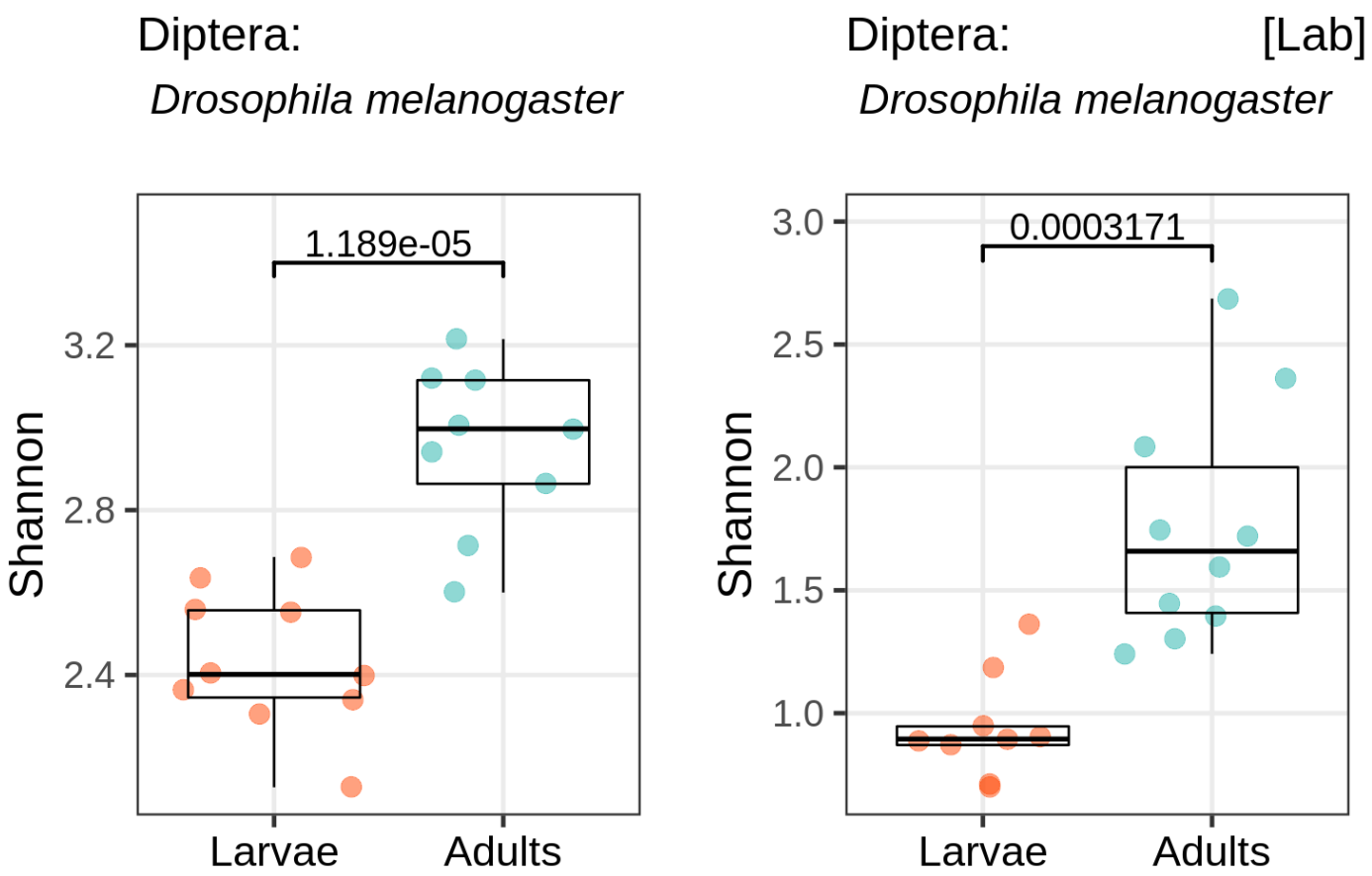
Diptera:
Drosophila melanogaster
1.189e-05
Shannon
3.2
2.8
2.4
Larvae
Adults
Diptera: [Lab]
Drosophila melanogaster
0.0003171
Shannon
3.0
2.5
2.0
1.5
1.0
Larvae
Adults

(d)

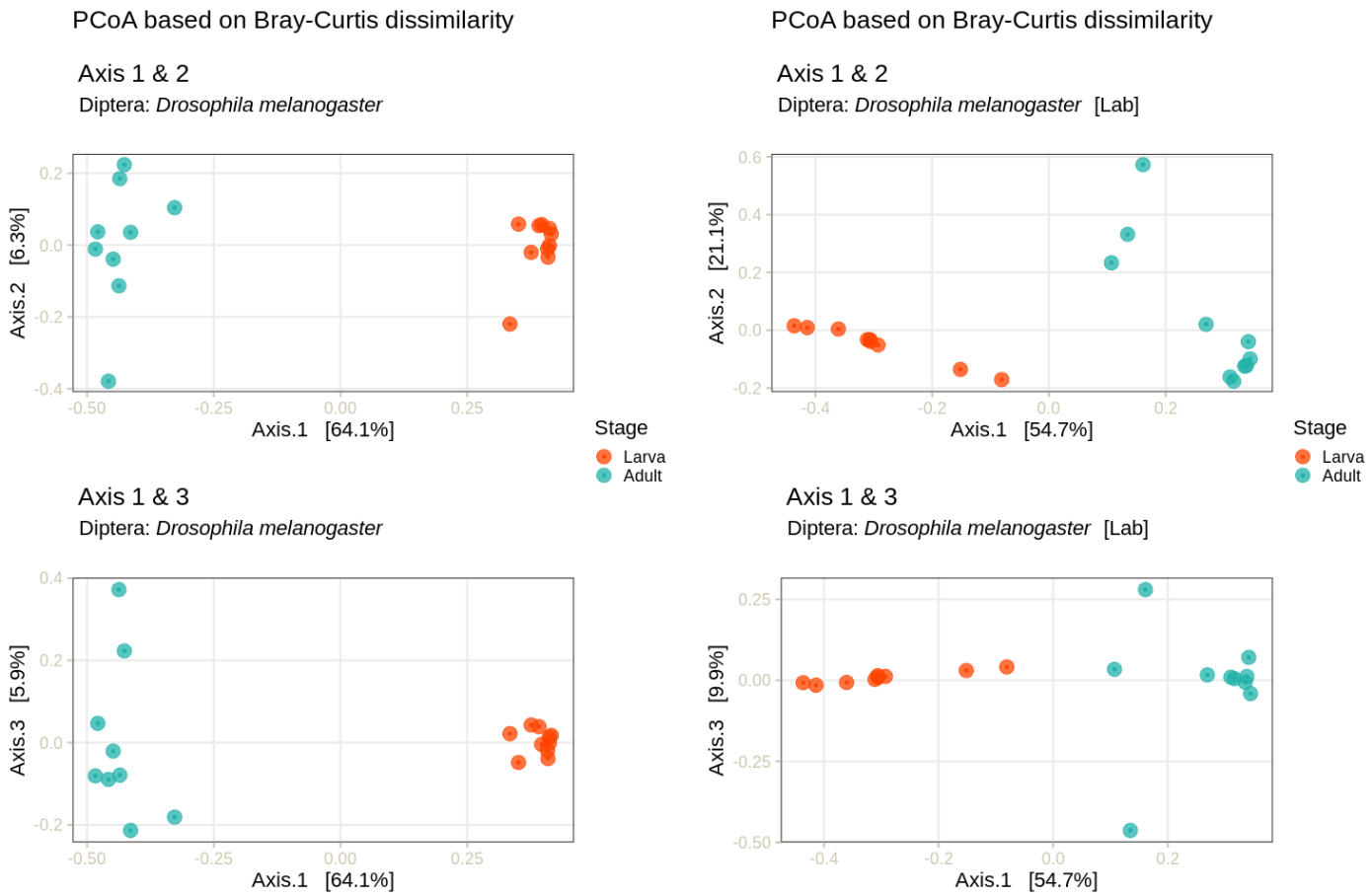

Figure S16: *Drosophila melanogaster* (Diptera) (a) microbiome composition assessed by 16S rRNA gene sequencing. Presented are the relative abundances of the bacterial genera for larval (left) and adult (right) samples. Shown are 99% of the genera. The remaining genera are shown as "Other." (b) Microbiome composition of laboratory-reared *Drosophila melanogaster*. (c) Box plots of alpha-diversity indices (Shannon diversity) comparing larvae and adults for field-collected (left; Two-sample t-test, t = 6.0954, df = 17, p-value = 1.189e-05) and laboratory-reared *Drosophila melanogaster* (right; Two-sample t-test, t = 4.891, df = 12.675, p-value = 0.0003171). (d) Principal coordinate analysis (PCoA) plot based on bray-curtis distances for field-collected (left) and laboratory-reared *Drosophila melanogaster* (right). The percentage of the total variance explained by each PC is indicated in parentheses.

(**a**)

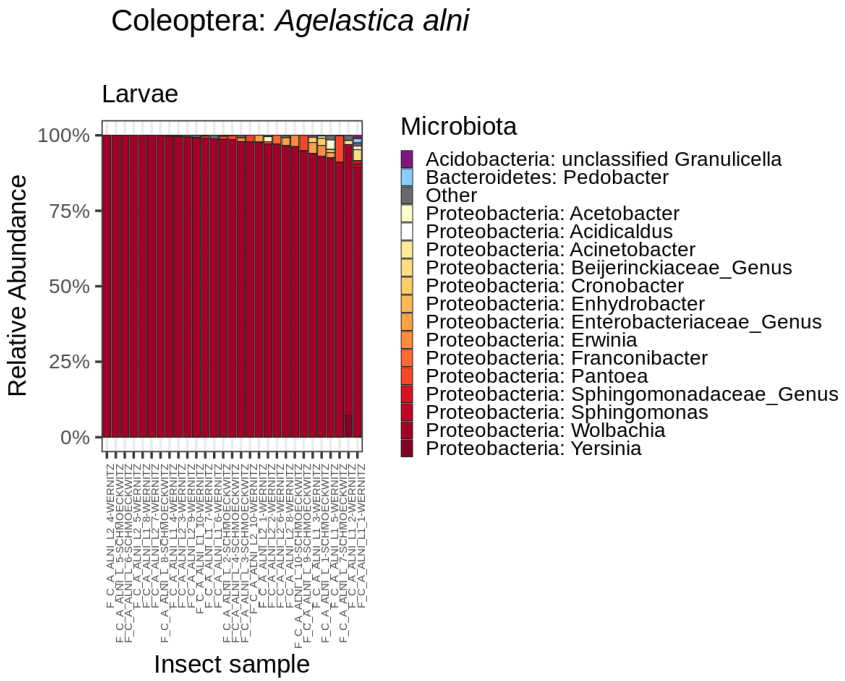
Coleoptera: *Agelastica alni*
Larvae
Relative Abundance
100%
75%
50%
25%
0%
Insect sample
Microbiota
Acidobacteria: unclassified Granulicella
Bacteroidetes: Pedobacter
Other
Proteobacteria: Acetobacter
Proteobacteria: Acidicaldus
Proteobacteria: Acinetobacter
Proteobacteria: Beijerinckiaceae_Genus
Proteobacteria: Cronobacter
Proteobacteria: Enhydrobacter
Proteobacteria: Enterobacteriaceae_Genus
Proteobacteria: Erwinia
Proteobacteria: Franconibacter
Proteobacteria: Pantoea
Proteobacteria: Sphingomonadaceae_Genus
Proteobacteria: Sphingomonas
Proteobacteria: Wolbachia
Proteobacteria: Yersinia

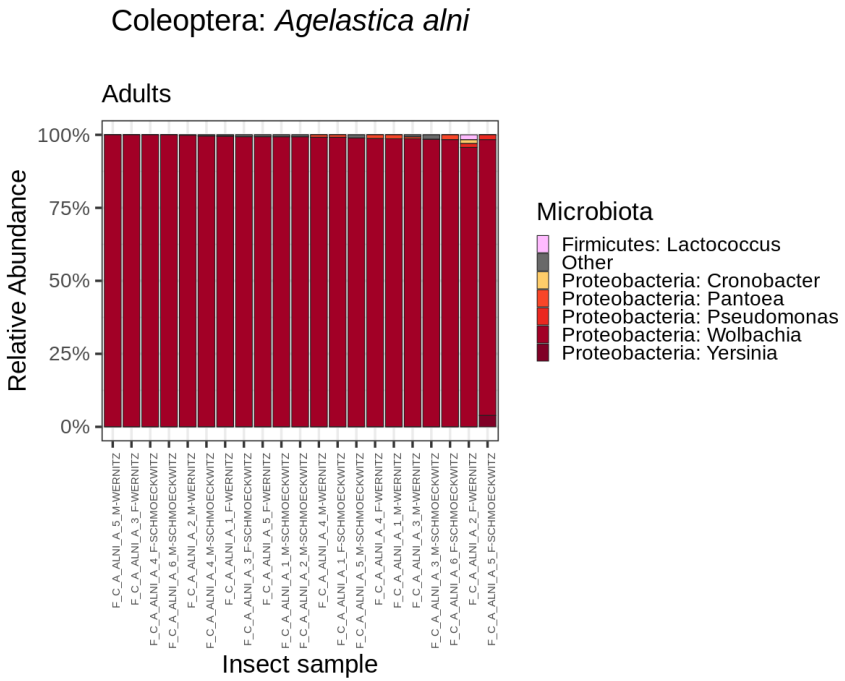
Coleoptera: *Agelastica alni*
Adults
Relative Abundance
100%
75%
50%
25%
0%
Insect sample
Microbiota
Firmicutes: Lactococcus
Other
Proteobacteria: Cronobacter
Proteobacteria: Pantoea
Proteobacteria: Pseudomonas
Proteobacteria: Wolbachia
Proteobacteria: Yersinia

(**b**)

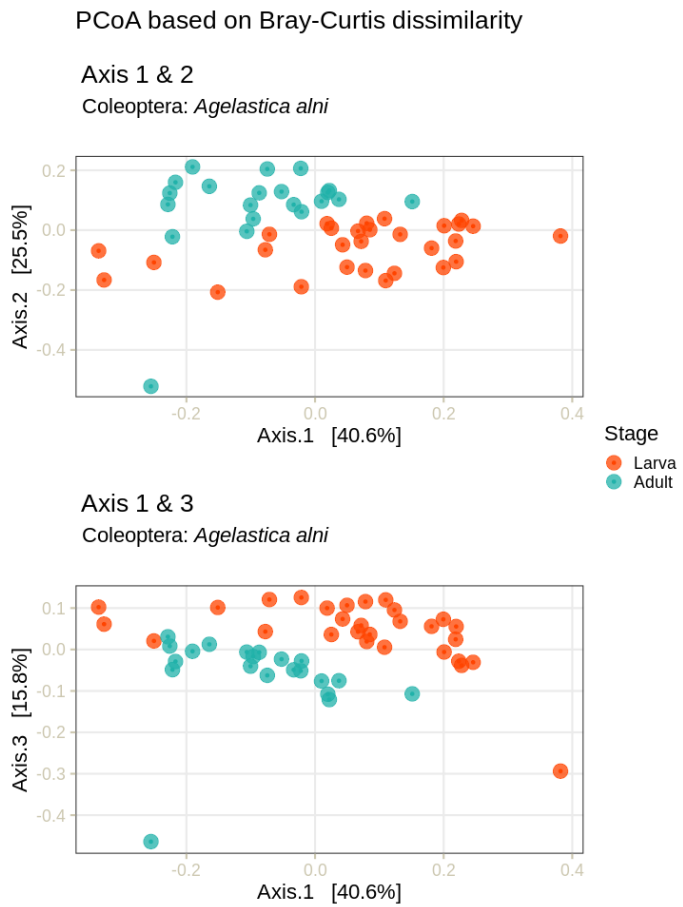

Figure S17: *Agelastica alni* (Coleoptera) (a) microbiome composition assessed by 16S rRNA gene sequencing. Presented are the relative abundances of the bacterial genera for larval (left) and adult (right) samples. Shown are 99% of the genera. The remaining genera are shown as "Other." (b) Principal coordinate analysis (PCoA) plot based on bray-curtis distances. The percentage of the total variance explained by each PC is indicated in parentheses. **Note**: *Agelastica alni* was excluded from the final analysis (see supplement for more details)

(**a**)

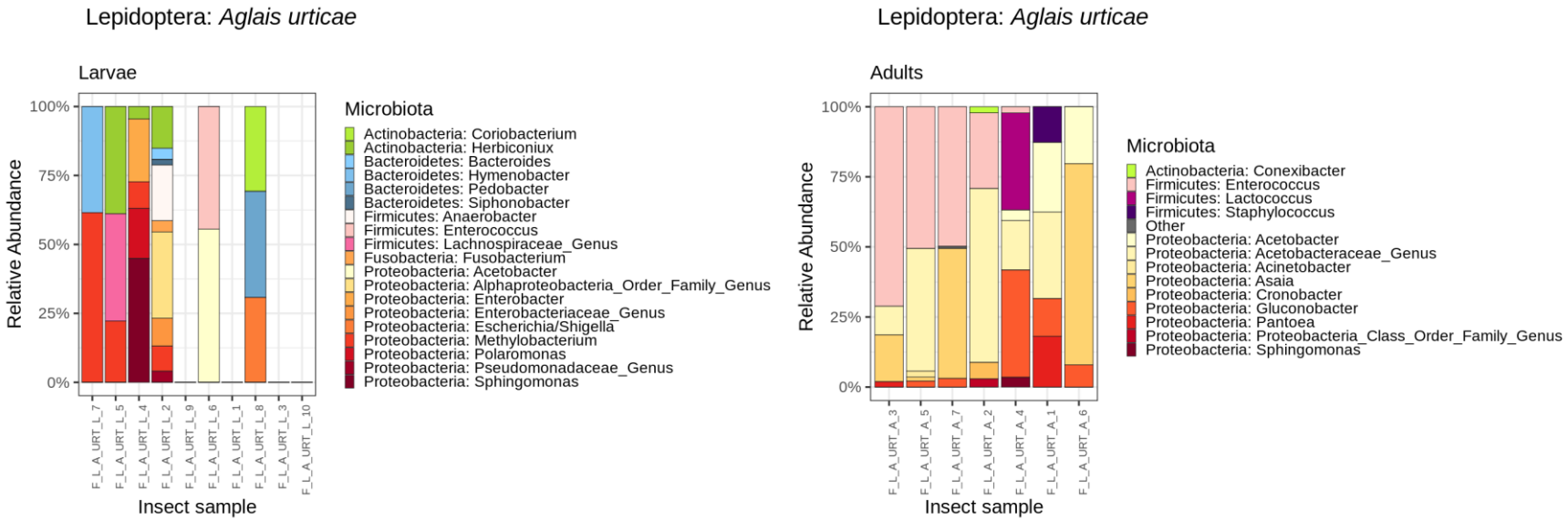
Lepidoptera: Aglais urticae
Larvae
Relative Abundance
100%
75%
50%
25%
0%
F_L_A_URT_L_7
F_L_A_URT_L_5
F_L_A_URT_L_4
F_L_A_URT_L_2
F_L_A_URT_L_9
F_L_A_URT_L_6
F_L_A_URT_L_1
F_L_A_URT_L_8
F_L_A_URT_L_3
F_L_A_URT_L_10
Insect sample
Microbiota
Actinobacteria: Coriobacterium
Actinobacteria: Herbiconiux
Bacteroidetes: Bacteroides
Bacteroidetes: Hymenobacter
Bacteroidetes: Pedobacter
Bacteroidetes: Siphonobacter
Firmicutes: Anaerobacter
Firmicutes: Enterococcus
Firmicutes: Lachnospiraceae_Genus
Fusobacteria: Fusobacterium
Proteobacteria: Acetobacter
Proteobacteria: Alphaproteobacteria_Order_Family_Genus
Proteobacteria: Enterobacter
Proteobacteria: Enterobacteriaceae_Genus
Proteobacteria: Escherichia/Shigella
Proteobacteria: Methylobacterium
Proteobacteria: Polaromonas
Proteobacteria: Pseudomonadaceae_Genus
Proteobacteria: Sphingomonas
Lepidoptera: Aglais urticae
Adults
Relative Abundance
100%
75%
50%
25%
0%
F_L_A_URT_A_3
F_L_A_URT_A_5
F_L_A_URT_A_7
F_L_A_URT_A_2
F_L_A_URT_A_4
F_L_A_URT_A_1
F_L_A_URT_A_6
Insect sample
Microbiota
Actinobacteria: Conexibacter
Firmicutes: Enterococcus
Firmicutes: Lactococcus
Firmicutes: Staphylococcus
Other
Proteobacteria: Acetobacter
Proteobacteria: Acetobacteraceae_Genus
Proteobacteria: Acinetobacter
Proteobacteria: Asaia
Proteobacteria: Cronobacter
Proteobacteria: Gluconobacter
Proteobacteria: Pantoea
Proteobacteria: Proteobacteria_Class_Order_Family_Genus
Proteobacteria: Sphingomonas

(b)

Lepidoptera: *Aglais urticae* [Lab]

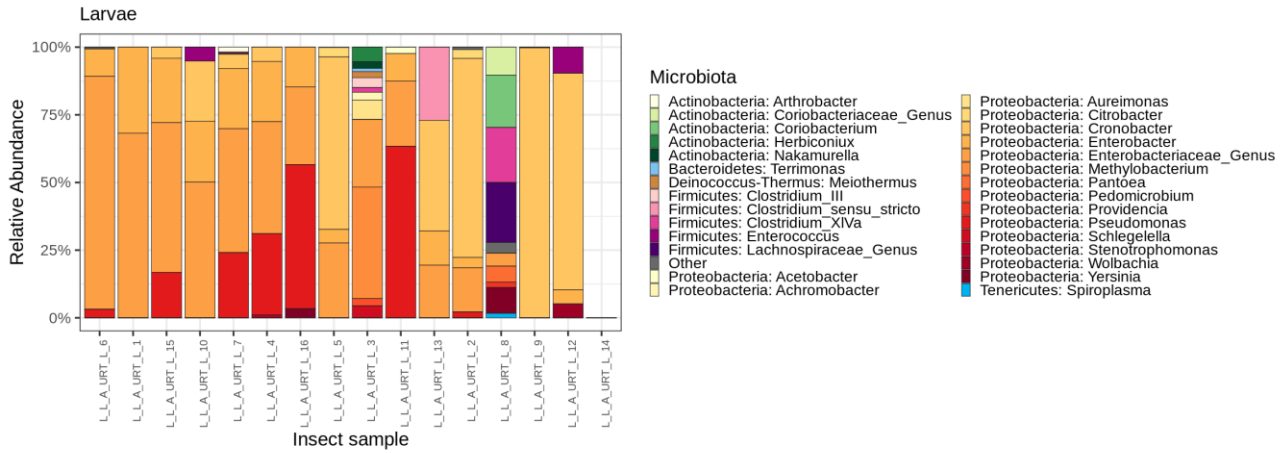

Lepidoptera: *Aglais urticae* [Lab]

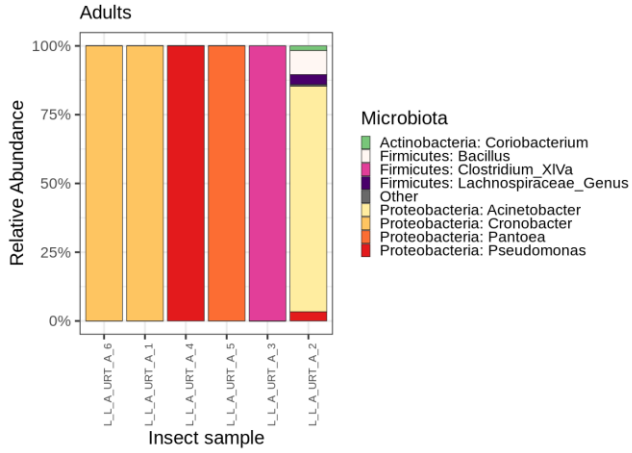

(**c**)

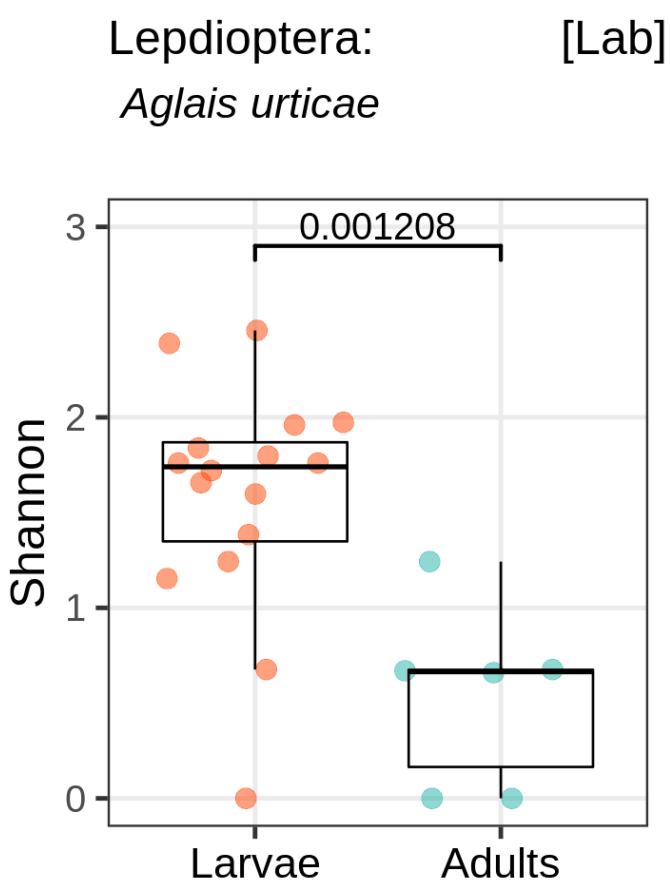
Lepdioptera:
[Lab]
Aglais urticae
0.001208
Shannon
3
2
1
0
Larvae
Adults

(d)

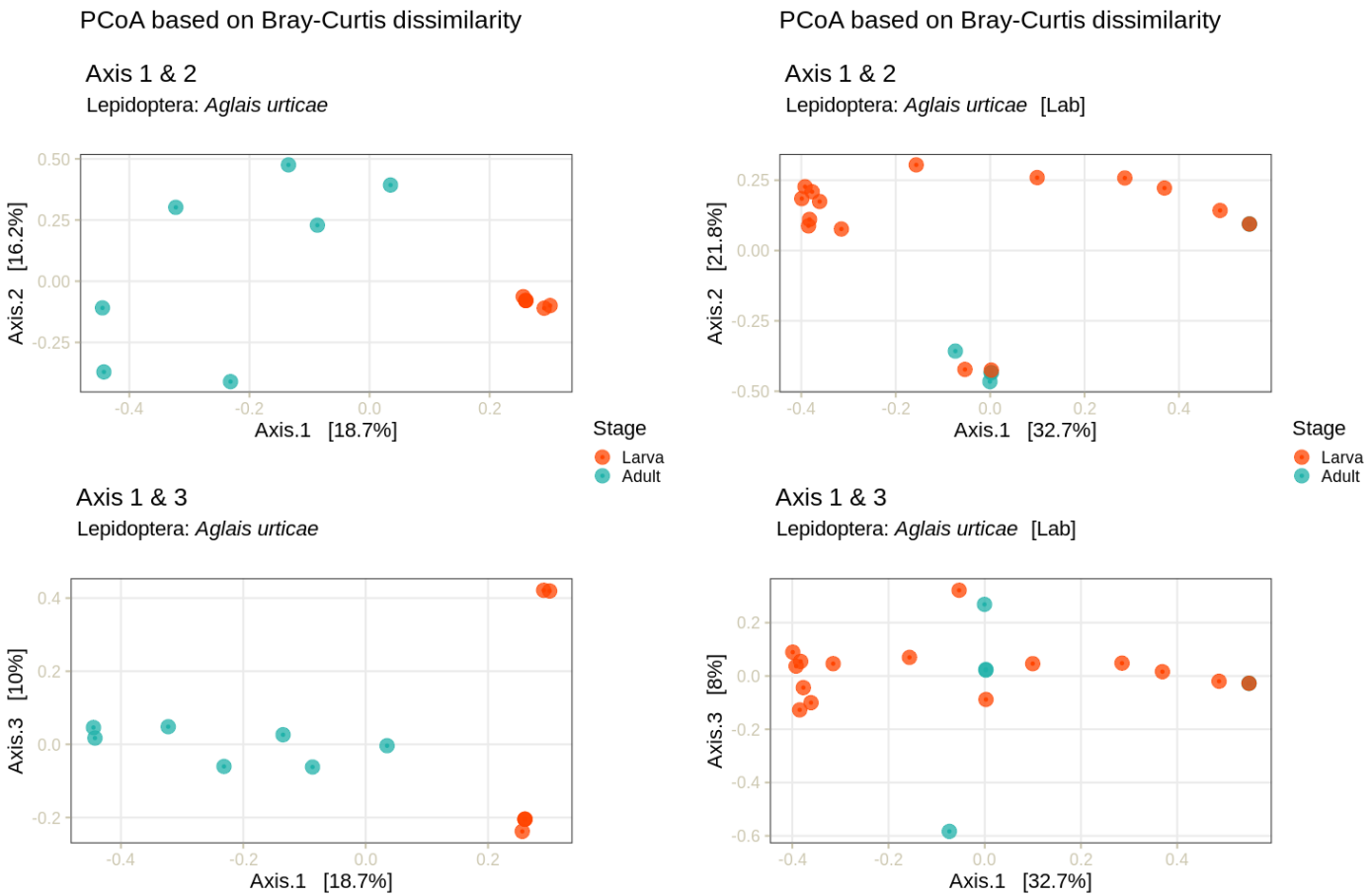

Figure S18: *Aglais urticae* (Lepidoptera) (a) microbiome composition assessed by 16S rRNA gene sequencing. Presented are the relative abundances of the bacterial genera for larval (left) and adult (right) samples. Shown are 99% of the genera. The remaining genera are shown as "Other." (b) Microbiome composition of laboratory-reared *Aglais urticae.* (c) Box plots of alpha-diversity indices (Shannon diversity) comparing larvae and adults of laboratory-reared *Aglais urticae* (Two-sample t-test ,t = -3.7686, df = 20, p-value = 0.001208). (d) Principal coordinate analysis (PCoA) plot based on bray-curtis distances for field-collected (left) and laboratory-reared *Aglais urticae* (right). The percentage of the total variance explained by each PC is indicated in parentheses. **Note**: Field-collected *Aglais urticae* were excluded from the final analysis (see supplement for more details)

APPENDIX CHAPTER II

Table 1: Origin of the field-collected insects. **Note**: [*1] 1 replicate equals 40 individuals, [*2] 1 replicate equals 10 individuals, [*3] 1 replicate equals 30 individuals

Order	Field-collected species	Location	Lon	Lat	Date	No of Larvae	No of Pupae	No of Adults
Orthoptera	*Chorthippus parallelus*	Wernigerode, Germany	10.776667	51.835833	June 2018	16	na	9
	Chorthippus dorsatus	Vienenburg, Germay	10.565278	51.950833	June 2018	10	na	16
	Metrioptera roeselii	Oker, Wernigerode, Germany	10.360944	52.523844	June 2018	2	na	7
Hemiptera	*Pyrrhocoris apterus*	Treptower Park, Berlin, Germany	13.47	52.490278	Apr – May 2018	11	na	12
	Pyrrhocoris apterus	Zoology, Freie Universität Berlin	13.306653	52.45414	Apr – June 2018	22	na	14
	Graphosoma lineatum	Nature reserve Drömling, Germany	11.131111	52.4825	May – June 2018	21	na	2
	Alleyrodes peroletella	Estedt, Germany	11.3585	52.5759	Aug 2018	10 [*1]	na	10 [*1]
Thysanoptera	*Francliniella occidentalis*	Thaer-Institute of Agricultural and Horticultural Sciences, Humboldt-Universität Berlin, Germany	13.299165	52.468107	Sept 2018	10 [*2]	na	10 [*2]
Coleoptera	*Agelastica alni*	Wernitz, Germany	11.231667	52.487778	May – July 2018	20	na	10
	Agelastica alni	Watersport centre Schmoeckwitz, Humboldt-Universität Berlin, Germany	13.649167	52.377778	May – July 2018	10	na	12
	Gastrophysa viridule	Treptower Park, Berlin, Germany	13.47	52.490278	July 2018	12	na	11
	Melolontha melolontha	Wernitz, Germany	11.231667	52.487778	May – June 2018	10	na	10
	Melolontha	Magdeburg, Germany	11.616667	52.133333	May – June 2018	10	na	10
	Tenebrio molitor	Letovanić, Croatia	16.17127968	45.485598	July 2018	12	na	14
	Leptinotarsa decemlineata	Magdeburg, Germany	11.65232	52.13183	June – Aug 2018	23	na	7
Hymenoptera	*Osmia cornuta*	Berlin, Germany	13.322082	52.486689	Apr – May 2018	18	11	12
	Osmia bicornis	Berlin, Germany	13.470234	52.482677	Apr – June 2018	12	5	5
	Neodiprion sertifer	Finnish Forest Research Institute, Vantaa Research Centre, Asikkala, Finland	26.083056	60.75	July 2018	26	7	13
Lepidoptera	*Aglais urticae*	Wernigerode, Germany	13.361961	52.401887	June – Aug 2018	10	na	10
	Aglais io	Nature conservation station Marienfelde, Germany	13.361961	52.401887	July – Oct 2018	13	na	10
Diptera	*Drosophila melanogaster*	Berlin, Germany	13.470234	52.482677	July 2018	10 [*3]	na	10 [*3]

APPENDIX CHAPTER II

Table 2: Origin of the laboratory-reared insects. **Note**: [*2] 1 replicate equals 10 individuals, [*3] 1 replicate equals 30 individuals

Order	Laboratory – reared species	Origin	No of Larvae	No of Pupae	No of Adults
Thysanoptera	*Francliniella occidentalis*	Institute of Biology, Developmental Biology, Martin-Luther-Universität Halle-Wittenberg, Germany	3 [*2]	na	2 [*2]
Coleoptera	*Tenebrio molitor*	Institute of Biology, Applied Zoology / Animal Ecology, Freie Universität Berlin, Germany	14	na	6
	Leptinotarsa decemlineata	Julius Kühn-Institut (JKI) Federal Research Centre for Cultivated Plants, Kleinmachnow, Germany	15	na	9
Lepidoptera	*Aglais urticae*	Commercial supplier, Worldwide Butterflies Ltd., United Kingdom	16	na	6
Diptera	*Drosophila melanogaster*	Institute of Biology, Applied Zoology / Animal Ecology, Freie Universität Berlin, Germany	9 [*3]	na	10 [*3]

Table 3: Results of the Breusch-Pagan test for heteroscedasticity using the *ncvTest* function from the R package car.

	χ2	**df**	**pval**	
Beta-diversity	5.913532	1	**0.015025**	*****
Shannon-difference	0.018648	1	**0.891380**	
Larval Shannon indices	0.035221	1	**0.851130**	
Adult Shannon indices	3.850086	1	**0.049743**	*****

Table 4: Model qualities of the models testing beta-diversity.

Model	LogLik	Deviance	AIC	BIC	AICc
(1) Intercept model	-0.1694	0.3388	6.3388	8.4629	8.5206
(2) Model looking at contrast between the groups	1.5390	-3.0780	4.9220	7.4782	9.3664
(3) Modelling heteroscadasticity	3.9618	-7.9236	2.0764	5.2717	9.5764

APPENDIX CHAPTER II

Table 5: Results of the regression analyses controlled for phylogeny (multivariate linear mixed-effects models) testing differences in beta-diversity between hemi- and holometabolous insects.

Model		estimate	se	tval	df	pval	ci.lb	ci.ub	
(1) Intercept model	intercept	0.6970	0.1298	5.3693	15	**<.0001**	0.4203	0.9737	***
(2) Model looking at contrast between the groups	intercept	0.5183	0.1084	4.7808	14	**0.0003**	0.2858	0.7509	***
	Hemi_Holo	0.3639	0.1489	2.4441	14	**0.0284**	0.0446	0.6832	*
(3) Modelling heteroscadasticity	intercept	0.5346	0.1139	4.6925	14	**0.0003**	0.2902	0.7789	***
	Hemi_Holo	0.3123	0.1255	2.4888	14	**0.0260**	0.0432	0.5814	*

Table 6: Model qualities of the models testing Shannon-difference.

Model	LogLik	Deviance	AIC	BIC	AICc
(1) Intercept model	-1.6223	3.2445	9.2445	11.3687	11.4264
(2) Model looking at contrast between the groups	-0.7536	1.5073	9.5073	12.0635	13.9517

Table 7: Results of the regression analyses controlled for phylogeny (multivariate linear mixed-effects models) testing differences in Shannon-difference between hemi- and holometabolous insects.

Model		estimate	se	tval	df	pval	ci.lb	ci.ub	
(1) Intercept model	intercept	0.6406	0.1992	3.2158	15	**0.0058**	0.2160	1.0652	**
(2) Model looking at contrast between the groups	intercept	0.5224	0.2583	2.0226	14	**0.0627**	-0.0316	1.0764	.
	Hemi_Holo	0.2786	0.3550	0.7850	14	**0.4455**	-0.4827	1.0400	

Table 8: Model qualities of the models testing larval Shannon indices.

Model	LogLik	Deviance	AIC	BIC	AICc
(1) Intercept model	-12.4805	24.9610	30.9610	33.0852	33.1429
(2) Model looking at contrast between the groups	-11.9702	23.9403	31.9403	34.4965	36.3847

APPENDIX CHAPTER II

Table 9: Results of the regression analyses controlled for phylogeny (multivariate linear mixed-effects models) testing differences in larval Shannon indices between hemi- and holometabolous insects.

Model		estimate	se	tval	df	pval	ci.lb	ci.ub	
(1) Intercept model	intercept	1.6947	0.1397	12.1299	15	**<.0001**	1.3969	1.9925	***
(2) Model looking at contrast between the groups	intercept	1.6006	0.2233	7.1668	14	**<.0001**	1.1216	2.0796	***
	Hemi_Holo	0.1586	0.2891	0.5488	14	**0.5918**	-0.4614	0.7787	

Table 10: Model qualities of the models testing adult Shannon indices.

Model	LogLik	Deviance	AIC	BIC	AICc
(1) Intercept model	-14.9485	29.8971	35.8971	38.0212	38.0789
(2) Model looking at contrast between the groups	-14.2979	28.5958	36.5958	39.1520	41.0402
(3) Modelling heteroscadasticity	-12.5639	25.1278	35.1278	38.3230	42.6278

Table 11: Results of the regression analyses controlled for phylogeny (multivariate linear mixed-effects models) testing differences in adult Shannon indices between hemi- and holometabolous insects.

Model		estimate	se	tval	df	pval	ci.lb	ci.ub	
(1) Intercept model	intercept	2.0095	0.1655	12.1430	15	**<.0001**	1.6567	2.3622	***
(2) Model looking at contrast between the groups	intercept	1.9127	0.2535	7.5447	14	**<.0001**	1.3689	2.4564	***
	Hemi_Holo	0.1745	0.3401	0.5132	14	**0.6158**	-0.5549	0.9040	
(3) Modelling heteroscadasticity	intercept	1.9220	0.3389	5.6713	14	**<.0001**	1.1951	2.6488	***
	Hemi_Holo	0.1803	0.3709	0.4861	14	**0.6344**	-0.6152	0.9758	

Table 12: Table of results for the visualised models.

Visualised model	Group	estimate	Lower CL	Upper CL	Lower PR	Upper PR
Heteroscadasticity model for beta-diversity	Hemimetabola	0.5345597	0.2902310	0.7788884	-0.07364454	1.1427639
	Holometabola	0.8468568	0.7340107	0.9597029	0.73401068	0.9597029
Contrast model for Shannon difference	Hemimetabola	0.5224223	-0.03156525	1.07641	-0.4557460	1.500591
	Holometabola	0.8010720	0.17886444	1.42328	-0.2172862	1.819430
Contrast model for larval Shannon indices	Hemimetabola	1.600569	1.121574	2.079564	0.3496938	2.851443
	Holometabola	1.759216	1.365476	2.152956	0.5384447	2.979988
Heteroscadasticity model for adult Shannon indices	Hemimetabola	1.921959	1.195109	2.648808	-0.09927765	3.943195
	Holometabola	2.102263	1.779066	2.425459	1.17035937	3.034166

Table 13: Results of perMANOVA testing differences in Beta-diversity between life stages per species collected from the field.

Order	Field – collected species	Factor	Df	Sum Sq	Mean Sq	Pseudo-F	R^2	P	group dispersions
Orthoptera	*Chorthippus parallelus*	Life stage	1	0.4454	0.44540	1.8122	0.07304	**0.121**	homogenous
		Residuals	23	5.6528	0.24577		0.92696		
		Total	24	6.0982			1.00000		
	Chorthippus dorsatus	Life stage	1	0.7328	0.73280	3.2021	0.12221	**0.019 ***	homogenous
		Residuals	23	5.2635	0.22885		0.87779		
		Total	24	5.9963			1.00000		
	Metrioptera roeselii	Life stage	1	0.27721	0.27721	0.99211	0.12414	**0.416**	homogenous
		Residuals	7	1.95587	0.27941		0.87586		
		Total	8	2.23308			1.00000		
Hemiptera	*Pyrrhocoris apterus*	Life stage	1	0.5017	0.50169	3.0134	0.04937	**0.002 ****	homogenous
		Population	1	0.3371	0.33713	2.0250	0.03318	0.034 *	
		Residuals	56	9.3232	0.16649		0.91746		
		Total	58	10.1621			1.00000		
	Graphosoma lineatum	Life stage	1	0.002420	0.0024199	0.96475	0.04392	**0.404**	homogenous
		Residuals	21	0.052674	0.0025083		0.95608		
		Total	22	0.055094			1.00000		
	Alleyrodes peroletella	Life stage	1	0.31711	0.31711	2.0528	0.10237	**0.058**	homogenous
		Residuals	18	2.78048	0.15447		0.89763		
		Total	19	3.09759			1.00000		
Thysanoptera	*Francliniella occidentalis*	Life stage	1	0.34693	na	0.8665	0.17805	**0.700**	homogenous
		Residuals	4	1.60158	na		0.82195		
		Total	5	1.94850			1.00000		
Coleoptera	*Agelastica alni*	**excluded**							
	Gastrophysa viridula	Life stage	1	3.0512	3.05117	17.521	0.45485	**0.001 *****	heterogenous
		Residuals	21	3.6569	0.17414		0.54515		
		Total	22	6.7081			1.00000		
	Melolontha melolontha	Life stage	1	5.0221	5.0221	19.4543	0.33561	**0.001 *****	heterogenous
		Population	1	0.3905	0.3905	1.5128	0.02610	0.134	

		Residuals	37	9.5515	0.2581		0.63829		
		Total	39	14.9641			1.00000		
	Tenebrio molitor	Life stage	1	0.9748	0.97482	3.3482	0.12243	**0.001 *** **	homogenous
		Residuals	24	6.9875	0.29114		0.87757		
		Total	25	7.9623			1.00000		
	Leptinotarsa decemlineata	Life stage	1	0.4587	0.45866	1.2788	0.04368	**0.228**	homogenous
		Residuals	28	10.0430	0.35868		0.95632		
		Total	29	10.5016			1.00000		
Hymenoptera	*Osmia cornuta*	Life stage	1	0.9475	0.94753	2.7374	0.09525	**0.023 ***	homogenous
		Residuals	26	8.9998	0.34614		0.90475		
		Total	27	9.9473			1.00000		
	Osmia bicornis	Life stage	1	1.2385	1.23846	4.0532	0.19252	**0.001 *** **	heterogenous
		Residuals	17	5.1943	0.30555		0.80748		
		Total	18	6.4328			1.00000		
	Neodiprion sertifer	Life stage	1	0.5352	0.53521	2.0298	0.05201	**0.032 ***	heterogenous
		Residuals	37	9.7561	0.26368		0.94799		
		Total	38	10.2913			1.00000		
Lepidoptera	*Aglais urticae*	**excluded**							
	Aglais io	Life stage	1	1.0125	1.01253	2.4208	0.12465	**0.003 ** **	homogenous
		Residuals	17	7.1105	0.41827		0.87535		
		Total	18	8.1231			1.00000		
Diptera	*Drosophila melanogaster*	Life stage	1	1.22434	1.22434	41.677	0.71028	**0.001 *** **	heterogenous
		Residuals	17	0.49941	0.02938		0.28972		
		Total	18	1.72375			1.00000		

Table 14: Results of perMANOVA testing differences in Beta-diversity between life stages per species collected from laboratory colonies.

Order	**Field – species**	**Factor**	**Df**	**Sum Sq**	**Mean Sq**	**Pseudo-F**	**R^2**	**P**	**group dispersions**
Thysanoptera	*Francliniella occidentalis*	Life stage	1	0.071812	0.071812	1.5018	0.3336	**0.200**	homogenous
		Residuals	3	0.143449	0.047816		0.6664		
		Total	4	0.215261			1.00000		
Coleoptera	*Tenebrio molitor*	Life stage	1	1.0638	1.06380	4.0714	0.18446	**0.003 ** **	heterogenous
		Residuals	18	4.7032	0.26129		0.81554		
		Total	19	5.7670			1.00000		
	Leptinotarsa decemlineata	Life stage	1	0.11578	0.115776	2.0327	0.08458	**0.072**	homogenous
		Residuals	22	1.25303	0.056956		0.91542		
		Total	23	1.36881			1.00000		
Lepidoptera	*Aglais urticae*	Life stage	1	0.9213	0.92129	2.7522	0.12653	**0.014 ***	homogenous
		Residuals	19	6.3602	0.33475		0.87347		
		Total	20	7.2815			1.00000		
Diptera	*Drosophila melanogaster*	Life stage	1	1.5345	1.53450	17.001	0.50001	**0.001 *** **	heterogenous
		Residuals	17	1.5344	0.09026		0.49999		
		Total	18	3.0689			1.00000		

Table 15: Results of perMANOVA testing differences in beta-diversity between life stages for all data pooled.

Factor	Df	SumSq	R^2	Pseudo-F	P		dispersion
Species	15	84.042	0.42094	23.3353	**0.001**	***	heterogenous
Life stage	2	1.892	0.00948	3.9407	**0.001**	***	
Species x Life stage	17	18.878	0.09456	4.6251	**0.001**	***	
Residuals	395	94.840	0.47502				
Total	429	199.653	1.00000				

Table 16: Analysis of variance table for linear model fits to compare alpha diversities between larval and adult life stages and populations per species. Shown are the two field-collected species which originated from two different locations.

Order	Field – collected species	Factor	Df	Sum Sq	Mean Sq	Pseudo-F	P
Hemiptera	*Pyrrhocoris apterus*	Life stage	1	0.0116	0.011604	0.1425	**0.7072**
		Population	1	0.1827	0.182706	2.2443	**0.1397**
		Residuals	56	4.5589	0.081408		
Coleoptera	*Melolontha melolontha*	Life stage	1	0.3567	0.35672	1.7861	**0.1896**
		Population	1	0.0053	0.00532	0.0266	**0.8713**
		Residuals	37	7.3897	0.19972		

APPENDIX CHAPTER II

Table 17: Mean Beta-diversities.

Order	Species	Mean Beta-diversity	SD	SE	No of Adult	No of Larvae
Orthoptera	*Chorthippus dorsatus*	0,712	0,236	0,142	15	10
	Metrioptera roeselli	0,707	0,174	0,236	7	2
	Chorthippus parallelus	0,656	0,336	0,131	9	16
Hemiptera	*Aleyrodes proletella*	0,561	0,163	0,126	10	10
	Graphosoma lineatum	0,039	0,050	0,008	15	8
	Pyrrhocoris apterus	0,565	0,198	0,074	26	33
Thysanoptera	*Frankliniella occidentalis*	0,872	0,072	0,356	3	3
Hymenoptera	*Osmia bicornis*	0,911	0,142	0,186	8	11
	Osmia cornuta	0,874	0,186	0,146	12	16
	Neodiprion sertifer	0,694	0,198	0,102	13	26
Coleoptera	*Gastrophysa viridula*	0,923	0,073	0,193	11	12
	Melolontha melolontha	0,999	0,003	0,158	20	20
	Tenebrio molitor	0,822	0,123	0,161	14	12
	Leptinotarsa decemlineata	0,846	0,216	0,155	7	23
Lepidoptera	*Aglais io*	0,961	0,108	0,220	7	12
Diptera	*Drosophila melanogaster*	0,936	0,048	0,215	9	10

Table 18: Results of t-tests used to compare larval and adult Alpha-diversities (Shannon) of the field-collected insect species. Also listed are the effect sizes (Hedges` g).

Order	Field – collected species	Test parameters					Hedges` g			
		Statistical test	W	T	Df	P	Estimate	Effect size	Lower 95% CI	Upper 95% CI
Orthoptera	*Chorthippus parallelus*	Two sample t-test	na	-0.726	23	**0.475**	-0.292	small	-1.130	0.545
Orthoptera	*Chorthippus dorsatus*	Two sample t-test	na	0.744	23	**0.465**	0.294	small	-0.527	1.115
Orthoptera	*Metrioptera roeselii*	Two sample t-test	na	1.120	7	**0.300**	0.798	medium	-0.933	2.529
Hemiptera	*Pyrrhocoris apterus*	Two sample t-test	na	-0.373	57	**0.710**	-0.097	negligible	-0.615	0.422
Hemiptera	*Graphosoma lineatum*	Two sample t-test	na	-2.313	21	**0.031** *	-0.976	large	-1.900	-0.052
Hemiptera	*Alleyrodes peroletella*	Two sample t-test	na	0.769	18	**0.452**	0.329	small	-0.577	1.235
Thysanoptera	*Francliniella occidentalis*	Two sample t-test	na	1.688	4	**0.167**	1.103	large	-0.844	3.049
Coleoptera	*Agelastica alni*	**excluded**								
Coleoptera	*Gastrophysa viridule*	Welch-test	na	0.612	13	**0.551**	0.255	small	-0.585	1.095
Coleoptera	*Melolontha melolontha*	Two sample t-test	na	-1.354	38	**0.184**	0.420	small	-1.054	0.215
Coleoptera	*Tenebrio molitor*	Two sample t-test	na	0.359	24	**0.723**	0.137	negligible	-0.650	0.924
Coleoptera	*Leptinotarsa decemlineata*	Two sample t-test	na	2.128	28	**0.042** *	0.894	large	0.003	1.784
Hymenoptera	*Osmia cornuta*	Two sample t-test	na	4.080	26	**3.8E-4** ***	1.513	large	0.650	2.375
Hymenoptera	*Osmia bicornis*	Two sample t-test	na	2.162	17	**0.045** *	0.960	large	-0.028	1.947
Hymenoptera	*Neodiprion sertifer*	Two sample t-test	na	1.029	37	**0.310**	0.342	small	-0.336	1.021
Lepidoptera	*Aglais urticae*	**excluded**								
Lepidoptera	*Aglais io*	Wilcoxon test	90	na	na	**0.027** *	1.217	large	0.272	2.162
Diptera	*Drosophila melanogaster*	Two sample t-test	na	6.095	17	**1.2E-5** ** *	2.675	large	1.401	3.949

APPENDIX CHAPTER II

Table 19: Results of t-tests used to compare larval and adult Alpha diversities (Shannon) with effect sizes (Hedges` g) for the laboratory-reared insect species.

Order	Laboratory – reared species	Test parameters					Hedges` g			
		Statistical test	W	T	Df	P	estimate	Effect size	Lower 95% CI	Upper 95% CI
Thysanoptera	*Francliniella occidentalis*	Two sample t-test	na	-4.096	3	**0.026 ***	-2.719	**large**	-5.622	0.1832555
Coleoptera	*Tenebrio molitor*	Two sample t-test	na	-0.638	18	**0.531**	-0.298	**small**	-1.285	0.688
	Leptinotarsa decemlineata	Two sample t-test	na	0.234	22	**0.817**	0.095	**negligible**	-0.749	0.940
Lepidoptera	*Aglais urticae*	Two sample t-test	na	-3.769	20	**0.001 ****	-1.736	**large**	-2.830	-0.641
Diptera	*Drosophila melanogaster*	Welch-test	na	4.891	12	**3.2E-4 *****	2.068	**large**	0.921	3.214

Table 20: Shannon indices and evenness for the species from laboratory colonies.

Order	Species	Life stage	N	Hs	SD (Hs)	E	SD (E)
Thysanoptera	*Francliniella occidentalis*	Larva	3	**2.067**	0.338	**0.633**	0.062
		Adult	2	**0.948**	0.200	**0.462**	0.016
Coleoptera	*Tenebrio molitor*	Larva	14	**1.377**	0.793	**0.641**	0.273
		Adult	6	**1.158**	0.363	**0.732**	0.164
	Leptinotarsa decemlineata	Larva	15	**1.515**	0.295	**0.768**	0.077
		Adult	9	**1.545**	0.324	**0.751**	0.103
Lepidoptera	*Aglais urticae*	Larva	16	**1.585**	0.609	**0.760**	0.220
		Adult	6	**0.541**	0.475	**0.883**	0.163
Diptera	*Drosophila melanogaster*	Larva	9	**0.940**	0.212	**0.580**	0.118
		Adult	10	**1.758**	0.479	**0.704**	0.126

APPENDIX CHAPTER II

Table 21: Shannon indices and evenness for the field-collected species.

Order	Species	Life stage	N	Hs	SD (Hs)	E	SD (E)
Orthoptera	*Chorthippus parallelus*	Larva	16	**1.602**	0.775	**0.668**	0.175
		Adult	9	**1.393**	0.671	**0.662**	0.175
	Chorthippus dorsatus	Larva	10	**1.418**	0.745	**0.707**	0.169
		Adult	15	**1.523**	0.587	**0.793**	0.155
	Metrioptera roeselii	Larva	2	**1.884**	0.515	**0.744**	0.187
		Adult	7	**2.434**	0.627	**0.765**	0.075
Hemiptera	*Pyrrhocoris apterus*	Larva	33	**1.957**	0.292	**0.782**	0.082
		Adult	26	**1.929**	0.284	**0.819**	0.059
	Graphosoma lineatum	Larva	8	**0.676**	0.024	**0.802**	0.214
		Adult	15	**0.775**	0.166	**0.707**	0.165
	Alleyrodes peroletella	Larva	10	**1.656**	0.362	**0.875**	0.125
		Adult	10	**1.791**	0.423	**0.868**	0.052
Thysanoptera	*Francliniella occidentalis*	Larva	3	**2.664**	0.892	**0.858**	0.057
		Adult	3	**3.607**	0.373	**0.891**	0.020
Coleoptera	*Agelastica alni*	**excluded**					
	Gastrophysa viridule	Larva	12	**1.508**	0.354	**0.813**	0.076
		Adult	11	**1.680**	0.870	**0.648**	0.250
	Melolontha melolontha	Larva	20	**2.501**	0.476	**0.887**	0.040
		Adult	20	**2.312**	0.403	**0.778**	0.087
	Tenebrio molitor	Larva	12	**2.123**	0.466	**0.784**	0.089
		Adult	14	**2.185**	0.409	**0.775**	0.099
	Leptinotarsa decemlineata	Larva	23	**1.572**	0.761	**0.778**	0.150
		Adult	7	**2.311**	0.944	**0.768**	0.096
Hymenoptera	*Osmia cornuta*	Larva	16	**0.954**	0.407	**0.723**	0.149
		Pupa	8	**1.268**	0.611	**0.699**	0.122
		Adult	12	**1.683**	0.540	**0.843**	0.104
	Osmia bicornis	Larva	11	**1.089**	0.279	**0.744**	0.126
		Pupa	5	**1.011**	0.335	**0.814**	0.172
		Adult	8	**1.802**	1.054	**0.790**	0.143
	Neodiprion sertifer	Larva	26	**1.570**	0.941	**0.712**	0.179
		Pupa	7	**2.123**	0.497	**0.748**	0.086
		Adult	13	**1.874**	0.701	**0.665**	0.131
Lepidoptera	*Aglais urticae*	**excluded**					
	Aglais io	Larva	13	**0.330**	0.463	**0.752**	0.390
		Adult	9	**1.102**	0.782	**0.551**	0.352
Diptera	*Drosophila melanogaster*	Larva	10	**2.437**	0.170	**0.908**	0.024
		Adult	9	**2.953**	0.199	**0.900**	0.025

APPENDIX CHAPTER II

Table 22: The three most abundant bacterial taxa per insect host are listed based on relative abundances of merged larval and adult life stages.

Origin	Species	Stage	Phylum	Genus	Note
Field	*Agelastica alni*	Larvae	Proteobacteria	Wolbachia	**Excluded** *from the final analysis*
			Proteobacteria	Enterobacteriaceae_Genus	
			Proteobacteria	Pantoea	
		Adults	Proteobacteria	Wolbachia	
			Other		
	Aglais io	Larvae	Proteobacteria	Pantoea	
			Proteobacteria	Pseudomonas	
			Proteobacteria	Enterobacter	
		Adults	Proteobacteria	Acinetobacter	
			Proteobacteria	Enterobacter	
			Proteobacteria	Enterobacteriaceae_Genus	
	Aglais urticae	Larvae	Proteobacteria	Methylobacterium	**Excluded** *from the final analysis*
			Proteobacteria	Sphingomonas	
			Actinobacteria	Herbiconiux	
		Adults	Proteobacteria	Gluconobacter	
			Proteobacteria	Acetobacteraceae_Genus	
			Firmicutes	Enterococcus	
	Aleyrodes proletella	Larvae	Proteobacteria	Arsenophonus	
			Proteobacteria	Proteobacteria_Class_Order_Family_Genus	
			Other		
		Adults	Proteobacteria	Arsenophonus	
			Proteobacteria	Proteobacteria_Class_Order_Family_Genus	
			Proteobacteria	Massilia	*Equally abundant*
			Proteobacteria	Pantoea	
	Chorthippus dorsatus	Larvae	Proteobacteria	Proteobacteria_Class_Order_Family_Genus	
			Proteobacteria	Alphaproteobacteria_Order_Family_Genus	
			Proteobacteria	Pantoea	
		Adults	Proteobacteria	Sphingomonas	
			Proteobacteria	Pantoea	
			Proteobacteria	Proteobacteria_Class_Order_Family_Genus	
	Chorthippus parallelus	Larvae	Bacteria_Phylum	uncultured bacterium	
			Proteobacteria	Proteobacteria_Class_Order_Family_Genus	
			Proteobacteria	Pantoea	
		Adults	Proteobacteria	Proteobacteria_Class_Order_Family_Genus	
			Proteobacteria	Alphaproteobacteria_Order_Family_Genus	

APPENDIX CHAPTER II

Origin	Species	Stage	Phylum	Genus	Note
			Proteobacteria	Pantoea	
	Drosophila melanogaster	Larvae	Proteobacteria	Gluconobacter	
			Proteobacteria	Komagataeibacter	
			Firmicutes	Lactobacillus	*Equally abundant*
			Proteobacteria	Enterobacteriaceae_Genus	
		Adults	Proteobacteria	Acetobacter	
			Proteobacteria	Alphaproteobacteria_Order_Family_Genus	
			Actinobacteria	Corynebacterium	
	Frankliniella occidentalis	Larvae	Firmicutes	Ruminococcaceae_Genus	
			Proteobacteria	Enterobacteriaceae_Genus	
			Proteobacteria	Pantoea	
		Adults	Firmicutes	Firmicutes_Class_Order_Family_Genus	
			Proteobacteria	Acetobacteraceae_Genus	
			Proteobacteria	Enterobacteriaceae_Genus	
	Gastrophysa viridule	Larvae	Proteobacteria	Cronobacter	
			Proteobacteria	Enterobacteriaceae_Genus	
			Proteobacteria	Pseudomonas	
		Adults	Firmicutes	Lactococcus	
			Proteobacteria	Pseudomonas	
			Proteobacteria	Yersinia	
	Graphosoma lineatum	Larvae	Proteobacteria	Pantoea	
			Other		
		Adults	Proteobacteria	Alphaproteobacteria_Order_Family_Genus	
			Proteobacteria	Pantoea	
			Proteobacteria	Serratia	
	Leptinotarsa decemlineata	Larvae	Proteobacteria	Pseudomonas	
			Proteobacteria	Enterobacteriaceae_Genus	
			Proteobacteria	Pantoea	
		Adults	Acidobacteria	Gp6_Family_Genus	
			Proteobacteria	Gammaproteobacteria_Order_Family_Genus	
			Proteobacteria	Pseudomonas	
	Melolontha melolontha	Larvae	Firmicutes	Ruminococcaceae_Genus	
			Firmicutes	Clostridium_XlVb	
			Bacteroidetes	Proteiniphilum	
		Adults	Synergistetes	Synergistes	
			Firmicutes	Ruminococcaceae_Genus	

APPENDIX CHAPTER II

Origin	Species	Stage	Phylum	Genus	Note
			Firmicutes	Clostridiales	
	Metrioptera roeselii	Larvae	Firmicutes	Lactobacillus	
			Firmicutes	Lactococcus	
			Proteobacteria	Pantoea	
		Adults	Proteobacteria	Proteobacteria_Class_Order_Family_Genus	
			NA_Phylum	NA	
			Proteobacteria	Sphingomonas	
	Neodiprion sertifer	Larvae	Proteobacteria	Yersinia	
			Proteobacteria	Enterobacteriaceae_Genus	
			Proteobacteria	Pseudomonas	
		Adults	Proteobacteria	Pseudomonas	
			Proteobacteria	Enterobacteriaceae_Genus	
			Proteobacteria	Stenotrophomonas	
	Osmia bicornis	Larvae	Firmicutes	Lachnospiraceae_Genus	
			Proteobacteria	Enterobacter	
			Proteobacteria	Pantoea	
		Adults	Tenericutes	Spiroplasma	
			Proteobacteria	Pantoea	*Equally abundant*
			Proteobacteria	Pseudomonas	
			Proteobacteria	Enterobacteriaceae_Genus	
			Proteobacteria	Sphingomonas	
	Osmia cornuta	Larvae	Firmicutes	Brevibacillus	
			Firmicutes	Staphylococcus	
			Proteobacteria	Enterobacteriaceae_Genus	
		Adults	Proteobacteria	Pseudomonas	
			Proteobacteria	Acinetobacter	
			Proteobacteria	Pantoea	
	Pyrrhocoris apterus	Larvae	Actinobacteria	Coriobacterium	
			Firmicutes	Clostridium_XlVa	
			Firmicutes	Lachnospiraceae_Genus	
		Adults	Actinobacteria	Coriobacterium	
			Firmicutes	Clostridium_XlVa	
			Actinobacteria	Gordonibacter	
	Tenebrio molitor	Larvae	Firmicutes	Lactococcus	
			Firmicutes	Clostridium_sensu_stricto	
			Firmicutes	Weissella	
		Adults	Firmicutes	Lactococcus	

APPENDIX CHAPTER II

Origin	Species	Stage	Phylum	Genus	Note
			Proteobacteria	Pantoea	
			Actinobacteria	Brevibacterium	
Laboratory	*Aglais urticae*	Larvae	Proteobacteria	Enterobacteriaceae_Genus	
			Proteobacteria	Pseudomonas	
			Proteobacteria	Methylobacterium	
		Adults	Proteobacteria	Cronobacter	
			Proteobacteria	Pseudomonas	
			Other		
	Drosophila melanogaster	Larvae	Proteobacteria	Acetobacter	
			Bacteroidetes	Bacteroides	
			Bacteroidetes	Parabacteroides	
		Adults	Proteobacteria	Acetobacter	
			Firmicutes	Lactococcus	
			Proteobacteria	Pantoea	
	Frankliniella occidentalis	Larvae	Proteobacteria	Acinetobacter	
			Proteobacteria	Enterobacteriaceae_Genus	
			Proteobacteria	Wolbachia	
		Adults	Proteobacteria	Enterobacter	
			Proteobacteria	Enterobacteriaceae_Genus	
			Actinobacteria	Micrococcus	
	Leptinotarsa decemlineata	Larvae	Proteobacteria	Enterobacter	
			Proteobacteria	Enterobacteriaceae_Genus	
			Firmicutes	Lactococcus	
		Adults	Proteobacteria	Enterobacter	
			Proteobacteria	Enterobacteriaceae_Genus	
			Firmicutes	Lactococcus	
	Tenebrio molitor	Larvae	Proteobacteria	Enterobacteriaceae_Genus	
			Proteobacteria	Stenotrophomonas	
			Firmicutes	Leuconostoc	
		Adults	Firmicutes	Enterobacter	
			Proteobacteria	Enterobacteriaceae_Genus	
			Proteobacteria	Lactococcus	

Reads

We obtained a dataset of 1 058 765 reads across 615 insect samples. After filtering chloroplasts and mitochondrial sequences, the dataset consisted of 646 011 reads, which we used for further analyses. The average number of reads was 1129.39 ± 769.67 SD per sample. For more details, see figure S19 and table S1.

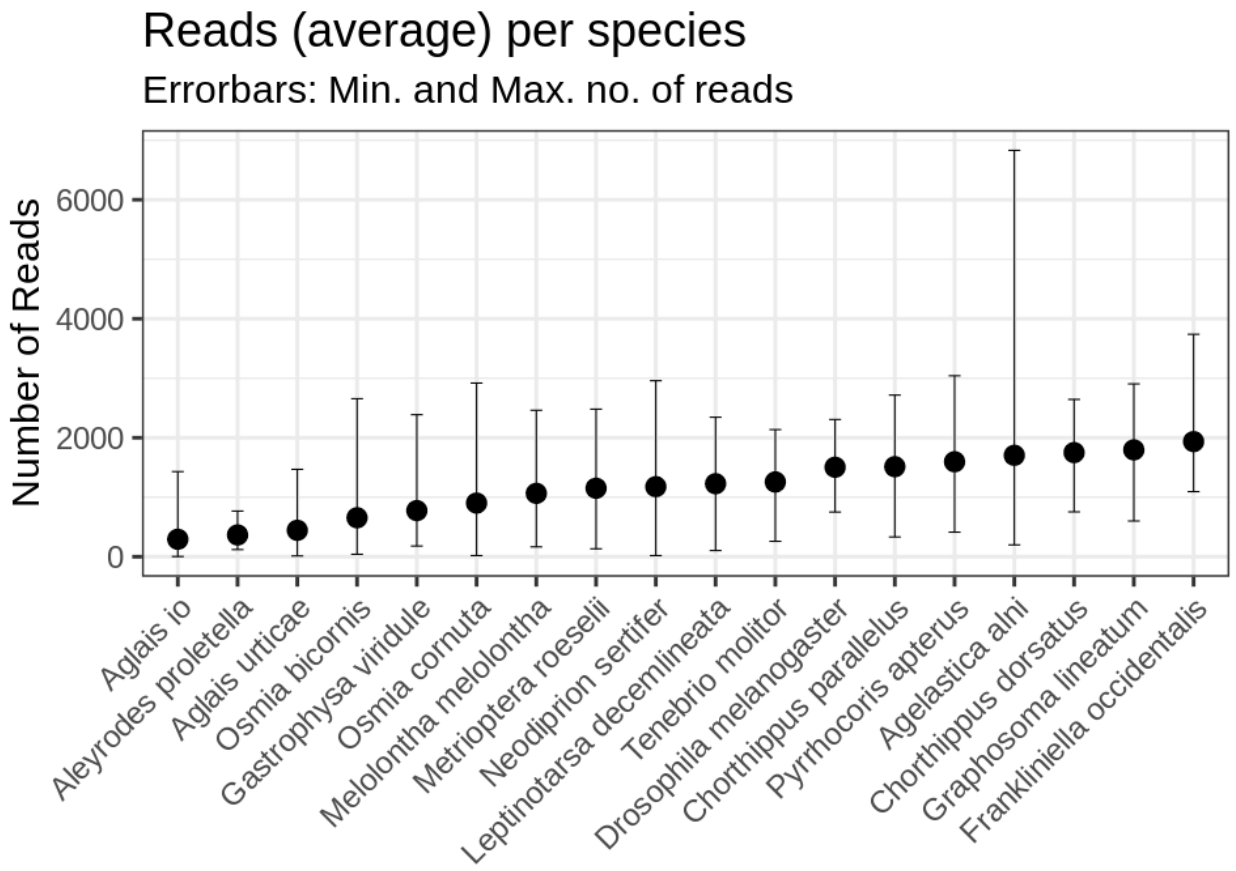

Figure S19: The average number of reads per species. The error bars show the minimum and the maximum number of reads.

APPENDIX CHAPTER II

Table 23: Number of reads per species.

Species	Average no of reads	Median no of reads	Total no of reads	Min. no of reads	Max. no of reads	Sparsity
Agelastica alni	1704.5	1594.5	85227.0	199.0	6830.0	0.996
Aglais io	294.2	31.0	5589.0	4.0	1431.0	0.999
Aglais urticae	444.3	169.0	5776.0	13.0	1469.0	0.998
Aleyrodes proletella	366.3	309.0	7325.0	120.0	768.0	0.997
Chorthippus dorsatus	1750.4	1787.0	43759.0	754.0	2644.0	0.996
Chorthippus parallelus	1513.7	1643.0	37842.0	333.0	2716.0	0.995
Drosophila melanogaster	1504.2	1432.0	28579.0	751.0	2307.0	0.992
Frankliniella occidentalis	1935.0	1790.5	11610.0	1094.0	3739.0	0.983
Gastrophysa viridule	775.2	679.0	17829.0	180.0	2387.0	0.996
Graphosoma lineatum	1796.2	1816.0	41313.0	601.0	2906.0	0.999
Leptinotarsa decemlineata	1227.4	1189.5	36821.0	105.0	2345.0	0.994
Melolontha melolontha	1065.4	1010.0	42617.0	166.0	2461.0	0.992
Metrioptera roeselii	1151.7	1020.0	10365.0	133.0	2481.0	0.990
Neodiprion sertifer	1177.3	1155.0	54157.0	20.0	2958.0	0.993
Osmia bicornis	655.1	509.5	15723.0	42.0	2656.0	0.997
Osmia cornuta	901.8	766.0	32466.0	20.0	2919.0	0.997
Pyrrhocoris apterus	1596.3	1567.0	94182.0	413.0	3042.0	0.995
Tenebrio molitor	1256.3	1228.5	32664.0	260.0	2136.0	0.993

APPENDIX CHAPTER II

Exclusion *Agelastica alni* and *Aglais urticae* from the field-collected dataset

We excluded two field-collected insect species from the final analysis, as they consisted mainly of contaminants: the coleopteran *Agelastica alni* and the lepidopteran *Aglais urticae*. *Agelastica alni* was excluded due to its very high abundance of the endosymbiont Wolbachia, which made up the entire microbial composition within most samples. Dobson et al. (1999) found Wolbachia in various insect tissues, e.g. reproductive tissues, brain and Malpighian tubules, and we homogenised the entire insect prior DNA extraction to use a standardised method for all insect samples (see Material and Methods for more details). Therefore, these sequences could not be known originated from the gut. Also, if the gut microbial biomass is low, the amount of contaminant DNA increases (Karstens et al., 2019). We also found low microbial biomasses in the lepidopteran *Aglais urticae*. The microbial composition of this butterfly species consisted mainly of Anaerobacter, Bacteroides known contaminants of negative control samples (Kartsens et al., 2019), Pedobacter and Methylobacterium known contaminants of DNA extraction kit reagents (Paniagua Voirol et al, 2020; Salter et al., 2014). Other sequences were abundant in low numbers. Therefore, we could not get meaningful results for *A. urticae*. Our result is consistent with the findings of low microbial densities in caterpillars (Hammer et al. 2017).

Ordination plots for all species pooled

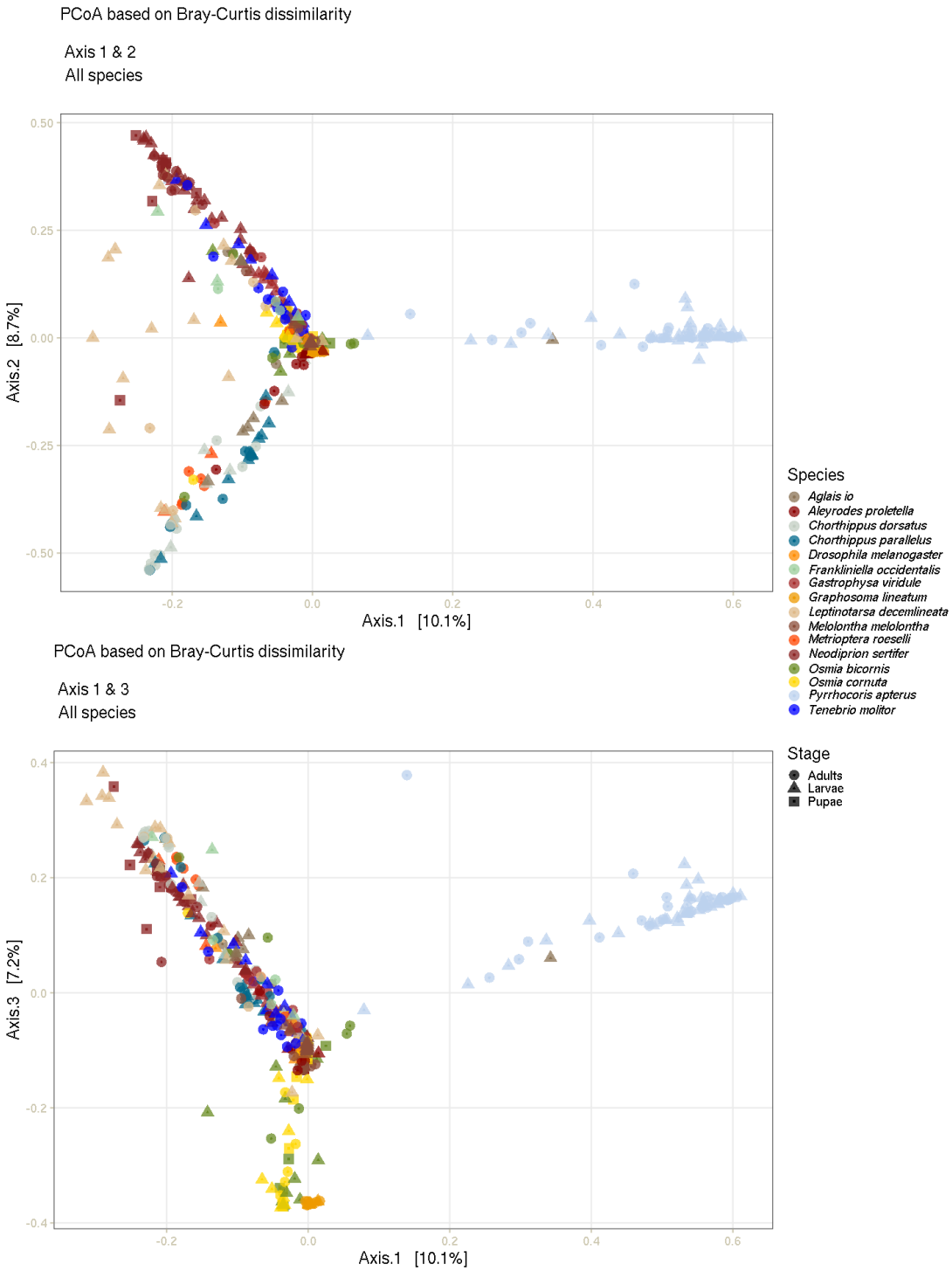

Figure S20: Principal coordinate analysis (PCoA) plot based on bray-curtis distances. The percentage of the total variance explained by each PC is indicated in parentheses.

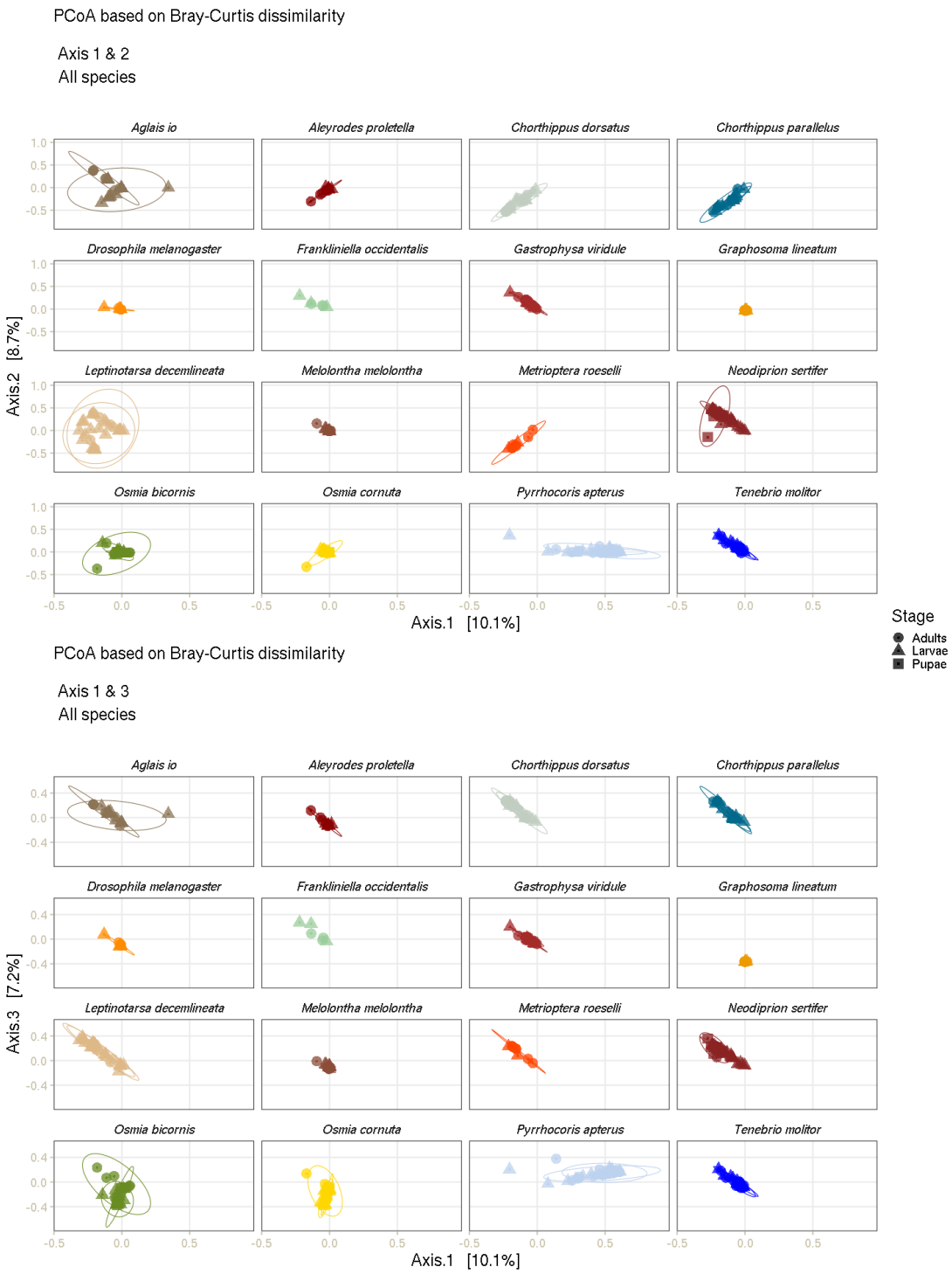

Figure S21: Principal coordinate analysis (PCoA) subplots based on bray-curtis distances per species. The percentage of the total variance explained by each PC is indicated in parentheses.

Appendix chapter III

Immune gene regulation in the gut during metamorphosis in two holo- versus a hemimetabolous insect

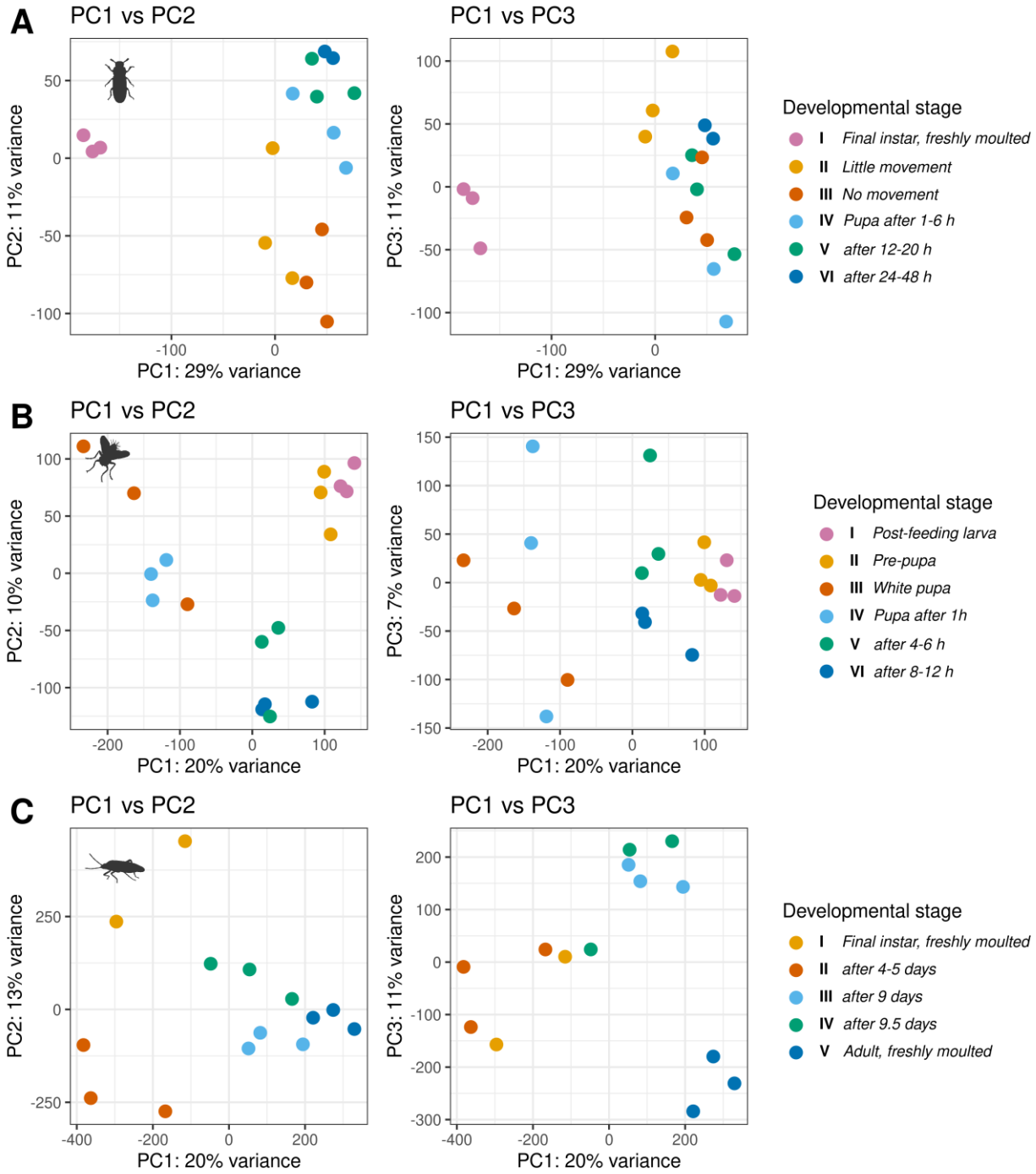

Figure 4: Principle components analysis (PCA) of *Tenebrio molitor* (A), *Calliphora vicina* (B) and *Pyrrhocoris apterus* (C) for examining the relationships between the developmental stages.

APPENDIX CHAPTER III

Table 2: Shown are the immune effectors of *Tenebrio molitor* and their normalized read counts for each differentially (corrected p-value <= 0.05) and non-differenially expressed (corrected p-value > 0.05) immune effector (averaged over all six developmental stages). Also shown are the read count means for each effector family and the overall mean.

	Effector family	Effector	No. of stages	Normalized read counts (averaged over all developm. stages)	SE (effector)	No. of effectors	Normalized read counts (averaged over the effectors for each effector family)	SE (effector family)
DIFFERENTIALLY EXPRESSED	Defensins	*Tenecin 1*	6	19,962.58	5,197.76	1	19,962.58	*NA*
	Cecropin	*Cecropin*	6	14,212.53	3,375.86	1	14,212.53	*NA*
	Attacins	*Attacin 1*	6	14,966.46	4,040.99	3	8,527.91	3,386.85
		Tenecin 4	6	7,130.99	4,806.18			
		Attacin 2	6	3,486.27	2,078.95			
	Coleoptericins	*Tenecin 2*	6	15,297.60	4,707.64	3	8,251.07	3,575.68
		Coleoptericin B	6	5,784.32	2,126.77			
		Coleoptericin A	6	3,671.30	1,672.61			
	Phenoloxidase	*Prophenoloxidase*	6	8,203.03	1,600.89	1	8,203.03	*NA*
	Lysozymes	*I-type lysozyme 2*	6	15,170.30	2,993.22	3	5,120.68	5,024.85
		Lysozyme 1	6	131.21	58.10			
		I-type lysozyme 1	6	60.53	19.78			
	Thaumatin	*Tenecin 3*	6	2,547.69	1,170.71	1	2,547.70	*NA*
			Mean:	**8,509.60**	**1,844.99**			
NOT	Attacin	*Attacin*	6	158.44	76.18	1	158.44	*NA*

APPENDIX CHAPTER III

Table 3: Shown are the immune effectors of *Calliphora vicina* and their normalized read counts for each differentially (corrected p-value <= 0.05) and non-differenially expressed (corrected p-value > 0.05) immune effector (averaged over all six developmental stages). Also shown are the read count means for each effector family and the overall mean.

	Effector family	Effector	No. of stages	Normalized read counts (averaged over all developm. stages)	SE (effector)	No. of effectors	Normalized read counts (averaged over the effectors for each effector family)	SE (effector family)
DIFF. EXPRESSED	Attacins	*Attacin a*	6	1,290.21	446.21	2	975.87	314.34
		Attacin b	6	661.53	188.39			
	Lysozymes	*Lysozyme b*	6	1,044.45	386.54	2	759.98	284.47
		Lysozyme a	6	475.51	106.17			
	Diptericins	*Diptericin b*	6	520.13	8.44	2	268.79	251.34
		Diptericin a	6	17.45	146.24			
			Mean:	**668.21**	**183.58**			
NOT	Attacins	*Attacin a*	6	691.35	165.20	10	111.28	70.54
		Attacin b	6	264.71	111.07			
		Attacin c	6	153.53	43.36			
		Attacin d	6	5.02	1.87			
		Attacin e	6	0.85	0.14			
		Attacin f	6	0.50	0.17			
		Attacin g	6	0.41	0.12			
		Attacin h	6	0.41	0.12			
		Attacin i	6	0.37	0.08			
		Attacin j	6	0.27	0.05			
	Cecropins	*Cecropin a*	6	389.33	101.91	4	110.63	93.34
		Cecropin b	6	42.98	10.38			
		Cecropin c	6	8.90	2.73			
		Cecropin d	6	1.32	0.57			

Diptericins	*Diptericin a*	6	345.89	55.33	10	55.07	36.04
	Diptericin b	6	163.72	20.45			
	Diptericin c	6	27.68	14.80			
	Diptericin d	6	4.78	1.04			
	Diptericin e	6	1.53	0.82			
	Diptericin f	6	2.45	0.78			
	Diptericin g	6	2.32	0.74			
	Diptericin h	6	0.52	0.31			
	Diptericin i	6	1.29	0.28			
	Diptericin j	6	0.50	0.14			
Defensin	*Defensin*	6	26.73	9.49	1	26.73	*NA*
Lysozymes	*Lysozyme a*	6	21.26	5.93	3	7.53	6.87
	Lysozyme b	6	1.04	0.24			
	Lysozyme c	6	0.29	0.08			
Coleoptericins	*Coleoptericin a*	6	3.79	1.24	2	3.30	0.49
	Coleoptericin b	6	2.81	1.75			
		***Mean**:*	**72.22**	**28.71**			

APPENDIX CHAPTER III

Table 4: Shown are the immune effectors of *Pyrrhocoris apterus* and their normalized read counts for each differentially (corrected p-value <= 0.05) and non-differenially expressed (corrected p-value > 0.05) immune effector (averaged over all six developmental stages). Also shown are the read count means for each effector family and the overall mean.

	**Effector family**	**Effector**	**No. of stages**	**Normalized read counts** (averaged over all developm. stages)	**SE (effector)**	**No. of effectors**	**Normalized read counts** (averaged over the effectors for each effector family)	**SE (effector family)**
DIFF. EXPR.	Phenoloxidase	*Phenoloxidase*	5	29.24	13.90	1	29.24	*NA*
	Lysozymes	*C-type lysozyme*	5	41.21	15.32	2	24.68	16.53
		Lysozyme	5	8.15	4.15			
			Mean:	**26.20**	**9.66**			
NOT	Lysozymes	*I-type lysozyme b*	5	45.20	12.00	5	17.88	7.97
		C-type lysozyme a	5	25.40	6.48			
		I-type lysozyme a	5	11.98	3.13			
		I-type lysozyme ac	5	5.95	1.94			
		C-type lysozyme b	5	0.88	0.53			
			Mean:	**17.88**	**7.97**			

Appendix chapter IV

Complete metamorphosis and fast larval growth in insects

APPENDIX CHAPTER IV

Table 1: Keywords used to search ZOBODAT for literature on insect growth. Also shown are the number of insects for each insect order that we used for the final dataset, the number of publications that fit all criteria and the number of publications with an existing PDF file on ZOBODAT from the initial search.

	Search terms		No. of publications (initial search)	No. of publications that fit all criteria	Species number
	Keywords (from Misof et al, 2014)	German names and synonyms			
HEMIMETABOLA	Archaeognatha	Felsenspringer	18	0	0
	Zygentoma	Fischchen	10	0	0
	Odonata	Libelle; Wasserjungfer	928	5	5
	Ephemeoptera	Eintagsfliege	80	0	0
	Zoraptera	Bodenlaus	4	1	1
	Dermaptera	Ohrwurm	50	0	0
	Plecoptera	Steinfliege	546	0	0
	Orthoptera	Heuschrecke	538	2	10
	Mantophasmatodea	Gladiatorschrecke; Gladiator; Fersenläufer	4	0	0
	Grylloblattodea	Grillenschabe; Notoptera	0	0	0
	Embioptera	Tarsenspinner; Fersenspinner	4	0	0
	Phasmatodea	Gespenstschrecke; Phasmida; Phasmiden	37	1	1
	Mantodea	Fangschrecke; Gottesanbeterin	104	0	0
	Blattodea	Schabe; Blatteria	61	1	1
	Isoptera	Termiten	143	0	0
	Thysanoptera	Fransenflügler; Thrips; Blasenfüße; Gewittertierchen; Gewitterwürmer	76	0	0
	Hemiptera	Schnabelkerfe; Rhynchota	584	2	2
	Psocodea	Staublaus; Psocoptera	7	1	1
HOLOMETABOLA	Hymenoptera	Hautflügler	3526	0	0
	Raphidioptera	Kamelhalsfliege	112	0	0
	Megaloptera	Großflügler; Schlammfliege	40	0	0
	Neurotera	Netzflügler; Planipennia	292	0	0
	Strepsiptera	Fächeflügler	41	0	0
	Coleoptera	Käfer	5478	6	6
	Trichoptera	Köcherfliege	678	0	0
	Lepidopera	Schmetterling	4791	5	5

Siphonaptera	Flöhe	68	0	0
Mecoptera	Schnabelfliege; Schnabelhafte	5	0	0
Diptera	Zweiflügler	2014	1	1

Table 2: The insect species with variability in the number of instars weighted GR, RGR and PGR were calculated with the respective pupation and adult eclosion rates, respectively.

	Insect	No. of instars	Rate [%]
HEMIMETABOLA	*Eucorydia yasumatsui*	8	27.27
		9	68.18
		10	4.55
HOLOMETABOLA	*Tenebrio molitor*	14	5.63
		15	19.39
		16	21.98
		17	28.32
		18	15.05
		19	6.29
		20	2.5
	Zophobas atratus	13	2.86
		14	11.43
		15	17.14
		16	25.71
		17	25.71
		18	17.14
	Lasiocampa pini	4	7.14
		5	69.05
		6	19.05
		7	4.76

APPENDIX CHAPTER IV

Table 3: Results of the regression analyses controlled for phylogeny (multivariate linear mixed-effects models) testing differences in growth estimates (GR, RGR, PGR) between hemi- and holometabolous insects.

	Model		Estimate	SE	T-value	Df	P-value	Lower CI	Upper CI	
GR	(1) Intercept model	Intercept	1.314	0.025	52.573	32	**<.0001**	1.263	1.365	***
	(2) Model looking at contrast between the groups	Intercept	1.272	0.030	43.172	31	**<.0001**	1.212	1.332	***
		Hemi_Holo	0.141	0.054	2.609	31	**0.0139**	0.031	0.252	*
	(3) Modelling heteroscadasticity	Intercept	1.272	0.018	70.276	31	**<.0001**	1.236	1.309	***
		Hemi_Holo	0.188	0.078	2.404	31	**0.0224**	0.029	0.348	*
RGR	(1) Intercept model	Intercept	0.023	0.003	7.156	32	**<.0001**	0.016	0.029	***
	(2) Model looking at contrast between the groups	Intercept	0.019	0.004	4.737	31	**<.0001**	0.011	0.027	***
		Hemi Holo	0.018	0.008	2.286	31	**0.0293**	0.002	0.035	*
	(3) Modelling heteroscadasticity	Intercept	0.018	0.002	7.922	31	**<.0001**	0.013	0.022	***
		Hemi_Holo	0.055	0.022	2.548	31	**0.0160**	0.011	0.099	*
PGR	(1) Intercept model	Intercept	3.738	0.739	5.061	32	**<.0001**	2.233	5.243	***
	(2) Model looking at contrast between the groups	Intercept	2.273	0.779	2.917	31	**0.0065**	0.684	3.863	**
		Hemi_Holo	5.347	1.539	3.474	31	**0.0015**	2.208	8.486	**
	(3) Modelling heteroscadasticity	Intercept	2.074	0.265	7.813	31	**<.0001**	1.532	2.615	***
		Hemi_Holo	7.930	2.669	2.971	31	**0.0057**	2.487	13.373	**

APPENDIX CHAPTER IV

Table 4: Results of the regression analyses controlled for phylogeny (multivariate linear mixed-effects models) testing differences in Mean DT between hemi- and holometabolous insects.

Model		Estimate	SE	T-value	Df	P-value	Lower CI	Upper CI	
(1) Intercept model	Intercept	14.8696	1.9244	7.7270	29	**<.0001**	10.9338	18.8053	***
(2) Model looking at contrast between the groups	Intercept	18.3097	1.7979	10.1841	28	**<.0001**	14.6269	21.9925	***
	Hemi_Holo	-11.0502	2.8262	-3.9100	28	**0.0005**	-16.8393	-5.2611	***

Table 5: The regression analysis results controlled for phylogeny testing differences in GR, RGR and PGR between hemi- and holometabolous insects for the reduced dataset without the three Gryllidae species measured in ten-day intervals (phylogenetic linear mixed-effects models with specified variance structure by modelling heteroscedasticity).

Growth estimate		Estimate	SE	T-value	Df	P-value	Lower CI	Upper CI	
GR	Intercept	1.277	0.020	64.083	28	**<.0001**	1.236	1.318	***
	Hemi_Holo	0.184	0.079	2.332	28	**0.027**	0.022	0.345	*
RGR	Intercept	0.018	0.003	6.802	28	**<.0001**	0.013	0.023	***
	Hemi_Holo	0.055	0.022	2.541	28	**0.017**	0.011	0.099	*
PGR	Intercept	2.068	0.307	6.747	28	**<.0001**	1.440	2.696	***
	Hemi_Holo	7.936	2.673	2.969	28	**0.006**	2.460	13.412	**

APPENDIX CHAPTER IV

Table 6: Table of results for the visualised models showing the plotted group estimates with their respective confidence intervals (CI) and prediction intervals (PR).

Visualised model	Growth	Estimate	Lower CI	Upper CI	Lower PR	Upper PR	Note
Heteroscadasticity model for **GR**	Hemimetabola	0.240	0.211	0.269	0.135	0.345	
	Holometabola	0.341	0.237	0.446	0.029	0.654	
Heteroscadasticity model for **RGR**	Hemimetabola	-4.115	-4.419	-3.812	-5.539	-2.691	*Log-transformed*
	Holometabola	-2.860	-3.721	-1.999	-5.963	0.243	*Log-transformed*
Heteroscadasticity model for **PGR**	Hemimetabola	0.445	0.087	0.804	-0.885	1.775	*Log-transformed*
	Holometabola	1.019	-0.034	2.071	-1.544	3.582	*Log-transformed*
Contrast model for **Mean GP**	Hemimetabola	0.240	0.211	0.269	0.135	0.345	
	Holometabola	0.341	0.237	0.446	0.029	0.654	

Table 7: Mean GR, RGR and PGR estimates for each species with the respective standard errors ordered by ascending PGR within Hemimetabla and Holometaola, respectively.

	Order	Species	Instars		GR	GR SE	RGR	RGR SE	PGR	PGR SE	Weighted
			No	Used							
HEMIMETABOLA	Phasmatodea	*Dixippus morosus*	6	6	1.082	0.056	0.003	0.002	0.340	0.217	No
	Blattodea	*Eucorydia yasumatsui*	10	10	1.199	0.028	0.004	0.001	0.413	0.099	Yes
	Odonata	*Aeshna tuberculifera*	30	29	1.203	0.023	0.011	0.002	1.245	0.227	No
	Zoraptera	*Zorotypus caudelli*	5	5	1.183	0.059	0.011	0.004	1.291	0.503	No
	Orthoptera	*Trilophidia conturbata*	5	5	1.258	0.112	0.011	0.005	1.352	0.561	No
	Odonata	*Leucorrhinia dubia*	13	13	1.211	0.025	0.013	0.003	1.409	0.298	No
	Odonata	*Nasiaeschna pentacantha*	15	13	1.256	0.012	0.013	0.002	1.435	0.265	No
	Orthoptera	*Acrida sp.*	7	7	1.331	0.029	0.013	0.002	1.514	0.205	No
	Orthoptera	*Acrotylus angulatus*	5	5	1.276	0.037	0.014	0.002	1.644	0.277	No
	Orthoptera	*Acheta domesticus*	10	10	1.211	0.072	0.018	0.006	2.107	0.719	No
	Orthoptera	*Oedaleus nigrofasciatus*	5	5	1.314	0.049	0.018	0.003	2.115	0.391	No
	Orthoptera	*Zonocerus elegans*	5	4	1.415	0.059	0.019	0.003	2.254	0.448	No
	Orthoptera	*Teleogryllus commodus*	10	10	1.237	0.075	0.020	0.006	2.367	0.753	No
	Orthoptera	*Gryllus assimilis*	10	10	1.241	0.075	0.020	0.006	2.406	0.746	No

	Orthoptera	*Acanthacris ruficornis*	7	6	1.413	0.171	0.020	0.009	2.651	1.329	No
	Psocodea	*Pediculus humanus corpor*	3	2	1.387	0.024	0.023	0.003	2.735	0.381	No
	Orthoptera	*Aiolopus thalassinus*	5	5	1.339	0.065	0.024	0.004	2.806	0.562	No
	Odonata	*Anax junius*	13	12	1.280	0.037	0.029	0.011	3.394	1.313	No
	Hemiptera	*Psammotettix alienus*	5	4	1.265	0.026	0.037	0.004	4.139	0.431	No
	Odonata	*Erythemis simplicicollis*	13	12	1.261	0.020	0.048	0.007	5.424	0.843	No
	Hemiptera	*Limnogeton fieberi*	5	4	1.400	0.020	0.047	0.013	5.621	1.620	No
HOLOMETABOLA	Lepidoptera	*Epilobophora sabinata teriolensis*	5	3	1.510	0.049	0.008	0.003	0.973	0.326	No
	Coleoptera	*Cucujus cinnaberinus*	6	5	1.199	0.025	0.009	0.002	1.019	0.287	No
	Coleoptera	*Tenebrio molitor*	20	19	1.144	0.024	0.015	0.003	1.613	0.271	Yes
	Lepidoptera	*Lasiocampa pini*	7	6	1.352	0.078	0.019	0.007	2.269	0.856	Yes
	Lepidoptera	*Saturnia pyri*	6	5	1.620	0.137	0.088	0.022	11.728	3.155	No
	Lepidoptera	*Ephestia kuehniella*	6	6	1.568	0.068	0.096	0.012	12.265	1.683	No
	Coleoptera	*Melasoma populi*	4	4	1.500	0.308	0.089	0.046	12.663	7.742	No
	Lepidoptera	*Hyles livornica*	5	2	1.733	0.267	0.111	0.063	15.417	9.583	No
	Coleoptera	*Zophobas atratus*	18	18	1.186	0.017	0.021	0.002	17.344	0.267	Yes
	Coleoptera	*Tribolium confusum*	6	6	1.463	0.084	0.138	0.035	17.344	5.163	No
	Coleoptera	*Andrector ruficornis*	3	3	1.642	0.168	0.263	0.081	34.692	11.914	No
	Diptera	*Lucilia sericata*	3	2	2.072	0.158	1.012	0.192	149.987	34.534	No

APPENDIX CHAPTER IV

Table 8: The mean and total durations of the growth period (in days) for each insect species; ordered by ascending Mean GP (estimate) within Hemimetabla and Holometaola, respectively. For the Total GP, four species were excluded because either the duration of the growth period for the first or the last immature stage were not reported.

	Order	Species	Instars		Mean GP		Total GP
			No	Used	Estimate	SD	
HEMIMETABOLA	Odonata	*Erythemis simplicicollis*	13	13	6.385	0.978	83.000
	Hemiptera	*Psammotettix alienus*	5	5	6.460	0.761	32.300
	Hemiptera	*Limnogeton fieberi*	5	5	9.601	3.294	48.005
	Psocodea	*Pediculus humanus corpor*	3	3	12.037	3.021	36.110
	Orthoptera	*Aiolopus thalassinus*	5	5	12.800	2.267	64.000
	Zoraptera	*Zorotypus caudelli*	5	5	15.457	1.461	77.285
	Orthoptera	*Oedaleus nigrofasciatus*	5	5	16.000	2.000	80.000
	Orthoptera	*Acrotylus angulatus*	5	5	17.400	1.122	87.000
	Orthoptera	*Acanthacris ruficornis*	7	7	19.214	3.175	134.500
	Orthoptera	*Trilophidia conturbata*	5	5	20.000	1.265	100.000
	Orthoptera	*Zonocerus elegans*	5	5	20.400	1.806	102.000
	Orthoptera	*Acrida sp.*	7	7	22.714	1.300	159.000
	Phasmatodea	*Dixippus morosus*	6	6	23.278	1.315	139.667
	Odonata	*Anax junius*	13	13	24.846	9.324	323.000
	Odonata	*Nasiaeschna pentacantha*	15	14	28.564	6.093	*excluded*
	Odonata	*Aeshna tuberculifera*	15	15	33.778	5.598	506.667
	Odonata	*Leucorrhinia dubia*	13	13	34.538	13.667	449.000
	Blattodea	*Eucorydia yasumatsui*	10	10	73.722	12.205	737.224
HOLOMETABOLA	Diptera	*Lucilia sericata*	3	3	0.986	0.259	2.958
	Coleoptera	*Andrector ruficornis*	3	3	2.304	0.838	6.912
	Coleoptera	*Tribolium confusum*	6	6	3.083	0.503	18.500
	Coleoptera	*Melasoma populi*	4	4	4.500	0.866	18.000
	Lepidoptera	*Ephestia kuehniella*	6	6	4.833	0.543	29.000
	Lepidoptera	*Saturnia pyri*	6	5	6.000	0.707	*excluded*
	Lepidoptera	*Hyles livornica*	5	5	7.400	0.872	37.000
	Coleoptera	*Zophobas atratus*	18	18	9.676	0.717	174.160
	Coleoptera	*Tenebrio molitor*	20	20	12.095	1.252	241.900
	Coleoptera	*Cucujus cinnaberinus*	6	5	29.408	7.187	*excluded*
	Lepidoptera	*Lasiocampa pini*	7	7	43.143	25.752	302.000
	Lepidoptera	*Epilobophora sabinata teriolensis*	5	4	67.000	37.050	*excluded*

APPENDIX CHAPTER IV

Table 9: Listed is the per species information about the rearing temperature, where the study was conducted (field or laboratory), and whether living or exuviae were measured. Also listed are the sample sizes for each species. These numbers are mean values due to variation of the sample sizes throughout insect development (some specimens died during an experiment, for instance).

	Order	Species	N	Laboratory / Field	Temp	living insect
HEMIMETABOLA	Blattodea	*Eucorydia yasumatsui*	18	Laboratory	18-24	living
	Hemiptera	*Limnogeton fieberi*	25	Laboratory	28	living
		Psammotettix alienus	50	Laboratory	>20	living
	Odonata	*Aeshna tuberculifera*	4	Laboratory	RT	exuvie and living
		Anax junius	13	Laboratory	10 - 31.6	exuvie
		Nasiaeschna pentacantha	NA	Laboratory	RT	exuvie
		Erythemis simplicicollis	1	Laboratory	RT	exuvie
		Leucorrhinia dubia	NA	Field	RT	living
	Orthoptera	*Acanthacris ruficornis*	7	Laboratory	Africa	living
		Acrida sp.	270	Laboratory	Africa	living
		Acrotylus angulatus	45	Laboratory	Africa	living
		Aiolopus thalassinus	60	Laboratory	Africa	living
		Oedaleus nigrofasciatus	120	Laboratory	Africa	living
		Trilophidia conturbata	45	Laboratory	Africa	living
		Acheta domesticus	50	Laboratory	25	living
		Gryllus assimilis	50	Laboratory	25	living
		Teleogryllus commodus	50	Laboratory	25	living
		Zonocerus elegans	2	Laboratory	Africa	living
	Phasmatodea	*Dixippus morosus*	3	Laboratory	20	living
	Psocodea	*Pediculus humanus corpor*	70	Laboratory	RT	living
	Zoraptera	*Zorotypus caudelli*	2	Laboratory	26	living
HOLOMETABOLA	Coleoptera	*Andrector ruficornis*	5	Laboratory	28	living
		Melasoma populi	10	Laboratory	RT	living
		Cucujus cinnaberinus	14	Laboratory	22	living
		Tenebrio molitor	10	Laboratory	25	living
		Tribolium confusum	50	Laboratory	30	living
		Zophobas atratus	10	Laboratory	25	living

Diptera	*Lucilia sericata*	100	Laboratory	25	living
Lepidoptera	*Epilobophora sabinata teriolensis*	9	Field	shady and cool	living
	Lasiocampa pini	32	Lab. / Field	RT	living
	Ephestia kuehniella	25	Laboratory	30	living
	Saturnia pyri	NA	Laboratory	RT	living
	Hyles livornica	15	Laboratory	<20	living

Table 10: References of the growth data.

	Species	Author	Title	Journal	Vol, No., pp.	Year	Language
HEMIMETABOLA HEMIPTERA BLATTODEA	*Eucorydia yasumatsui*	Fujita Mari, Ryuichiro Machida	Reproductive biology and postembryonic development of a polyphagid cockroach Eucorydia yasumatsui Asahina (Blattodea: Polyphagidae)	Arthropod Systematics & Phylogeny	72, 2, 193-211	2014	Eng
	Limnogeton fieberi	J. Voelker	Untersuchungen zu Ernährung, Fortpflanzungsbiologie und Entwicklung von Limnogeton fieberi Mayr (Belostomatidae, Hemiptera) als Beitrag zur Kenntnis von natürlichen Feinden tropischer Wasserschnecken	Entomologische Mitteilungen aus dem Zoologischesn Staatsinstitut u. Zoologischen Museum Hamburg	3,60	1968	Ger
	Psammotettix alienus	Binari Manurung, Werner Witsack, Egon Fuchs, Silke Mehner	Zur Embryonal-und Larvalentwicklung der Zikade Psammotettix alienus (DAHLBOM, 1851):(Hemiptera, Auchenorrhyncha)	Cicadina	4, 49-58	2001	German
ODONATA	*Aeshna tuberculifera*	Elsie Lincoln	Growth in Aeshna Tuberculifera (Odonata)	Proceedings of the American Philosophical Society	83, 5, 589-605	1940	Eng
	Anax junius	Philip P. Calvert	The Rates of Growth, Larval Development and Seasonal Distribution of Dragonflies of the Genus Anax (Odonata: Æshnidæ)	Proceedings of the American Philosophical Society	73, 1, 1-70	1934	Eng
	Nasiaeschna pentacantha	S.W. Dunkle	Larval growth in Nasiaeschna pentacantha (Rambur)(Anisoptera: Aeshnidae)	Odonatologica	14, 1, 29-35	1985	Eng
	Erythemis	George H.	Life-history of the dragofly,	Annals of the	34, 1,	1941	Eng

APPENDIX CHAPTER IV

	Species	Author	Title	Journal	Vol, No., pp.	Year	Language
	simplicicollis	Bick	Erythemis simplicicollis (Say)	Entomological Society of America	215-230		
	Leucorrhinia dubia	Fritz Prenn	Aus der Nordtiroler Libellenfauna	Buch; Verlag: K.k.zoologisch-botanische Gesellschaft, Wien		1929	German
ORTHOPTERA	*Acanthacris ruficornis* *Acrida sp.* *Acrotylus angulatus* *Aiolopus thalassinus* *Oedaleus nigrofasciatus* *Trilophidia conturbata* *Zonocerus elegans*	Julia Chesler	Observations on the biology of some South African Acrididae (Orthoptera)	Transactions of the Royal Entomological Society of London	87, 14, 313-351	1938	Eng
	Acheta domesticus *Gryllus assimilis* *Teleogryllus commodus*	Robert Sturm	Längen- und Gewichtsentwicklung der Larven verschiedener Grillenarten (Orthoptera: Gryllidae) vom Zeitpunkt des Ausschlüpfens bis zur Adulthäutung	Linzer biologische Beiträge	35, 1, 487-498	2003	German
PHASMATODEA	*Dixippus morosus*	Eidmann	Untersuchungen über Wachstum und Häutung der Insekten	Zeitschrift für Morphologie und Ökologie der Tiere	2, 3-4, 567-610	1924	German
PSOCODEA	*Pediculus humanus corpor*	P.A. Buxton	Studies on the growth of Pediculus (Anoplura)	Parasitology	30,1, 65-84	1938	Eng
	Pediculus humanus corpor	P.A. Buxton	The biology of the body louse (Pediculus humanus corporis: Anoplura) under experimental conditions	Parasitology	32, 3, 303-312	1940	Eng
	Zorotypus caudelli	Yuta Mashimo, Rolf G. Beutel,	Postembryonic development of the ground louse Zorotypus caudelli Karny (Insecta: Zoraptera: Zorotypidae)	Arthropod Systematics & Phylogeny	72, 1, 55-71	2014	Eng

APPENDIX CHAPTER IV

		Species	Author	Title	Journal	Vol, No., pp.	Year	Language
	ZORAPTERA		Romano Dallai, Chow-Yang Lee, Ryuichiro Machida					
HOLOMETABOLA	COLEOPTERA	*Andrector ruficornis*	Wolfgang Heyer, Maria Luisa Chiang Lok, Bienvenido Cruz	Zum Einfluss der Temperatur und Wirtspflanze auf die Entwicklung von Andrector ruficornis (Oliv.) (Coleoptera: Chrysomelidae)	Beiträge zur Entomologie	38, 1, 183-188	1988	German
		Melasoma populi	A. Willer	Beobachtungen zur Biologie von Melasoma populi L.	Zeitschrift für wissenschaftliche Insektenbiologie	15, 65-73	1919	German
		Cucujus cinnaberinus	Ulrich Straka	Zur Biologie des Scharlachkäfers Cucujus cinnaberinus (Scopoli, 1763)	Beiträge zur Entomofaunistik	8, 11-26	2008	German
		Tenebrio molitor	Jong Bin Park, Won Ho Choi, Seong Hyun Kim, Hyo Jung Jin, Yeon Soo Han, Yong Seok Lee, Nam Jung Kim	Developmental characteristics of Tenebrio molitor larvae (Coleoptera: Tenebrionidae) in different instars	International Journal of Industrial Entomology	28, 1, 5-9	2014	Eng
		Tribolium confusum	Tom A. Brindley	The Growth and Development of Ephestia Kuehniella Zeller (Lepidoptera) and Tri-Bolium Confusum Duval (Coleoptera) under Controlled Conditions of Temperature and Relative Humidity	Annals of the Entomological Society of America	23, 4, 741-757	1930	Eng
		Zophobas atratus	Sun Young Kim, Hong Geun Kim, Sung Ho Song, Nam Jung Kim	Developmental characteristics of Zophobas atratus (Coleoptera: Tenebrionidae) larvae in different instars	International Journal of Industrial Entomology	30, 2, 45-49	2015	Eng
	DIPTERA	*Lucilia sericata*	Martin Grassberger, Christian Reiter	Effect of temperature on Lucilia sericata (Diptera: Calliphoridae) development with special reference to the isomegalen-and isomorphen-diagram	Forensic Science International	120, 1-2, 32-36	2001	Eng
		Epilobophora	Wilhelm	Die Entwicklung von	Zeitschrift des	27,	1942	German

APPENDIX CHAPTER IV

	Species	Author	Title	Journal	Vol, No., pp.	Year	Language
LEPIDOPTERA	*sabinata teriolensis*	Mack	Nothopteryx (Lobophora) sabinata H.-Schäf.f von teriolensis Kitt	Wienerr Entomologen-Vereins	16-22		
	Lasiocampa pini	Karl Eckstein	Beiträge zur Kenntnis des Kiefernspinners Lasiocampa (Gastropacha, Dendrolimus) pini L.	Zoologische Jahrbücher, Abteilung für Systematik, Geographie und Biologie der Tiere	31, 59-164	1911	German
	Ephestia kuehniella	Tom A. Brindley	The Growth and Development of Ephestia Kuehniella Zeller (Lepidoptera) and Tri-Bolium Confusum Duval (Coleoptera) under Controlled Conditions of Temperature and Relative Humidity	Annals of the Entomological Society of America	23, 4, 741-757	1930	Eng
	Saturnia pyri	Oliver Eitschberger	Die Biologie und Metamorphose des Wiener Nachtpfauenauges Saturnia pyri ([Denis & Schiffermüller], 1775)	Neue Entomologische Nachrichten	148-171	2010	German
	Hyles livornica	M. Gillmer	Ein Beitrag zur Entwicklungsgeschichte von Phryxus livornica, Esp.	Entomologische Zeitschrift	70-72	1904	German

Growth trajectories

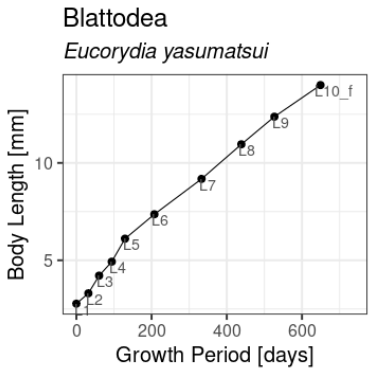

Figure 4: Growth trajectory of the Blattodea species (mean values).

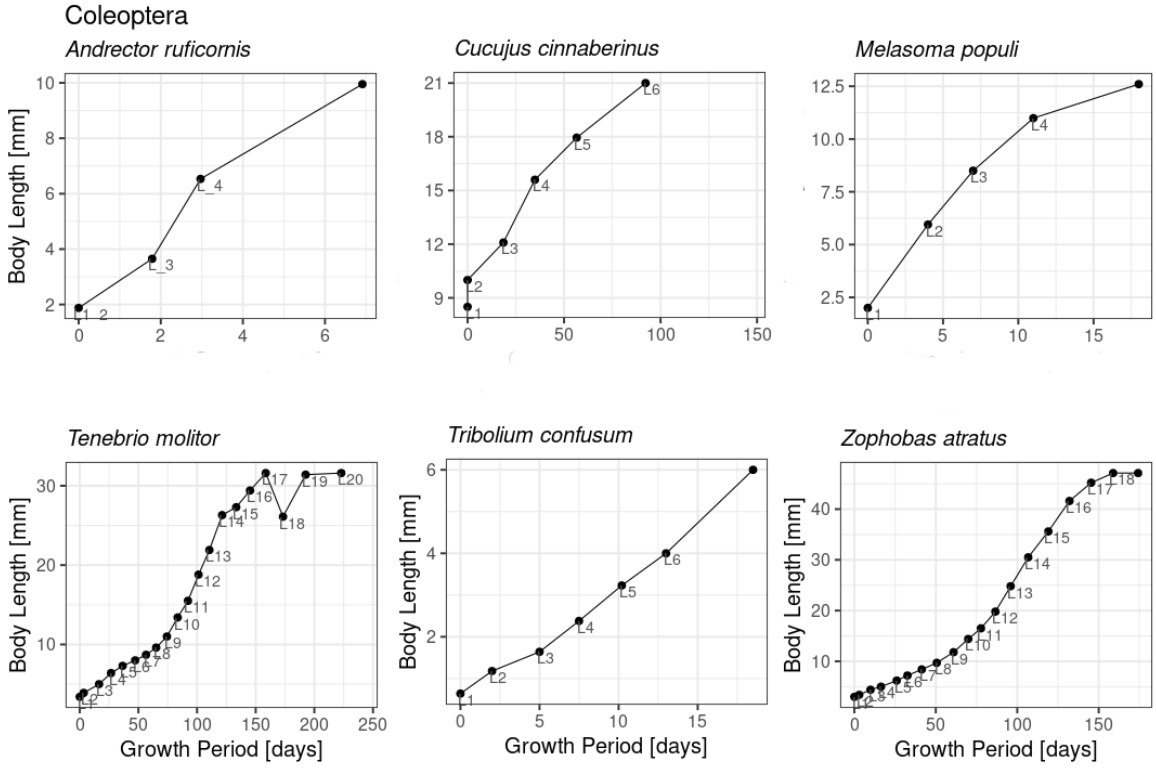

Figure 5: Growth trajectory of the Coleoptera species (mean values).

APPENDIX CHAPTER IV

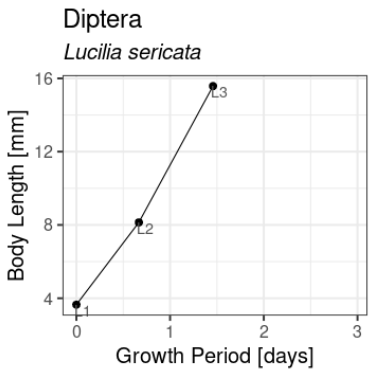

Figure 6: Growth trajectory of the Blattodea species (mean values).

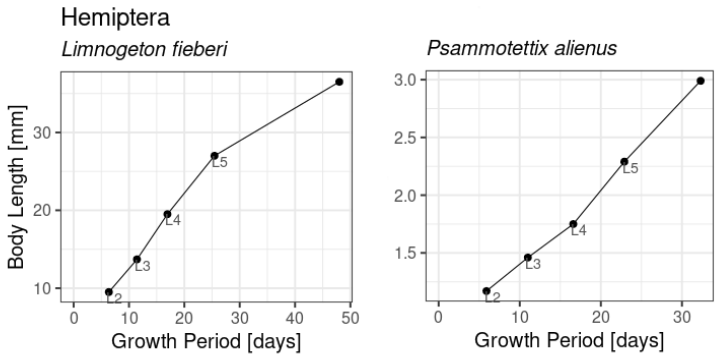

Figure 7: Growth trajectory of the Hemiptera species (mean values).

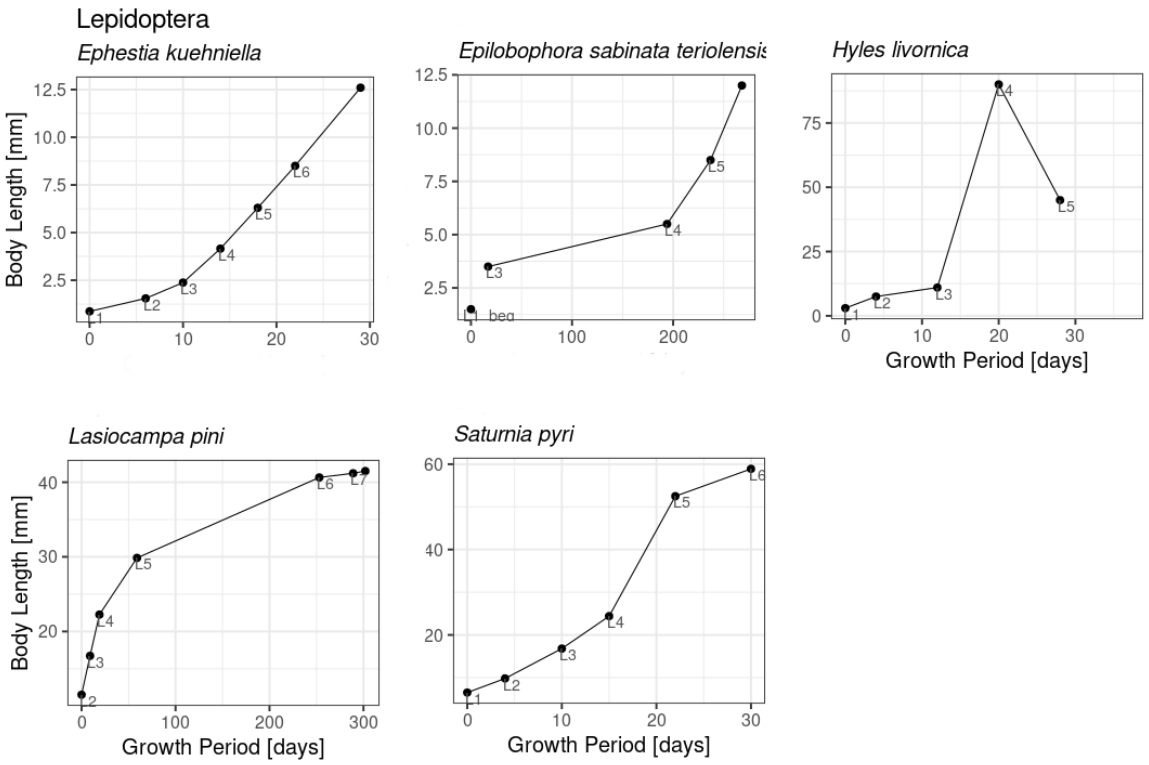

Figure 8: Growth trajectory of the Lepidoptera species (mean values).

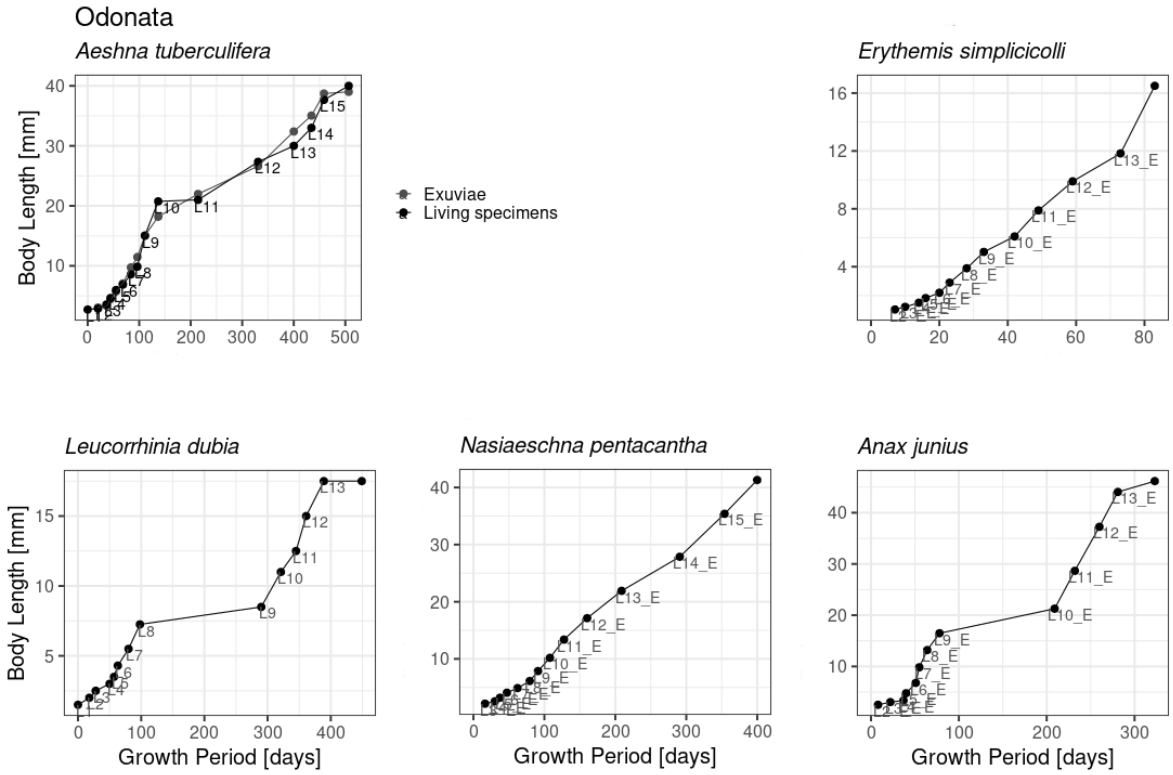

Figure 9: Growth trajectory of the Odonata species (mean values). Living specimens and exuviae were measured for *Aeshna tuberculifera*.

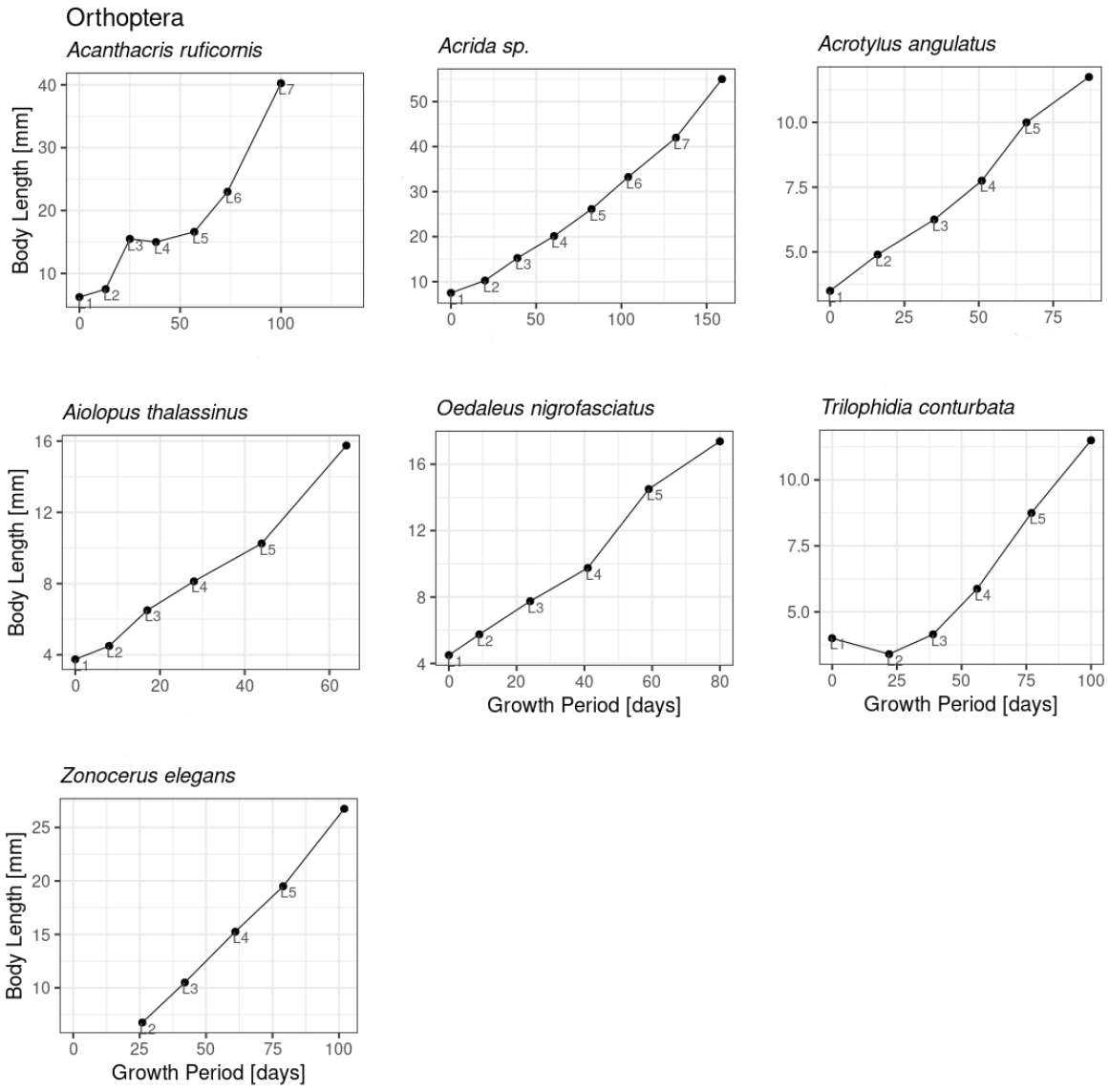

Figure 10: Growth trajectory of the Orthoptera species (mean values), without the three Gryllidae species.

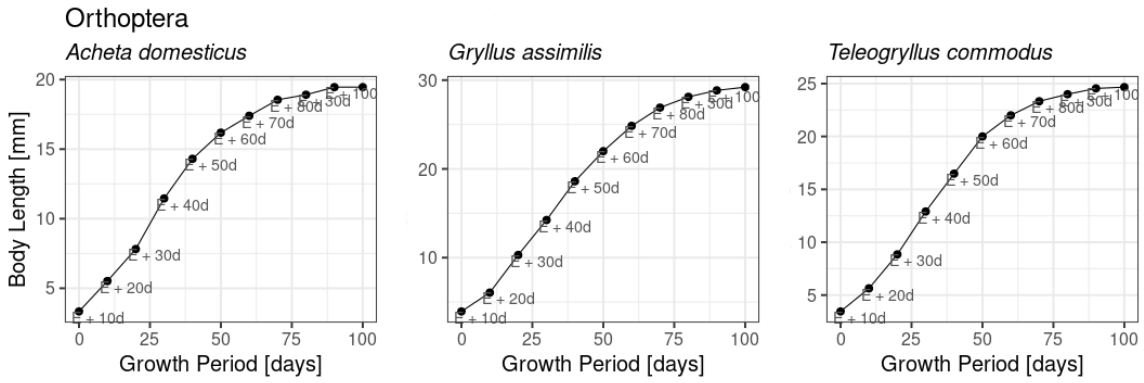

Figure 11: Growth trajectory of the Gryllidae species (mean values) measured in a ten-days interval.

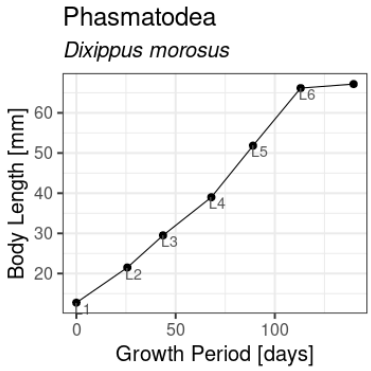

Figure 12: Growth trajectory of the Phasmatodea species (mean values).

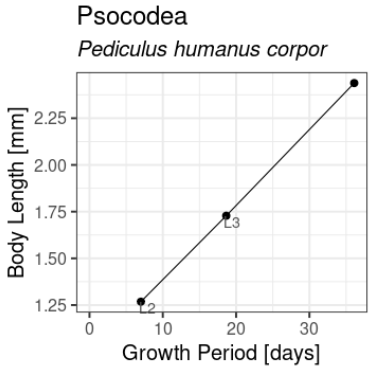

Figure 13: Growth trajectory of the Psocodea species (mean values).

APPENDIX CHAPTER IV

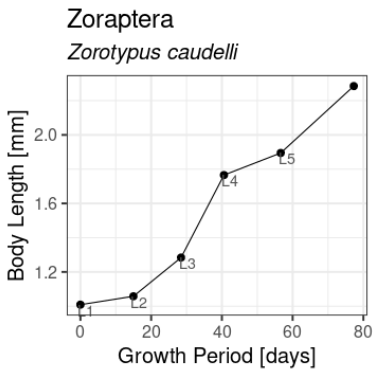

Figure 4: Growth trajectory of the Zoraptera species (mean values).

References

T. Münkemüller, S. Lavergne, B. Bzeznik, S. Dray, T. Jombart, K. Schiffers, W. Thuiller, How to measure and test phylogenetic signal. *Methods in Ecology and Evolution* **3.4**, 743-756 (2012).

S. Dray, *Adephylo package* (2018).

S. L. Dobson, *et al.*, Wolbachia infections are distributed throughout insect somatic and germ line tissues. *Insect Biochemistry and Molecular Biology* **29**, 153–160 (1999).

L. Karstens, *et al.*, Controlling for Contaminants in Low-Biomass 16S rRNA Gene Sequencing Experiments. *mSystems* **4** (2019).

L. Paniagua Voirol, G. Valsamakis, M. Yu, P. Johnston, M. Hilker, How the "kitome" influences the characterisation of bacterial communities in lepidopteran samples with low bacterial biomass. *Journal of Applied Microbiology* (2020) https:/doi.org/10.1111/JAM.14919.

S. J. Salter, *et al.*, Reagent and laboratory contamination can critically impact sequence-based microbiome analyses. *BMC Biol* **12**, 87 (2014).

T. J. Hammer, D. H. Janzen, W. Hallwachs, S. P. Jaffe, N. Fierer, Caterpillars lack a resident gut microbiome. *Proc Natl Acad Sci USA* **114**, 9641–9646 (2017).

ACKNOWLEDGEMENTS

First and foremost, I thank my supervisor Prof. Dr Jens Rolff, for making this thesis possible by giving me the opportunity to become a member of his group. I am very grateful for your guidance through academia, entrusting me with responsible and stimulating tasks and for being such a great role model. I learned a lot from you. I am very thankful to Sophie Armitage for the productive and inspiring mentoring meetings, her guidance through the depth of academia, and her feedback. I am very grateful for your constant positive input. Thanks a lot to Paul Johnston for all the tremendous computational input, hours of online meetings whenever I was facing a problem, and being such amicable and fun support. I also thank Prof. Dr Dino McMahon and Prof. Dr Michael Monaghan not only for accepting to supervise my work, but also for making time for productive discussions and giving me great input during supervisory meetings.

Thanks to Elisa Bittermann for her support in the laboratory, the tons of orders and your lovely character. I would have been lost many times in the laboratory without you. I also thank Luisa Linke, Marlene Finger and Jia Clara Kim for being enjoyable students and for their support in the laboratory. Thanks to Felix Mende, Carl Bukowski and Josh Kim, who greatly supported me as HiWis. I also express my gratitude to the Rolff group, which created an inspiring and fun environment. Thanks to Dirk ´Dr Miko` Mikolajewski for his open door and the tea breaks.

I am very thankful to my partner Martin Friedrichs-Manthey for always supporting me emotionally and the fruitful discussions about science and life. Many thanks to my son Loke who always knows

how to make me smile. This thesis is dedicated to you. Last but not least, I thank my sisters Lisa Manthey and Carla Weckwerth for always giving me emotional support, and for being great aunts.

PUBLICATIONS

Published

Scharnweber, K., Peura, S., Attermeyer, K., Bertilsson, S., Bolender, L., Buck, M., Einarsdóttir, K., Garcia, S.L., Gollnisch, R., Grasset, C., Groeneveld, M., Hawkes, J.A., Lindström, E.S., **Manthey, C.**, Övergaard, R., Rengefors, K., Sedano-Núñez, V.T., Tranvik, L.J. and Székely, A.J. (2021), Comprehensive analysis of chemical and biological problems associated with browning agents used in aquatic studies. Limnol Oceanogr Methods. (https://doi.org/10.1002/lom3.10463)

Agha, R., Saebelfeld, M., **Manthey, C.**, Rohrlack, T., & Wolinska, J. (2016). Chytrid parasitism facilitates trophic transfer between bloom-forming cyanobacteria and zooplankton (Daphnia). Scientific Reports, 6(1), 1-9. (https://doi.org/10.1038/srep35039)

In revision

Manthey, C., Johnston, P. R., Shinichi, N., & Rolff, J. (2021). Complete metamorphosis and microbiota turnover in insects. bioRxiv. (https://doi.org/10.1101/2021.06.15.448481) (**CHAPTER II**)

In prep.

Manthey, C., Monaghan, M.T., Steiner, U., & Rolff, J. (2022). Holometaboly facilitates fast growth. (In prep.) (**CHAPTER IV**)

Manthey, C., Johnston, P. R., & Rolff, J. (2022). Immune gene regulation during metamorphosis. (In prep.) (**CHAPTER III**)

DECLARATION OF INDEPENDENCE

Herewith I certify that I have prepared and written my thesis independently and that I have not used any sources and aids other than those indicated by me. Intellectual property of other authors has been marked accordingly. I also declare that I have not applied for an examination procedure at any other institution and that I have not submitted the dissertation in this or any other form to any other faculty as a dissertation.

Berlin, 20th May 2022

Christin Manthey